INFORMATION TO USERS

This manuscript has been reproduced from the microfilm master. UMI films the text directly from the original or copy submitted. Thus, some thesis and dissertation copies are in typewriter face, while others may be from any type of computer printer.

The quality of this reproduction is dependent upon the quality of the copy submitted. Broken or indistinct print, colored or poor quality illustrations and photographs, print bleedthrough, substandard margins, and improper alignment can adversely affect reproduction.

In the unlikely event that the author did not send UMI a complete manuscript and there are missing pages, these will be noted. Also, if unauthorized copyright material had to be removed, a note will indicate the deletion.

Oversize materials (e.g., maps, drawings, charts) are reproduced by sectioning the original, beginning at the upper left-hand corner and continuing from left to right in equal sections with small overlaps. Each original is also photographed in one exposure and is included in reduced form at the back of the book.

Photographs included in the original manuscript have been reproduced xerographically in this copy. Higher quality 6" x 9" black and white photographic prints are available for any photographs or illustrations appearing in this copy for an additional charge. Contact UMI directly to order.

UMI

A Bell & Howell Information Company
300 North Zeeb Road, Ann Arbor MI 48106-1346 USA
313/761-4700 800/521-0600

The Development and Application of a Sequence-Selective DNA Sensor

Kelly M. Millan

A Thesis

In

The Department

of

Chemistry and Biochemistry

Presented in Partial Fulfilment of the Requirements

for the Degree of Doctor of Philosophy at

Concordia University

Montreal, Quebec, Canada

1997

Abstract

The Development and Application
of a Sequence-Selective DNA Sensor

Kelly M. Millan, Ph.D.
Concordia University, 1997

DNA has been covalently immobilized onto glassy carbon electrodes and stearic acid modified carbon paste electrodes using water soluble carbodiimide and hydroxysuccinimide reagents. This promotes coupling between surface carboxylic acid groups and guanine bases. Preliminary results with model compounds suggest that coupling occurs at the N1 imino position of the guanine base. Octadecylamine modified carbon paste electrodes (ODACPEs) have been modified with DNA via a phosphoramidate bond between the 5'phosphate and the primary amine of octadecylamine. Immobilized DNA was detected voltammetrically with either $Co(bpy)_3^{3+}$, $Co(phen)_3^{3+}$, $Os(bpy)_3^{2+}$, three complexes which exhibit quasireversible one electron redox activity and associate selectively with double-stranded DNA, or with a daunomcyin-glucose oxidase conjugate with a ferrocene mediator.

Voltammetric peak currents obtained with a poly(dG)poly(dC)-modified GCE depend on $Co(bpy)_3^{3+}$ concentrations in a nonlinear fashion and indicate saturation binding with immobilized DNA. Ferrocene derivatives which do not bind selectively to dsDNA yield linear calibration curves (i_p vs concentration) at both DNA-modified and unmodified GCEs. Voltammetric peak currents for $Co(phen)_3^{3+}$ reduction were used to estimate the constant local DNA concentration at the modified electrode surface; a binding site size of 5 base pairs and an association constant of $1.74 \times 10^3\ M^{-1}$ yield 8.6 ± 0.2 mM base pairs.

A prototype sequence-selective DNA sensor was developed by immobilizing a 20-mer oligo$(dT)_{20}$ following its enzymatic elongation with dG residues, which yielded the species oligo$(dT)_{20}(dG)_{99}$. An increase in peak current was obtained after hybridization with target DNA. The single-stranded probe at the GCE surface is regenerated after rinsing the sensor in hot distilled water. These results demonstrate that this sensor can be used as a reusable sequence-selective biosensor for DNA.

A comparison of batch and *in situ* hybridization rates of an immobilized poly(dT) demonstrated that hybridization occurred at a faster rate under high ionic strength in the absence of a hybridization indicator and yielded a detection limit of 100 ng/mL.

This technique was applied to DNA sensors selective for the ΔF508 deletion region of human DNA. These sensors were capable of selectively detecting their target sequences when hybridization occurred at 43 °C.

Acknowledgements

I would like to thank my supervisor, Dr. S. Mikkelsen, for her advice, support, and invaluable assistance in carrying out my Ph.D research. I would also like to thank Dr. Susan Mikkelsen and Dr. Ann English for being significant role models in my life. A special thanks for their joint group meetings, for which at the time I had to endure, but now realize that they made me a better scientist. I would also like to thank them for challenging me to be the best I can be.

I would like to thank the members of my committee, Dr. Powlowski, Professor Baldwin and Joanne Turnbull, for their support. A special thanks to Professor Baldwin and Dr. Pallen for their kindness and advice.

Thanks to the departmental secretaries, Carol Coutts, Kathy Usas, Donna Gordon, and Mary at Graduate studies for going beyond the call of duty and always having time to help. I would also like to thank the technical staff (especially Miriam, Jimmy and Paul) for helping the graduate students when we needed it.

I would especially like to thank Beata Kolakowski and George Tspairalis for their continued moral support and for providing laughter, fun, and friendship. I would also like to thank Suzanne for providing humour when least expected.

Thanks to my friends Lucy, Alexandra, Elizabeth, and Janet for being true friends. Without their constant encouragement and support this project would have been much more difficult. I would like to thank Roch for working all hours of the night to help with my conference presentations.

I would like to thank my nephew and niece, Shayne and Kaley for bringing me an immeasurable amount of joy. Their smiles and laughter bring sense to this world..

Finally, I would thank my mother and father for having enough patience to see me through my Ph.D. This degree would not have been possible without their love and support.

In loving memory of Neil J. Millan (1931-1994)

Table of Contents

List of Figures and Schemes

List of Tables

Abbreviations

A	Ampere
A	Area
ACN	Acetonitrile
ARMS	Amplification refractory mutant system
ASO	Allele specific oligonucleotide
CA	Chronoamperometry
CCM	Chemical cleavage of mismatch
CDCE	Constant denaturing capillary electrophoresis
$CDCl_3$	Deuterated chloroform
CD_3OD	Deuterated methanol
CF	Cystic fibrosis
CFTR	Cystic fibrosis transmembrane conductance regulator
$Co(bpy)_3^{3+}$	Tris (2,2' bipyridine)cobalt(III)
$Co(phen)_3^{3+}$	Tris(1,10 phenanthroline)cobalt(III)
CPE	Carbon paste electrode
CPG	Controlled-pore-glass
CV	Cyclic voltammetry
DAF	Dimethylaminomethyl Ferrocene
Daunomycin-GOx	Daunomycin-glucose oxidase conjugate
D_6-DMSO	Deuterated dimethylsulfoxide
DGGE	Denaturing gradient gel electrophoresis

DMF	Dimethylformamide
cDNA	complementary DNA
DNA	Deoxyribonucleic acid
dsDNA	Double-stranded DNA
ssDNA	Single-stranded DNA
DPV	Differential pulse voltammetry
ECL	Electrogenerated chemiluminescent
EDC	1-[3-(dimethylamino)propyl]-3-ethylcarbodiimide hydrochloride
FCA	Ferrocene carboxylic acid
GCE	Glassy carbon electrode
HPLC	High performance liquid chromatography
I	Current
i_p	Peak current
IRT	Immunoreactive trypsin
LAPS	Light addressable potentiometric sensor
NBF	Nucleotide binding fold
NHS	N-hydroxysulfosuccinimide
ODA	Octadecylamine
ODA-CPE	Octadecylamine carbon paste electrode
$Os(bpy)_3^{2+}$	Tris (2,2' bipyridine)osmium(II)
PAGE	Polyacrylamide gel electrophoresis

PCR	Polymerase chain reaction
QCM	Quartz crystal microbalance
R	Resistance
RFLP	Restriction fragment length polymorphism
$Ru(phen)_3^{2+}$	Tris(1,10 phenanthroline)ruthenium(II)
SA	Stearic acid
SACPE	Stearic acid carbon paste electrode
SAW	Surface acoustic wave
SCE	Saturated calomel electrode
SSB	Single-stranded binding protein
SSCP	Single-stranded conformational polymorphism
TAG	2',3',5' triacetylguanosine
T_m	Melting temperature
TBR	Tris (2,2' bipyridine)ruthenium(II)
TPA	Tripropylamine
TSM	Thickness shear mode
V	Voltage

Chapter 1

Introduction

Advances in molecular genetics have given us a greater understanding of the relationship between genetics and human disease. The human genome consists of about 10^5 genes which are coded for by 3 to 5% of the total 3×10^9 base pairs of the human genome.[1] The identification of the correct sequences of nucleic acids which code for biologically necessary proteins have affected the ways in which human disease is diagnosed. Alterations in the normal sequence can cause genetic diseases such as sickle cell anaemia and cystic fibrosis. DNA sequences associated with disease differ from normal sequences by changes due to a point mutation which results from a one nucleotide substitution or to larger changes such as deletions, insertions, repetitions, and translocations of DNA segments. Techniques of positional cloning identify disease genes based solely on their chromosomal location. This has led to the genetic identification of many diseases and will allow for the identification of many others[2].

Until recently clinical laboratories have had a limited role in diagnosing genetic disease. Rapid developments in genetic diagnostics have led to pre-and postnatal detection of genetic disorders. Genetic diagnostics can also be applied to any disease state which results in an alteration in the normal DNA sequence. Detecting specific sequences of DNA which are not normally found in the human genome can allow for the diagnosis of viral and bacterial infections as well as for the early detection of precancerous and cancerous cells. The early diagnosis of heritable disorders, cancer, and infectious diseases will allow early treatment

which could control or correct for the disease state. Gene therapy is now being used to control many genetic disorders.[3,4]

1.1 Sample Preparation

Depending upon the technique used to detect hybridization, assays or DNA sensors, the requirements for purity change. For example, analysis by Southern blotting requires DNA of high purity. Impurities can inhibit restriction enzyme cleavage at its particular recognition site and this can lead to anomalous results[5]. Pure samples of DNA are not always necessary; some techniques involved in DNA diagnostics, such as PCR, only require crudely isolated samples[6].

Typical preparation of genomic DNA samples begin with cell lysis using lysozyme, alkali, detergents, or heat. Proteins can then be digested with proteinase K. Digested protein and carbohydrate are then removed by extracting with phenol and chloroform. Proteins are soluble in the phenol chloroform mixture and DNA is left behind in the aqueous layer. The remaining DNA is then concentrated by precipitation with ethanol and sodium acetate. This method does not remove all protein and carbohydrate and a high percentage of DNA is lost. Chaotropic agents such as guanidinium thiocyanate have been used to extract DNA and RNA but interfere with hybridization and thus cannot be used with any method that relies on hybridization to detect a DNA sequence. DNA isolation has been automated and through the use of the DNA Extractor DNA of a higher quality than that obtained from manual methods can be isolated.[1]

One of the most important developments in molecular biology has been that of the Polymerase Chain Reaction (PCR). PCR is an enzymatic technique used to exponentially

increase the copy number or concentration of a selected segment of DNA or RNA. This allows for the genetic analysis of samples that would otherwise have too low a DNA concentration for routine diagnosis. Using PCR, a single copy of the target DNA is sufficient to start the amplification reaction. Thus amplification of a single cell can be performed with confidence.[7] This technique relies on a thermostable DNA polymerase enzyme, Taq DNA polymerase,from the bacterium *Thermus aquaticus*. A DNA polymerase is an enzyme that synthesizes new DNA strands from a primed template strand. Two DNA primers are selected which have complementary sequences to outlying regions of the segments to be amplified. One primer is complementary to the 3'end of one copy and the other is complementary to the 3' end of the other copy. The procedure consists of three stepwise operations, which are sequentially performed: DNA denaturation followed by primer annealing and finally primer extension/amplification. These operations can be performed in one reaction vial and are only controlled by temperature. DNA denaturation occurs at temperatures above 90 C, annealing of primers to their complementary target occur at temperatures between 37 and 55 C. After the primers are annealed to their target sequences the temperature is raised to the optimal temperature for extension by the DNA polymerase. Figure 1 illustrates how this cycle of denaturation, annealing, and extension occurs. The cycle is be repeated up to 30 times, and the products of one round of amplification can serve as templates for all other cycles. Each cycle exponentially increases the DNA copy number. Thus the theoretical yield for amplification is 2^n-1, where n is the number of cycles. The discovery of a DNA polymerase which is thermostable has made this technique amenable to automation. Taq DNA polymerase can survive extended incubations at 95° C without any significant decrease in its activity. Two

other heat stable DNA polymerase have been identified, these have 3'-5' exonuclease activity which reduces the rate of misincorporation of nucleotides. Vent polymerase and Pfu polymerase were isolated from *Thermococcus litoralis* and *Pyrococcus furiosus*, respectively.[8] Taq polymerase does not have this proofreading capability.

Analysis of genetic mutations begins with amplification of the sequence of interest followed by selective hybridization with a sequence-selective oligonucleotide probe and an appropriate detection method.[1] Oligonucleotide probes are short sequences of ssDNA, of 15 to 20 nucleotides in length. This length is sufficient to recognize a unique sequence in a random DNA sequence of six billion bases, such as the human genome, and at the same time is short enough to permit selective hybridization under controlled conditions with its exact complementary sequence.[9] Under specific conditions of temperature and ionic strength hybridization will be destabilized by a single base mismatch between probe and target sequences. Longer probes are not as selective. A DNA probe's selectivity is determined by its ability to form a heteroduplex with its target sequence via Watson-Crick base pairs during hybridization. The selectivity of DNA hybridization is determined by the ability of the purine and pyrimidine bases, which make up the nucleotides, to hydrogen bond only to their specific complementary base. Guanosine will only hydrogen bond to cytidine and adenosine with thymidine. Thus if the target DNA is the complementary sequence to the probe, the bases of the two sequences pair off and form a stable hybrid. If the two sequences are not complementary, hybridization will not occur as readily or under the same conditions. Thus hybridization conditions can be adjusted according to the required stringency of detection. A DNA probe is thus capable of detecting the presence of a target sequence of DNA which is

linked to a hereditary disorder, or to the presence of a particular strain of bacteria or virus.

In order for an oligonucleotide probe to be able to determine the presence of a particular sequence of DNA it must be modified such that it can be detected, by standard methods, in the presence of a large excess of non-target DNA. This modification of the DNA probe must not interfere with its ability to hybridize with its complementary sequence. For example, modifying an oligonucleotide probe with a radioactive isotope does not interfere with hybridization to its complement and allows for detection by autoradiography[10].

1.2 Assays for Sequence-Selective DNA Detection

Restriction mapping is often used in DNA analysis. In this technique, DNA is treated with a particular restriction endonuclease enzyme. There are many restriction enzymes commercially available, and each restriction enzyme recognizes a particular pallindromic base sequence of about 4 - 8 base pairs. The restriction enzyme will selectively cleave double-stranded DNA at any site with that base sequence[11]. Restriction enzymes have two important functions. First, they cleave DNA into smaller double-stranded fragments which are more convenient to analyze. Second, since each restriction enzyme will only cleave double-stranded DNA with a particular known recognition sequence they can be used to identify the presence or absence of that sequence. Sometimes an alteration in the normal genetic sequence, which can lead to a heritable disorder, can result in the creation or elimination of a recognition sequence for a particular restriction enzyme. If these sites are created or eliminated the lengths of the fragments generated by enzymatic cleavage will change. The sizes of the fragments generated can then be determined by gel electrophoresis.

Electrophoresis separates DNA based on its size. A small sample of DNA is placed

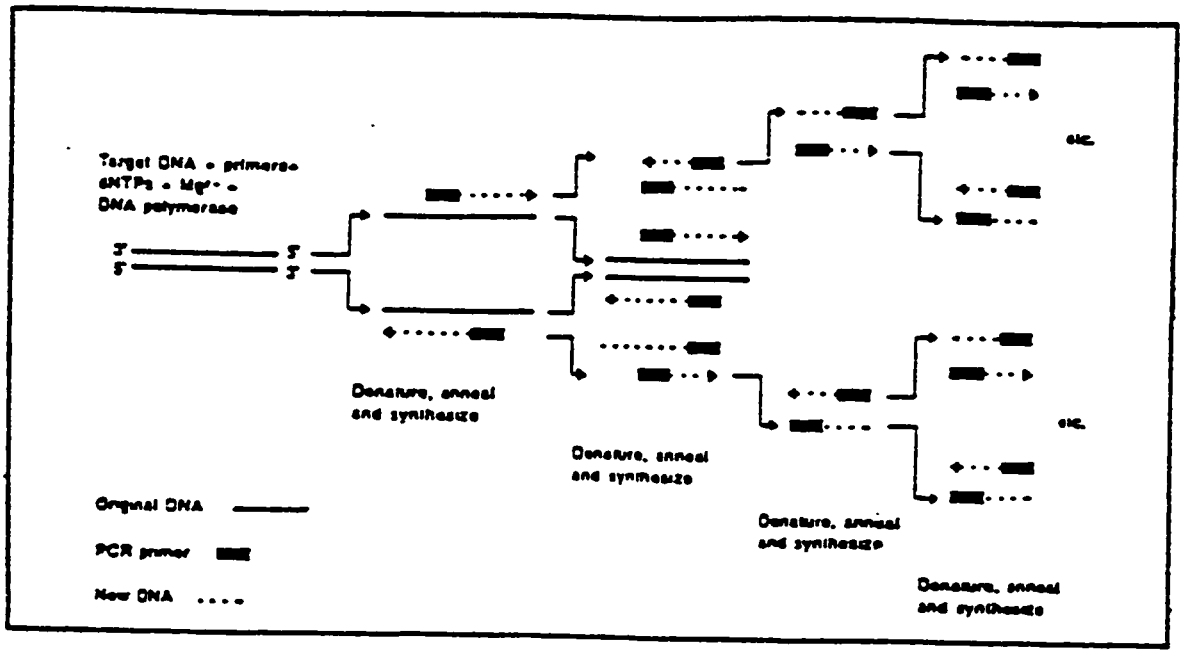

Figure 1.1: Diagram of the Polymerase Chain Reaction.[8]

in a well cut into a gel which acts as a sieving matrix through which DNA can migrate. The ends of the gel are exposed to an electrolyte solution and an electric field is applied across the gel. Since each nucleotide has associated with it a negatively charged phosphate group, DNA has a constant charge to mass ratio. Thus the DNA will migrate towards the positively charged anode at rates dependent only of the size of the DNA strand. The electrophoretic mobility of DNA is inversely proportional to the logarithm of its length, or molecular weight, within a certain range[12].

The DNA separated by electrophoresis can be visualized by staining with a dye or fluorophore which interacts selectively with double-stranded DNA. Restriction enzyme digestion of genomic DNA creates many fragments of the same and differing lengths, too many to completely separate by electrophoresis. The pattern produced by a simple staining procedure would be uninterpretable. Restriction fragments containing a particular sequence can be identified by hybridization with a labelled oligonucleotide probe. This probe's DNA sequence is complementary to a particular site on the restriction fragment, or to any fragment of interest.

Restriction mapping and Southern blot analysis are routinely used in laboratories for the identification of heritable diseases. Southern blotting is a technique that allows the transfer of electrophoretically-separated DNA fragments to a nitrocellulose membrane, to allow subsequent detection using oligonucleotide probes. Since only single-stranded DNA will adsorb to nitrocellulose and hybridize to its complementary probe sequence, the DNA is denatured before it is transferred to the nitrocellulose. The entire separation pattern is then transferred to the nitrocellulose membrane by buffer flow. DNA sequences can then be

detected following hybridization with labelled oligonucleotide probes.[12]

β°-Thalassemia, which results from a single nucleotide change in the β-globin gene, has been identified by restriction mapping and Southern Blot analysis. The enzyme Hph I is known to cleave DNA at the 5' end of β-globin large intervening sequence, IVS 2. The single nucleotide which results in the defective gene causes a change at this restriction enzyme recognition site. Thus the size of the fragment(s) generated after digestion with Hph I will be different for the normal and defective genes. A 1000 bp or 900 bp fragment will be generated for the defective and normal genes, respectively, which is consistent with the loss of the HphI cleavage site in the mutated sequence. The fragments generated are hybridized to a ^{32}P-labelled probe complementary to the IVS 2 sequence[13]. DNA fragments created by restriction enzyme mapping can be separated by gel electrophoresis and visualized by autoradiography.

There are many problems associated with restriction mapping and Southern blot analysis. The most obvious is that not all mutations result in a change at a restriction enzyme cleavage site. Therefore these methods cannot be used universally for genetic diagnostics.

This problem can be overcome by a related technique called slot or dot blotting. In this technique the sample is immobilized directly onto nitrocellulose without the need for restriction enzymes or electrophoresis. Labelled probes, usually radio-labelled, which are complementary to a unique sequence and can discriminate between the defective and nondefective gene sequence, are then hybridized under stringent conditions, to its immobilized complement. These probes are sometimes referred to as allele specific oligonucleotides. The presence or absence of a particular sequence is determined by measuring the signal intensity resulting from the label on the probe sequence.[4] Dot blotting and Southern blotting are very

similar and share some of the same problems. Binding of single-stranded DNA to nitrocellulose is a very time-consuming process. Also, radioactive labelled probes are hazardous, require expensive equipment and inconvenient to work with on a routine basis. ^{32}P-labelled probes have a very short half-life and therefore are only useful for a few days. ^{3}H labelled probes require long exposure times, sometimes weeks. All radio-labelled probes require a darkroom for photography, or an expensive scintillation counter, and handling and disposal of radioactive isotopes is hazardous and expensive.

There are many nonisotopic probes. The most commonly used non-radioactive probes are based on biotin which is detected by its strong affinity for avidin or streptavidin. If an enzyme is linked to avidin the probe can be detected by a coloured product of the enzyme reaction. If nonisotopic probes are to be used the immobilized nucleic acid must be free of protein and other contaminants to prevent nonspecific background signals[14].

In conjunction with PCR, restriction fragment length polymorphism (RFLP) does not require the use of radioactive probes. When a segment of DNA is amplified by PCR the primers are chosen such that there is a reasonably short distance between them. This allows for the creation of amplified DNA with only one possible restriction enzyme cleavage site for either the mutant or nonmutant sequence. Digestion with a restriction enzyme will create different length DNA fragments depending upon the sequence. The fragments produced can be run on an electrophoresis gel and visualized by staining with a DNA-binding fluorescent dye, such as ethidium bromide. The CS.7/Hha I polymorphism close to the cystic fibrosis locus on chromosome number 7 can be detected in such a manner.[7]

An easier alternative to PCR/RFLP analysis that allows deletions or additions to be

detected involves electrophoresis of a PCR amplified DNA segment under specific conditions which can separate DNA varying in length by only 3 bases. The ΔF508 deletion, a three base deletion on chromosome 7, which is linked to cystic fibrosis, can be separated from its normal counterpart on a 10-12% non-denaturing or an 8% denaturing gel.[7] This technique is not universal and can only be applied to the detection of DNA length alterations of 3 or more base pairs.

Denaturing Gradient Gel Electrophoresis (DGGE) is an electrophoretic technique in which double-stranded DNA fragments are separated on a gel with a gradient of increasing denaturant concentration. DNA fragments possess small regions of DNA which undergo cooperative strand dissociation under different denaturant conditions, resulting in incomplete hybridization of the whole DNA fragment. As DNA fragments move through the gel into higher concentrations of denaturant the least stable duplex regions undergo strand dissociation, followed by the more stable regions. Incomplete denaturation results in a decrease in mobility of the DNA fragment. DNA sequences suitable for DGGE separation must have a high stability melting domain and a low stability melting domain such that within certain denaturing conditions a stable partially melted intermediate exists. Alterations of the base sequence in the melting domain result in a change in the melting temperature (T_m), and this creates a change in the stability of that region towards denaturants. The problem with DGGE is that base substitutions in the regions of highest stability cannot be detected since once the most stable melting domain undergoes strand dissociation complete denaturation occurs and the resolving capability of the gel is lost.

In a variation of DGGE, a PCR-amplified target sequence is hybridized with a an

excess of the "normal" probe sequence. Hybridization occurs between mismatched sequences at the appropriate temperature and ionic strength. The resulting heteroduplex is electrophoresed on a gel with increasing concentrations of denaturant. Regions containing a mismatch will denature more easily than a perfectly matched duplex. This allows for the separation of DNA with a single base substitution. The difficulties associated with this method of DNA analysis include the use of radioactive labels and high temperatures (60 °C). This technique can require several days for completion, and due to the high temperatures and the use of radioisotopes can cause DNA strand breakage. This differential melting process has been adapted to constant denaturant capillary electrophoresis (CDCE)[15]. Using CDCE in conjunction with fluorescent DNA labels the absolute limit of detection is 3×10^4 molecules.

Other methods have been developed which take advantage of gel electrophoresis and various DNA-modifying enzymes. One such method has combined gel electrophoresis, a thermostable DNA ligase from the bacterium *Thermus thermophilus*, and the technique of thermal cycling.[16] This assay uses four DNA probes which represent adjacent sequences on the two complementary stands of the target sequence. The target DNA serves as a template for which the probes can selectively hybridize under controlled conditions. If the probe sequences are complementary and hybridize to their respective target sequences, they will be perfectly aligned with the 3' end of one probe adjacent to the 5'end of the other. The DNA ligase will catalyze the formation of the phosphodiester bond to join the probes together. Each temperature cycle results in an approximate doubling of ligated probes with a size equal to the sum of the reactant probes. If there is a mismatch at the ligation site the enyzme will not ligate the probes and no product will be detected. Thus, with appropriate design of the DNA

probes, this assay can be adapted to the analysis of heritable disorders.

A modification of this strategy was designed which chemically ligates probe oligonucleotides. The two probes are complementary to adjacent sites on the same target sequence of DNA. The DNA probes are chemically modified so that the 3' end of one oligonucleotide is reactive towards the 5'end of the other. The 5' terminus is modified with a nucleophilic phoshorothioate which is reactive towards an electrophilic α-halo acyl derivative (bromoacetomido) modified at the 3'end[17]. Figure 1.2 shows the structures of two chemically modified probes and their reaction product. The target sequence serves as a template for which the probes can selectively hybridize under controlled conditions. If the probe sequences are complementary and hybridize to the target sequence, they will be perfectly aligned with the 3' end of one probe adjacent to the 5'end of the other. When the nucleophilic phosphorothioate comes into contact with the electrophilic bromoacetomido group, the two oligonucleotides chemically ligate. A single-base mismatch results in a reduction in the rate of this chemical autoligation. Thus the presence or absence of a single-base mutation can be detected by determining the size of the resulting oligonucleotide probes.[18].

Other methods for the detection of single-base mutations rely on chemical or enzymatic modification of single-base mismatches. The enzymes ribonuclease A, ribonuclease T, or S1 nuclease will degrade single-stranded but not double-stranded nucleic acids. Heteroduplex strands formed between the complementary strands of a deletion, insertion, or base substitution mutant and the nonmutant sequences creates a single-stranded loop or an unpaired base at the site of the mutation. If a heteroduplex is formed between RNA and DNA

the ribonuclease enzymes RNase A or T1, will cleave at the site of unpaired RNA bases.[19,20] For S1 nuclease[21] cleavage occurs at unpaired DNA bases. Electrophoresis is used to examine the size of the resulting fragments after digestion with one of the above enzymes.

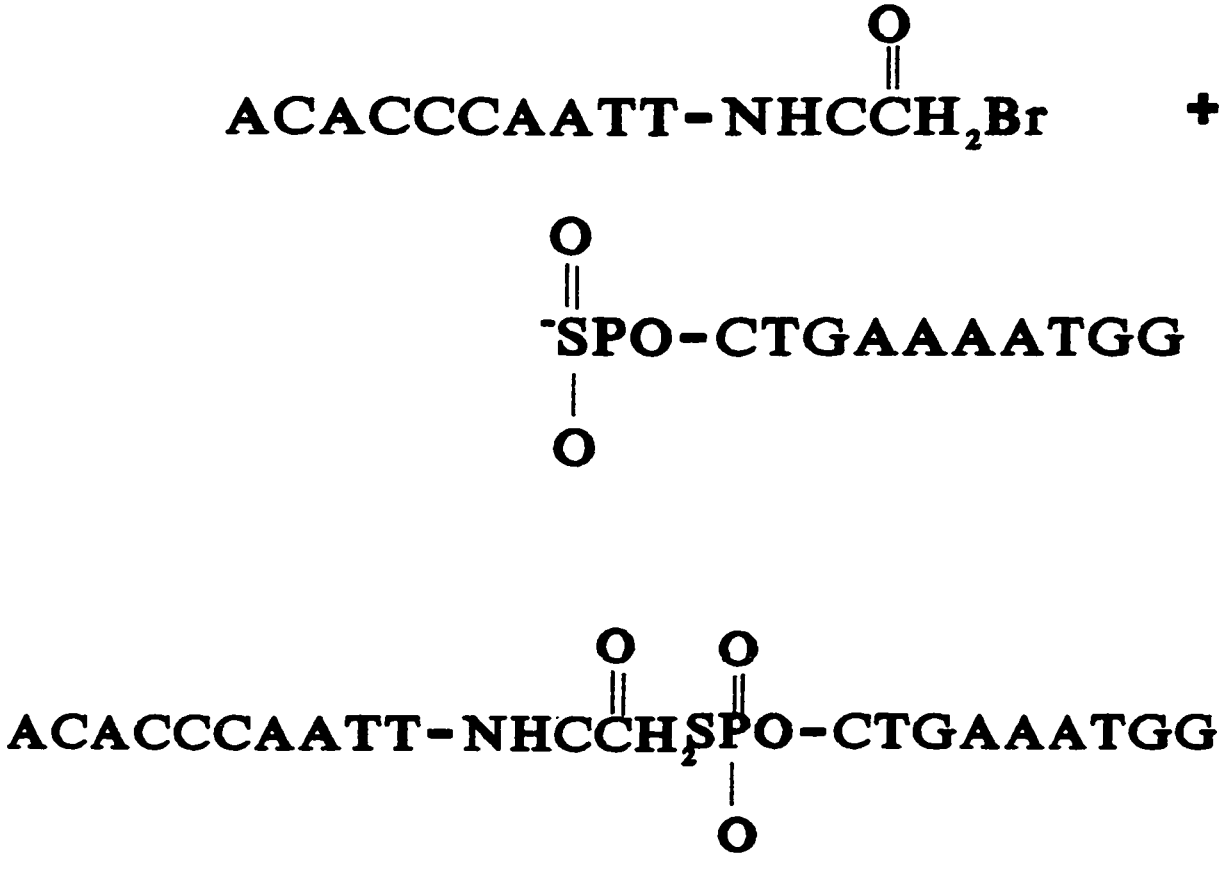

Figure 1.2 The structures of a phosphorthioate-modified, an α-halo acyl derivatized probe and the ligated product.[18]

Similar methods involve the chemical cleavage of unpaired nucleotides. One such method involves reacting mismatched cytosine and thymine bases with hydroxylamine and osmium tetroxide, respectively, followed by chemical cleavage with piperidine[22]. Water soluble carbodiimides can also be used to chemically modify mismatched guanosine and thymine residues.[23] The modified DNA is then amplified by Taq DNA polymerase under conditions in which the extension of the primers is terminated at the site of any carbodiimide-modified Gs or Ts. In this assay single-base mutations are detected by electrophoretically determining the size of PCR products which are shorter than the full length product.

Figure 1.3 summarizes the different DNA assays discussed which are available for the diagnosis of heritable disorders.

1.3 DNA Biosensors

Recent efforts have focused on the development of a DNA biosensor for a less hazardous, more cost-effective, and simpler approach to DNA analysis. These sensors all employ single-stranded DNA bound to the surface of a transducer. Electrochemical, piezoelectric, surface plasmon resonance, and chemiluminescent devices are all under development.

Although the detection event is different for each transducer used, all rely on hybridization for selectivity. The transducers must be able to generate different signals for double and single-stranded DNA. The DNA sensors developed to date rely on the ability to discriminate between double and single-stranded DNA either directly by surface mass in a reagentless sensor, or indirectly, through the use of detection probes or hybridization indicators. Detection probes are short oligonucleotides approximately 20 bases long which

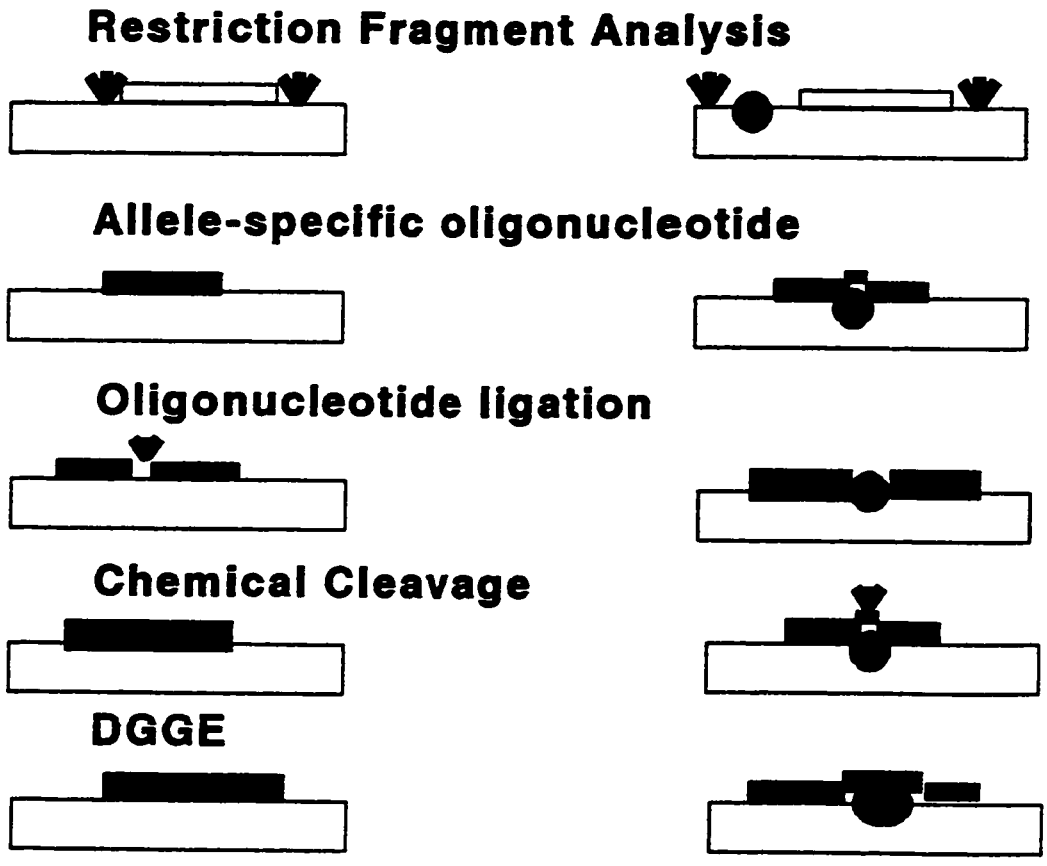

Figure 1.3 DNA Assays capable of diagnosing heritable disorders. The diagram on the left represents the analysis of the normal target sequence and on the right the diagram represents the mutated sequence.

are covalently bound to a label which can be directly detected. Examples of labels are flourophores, chemiluminescent compounds, and enzymes.[4] Hybridization indicators are compounds which selectively interact with double-stranded DNA and can easily be detected with an appropriate transducer.[24]

1.3.1 Reagentless DNA sensors

Reagentless DNA sensors detect the hybridization event directly through an increase in mass. In this type of sensor there is no need for modification of the probe oligonucleotide or the target sequence with a detecting element. The probe is immobilized to the surface of the transducer and the presence of the target sequence is detected directly through hybridization.

Piezoelectric devices detect the presence of the target sequence directly by sensing an increase in mass upon hybridization to the probe sequence. Piezoelectric devices rely on the generation of acoustic waves. This class of sensor is composed of piezoelectric material with one or more metal transducers on its surface. The piezoelectric material is usually quartz crystal, A-T cut quartz for thickness shear mode devices (TSM), and S-T cut quartz for surface acoustic wave devices (SAW). The transducer applies a sinusoidal voltage across the piezoelectric material at its resonance frequency, for a TSM device such as a quartz crystal microbalance (QCM), or at a frequency controlled by the periodicity of the interdigital transducer, for a SAW device. The transducer metal is usually chosen for its chemical inertness or for its acoustic match to the piezoelectric material. A layer can be added to the surface of the piezoelectric material that can bind the analyte being measured. Regardless of the type of piezoelectric device the measurements are the same. Changes in wave velocity,

frequency, and/or amplitude are measured and correlated to direct changes in mass[25]. The response of the TSM sensor to added mass is shown in equation 1:

$$\Delta f = -C_t F^2 \Delta m \qquad (1)$$

where Δf is the change in frequency, C_t is a constant and depends on the piezoelectric material, F is the resonant frequency, and Δm is the change in mass.

For a DNA biosensor the SAW device has the drawback that it can only be used in the gas phase and cannot be used for solutions of DNA. This is because the SAW device radiates compressional waves into the liquid medium and this causes the signal to be attenuated.[25] The QCM, a TSM device has had considerable attention as a DNA sensor since it can be used in either the gas or liquid phase.

In the first TSM device reported, nucleic acid probes were covalently bound to a polymer-modified surface of an A-T cut quartz crystal. A random copolymer of styrene and acrylic acid was attached to the quartz piezoelectric material. A poly(A) probe was covalently bound to the polymer carboxylic acid groups using the coupling reagent 1-ethyl-3-(3-dimethylaminopropyl) carbodiimide. A decrease in frequency was observed after each step of addition of polymer, binding the probe DNA, and hybridization to the target sequence. However, this sensor had to be dried before frequency measurements could be taken. Constant humidity was also necessary during measurements. Calibration of the crystal illustrated a linear decrease in frequency with increase in mass, (0.5 Hz/ng ± 28 Hz)[26].

In another device, hybridization and detection were performed in the liquid phase. The probe oligonucleotide sequences containing a terminal thiol group were immobilized through

chemisorption onto the gold electrodes of a QCM. The resonant frequency decreased with the mass of the probe DNA bound to the QCM. Upon addition of the target sequence, another decrease in frequency occurred. A decrease in frequency of 560 ± 10 Hz was observed after addition of the target sequence. This indicates an increase in mass, which is attributed to the hybridization of the target sequence to the immobilized probe DNA. Calibration of this device showed that a frequency decrease of 1 Hz corresponded to a mass increase of 1.05 ng on the QCM electrode both in aqueous solution and in air. The reported detection limit of this DNA sensor is 10 fmol of a 7249 base pair target DNA[27].

The most recently reported TSM piezoelectric device for the direct detection of DNA uses acoustic network analysis.[28] This is a passive method to analyze acoustic waves when liquid is in contact with the electrodes, as it is during hybridization of the target sequence to the surface-immobilized probe. The DNA probe is adsorbed onto a palladium layer by interactions of the phosphate and ribose groups of the probe with oxide oxygen of the palladium. A fine layer of palladium oxide is sputtered onto the gold electrodes which are in contact with the A-T cut quartz crystal. Once again a decrease in frequency is directly related to the increase in mass upon hybridization of the target sequence. A detection limit of 1.5 fmol has been reported for target DNA of 3955 base pairs.

In addition to piezoelectric devices, optical transducers are also under investigation for reagentless DNA sensors. Optical transducers have included surface plasmon resonance[29] and reflectometry[30] devices.

Like its piezoelectric counterpart pseudo-Brewster angle reflectometry can also be used in a reversible and reagentless DNA sensor. The principle of reflectometry is that

hybridization of the target DNA sequence to the immobilized probe is detected directly by a change in refractive index at the transducer surface. A thin layer of either nitrocellulose or aminosilane is coated onto the surface of silicon chips. This layer can be used for the covalent or adsorptive binding of DNA or poly-L-lysine which would electrostatically bind to the DNA phosphate backbone. The binding of single-stranded DNA through the phosphate groups allows the nucleotides to hybridize to their complement. In pseudo-Brewster angle reflectometry, plane polarized laser light strikes the silicon surface. At the Brewster angle for silicon (71°), the reflected light is attenuated and any change in refractive index causes an increase in reflected light intensity at the Brewster angle for silicon. After immobilization of the single-stranded probe DNA there is an increase in reflected light intensity. Hybridization with the immobilized probe alters the refractive index of the modified surface and this creates another increase in reflected light intensity at the Brewster angle. In one example, salmon sperm DNA was used as a high molecular weight probe.[30] Future studies with this method require its characterization with smaller probe sequences to determine whether it can be used for diagnosis of heritable disorders. Similar in principle with reflectometry is surface plasmon resonance. Surface plasmons are quanta of oscillations produced at metal-glass interfaces by resonant excitation of electrons in the metal by electron beams or light[31]. When plane polarized light is focused onto a metal surface, light energy is transferred to the metal surface layer, and a decrease in the intensity of the reflected light is observed. The metal can be modified with a biomolecule which alters the refractive index of the media near the surface. Surface plasmons are sensitive to changes in the refractive index of the media near the transducer surface. Therefore binding of ssDNA to the metal surface and hybridization to its

complement can be detected by an increase in reflectivity for light angle plotted. This device has applications as a DNA sensor but has generally been used for the detection of receptor-ligand binding. One group has used this to study the lactose-repressor binding to the lac operon.[32].

Although the three methods for detection of the presence of a target sequence are different, they share a common modality in that they do not require labels such as enzymes or fluorophores to detect hybridization of the target to the probe sequence.

1.3.2 Reagent-Dependent DNA Sensors.

Other DNA sensors have been developed in which the hybridization event is detected indirectly through the modification of either the target and/or probe sequence with a detectable label. Thus the presence of the target sequence is determined on the basis of the signal generated by a secondary compound bound closely to the transducer through its association with the DNA duplex. A detection probe, which is complementary to a specific section of the target DNA, is modified with an electroactive or chemiluminescent compound, a fluorophore, or an enzyme which catalyzes a reaction that produces a coloured product. For indirect methods the common theme is to capture the target sequence at the surface of the transducer and have the detection compound be brought to the surface through the presence of double-stranded DNA. Optical[33,34], electrochemiluminescent[35], and electrochemical methods[36,37,38a,b,c] have all made use of indirect detection of a target sequence.

Graham and Squirrell[33] have developed a fibre optic evanescent wave DNA sensor by covalently binding probe oligonucleotides with a terminal amino group to a silanized waveguide surface. This system takes advantage of total internal reflection for detection.

When light is transmitted through the optical fibre, part of that light is totally internally reflected and part will pass through the quartz optical fibre and enter the evanescent zone near the external surface of the fibre. The effective depth of the evanescent zone was calculated to be 100 nm. Of the light transmitted through this zone, part will be reflected back into the cable and become part of the total internal reflection. When the fluorophore label is present within the evanescent zone, and light at the excitation wavelength for that fluorophore is transmitted into this zone, the fluorophore is excited and emits light at its emission wavelength. This emitted light becomes part of the total internal reflection.

In this study[33] the detection probe sequences were modified with fluorescein and the target sequences were immobilized onto the transducer. Thus hybridization causes the fluorescein-labelled probe to be brought into the area within the evanescent zone. The fluorescein label is then detected by light intensity at the emission wavelength.

The lengths of the probes were varied to determine the effect of probe length on signal response. It was determined that there was little difference in signal between a 16-20-mer or a 204-mer immobilized onto the surface of the optical fibre. There was also little difference found between the detection probe being complementary to the distal or proximal end of the 204-mer. This indicates that the 204 mer stays within the confines of the evanescent zone. This will allow for the design of a "sandwich" type assay where a short capture probe is immobilized onto the transducer. It is capable of hybridizing to the target sequence and bringing the target into the evanescent zone. The capture and detection probes are complementary to different sequences present in the target DNA. The detection probe possesses a fluorescent label, which is brought into the evanescent zone upon hybridization.

Thus the target sequence does not require modification and is free in solution to hybridize to both the capture and detection probes. The reported detection limit for this sensor is 1 pmole using a 204 bp PCR amplified target sequence and 16- 20 mer capture and detection probes.

An automated fiber-optic evanescent wave biosensor based on the same principles outlined above has been recently developed as a reusable DNA biosensor. Biotinylated capture DNA is immobilized onto the surface of quartz fibers via the strong interaction between streptavidin and biotin. Target DNA is labelled with fluorescein, and detection of hybridization is based on fluorescence excitation and detection in the evanescent field of the quartz fiber. The sensor's reusability was tested over 200 cycles of repeat denaturation and hybridization cycles. These cycles had a duration of 35 minutes. Regeneration of the single-stranded probe was achieved by either thermal or chemical regeneration. After 200 cycles the net signal decreased by 50%. However, the signal loss during the repeat regeneration was nearly single exponential, and a correction factor can be applied. The detection limit for direct detection of a 16-mer fluorescein-modified target DNA is 2.0×10^{-13} M (2 fmol). Competitive hybridization assays for the detection of the unlabeled complementary 16-mer target DNA is 1.1×10^{-9} (132 pmol).[39]

Another fibre optic evanescent wave DNA sensor uses the same technology except that a hybridization indicator acts as the detection element.[34] In this device single-stranded probe DNA is immobilized onto a quartz optical fibre by synthesizing the oligonucleotide on a 5'-O-dimethoxytrityl-2'-deoxythmidine-modified optical fibre, by the solid-phase phoshphoramidite method. The target sequence is then free to hybridize to its immobilized complement and the resulting heteroduplex is detected with ethidium bromide. Ethidium

bromide acts as a hybridization indicator since it is a fluorescent compound which intercalates into the base stacking region and, in some cases the major groove of the DNA duplex. The reported detection limit for this prototype DNA sensor based on an oligo$(dT)_{20}$ probe and an oligo$(dA)_{20}$ target sequence is 1.3 fmole. The sensitivity of this device is limited by the association constant of ethidium bromide with DNA and due to the high background fluorescence produced by contaminants in biological samples.[40] This problem may be overcome by time-resolved fluorescence[31], using a lanthanide complex which selectively interacts with double-stranded DNA.

Another optical method for DNA detection is unique in the sense that it takes advantage of the electrochemiluminescence (ECL) of a labelled detection probe. In ECL, luminescence is measured from a compound whose active state is produced in an electrochemical cell.

This electrochemiluminescence-based DNA detection system has been applied to PCR product quantitation.[35] In order to capture the PCR product one of the primers for the PCR reaction is modified with biotin, so that it will bind to streptavidin coated magnetic beads. The captured PCR product is then denatured and hybridized to the detection probe. The detection probe is sequence-selective and will only hybridize to the exact complement under controlled conditions. The magnetic beads with the captured PCR product are injected into a flow-through electrochemical cell where a magnetic arm traps the beads at the working electrode surface. Hybridization between the detection probe and the denatured biotinylated PCR-amplified product will occur only if they are exactly complementary. The detection probe is labelled with the luminophore tris (2,2' bipyridine) ruthenium(II) (TBR). In this ECL

process both TBR and a reactant TPA (tripropylamine), are oxidized at the electrode surface. The oxidized TPA, which is added in the reaction buffer, is converted to an unstable highly reducing intermediate via deprotonation which can then react with oxidized TBR to produce the excited reduced state. This electrochemical reaction is depicted in Figure 1.4. The label TBR in its excited state then emits light at 620 nm which is detected in the flow cell opposite the working electrode surface.[35] Light is emitted only when the TBR label is present, ie. when there is exact complementarity between probe and target.

Another procedure has been developed in which two modified sequence selective DNA primers are used in the PCR reaction. A biotinylated primer is used for capturing the target DNA and a second primer is conjugated to TBR. Thus under specified PCR conditions amplification will only occur if exact complementarity exists between the primers and the target DNA. This procedure does not require a denaturation step after PCR for hybridization of the detection probe and is therefore faster than the previous protocol. However, this procedure can only be applied when the PCR step is very selective and reproducible.

Recently, another ECL-based DNA sensor was reported whereby single-stranded DNA was immobilized onto the surface of an aluminum(III) alkanebisphosphonate film coated onto a gold electrode.[41,42] The DNA was bound noncovalently through ionic interactions between the negatively charged DNA phosphate backbone and the positively charged Al(III) surface. This interaction leaves the bases free to form hydrogen bonds with their complementary bases. The hybridization event is detected by the hybridization indicator $Ru(phen)_3^{2+}$. $Ru(phen)_3^{2+}$ associates selectively with double-stranded DNA through ligand intercalation.[41] After immobilization of the probe sequence, hybridization to its complement

and association with $Ru(phen)_3^{2+}$, the potential of the electrode is scanned from 0 to 1.6 V vs a saturated calomel electrode (SCE) in the presence of TPA. The electrogenerated chemiluminescence occurs by the reaction between $Ru(phen)_3^{3+}$, produced at oxidizing potentials, and the highly reducing intermediate formed from the deprotonation of oxidized TPA. This produces a $Ru(phen)_3^{2+*}$ which emits light and can be detected by a single-photon -counting apparatus. The electrogenerated chemiluminescence is only detected when $Ru(phen)_3^{2+}$ is near the surface of the electrode, which occurs when $Ru(phen)_3^{2+}$ intercalates into surface bound double-stranded DNA. Thus the presence of target DNA is determined by the intensity of light emitted.

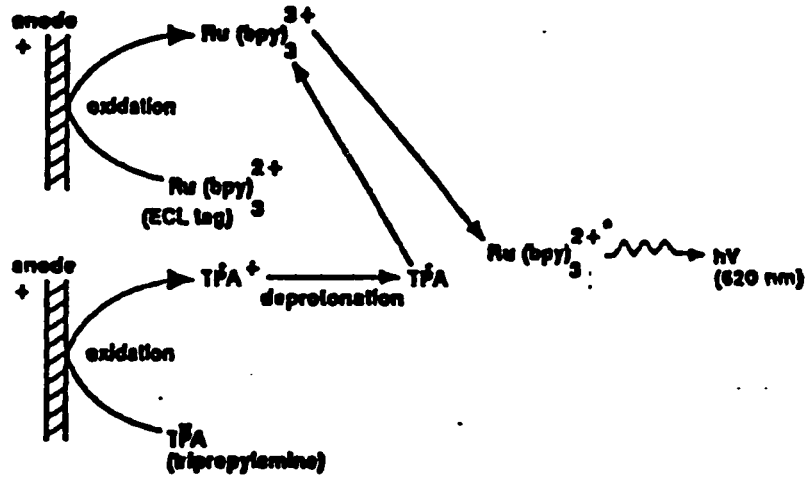

Figure 1.4: The ECL reaction. Figure taken from reference 35.

Electrochemical sensors are easy to work with since they are functional in turbid media, offer comparable instrumental sensitivity to other transducers, and can be miniaturized.[31] Electrochemical sensors are either potentiometric or amperometric. In potentiometry the current, i, is zero, and the potential, E, is a function of activity or concentration of analyte. If the activities for all but one species in a cell is known, the cell voltage can be related to the activity of the unknown species.[43].

pH is the most common measurement made in the chemistry laboratory[44]. The pH electrode is an ion-selective electrode composed of a thin membrane which separates the sample from an inner reference solution of the electrode. The reference solution contains the ion of interest at a constant activity. Outside the electrode is the sample of unknown activity. The pH electrode develops an electrical potential across the glass membrane that is proportional to the logarithm of the activity of the hydrogen ion in solution.[45] The classic potentiometric biosensor is a combination of a pH electrode with an immobilized enzyme. The enzyme confers selectivity, and catalyzes a reaction which produces a change in pH.

Kung et. al. have developed a rapid and reproducible method for quantifying total DNA concentrations using a pH electrode.[46] DNA is denatured and incubated at 37°C in the presence of three reagents: single-stranded DNA binding protein (SSB) conjugated with biotin, streptavidin, and an anti-DNA antibody labelled with the enzyme urease. The SSB protein strongly associates with single-stranded DNA, the biotin and streptavidin form a complex, and the Anti-DNA antibody binds to double-stranded DNA. The stable streptavidin-biotin-SSB-DNA-Ab-urease complex is captured onto a biotinylated nitrocellulose membrane since streptavidin possesses four biotin-binding sites. Since the urease activity is proportional

to DNA concentration, the hydrolysis of urea to ammonium and bicarbonate is detected through changes in pH using a light addressable potentiometric sensor (LAPS).

A similar system has also been used for the development of a sequence-selective DNA sensor.[37] This sensor has combined the LAPS with a sandwich type capture and detection system. A single-stranded capture probe is labelled with biotin, bound to streptavidin and then captured onto a nitrocellulose membrane modified with biotin. Complementary DNA hybridizes with the capture probe. The detection probe is labelled with fluorescein and is brought close to the membrane if hybridization occurs. The fluorescein label is then reacted with an anti-fluorescein-urease conjugate and the LAPS device is used to measure urease acitvity. Thus, the presence of the target sequence is determined by a change in pH.

Other electrochemical sensors have been developed which detect changes in current. These types of sensors measure current as a function of applied potential under conditions that polarize the working electrode. The current magnitude is related to the concentration of the analyte species at the electrode surface. These sensors are a subdivision of amperometric sensors called voltammetric biosensors.

Redox active compounds participate is electron transfer reactions with other compounds which can act as electron acceptors or donors, or with electrodes. When electrons are exchanged between an electrode and a redox-active species in solution, a current is produced which is related to the concentration of analyte species.

In voltammetry, current is measured as a function of applied potential, which is swept at a constant scan rate. For a nonadsorbed reversibly electroactive species the voltammetric peak current can be related to the concentration of the analyte by the Randles-Sevçik

equation:

$$i_p = (2.69 \times 10^3) n^{3/2} v^{1/2} A D^{1/2} C \quad (2)$$

where i_p is the peak current, n is the number of electrons, v is the scan rate, A is the surface area of the electrode, D is the diffusion coefficient of the electroactive species, C is its concentration, and the constant has been evaluated at 25 °C. A reversible electrochemical reaction possesses fast enough heterogenous kinetics to maintain an equilibrium between the concentrations of the reactant and product at the electrode surface as the applied potential of the electrode is varied, according to the Nernst equation.[43]

There are many voltammetric excitation signals. In linear scan voltammetry the applied potential is increased or decreased linearly through time at a constant scan rate and in cyclic voltammetry a triangular waveform is applied. In differential pulse voltammetry, pulses of constant amplitude are superimposed on a linear voltage ramp.

For voltammetric DNA sensors a standard three electrode cell is used with an amperometric working electrode, a reference and an auxillary electrode. The current is passed between the working and auxillary electrodes and the potential is applied between the working and reference electrodes. With this type of arrangement no current passes through the reference electrode and its potential remains constant.[47]

Cyclic voltammetry is used to study oxidation and reduction processes in various media, adsorption processes on surfaces, and electron-transfer reactions at modified electrode surfaces[47]. In cyclic voltammetry the potential is scanned in both directions. This gives rise to oxidation reactions when the applied potential is scanned in the positive direction, and

reductions when the applied potential is shifted in the negative direction. For a reversible electron transfer reaction the separation between anodic and cathodic peak potentials is given by equation 3.

$$E_{p,a}-E_{p,c}=2.22\frac{RT}{nF} \quad (3)$$

Where $E_{p,a}$ and $E_{p,c}$ are the anodic and cathodic peak potentials, respectively. Thus for a reversible, one electron transfer reaction at 25 °C the difference in peak potentials is 57 mV. The formal potential lies halfway between the two peak potentials. For an irreversible reaction the anodic and cathodic waves are drawn out, more separated, and are less well-defined.[47] For completely irreversible systems no peaks are observed.

Differential pulse voltammetry can be used to increase sensitivity. The enhanced sensitivity of pulsed methods is due mainly to an increase in faradaic currents, produced by charge transfer, and to a decrease in nonfaradaic or residual currents. Thus, the signal to noise ratio is greatly enhanced. Pulses of constant potential are superimposed onto a linear voltage ramp. Two current samples are taken, one before the pulse is applied, τ and one at a time late in the pulse, τ'. The result of a differential pulse experiment is a plot of current difference ($\delta i = i_{\tau'} - i_{\tau}$) versus base potential. The current difference is related to the concentration of analyte near the surface of the electrode by equations 4 and 5.[43]

$$(\partial i)_{max}=\frac{nFAD^{1/2}C}{\pi^{1/2}(\tau-\tau')^{1/2}}\times\frac{1-\sigma}{1+\sigma} \quad (4)$$

$$\sigma=\exp\frac{nF}{RT}\frac{\Delta E}{2} \quad (5)$$

For a more simplified approach to an electrochemical biosensor, chronoamperometry is used. In chronoamperometry the potential of the working electrode is held constant and current is measured as a function of time. The potential is switched to a potential beyond that where the analyte is electroactive and the limiting factor for electron transfer between analyte and electrode is the mass transfer of analyte to the electrode surface. The reduction or oxidation of the analyte at the surface of the electrode creates a concentration gradient. This causes a net flux of analyte to the surface which produces a current that is proportional to the concentration gradient between the electrode surface and the bulk solution. For a planar microelectrode the current is related to the concentration of the analyte in the bulk solution by the Cottrell equation (4):

$$i_t = i_d(t) = \frac{nFAD^{1/2}C}{\pi^{1/2}t^{1/2}} \qquad (6)$$

where i(t) is the current at time t, n is the number of electrons, F is Faraday's constant, A is the area of the electrode, D is the diffustion coefficient of the analyte, and C is concentration of analyte.

Three research groups have focused on a voltammetric means of detecting the presence of target DNA.[36, 38, 51, 52, 53, 54] The working electrodes have been glassy carbon (GCE), carbon paste (CPE), and gold. Oligonucleotide probes are immobilized at one end, and the sequence complementary to the target sequence is free to hybridize.

For voltammetric detection the analyte must be electroactive. Since DNA is electroinactive within the range of +1.2 to -0.9 mV vs. SCE, a redox-active indicator compound is used. The indicator is ideally electrochemically reversible within this range and

binds selectively to double-stranded DNA. These electroactive hybridization indicators can be either transition metal complexes or organic compounds. As shown in Figure 1.5, voltammetric peak currents expected for the indicator species are larger when double-stranded DNA is present on the working electrode surface, since this allows preconcentration of the indicator in the DNA layer. The development and testing of this type of DNA biosensor, using carbon electrode materials, is the subject of this thesis.

Tris(phenanthroline) and tris(bipyridine) transition metal complexes interact reversibly with double-stranded DNA through two distinct binding modes, electrostatic and intercalative. Photophysical studies of ruthenium polypyridine complexes suggest that electrostatic interactions occur between the positive transition metal polypyridine complex and the polyanionic sugar phosphate backbone in the minor groove of the double helix. The intercalative binding mode involves insertion of a planar aromatic ligand between the base pairs of the nucleic acid in an approximately perpendicular position to the double-helical axis, in the major groove. The intercalative binding mode may also have some electrostatic characteristics[48]. Two such polypyridine transition metal complexes, tris (1,10 phenantroline) cobalt (III) and tris (2.2' bipyridine) cobalt (III), have been used in this work as hybridization indicators for a sequence-selective DNA sensor.[38a,b,c] These complexes have reversible one-electron reductions with standard reduction potentials of 0.137 and 0.085 vs. SCE for the phenanthroline and bipyridine complexes respectively. In homogenous solutions these complexes interact with calf thymus DNA, with association constants and binding site sizes that have been determined electrochemically[49,50]. Through these studies it was determined that $Co(phen)_3^{3+}$ binds with $K= (2.6 \pm 0.4) \times 10^4\ M^{-1}$ with a binding site size of 5bp. The

analogous ruthenium complex binds mainly through intercalation. $Co(bpy)_3^{3+}$ binds with K= $(1.4 \pm 0.3) \times 10^4 M^{-1}$ and a binding site size of 3 base pairs. The bipyridyl ruthenium complex binds electrostatically.

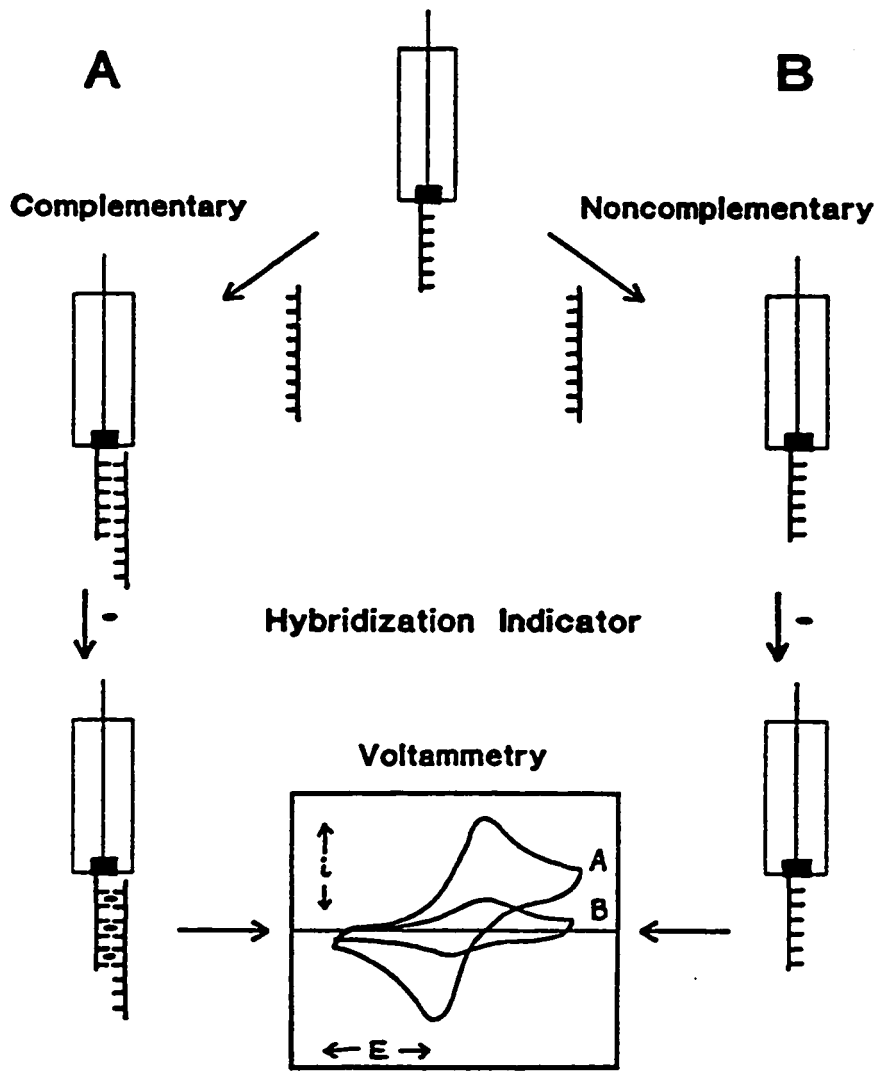

Figure 1.5 A schematic representation of a voltammetric DNA sensor.

In another voltammetric DNA sensor, developed during the course of this work, the design is essentially the same. Probe DNA, modified with a mercaptohexyl group, is immobilized onto a gold electrode surface by thiol chemisorption. The hybridization indicators used are organic dyes, such as Hoechst 33258, which are electroactive and bind preferentially to double-stranded DNA[36,51].

A modification of the DNA sensor based on immobilizing DNA onto GCEs and CPEs in conjunction with detection of hybridization with $Co(phen)_3^{3+}$ was recently developed. This sensor immobilizes ssDNA onto the surfaces of CPEs and GCEs via adsorption. The electrode is poised at a positive potential (1.7 V) followed by the adsorptive accumulation of DNA at a potential of +0.50 V. Hybridization with its complementary strand is then detected via the preconcentration of $Co(phen)_3^{3+}$ at the electrode surface. The method of detection is chronopotentiometry. The preconcentration of $Co(phen)_3^{3+}$ is determined by an increase in the chronopotentiometric peak. This method has been used for the detection of short DNA sequences related to the human immunodeficiency virus. The reported detection limit after a 30 minute hybridization is 4×10^{-9} M for the HIV-1 U5 LTR segment.[52] This method has also been applied with peptide nucleic acid (PNA) probes. PNAs are structural DNA analogues containing a N-(2-aminoethyl)-glycine-based pseudopeptide backbone. PNA probes hybridize to their target sequence at higher temperature, lower ionic strengths, with decreased hybridization times, and with greater specificity than DNA probes. A detection limit of 10 pmol following a 10 minute hybridization with a 15-mer target sequence was estimated.[53] Electrochemical adsorption of DNA onto microfabricated thick-film carbon electrodes has led to the present investigation of a thick-film electrochemical DNA sensor.[54]

Figure 1.6 summarizes and compares the results obtained for the DNA biosensors with reported detection limits.

Transducer	Immobilization Method	Probe DNA Length (base)	Target DNA Length (base)	Detection Method	Assay Time (min)	Detection Limit (Molar)
Potentiometric[46, 37]	Biotin-Streptavidin	20	114	Detection Probe	75	30 amol
Voltammetric (CPE)[38]	Covalent	18	4000	Hybridization Indicator	10	1.8 fmol
Voltammetric (CPE)[53]	Adsorption PNA probes	15	15	Hybridization Indicator	10	10 pmol
Voltammetric (Au)[36, 51]	Thiol Chemisorption	20	4200	Hybridization Indicator	60	0.1 amol
Electrogenerated Chemiluminescence[35]	Biotin-Streptavidin	20	110 1829	Detection Probe Hybridization Indicator	25	10 amol 200 amol
Surface Acoustic Wave [28]	Adsorption	4000	4000	Reagentless	180	1.5 fmol
Quartz Crystal Micro-Balance [27]	Thiol-Chemisorption	10	7249	Reagentless	60	10 fmol
Optical Fiber [33]	Covalent	16	16	Detection Probe	3	1 pmol
Optical Fiber [39]	Covalent	20	20	Hybridization Indicator	60	1.3 pmol
Optical Fiber [34]	Biotin-Streptavidin	16	16	Detection Probe	35	2 fmol
Surface Plasmon Resonance [31]	Adsorption	17	97	Reagentless	5	1 fmol

Figure 1.6 Comparison of DNA Biosensors.
[a]Values in parenthesis were calculated from reported detection limits, using a formula weight of 330 g/mol base.

1.4 Thesis Organization

This thesis summarizes research towards a voltammetric sequence-selective DNA biosensor that employs redox-active transition metal polypyridine complexes as hybridization indicators. In this biosensor single-stranded DNA is immobilized onto either glassy carbon electrodes or modified carbon paste electrodes. The transition metal polypyridine complexes bind selectively to double-stranded DNA over single-stranded DNA and produce a measurable electronic signal relative to this binding interaction. Larger voltammetric peak currents are obtained when double-stranded DNA is present at the electrode surface than single-stranded DNA.

Chapter 2 describes the experimental methods, which are common to the experiments reported in the later chapters.

Chapter 3 contains the results of research towards the development of a DNA sensor based on glassy carbon working electrodes (GCEs). It also covers the electrochemical characterization of a DNA-modified GCE and a prototype sequence-selective DNA sensor.

Chapter 4 includes the development of a sequence-selective nucleic acid biosensor based on modified carbon paste electrodes, optimization of the immobilization conditions, and a prototype carbon paste DNA sensor.

Chapter 5 includes optimization of hybridization conditions, hybridization kinetic studies and the determination of detection limits for target DNA.

Chapter 6 provides results of a cystic fibrosis biosensor selective for the ΔF508 deletion sequence which is associated with 70% of all cystic fibrosis illnesses. The development of this sensor includes the use of synthetic probes and target sequences followed

by actual human samples amplified by PCR.

Chapter 7 is concerned with determining the reactive site on the DNA molecule which is responsible for immobilization with the methods used.

Chapter 8 is a summary of the results presented in the previous chapters and provides suggestions for future work.

1.5 References

1. Landegren, U., Kaiser, R., Caskey, C.T., Hood, L., Science, 1988, 242, 229-236.

2. O'Brien, S. J.; *Nature New Biol.*, **1973**, 242, 52. (b) Bishop, J. O.; *Cell*, **1974**, 2, 81.

3. Ledley, F. D.; *Curr. Opin. Biotechnol.*, **1994, 5, 626.**

4. Boucher, R. C.; *Curr. Opin. Biotechnol.*, **1994**, 5, 639.

5. Matthews, J.A., Kricka, L. J., *Anal. Biochem.*, **1988**, 169, pp 1.

6. Remick, D. G.; Kunkel, S. L.; Holbrook, E. A.; Hanson, C. A.; Am. J. Clin. Pathol., 1990, S49

7. McPherson, M. J.; Quirke, P.; Taylor, G. R.; "PCR: A Practical Approach", Oxford University Press, New York, 1991, p. 17

8. Timmer, W. C.; Villalobos, J. M.; *J. Chem. Ed.*, **1990**, 70, 273.

9. Saiki, R. K., Walsh, P., S., Levenson, C. H., Erlich, H. A. Proc. Nat'l Acad. Sci. USA, **1989**, 86, 6230.

10. Conner, B. J.; Reyes, A. A.; Morin, C.; Itakura, K.; Teplitz, R. L.; Wallace, R. B.; Proc. Nat'l. Acad. Sci. USA, 1983, 80, 278.

11. Suzuki, D. T.; Griffith, A. J. F.; Miller, J. H.; Lewontin, R. C.; "An Introduction to Genetic Analysis", 3rd Ed.,

12. Southern, E.; Methods Enzymol., 1979, 68, 152-178

13. Baird, M.; Driscoll, C.; Schreiner, H.; Sciarratta, G.V.; Sansone, G.; Niazi, G.; Ramirez, F.; Bank, A.; Proc. Nat'l. Acad. Sci. USA, 1981, 78, 7, 4218.

14. Keller, G. H.; Huang, D. P.; Manak, M. M.; Anal. Biochem., 177,27, 1989

15. Khrapko, K.; Hanekamp, J. S.; Thilly, W. G.; Belenkii, A.; Foret, F.; Karger, B. L.; *Nucl. Acids Res.*, **1994**, 22, 3, 364.

16. Backman, K., Clin. Chem., 1992, 38, 3, 457.

17. Gryaznov, S. M.; Letsinger, R. L.; J. Am. Chem. Soc., 1993, 115, 3808.

18. Gryaznov, S. M.; Schultz, R.; Chaturvedi, S. K.; Letsinger, R. L.; Nucl. Acids Res., 1994, 22, 12.

19. Myers, R. M.; Larin, A.; Maniatis, T.; Science, 1985, 230, 1242.

20. Winter, E.; Yamamoto, F.; Almoguera, C.; Percuho, M.; Proc. Nat'l. Acad. Sci. USA, 1985, 82, 7575.

21. Shenk, T. E.; Rhodes, C.; Rigby, P. W.; Berg, P.; Proc. Nat'l. Acad. Sci. USA, 1975, 72, 3, 989.

22. Cotton, R. G. H.; Rodrigues, N. R.; Campbell, R. D.; Proc. Nat'l. Acad. Sci. USA, 1988, 85, 4397.

23. Ganguly, A.; Prockop D.J.; Nucl. Acids Res., 1990, 18, 13, 3933.

24. Millan, K. M.; Mikkelsen, S. R.; Anal. Chem., 1993, 65, 2317.

25. Grate, J. W.; Martin, S. J.; White, R. M.; Anal. Chem., 1993, 65, 21.

26. Fawcett, N.C.; Evans, J.A.; Chien, L.; Flowers, N.; Anal. Lett., 1988, 21, 7, 1099.

27. Okahata,Y.; Matsunobu, Y.; Ijiro, K.; Mukae, M.; Murakami, A.; and Makino, K.; J. Am. Chem. Soc., 1992, 114, 8299.

28. Su, H.; Kallury, K. M. R.; Thompson, M.; Anal. Chem., 1994, 66, 769.

29. Bondeson, K.; Frostell-Karlsson, A.; Fagerstam, L.; Mangusson, G.; Anal. Biochem., 1993, 214, 245.

30. Mandenius, C.F.; Chollet, A.; Mecklenburg, M.; Jundstrom, I.; Mosback, K.; Anal. Lett., 1989, 22, 2961.

31. Leech, D.; Chem. Soc. Rev., 1994, 205.

32. Bondeson, K.; Frostell-Karlsson, A.; Fagerstam, L.; Magnusson, G.; Anal. Biochem., 1993, 214, 245.

33. Graham, C. R.; Leslie, D.; Squirrell, D. J.; *Biosens. Bioelectron.*, 7, **1992**, 487-493.

34. Piunno, P.; Krull, A. E.; Urlich, J.; Hudson, R. H. E.; Damha, M. J.; Cohen, H.; *Anal. Chim. Acta*, **1994**, 288, 205.

35. DiCesare, J.; Grossman, B.; Katz, E.; Picozza, E.; Ragusa, R.; Woudenberg, T.; *BioTechniques*, **1993**, 15, 1, 152.

36. Hashimoto, K.; Ito, K.; Ishimori, Y.; *Anal. Chem.*, **1994**, 66, 3830.

37. Olson, J.D.; Panfili, P. R.; Zuk, R. F.; and Sheldon E. L.; *Mol. Cell. Probes*, **1991**, 5, 351.

38. (a) Millan, K. M.; Spurmanis, A. J.; Mikkelsen, S. R.; *Electroanalysis*, **1992**, 4, 929. (b) Millan, K. M.; Mikkelsen, S. R.; *Anal. Chem.*, **1993**, 65, 2317. (c) Millan, K. M.; Saraullo, A.; Mikkelsen, S. R.; *Anal. Chem.*, **1994**, 66, 2943.

39. Abel, A. P.; Weller, M. G.; Duveneck, G.L.; Ehrat, M.; Widmer, H. M.; *Anal. Chem.*, **1996**, 68, 17, 2905-2911.

40. Maniatis, T.; Fritsch, E. F.; and Sambrook, J.; (1982) "Molecular Cloning: A Laboratory Manual", **1982**, Cold Spring Harbor Laboratory, Cold Spring Harbor, NY., pp 468.

41. Xu, X-H., Yang, H. C.; Mallouk, T. E.; Bard, A. J.; *J. Am. Chem. Soc.*, **1994**, 116, 8386.

42. Xu, Xiao-Hong and Bard, Allen J., J. Am. Chem. Soc. 1995, 117, 2627-2631.

43. Bard, A. J.; Faulkner, L. R.; "Electrochemical Methods: Fundamentals and Applications", John Wiley & Sons, New York, 1980.

44. Turner, A. P. F.; Karube, I.; Wilson, G. S.; "Biosensors Fundamentals and Applications", Oxford Science Publications, 1987.

45. Harris, Daniel C.; "Quantitative Chemical Analysis", 2nd Edition, W. H. Freeman and Company, New York, 1987.

46. Kung, V. T.; Panfili, P. R.; Sheldon, E. L.; King, R. S.; Nagainis, P. A.; Gomez, B. Jr.; Ross, D. A.; Briggs, J.; Zuk, R. F.; *Anal. Biochem.*, **1990**, 187, 220.

47.Skoog, Douglas A.; Leary, James J.; "Principles of Instrumental Analysis" Fourth Edition, Saunders College

Publishing, 1992.

48. Pyle, A. M.; Rehmann, J. P.; Meshoyrer, R.; Kumar, C. V.; Barton, J. K.; *J. Am. Chem. Soc.*, **1989**, 111, 3051.

49. Carter, Michael T.; Bard, Allen J.; *J. Am. Chem. Soc.*, **1987**, 109, 7528.

50. Carter, M. T.; Rodriguez, M.; Bard, A. J.; *J. Am., Chem. Soc.*, **1989**, 111, 8901.

51. Hashimoto, K., Ito, K.; Ishimori, Y.; *Anal. Chim. Acta*, **1994**, 286, 219.

52. Wang, J.; Xiaohua, C.; Rivas, G.; Shiraishi, H.; Farias, P. A. M.; Dontha, N.; *Anal. Chem.*, **1996**, 68, 2629-2634.

53. Wang, J.; Palecek, Nielsen, P. E.; Rivas, G.; Cai, X.; Shiraishi, H.; Dontha, N.; Luo, D.; Farias, P. A. M.; *J. Am. Chem. Soc.*, **1996**, 118, 7667-7670.

54. Wang, J. Cai, X.; Tian, B.; Shiraishi, H.; *Analyst*, **1996**, 121, 965-969.

Chapter 2

Experimental

2.1 Materials and Instrumentation

(Dimethyaminomethyl)-ferrocene (DAF), ferrocenemonocarboxylic acid (FCA), and were obtained from Aldrich. Potassium dichromate ($K_2Cr_2O_7$) and 1-[3-(dimethylamino)propyl]-3-ethylcarbodiimide hydrochloride (EDC) were obtained from Aldrich or Sigma. Sulfo N-hydroxysuccinimide was obtained from Pierce or Fluka. Sodium chloride, mono- and dibasic potassium phosphate (Fisher), tris(hydroxymethyl)aminomethane (Tris, Sigma) and boric acid (Sigma) were of the best available quality. These chemicals were used as received from suppliers. Carbon powder, microcrystal gr. (graphite) was supplied by Johnson Matthey Electronics. Octadecylamine, stearic acid and potassium hexachloroosmate (IV) chloride were supplied by Aldrich. Acrylamide, N,N'-methylenebisacrylamide, urea, disodium ethylenediaminetetraacetate, bromophenol blue, and silver stain kits were also obtained from Bio Rad. Formamide and aminomethanamidine HCl were obtained from Sigma. HPLC grade acetonitrile was obtained from J T Baker, Anachemia, or Aldrich. Dimethylformamide, CD_3OD, CD_3OH, D_6 DMSO were obtained from Aldrich. 2',3',5'-Triacetylguanosine (TAG) was obtained from aldrich and NHS-fluorescein was obtained from Pierce. Deionized water was prepared by a Barnstead Type D4700 NANOpure™ Analytical Deionization System and was used in all solutions.

Tris(1,10-phenanthroline)cobalt(III) perchlorate and tris(2,2'-bipyridyl)cobalt(III) perchlorate were prepared as described by Dollimore and Gillard[1] using reagent grade

cobalt(II) chloride and bromine (Fisher), perchloric acid (Baker), and ligands 1,10 phenanthroline and 2,2' bipyridine (Aldrich). These complexes were recrystallized twice from water prior to use. Tris (2,2'bipyridine) osmium (II) chloride, $Os(bpy)_3^{2+}$ was prepared as described[2] using reagent grade potassium hexachloroosmate (IV) chloride and 2,2' bipyridine. The $Os(bpy)_3^{2+}$ was recrystalized from a minimum volume of 50% ethanol.

The daunomycin glucose oxidase conjugate (Daunomycin-GOx) was prepared by Fernando Battaglini as follows[3]; daunomycin (8 mg) and glucose oxidase (94 mg) were dissolved in 40 mL of 0.1 M potassium phosphate buffer, pH 7.0, 5 mL of this solution was saved as a control. To the remaining 35 mL were added 36 mg of sulfo-NHS and 0.6 g EDC. The reaction and control solutions were sealed with aluminum foil and incubated at 5 °C overnight. An Amicon microconcentrator (YM-30 cutoff filter) was used to concentrate the product mixture to 3.00 mL. This sample was applied to an 85 x 1.5 cm Sephadex G-15 column. When eluting with 0.1 M potassium phosphate buffer, pH 7.0, two distinct bands were observed, the first red-orange band containing the species of interest. The product was characterized using spectrophotometry to determine that the average number of daunomycin molecules bound to glucose oxidase was 4:1.[3]

Calf thymus DNA (Type 1, highly polymerized) was obtained from Sigma. Poly(dG)poly(dC), poly(dA)poly(dT), poly(dAdT), proteinase K (EC 3.4.21.14), terminal deoxynucleotidyl transferase (E.C. , type), sodium cacodylate buffer, DNA molecular weight markers, and 2' deoxyguanosine 5' triphosphate (dGTP) were obtained from Boehringer Mannheim and Sigma. DNA was purified[4] by incubation with 200 μg/mL proteinase K (Boehringer-Mannheim) for one hour at 50 °C, followed by phenol/chloroform extraction

until A_{260}/A_{280} values of between 1.6 and 1.8 were obtained.[2] Phenol:chloroform:isoamyl alcohol Ultrapure was obtained from Gibco BRL. Absorbance measurements were made using a Varian Cary 1 double-beam UV-visible spectrophotometer.

Oligo$(dT)_{20}$, oligo$(dA)_{20}$, oligo$(dG)_{20}$, and oligo$(dC)_{20}$, were prepared by the Department of Biology, Concordia University, using an Applied Biosystems 391 DNA synthesizer and standard β-cyanoethyl phosphoramidite coupling reactions. Oligo$(dT)_{18}$, oligo$(dA)_{18}$, poly(dA), and poly(dT) were obtained from Boehringer Mannheim or Sigma. The cystic fibrosis sequence (5' **GAA ACA CCA ATG ATA TTT 3'**) which is called probe 5916, its normal equivalent sequence (5' **GAA ACA CCA AAG ATG ATA** 3') called probe 5915 and their repsective complements were obtained from Queen's University DNA Synthesis Lab, referred to as oligo 6813 (5' **AAA TAT CAT TGG TGT TTC 3'**) and oligo 6814 (5' **TAT CAT CTT TGG TGT TTC** 3'), respectively.

The dG-elongated cystic fibrosis sequence (5' **GAA ACA CCA ATG ATA TTT GGG GGG GGG GGG GGG** 3') probe ΔF508M and the nonmutated sequences (5' **GAA ACA CCA AAG ATG ATA GGG GGG GGG GGG GGG** 3'), probe ΔF508NA, and (5' **CAC CAA AGA TGA TAT TTT GGG GGG GGG GGG GGG** 3'), probe ΔF508NB, with all their complementary sequences; (5' **AAA TAT CAT TGG TGT TTC** 3'), oligoΔF508M, (5' **TAT CAT CTT TGG TGT TTC** 3'), oligoΔF508NA, and (5' **AAA ATA TCA TCT TTG GTG** 3'), oligoΔF508NB were prepared in house by standard β-cyanoethyl phosphoramidite coupling reactions[5,6] on an Applied Biosystems 391 DNA synthesizer. Following synthesis, the diester oligonucleotides were cleaved from the controlled-pore-glass (CPG)[7] support by treatment with fresh, concentrated ammonium

hydroxide (Fisher) for one hour. The cyanoethyl protecting groups were removed from the bases by treatment with ammonium hydroxide at 55 °C for 8-15 hours. All reagents used for solid phase phosphoramidite DNA synthesis were obtained from Applied Biosystems. The probe ΔF508M was used to detect the ΔF508 deletion sequence and the probe ΔF508NB was used to detect the same region of DNA without the three-base deletion.

Glassy carbon working electrodes, carbon paste electrode holders, Ag/AgCl (3M NaCl) reference electrodes, and polishing materials were obtained from Bioanalytical Systems. Platinum wire auxiliary electrodes (0.5 mm diameter) were obtained from Fisher. A BAS100A potentiostat was used with a standard water-jacketed three-electrode cell at 25.0 ± 0.2 °C. Unless otherwise indicated, cyclic voltammetry was performed at 50 mV/s on 0.12 mM solutions of electroactive species prepared in 5 mM Tris buffer (pH 7.1) with 20 mM NaCl.

Electrophoresis was performed using gels cast in a Mini-Protean II cell (Bio Rad). Migration distances were measured with a Model FB910 densitometer (Fisher).

High performance liquid chromatography was performed using a Waters 510 HPLC pump with a Waters Lambda Max 481 LC spectrophotometric detector operated at 254 nm. The separation system was an Econosphere reversed phase C18 HPLC column (250 mm × 4.6 mm) with 5 μm particles. The number of theoretical plates for the column with phenol was 79510 and with Fraction 12 of the model compound (Chapter 7) it was 37251. NMR experiments were performed on a 500 MHz Varian NMR spectrometer at the Department of Chemistry at McGill University. Cellulose acetate syringe filters (0.2 μm, 25 mm) were obained from Baxter.

2.2 Methods

2.2.1 Generation of Functional Groups on the Surface of Electrodes.

2.2.1.1 *Glassy Carbon Electrodes*

Glassy carbon electrodes were polished with either 6μm and 1 μm diamond slurries or 0.3 μm and 0.05 μm alumina slurries, and sonicated in ethanol for approximately 5 minutes. Carboxylic acid groups were generated on the surface of glassy carbon electrodes (GCEs) by oxidization at +1.5 V for 15 s in an aqueous solution containing 2.5% $K_2Cr_2O_7$ and 10% HNO_3. This was followed by rinsing with deionized H_2O. Unmodified GCEs for control experiments were polished, sonicated, and oxidized as described above.

2.2.1.2 *Preparation of Carbon Paste Electrodes with Modifier.*

The carbon paste electrode was prepared by combining carbon powder (500 mg) and mineral oil (300 μL) in the presence of either octadecylamine or stearic acid modifier, using a mortar and pestle, varying the final quantity of modifier from 0.4 to 10% (w/w). The mixture was packed tightly into an electrode holder and polished to a smooth finish.

2.2.2 Immobilization of DNA.

2.2.2.1 *Coupling of DNA to Electrodes with 1-[3-(Dimethylamino)propyl]-3-ethylcarbodiimide Hydrochloride (EDC).*

The electrodes with surface functional groups were inverted and activated by evaporation to dryness of 50 μL of a solution containing 5 mM EDC in 0.020 M phosphate

buffer (pH 6.8). After rinsing, DNA was then coupled to the surface by evaporating to dryness 50 μL of 1 mg/mL DNA. In cases in which DNA was denatured prior to immobilization, the solutions were heated to 100 °C for more than 10 min. and then rapidly cooled to 0 °C. Electrodes modified by this procedure were rinsed and stored in 5 mM Tris buffer (pH 7.1) with 0.020 M NaCl at 4 °C.

2.2.2.2 *Coupling of DNA to Electrodes with EDC and N-Hydoxysulfosuccinimide (NHS).*

The electrodes were inverted and activated by evaporation to dryness of 50 μL of a solution containing 5 mM EDC and 8mM NHS in 0.020 M phosphate buffer (pH 6.8). After rinsing DNA was then coupled to the surface by evaporating to dryness 50 μL of 1 mg/mL DNA. DNA was denatured following the same procedure as given in Section 2.2.2.1. Electrodes were stored under the conditions described in the same section.

2.2.2.3 *Octadecylamine-Modified Carbon Paste Electrodes.*

DNA was immobilized onto the prepared octadecylamine-modified CPEs in a single step in which 100 μL of a solution of 0.10 M EDC and DNA or oligodeoxynucleotide in 0.010 M methylimidazole buffer, pH 8.2, was evaporated to dryness at room temperature. Modified CPEs were rinsed and stored in 5 mM Tris (pH 7.1) with 0.020 M NaCl at 4 °C.

2.2.3 Hybridization

2.2.3.1 *Hybridization of Synthetic Homopolymers.*

Hybridizations were performed at 25 °C by applying 50 μL of a 1 mg/mL solution of

target DNA in 0.020 M phosphate buffer (pH 6.8) to the surface of the single-stranded DNA-modified sensor for 15 min and then rinsing with 5 mM Tris buffer (pH 7.1) with 0.020 M NaCl.

For hybridization reactions studied by in situ voltammetry, the DNA sensor was immersed in a solution containing 60 μM of hybridization indicator in 5 mM Tris (pH 7.1) with 0.020 M NaCl at 25 °C. At time t = 0, an aliquot of a solution of DNA possessing a sequence complementary to the immobilized DNA was added. Magnetic stirring was continued throughout the experiment except during a voltammetric scan.

Hybridizations were also performed at high ionic strength in a solution containing 0.5 M NaCl and the complementary DNA sequence at different concentrations. Sensors were periodically removed from this solution, rinsed and placed in 60 μM hybridization indicator, 0.020 M NaCl, 5 mM Tris (pH 7.1) for the voltammeteric scans. The sensors were then rinsed and returned to the high ionic strength hybridization solution.

More stringent conditions were required for the selective hybridization of the cystic fibrosis target sequence. A 25 μL drop of analyte DNA was added to the surface of the inverted sensor and the incubation temperature was varied during hybridization.

2.2.3.2 *Hybridizations with the Synthetic Cystic Fibrosis Probe and Target.*

Hybridizations were performed at 43 °C by applying 50 μL of target DNA with varying concentrations in 5 mM Tris buffer (pH 7.1) with 0.50 M NaCl to the surface of the electrode for 30 minutes. To prevent evaporation to dryness, a solution of 5 mM Tris (pH 7.1) and 0.50 M NaCl was applied to the electrode surface periodically during hybridization.

2.2.3.3 *Hybridizations with the Cystic Fibrosis Probe and the PCR-Amplified Cystic Fibrosis Gene Product.*

PCR-amplified DNA containing the region in which the cystic fibrosis ΔF508 deletion occurs was provided by Dr. Rima Rosen of the Molecular Genetics Unit of the Montreal Children's Hospital. PCR of human genomic DNA samples was performed using standard Conditions.[8,9,10] The two PCR primers, GH352 and GH353 were based on the sequence of exon 10 in the CFTR cDNA. GH352 is located at postion 1524-1545 in the positive strand and has the sequence 5'-GACTTCACTTCTAATG-3'. GH352 is located at position 1696-1715 in the negative strand and has the sequence 5'-TCTTCTAGTTGGCATGCTTT-3'). The PCR-product (10 μL) was diluted with 200 μL of hybridization buffer [5 mM Tris buffer (pH 7.1) containing 0.50 M NaCl]. The diluted target DNA was denatured by heating to 100 °C for 15 min. The probe-immobilized GCE was submerged in the solution containing the target sequence and hybridizations were performed at 43 °C for 20 minutes. The sensor was then rinsed with hybridization buffer and analyzed in 1.2×10^{-4} M $Co(bpy)_3(ClO_4)_3$ in 5 mM Tris (pH 7.1) with 0.020 mM NaCl.

2.2.4 Denaturation of Immobilized Target DNA.

For GCEs denaturation of double-stranded DNA (dsDNA) was achieved by rinsing the sensor in hot (95 °C to 100 °C) deionized water for 10 - 30 minutes. With CPEs denaturation of dsDNA on the surface of the electrode was attempted by rinsing in hot deionized water at varying temperatures, by rinsing in various denaturants, such as 7-8 M

urea, 8M formamide, 8M guandinium HCl.[2]

2.2.5 Catalytic Elongation of Oligo$(dT)_{20}$ with Deoxyguanosine Residues.

Terminal dexoynucleotidyl transferase catalyzes the addition of deoxynucleotide residues to the 3'-end of DNA.[11] Oligo$(dT)_{18}$ (330 μg) was incubated with a 1000 fold or 100 fold molar excess of dGTP and terminal dexynucleotidyl transferase (250 units total, in aliquots of 50 units each at 0, 4, and 8, and 100 units at 12 hours) in 500 μL of sodium cacodylate buffer at 37 °C for 24 h as recommended by Boehringer. Products were purified by phenol/chloroform extraction, precipitated with ethanol and reconstituted to 1 mg/mL phosphate buffer.

2.2.6 Polyacrylamide Gel Electrophoresis

Polyacrylamide gels (% T=8.3, % C= 3.3) were cast and run in TBE buffer (0.134 M Tris, 0.081 M H_3BO_3, 0.0026 M EDTA, pH 8.8) containing 8M urea.[12] Separations of 2.5 μL of 1 mg/mL solutions of the purified terminal transferase reaction product and denatured DNA molecular weight markers were carried out at 100 V for 90 min. Purity of the synthetic nucleotides was determined by polyacrylamide electrophoresis, as described above. Visualization of the separated fragments was accomplished by silver staining, according to the protocol recommended by Bio Rad.

2.2.7 Cyclic Voltammetry of DNA-modified Electrodes

Cyclic voltammograms were run at 25 °C and 0.050 V/s on solutions containing

various concentrations of $Co(bpy)_3^{3+}$, $Co(phen)_3^{3+}$, FCA, and DAF, in 5 mM Tris buffer (pH 7.1) with either 0.020 M or 0.050 M NaCl. Scan rate experiments and peak current experiments were performed varying the scan rate between 0.010 V/s and 0.500 V/s on solutions containing 1.2×10^{-4} M of the electroactive species. Voltammetric titrations were performed at a scan rate of 0.050 V/s on solutions containing concentrations of complexes up to 4.0×10^{-4} M. For the cobalt complexes the potential was scanned from 0.500 V to -0.200 V, while for the ferrocene complexes (DAF and FCA), the potential was scanned from -0.200 V to 0.500 V. For $Os(bpy)_3^{2+}$ the potential was scanned from -0.200 to 0.900 V. The average of peak current and potential values of 5 scans were taken for both cathodic and anodic peaks.

2.2.8 Differential Pulse Voltammetry of DNA-modified GCEs

Glassy carbon electrodes were modified with denatured poly(dG)poly(dC) and examined by differential pulse voltammetry in solutions containing 1.2×10^{-4} M $Co(bpy)_3^{3+}$ in Tris buffer (pH 7.1) 0.020 M NaCl. Conditions for differential pulse voltammetry were as follows: the potential was scanned from 0.500 V to -0.200 V at a scan rate of 0.020 V/s. The pulse amplitude was varied from 0.050 V to 0.200 V in order to optimize the change in peak current between the unmodified electrode and the poly(dG)poly(dC)-modified electrode.

2.2.9 Chronoamperometry of DNA-modified GCEs

Unmodified GCEs and poly(dG)poly(dC)-modified GCEs were examined by chronoamperometry in solutions containing 1.2×10^{-4} M $Co(bpy)_3^{3+}$ in Tris buffer (pH 7.1)

0.020 M NaCl. The potential was stepped from 0.500 V to -0.200 V at t = 0, and current values were recorded every 12.5 ms for 0.250 s. Current values from blank solutions containing 5 mM Tris pH 7.1 0.020 M NaCl were subtracted from those obtained with solutions containing 1.2×10^{-4} M $Co(bpy)_3^{3+}$, 5 mM Tris pH 7.1 and 0.020 M NaCl. The corrected current values for unmodified and poly(dG)poly(dC)-modified GCEs were compared to determine the percent increase in signal between modified and unmodified GCEs.

2.2.10 Detection of DNA at the Surface of an Electrode with the Daunomycin-Glucose Oxidase (Daunomycin-GOx) Conjugate.

A 50 μL solution of 2.75 μM daunomycin-GOx conjugate was added to the surface of both the unmodified and poly(dG)poly(dC)-modified SACPEs and incubated for 10 minutes to allow for adsorption or intercalation. The electrode was then rinsed in potassium phosphate buffer (pH 7.1). The electrode was then placed in an electrochemical cell containing 0.05 mM ferrocene carboxylic acid (FCA) and 20.00 mM glucose. The potential was scanned at 5 mV/s from 0 mV to 650 mV.

2.2.11 Model Compound studies

2.2.11.1 The Reaction Between NHS-fluorescein and 2',3', 5' Triacetylguanosine with HPLC Pufification.

To a solution of NHS-fluorescein (0.050 g) in 1 mL of dimethylformamide (DMF) was added 2',3',5'-triacetylguanosine (0.010 g) and the reaction was allowed to proceed at

room temperature for 24 hours with constant stirring. DMF was removed by vacuum distillation. The reaction product(s) were redissolved in 40% (v/v) acetonitrile/water and filtered through a 0.2 μm filter, and purified by reversed phase isocratic HPLC with a 40% (v/v) acetonitrile/water on a phenyl column with a flow rate of 1.2 mL/min. Further separation was required to ensure purity of the separated products. Products which were fluorescent were further purified by reversed-phase HPLC with a 20 % (v/v), on the same phenyl column with a flow rate of 1.2 mL/min. The separated products were further purified by reversed-phase HPLC with a 10% (v/v) ACN:H2O on a C18 column with a flow rate of 0.5 mL/min. Reactants and products were detected by a UV/Vis detector at λ= 256 nm or λ = 490. TLC on silica plates with ethyl acetate was performed on the collected fractions to determine their purity.NMR experiments were performed on a 500 MHz Varian NMR spectrometer at the Department of Chemistry at McGill University.

2.2.11.2 The Reaction Between NHS-fluorescein and 2',3',5' triacetylguanosine with a crude purification of products by precipitation.

NHS-fluorescein and 2',3', 5' triaceytlguanosine were reacted as above and purified by precipitation with H_2O. The products were separated by filtration. The precipitate and supernatant were collected, dried by vacuum filtration, and dissolved in D_6DMSO. NMR experiments were performed on a 200 MHz Varian NMR spectrometer at the Department of Chemistry and Biochemistry at Concordia University.

2.2.11.3 The Reaction Between fluorescein and 2' Deoxyguanosine 5' triphosphate with a Crude Purification of Products by Precipitation

Fluorescein (0.1 g) was reacted with a 0.1 g of EDC and 0.2 g sulfo-NHS in distilled H_2O. A precipitate formed and the solution was centrifuged. The supernatant was discarded the precipitate was redissolved in dimethylformamide (DMF). This solution of the activated fluorescein was then reacted with 2' deoxyguanosine 5' triphosphate (10 mg). The product was then precipitated with H_2O and the supernatant and precipitate were isolated by centrifugation and then removing the supernatant. Solvent was removed from the supernatant and precipitate by vacuum filtration. The supernatant and precipitate were then redissolved in D_6DMSO. NMR experiments were performed on a 200 MHz Varian NMR spectrometer at the Department of Chemistry and Biochemistry at Concordia University by Dr. Colebrook.

2.11 References

1. Dollimore, L. S.; Gillard, R. D.; *J. Chem. Soc., Dalton Trans.*, **1973**, 933.

2. Creutz, C.; Chou, M.; Netzel, T. L.; Okhumura, M.; Sutin, N.; J. Am. Chem. Soc., **1980**,102, 1309.

3. Kolakowski, B.; Battaglini, F.; Lee, Y. S.; Kliromonos, G.; Mikkelsen, S. R.; Anal. Chem., 1996, 68, 1197.

4. Keller, G. H.; Manak, M. M.; "DNA Probes", Macmillan: New York, **1989**, pp 1-23.

5. Beaucage, S. L.; Caruthers, M. H.; *Tet. Lett. 22*, **1981**, 1859.

6. Beaucage, S. L.; Caruthers, M. H.; *United States Patent*, # 4,668,777, **1981**.

7. Adams, S. P.; Kavka, K. s.; Wykes, E. J.; Holder, S. B.; and Galluppi, G. R.; J. Am. Chem. Soc., 1983, 105, 661.

8. Rozen, R.; Schwartz, R. H.; Hilman, B. C.; Stanislovitis, P.; Horn, G. T.; Klinger, K.; Daigneault, J.; De Braekeleer, M.; Kerem, B.; Tsiu, L.; Fujiwara, T. M.; Morgan, K.; *Am J. Hum. Genet.*, **1990**, 47, 606-610.

9. Kerem, B.; Rommens, J. M.; Buchanan, J. A.; Markiewicz, D.; Cox, T. K.; Chakravarti, A.; Buchwald, M.; Tsui, L.; Science, 1989, 245, 1073-1079.

10. Klinger, K.; Horn, G. T.; Stanislovitis, P.; Schwartz, R. H.; Fujiwata, T. M.; Morgan, K.; Am. J. Hum. Genet., 1990,46, 983-987.

11. Deng, G.; Wu, R.; Methods Enzymol., 1983, 100, 96.

12. Sambrook, J.; Fritsch, E. F.; Maniatis, T.; "Molecular Cloning A Laboratory Manual" Second Edition, 1989, Cold Spring Harbor laboratory Press, pp. 11.23-11.28.

Chapter 3

DNA Biosensors Based on Glassy Carbon Electrodes

3.1 Introduction

The focus of this chapter is the investigation of a method for the covalent binding of single-stranded DNA (ssDNA) onto the surface of glassy carbon electrodes (GCEs), followed by hybridization with its complement and detection.[1,2] Immobilization must therefore not interfere with the capacity for the surface-bound DNA to hybridize.

Detection of the target DNA occurs voltammetrically through an electroactive hybridization indicator. DNA is electroinactive within the range of +1.2 to -0.9 mV vs. SCE[2]. Therefore a redox-active compound which is electrochemically active within this potential window can act as a hybridization indicator. There are four other characteristics which are useful for a hybridization indicator. First, binding of the indicator must be different for double-stranded (dsDNA) than for ssDNA, since the presence of the target sequence is determined by the formation of dsDNA at the surface of a transducer. A large association constant and small binding site size with dsDNA are preferred for high sensitivity and low detection limits. Finally, reversible electrochemistry is preferred since electrochemical methods are at their maximum sensitivity for reversible redox systems.[3]

For our studies with GCEs two transition metal complexes have been employed as hybridization indicators; tris(2,2' bipyridyl)cobalt(III)perchlorate, $Co(bpy)_3^{3+}$, and tris(1,10-phenanthroline)cobalt(III)perchlorate, $Co(phen)_3^{3+}$. The standard reduction potentials of $Co(bpy)_3^{3+}$ and $Co(phen)_3^{3+}$ are 0.085 V and 0.137 V vs SCE, respectively.[4] These standard

reduction potentials are well within the range where DNA is electroinactive. The separation of anodic and cathodic peak potentials, $\Delta Ep = 66$ mV for $Co(bpy)_3^{3+}$ and $\Delta Ep = 67$ mV for $Co(phen)_3^{3+}$ at a glassy carbon electrode indicate a quasireversible, one electron redox process.[4] At the surface of the electrode the presence of dsDNA causes the preconcentration of these hybridization indicators near the surface of the electrode, and this is detected by an increase in voltammetric peak current.[1,2]

$Co(bpy)_3^{3+}$ and $Co(phen)_3^{3+}$ are members of a class of compounds referred to as the transition metal polypyridine complexes. These complexes can interact reversibly with dsDNA in surface binding and/or intercalative modes[5,6]. In studies with mixed-ligand phenanthroline and bipyridine complexes of ruthenium(II) it was demonstrated by biophysical and spectroscopic methods that the surface-binding mode consists of the positively charged complex selectively residing in the minor groove of dsDNA. Tris (2,2' bipyridyl)ruthenium (II) binds electrostatically in the minor groove of dsDNA.[7] The intercalative binding mode of phenanthroline complexes involves π-stacking interactions. One of the complex's ligands is inserted between the base pairs of the nucleic acid. This binding mode is hydrophobic in nature and is selective for the major groove of dsDNA. Barton has demonstrated that tris-chelated transition metal complexes with phenanthroline ligands intercalate into the DNA helix but only the outer third of the phenanthroline ligand is available for π-stacking.[7] Thus only partial ligand insertion is possible, while the other two ancillary ligands rest near the surface of the major groove. This allows for electrostatic interactions between the charged metal core and the polyanionic sugar-phosphate backbone of the DNA helix. Selectivity for dsDNA is augmented by the π-stacking interactions for the phenanthroline complex, but both

modes are selective for dsDNA because of their groove binding sites.

The association constants of many transition metal polypyridine complexes have been measured by equilibrium dialysis[7], and spectroscopic[7] and voltammetric titrations[8]. Table 2.1 gives a list of relevant transition metal complexes, their DNA-association constants, and the method used to determine these values. The biophysical and spectroscopic studies on the ruthenium complexes illustrates the importance of the ligand on binding to DNA. The transition metal at the core of the complex produces a rigid well-defined structure of coordinated ligands[7].

Table 3.1 Association Constants for DNA-binding transition metal complexes.

Transition Metal Polypyridine Complex	**K_a x 10^3 (M^{-1}) Equilibrium Dialysis[7]**	**K_a x10^3 (M^{-1}) Absorption Titration[7]**	**K_a x 10^3 (M^{-1}) Voltammetric Titration[8]**
$Ru(bpy)_3^{2+}$	0.70 ± 0.13	----------	----------
$Ru(phen)_3^{2+}$	3.1 ± 0.1	5.50 ± 0.99	----------
$Fe(bpy)_3^{2+}$	----------	----------	1.4 ± 0.1 *
$Fe(phen)_3^{2+}$	----------	----------	14.70 ± 0.04
$Co(bpy)_3^{3+}$	----------	----------	14 ± 3
$Co(phen)_3^{3+}$	----------	----------	26 ± 4

*. The value of K_a for $Fe(bpy)_3^{3+}$ was obtained at 10 mM NaCl whereas all other voltammetric titrations were performed at 50 mM.

Voltammetric titrations involve measurements of peak current to determine the

concentrations of the free and bound forms of the complex. For a reversible redox couple, in the absence of specific adsorption, the peak current, i_p, is related to the apparent diffusion coefficient of the analyte, D_{app}, by the Randles-Sevcik equation:

$$i_p = (2.69 \times 10^5) n^{3/2} A v^{1/2} D_{app}^{1/2} C \qquad (1)$$

where n is the number of electrons involved in the half reaction, A is the area of the surface of the electrode, v is the potential scan rate, and C is the total concentration of analyte in the bulk solution. For a voltammetric titration of a DNA-binding complex with DNA a decrease in peak current will be observed as the DNA concentration is increased. This is due to the diffusion coefficient of the bound complex being much smaller than that of the free complex.

The apparent diffusion coefficient is related to the concentrations of both the free and bound forms of the complex, C_f and C_b, respectively. The equation relating these two parameters depends upon the model chosen for the binding kinetics. Equation 2 represents the relationship for the limit of fast binding kinetics:

$$D_{app}^{1/2} = (X_f D_f + X_b D_b)^{1/2} \qquad (2)$$

where X_f, X_b, are the mole fractions of the DNA-binding complex in the free and bound forms, respectively, and D_f and D_b are the diffusion coefficients for the free and bound forms, respectively. In this model, the mobile model, equilibration between the free and bound forms occurs at a faster rate than the faradaic reaction. In the static model, given by equation 3 equilibration does not occur during the time course of the voltammetric scan. The bound complex remains bound and the free complex stays free within the time frame of the

voltammetric experiment.

$$D_{app}^{1/2} = (X_f D_f^{1/2} + X_b D_b^{1/2}) \quad (3)$$

Equations 2 or 3 can be used to determine the free and bound concentrations of analyte from peak current values. Electrostatic association reactions are expected to occur rapidly with respect to the voltammetric time frame and therefore the mobile model can be assumed, at least for $Co(bpy)_3^{3+}$.

The values of D_f and D_b are determined by cyclic voltammetry (CV) experiments in which the ratio of DNA to analyte is varied by titrating a constant concentration of analyte with DNA. When the ratio of DNA:analyte is zero, the value of D_f is obtained through a plot of i_p vs. $v^{1/2}$ using the Randles-Sevcik equation (eq. 1). With DNA concentrations in large excess over analyte, a limiting value of D_{app}, D_b is determined[8]. The total current at any DNA to analyte ratio is

$$i_{p,c} = BC_t (D_f X_f + D_b X_b)^{1/2} \quad (4) \text{ mobile model}$$

$$i_{p,c} = B(D_f^{1/2} C_f + D_b^{1/2} X_b) \quad (5) \text{ static model}$$

where $B = 2.69 \times 10^5 n^{3/2} A v^{1/2}$, for reversible electrochemistry. The reaction governing the binding of the complex to DNA is given by equation 6:

$$ML_x^{n+} + BS \rightleftharpoons ML_x^{n+}\text{-}BS \qquad (6)$$

where ML_x^{n+} is the transition metal DNA-binding complex, BS is the DNA binding site, and ML_x^{n+}-BS is the DNA with its bound complex. The number of binding sites available is equal to the total concentration of base pairs divided by the binding site size in base pairs, n_s, for DNA saturated with analyte.

$$Number\ of\ Sites = \frac{[BP]_{total}}{n_s} \qquad (7)$$

In the simplest model, the association constant K of the DNA-binding complex with DNA can be obtained from equation 8.

$$K = \frac{C_b n_s}{C_f [BP]_f} \qquad (8)$$

where C_f and C_b are the concentrations of the free and bound complex, respectively, and $[BP]_f$ is the concentration of free (unoccupied) base pairs.

Using either the static or mobile model for D_{app}, equations 2 or 3, and determining the diffusion coefficients of the free and bound forms, the concentrations of free and bound analyte can be determined. Association constants and binding site sizes can be estimated by either fitting the voltammetric titration data to a Scatchard plot that assumes the simple equilibrium of equation 6, or to the McGee-von Hippel model.

For estimating DNA-complex interactions the data should be fit to the McGee-von Hippel equation 9:

$$\frac{r}{C_f} = K(1-nr)\frac{(1-nr)}{1-(n-r)r}^{(n-1)} \quad (9)$$

where

$$r = \frac{C_b}{[BP]_{tot}} \quad (10)$$

where K is the association constant for the DNA-complex interaction, $[BP]_{total}$ is the total concentration of DNA base pairs present, and n is the length of the binding site in base pairs. The McGee-von Hippel model is preferred for DNA-complex interactions since it takes into consideration that along the DNA lattice there may be overlapping potential binding sites at high DNA: complex ratios. It also accounts for incomplete saturation of the DNA with complex due to the size of the binding site.[9]

Bard et. al. performed a voltammetric titration of DNA-binding complexes with calf thymus DNA. The data were fit to a Scatchard plot to determine K_a and n, the DNA-binding constant and binding site size, respectively. The Scatchard plot is defined by equation 11:

$$\frac{r}{C_f} = K(1-nr) \quad (11)$$

where the variables have been defined in equations 9 and 10. Plotting r/C_f vs r results in a curved Scatchard plot with the slope equal to -K and n given by the x-intercept. Using this

method K and n were determined for $Co(phen)_3^{3+}$ and $Co(bpy)_3^{3+}$ in 50 mM NaCl. For $Co(phen)_3^{3+}$ K= 2.6 ± 0.4 x 10^4 M^{-1} and n= 5bp, for $Co(bpy)_3^{3+}$ K= 1.4 ± 0.3 x $10^4 M^{-1}$ and n= 3 bp, assuming the mobile model. The best fit curves were observed for the mobile equilibrium limit. Thus the mobile model best represents the binding interaction of these complexes to DNA.

In addition to changes in peak current amplitude, changes in formal potential of the redox couple are observed upon association with dsDNA. Carter et. al[8] adapted the Nernst equation for use with the equilibrium DNA-binding constants for each oxidation state for electroactive DNA-binding complexes. Equation 12 correlates the change in formal potentials for the free and DNA-bound species with the equilibrium constants for binding of the reduced and oxidized complex, assuming one discrete binding site.

$$E_{b^{o\prime}} - E_{f^{o\prime}} = 0.059 \log \frac{K_{2+}}{K_{3+}} \qquad (12)$$

A positive shift of 17 mV for the formal potential of $Co(phen)_3^{3+}$ upon addition of DNA indicates that the 2+ form is bound 1.9 times more strongly to DNA than the 3+ ion. This is consistent with a hydrophobic association between $Co(phen)_3^{3+}$ and dsDNA. $Co(bpy)_3^{3+}$ demonstrates a negative shift of -14 mV. This indicates that the 3+ ion is more strongly bound. This suggests electrostatic binding of $Co(bpy)_3^{3+}$ to the polyanionic DNA backbone. This study is in agreement with spectroscopic studies of the binding modes of ruthenium bipyridine and phenanthroline complexes with DNA.[7]

In addition to examining changes in formal potential, electrochemical characterization can include determining changes in the separation between anodic and cathodic peaks, ΔE_p.

Increases in peak separation with increasing scan rate may be the result of either IR drop or slow electron transfer kinetics. Standard rate constants for heterogenous electron transfer can be calculated from ΔE_p provided that IR drop is compensated for.

The development of a sequence-selective DNA biosensor begins with the investigation of a method for the covalent immobilization of DNA onto a glassy carbon electrode. Two methods have been used. Both involve the oxidation of a GCE to generate carboxylic acid groups on the surface. The carboxylic acid groups are then coupled to DNA using either a water soluble carbodiimide in the absence or presence of sulfo-N-hydroxysuccinimide (NHS). The coupling reagent 1-ethyl-3-(3-dimethylaminopropyl)carbodiimide hydrochloride (EDC) has been used to immobilize proteins[10]. EDC reacts with carboxylic acid groups and forms an *o*-acylisourea intermediate. The *O*-acylisourea is prone to nucleophilic attack, such as by groups such as primary amines found in proteins. This reaction produces an amide bond between the protein and the compound containing a carboxylate group. The *O*-acylisourea is unstable in aqueous solutions and is susceptible to hydrolysis, which regenerates the carboxylic acid and releases an N-substituted urea. The addition of NHS results in a more stable intermediate, an NHS ester. This ester is less susceptible to hydrolysis and is therefore useful in a two-step conjugation procedure[11]. Figure 3.1 shows a schematic for the immobilization of DNA onto GCEs using EDC and EDC/NHS as coupling reagents.

Covalent immobilizations using these two methods were attempted with various synthetic DNA sequences. DNA-modified electrodes were then characterized by cyclic voltammetry using four electroactive species, $Co(bpy)_3^{3+}$, $Co(phen)_3^{3+}$, dimethyaminomethyl ferrocene (DAF), and ferrocene carboxylic acid (FCA). The ferrocene derivatives were used

to examine electrostatic effects, since at neutral pH, DAF has a single positive, and FCA a single negative charge.

Phosphate buffers containing potassium and lithium counterions were examined for the immobilization procedure. K_3PO_4 and Li_3PO_4 were chosen on the basis of their abilities to promote the formation of G4-DNA.[13-15] G4-DNA is a term used to describe a stable highly ordered DNA structure formed from the self-association of guanosine nucleosides via Hoogsteen base pairing. The association of four parallel strands of DNA, each containing a minimum of three contiguous guanosine residues is dependent on the alkali metal cation present. The G4-DNA has a crown ether-like size selectivity for the binding of cations. The larger alkali metal potassium is the most effective in promoting the formation of G4-DNA, whereas the smaller lithium, is the least effective. Included in the family of highly ordered structures resulting from dG association are four-stranded intramolecular fold-back structures, and dimer foldback structures. Figure 3.2 shows a model structure of a Hoogsteen hydrogen-bonded guanine tetrad. The formation of G4-DNA may influence the immobilization through conformational changes with the DNA and by blocking a possible reactive site on the deoxyguanosine base.

A model 20-base ssDNA probe, oligothymidylic acid ($oligo(dT)_{20}$) was used as a probe sequence for the construction of a prototype DNA biosensor for the detection of $oligo(dA)_{20}$ and poly(dA). Hybridization and denaturation of this immobilized model probe were detected voltammetrically using $Co(bpy)_3^{3+}$. Attempts were made to hybridize this probe to noncomplementary sequences to study interferences.

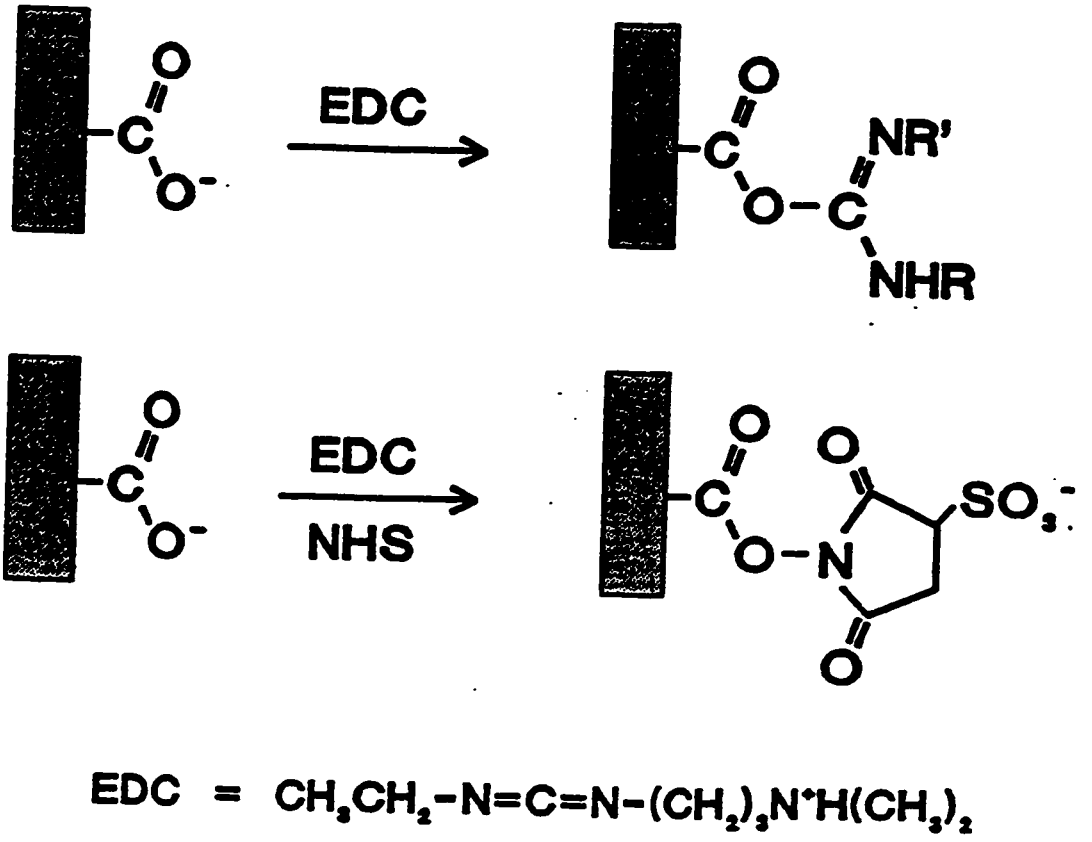

EDC = $CH_3CH_2-N=C=N-(CH_2)_3N^+H(CH_3)_2$

Figure 3.1 A scheme for the immobilization of DNA onto GCEs (a) using EDC and (b) EDC and NHS as coupling reagents.

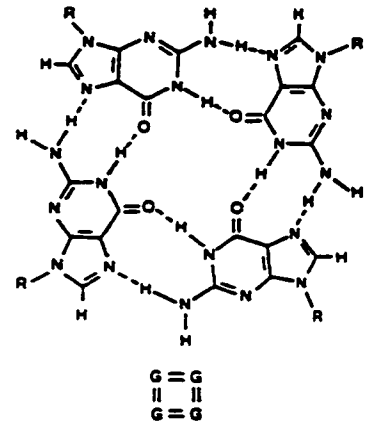

Figure 3.2 Model structure of a Hoogsteen hydrogen-bonded guanine.

To optimize the sensitivity of the sensors three different techniques were compared, differential pulse voltammetry (DPV), cyclic voltammetry (CV), and chronoamperometry (CA) with immobilized poly(dG)-poly(dC).

3.2 Results

3.2.1 Covalent Immobilization of DNA onto GCEs

3.2.1.1 A Water Soluble Carbodiimide as a Coupling reagent

GCEs were modified with DNA using EDC as a coupling reagent as described in section 2.2.2.1. Attempts were made to modify GCEs with native (double-stranded) and

denatured (single-stranded) calf-thymus DNA (42% GC content). Typical cyclic voltammograms obtained at a DNA-modified and an unmodified GCE are compared for $Co(bpy)_3^{3+}$ in Figure 3.3. The increase in peak current for the DNA-modified GCE indicates the presence of dsDNA at the surface of the electrode. Voltammetric titrations of DNA-modified and unmodified electrodes were performed in the presence of 0.020 M NaCl by measuring cathodic peak currents at 50 mV/sec as a function of $Co(bpy)_3^{3+}$ concentration. Figure 3.4 shows voltammetric calibration curves obtained at GCEs unmodified and modified with native calf thymus DNA, denatured calf-thymus DNA with or without the coupling reagent EDC. At 0.12 mM $Co(bpy)_3^{3+}$ the resulting voltammograms yielded responses of 1.1 μA for an unmodified GCE and 3.1 μA for a denatured calf-thymus DNA-modified GCE (Figure 3.4). No significant increase in peak current was observed for GCEs modified with native calf-thymus DNA (1.2 μA) or GCEs modified with denatured calf-thymus DNA without EDC (1.4 μA). This reveals that only ssDNA can be covalently bound to EDC-activated GCEs. This indicates that it is one of the bases which is capable of binding to activated GCEs and not the 5'-phosphate or the 3'-hydroxyl of the DNA strand.

To determine which group(s) present in DNA is (are) reactive, two species of synthetic homologous DNA were tested for their ability to bind to activated GCEs: denatured poly(dA)poly(dT), and denatured poly(dG)poly(dC). These are high molecular weight DNA with one strand containing repeats of one nitrogenous base and the other strand containing repeats of the complementary base. Upon denaturation complementary single-stranded homopolymers are produced. Figure 3.5 shows voltammetric titrations with $Co(bpy)_3^{3+}$ at synthetic DNA-modified GCEs. At 0.12 mM $Co(bpy)_3^{3+}$ the resulting voltammetric response

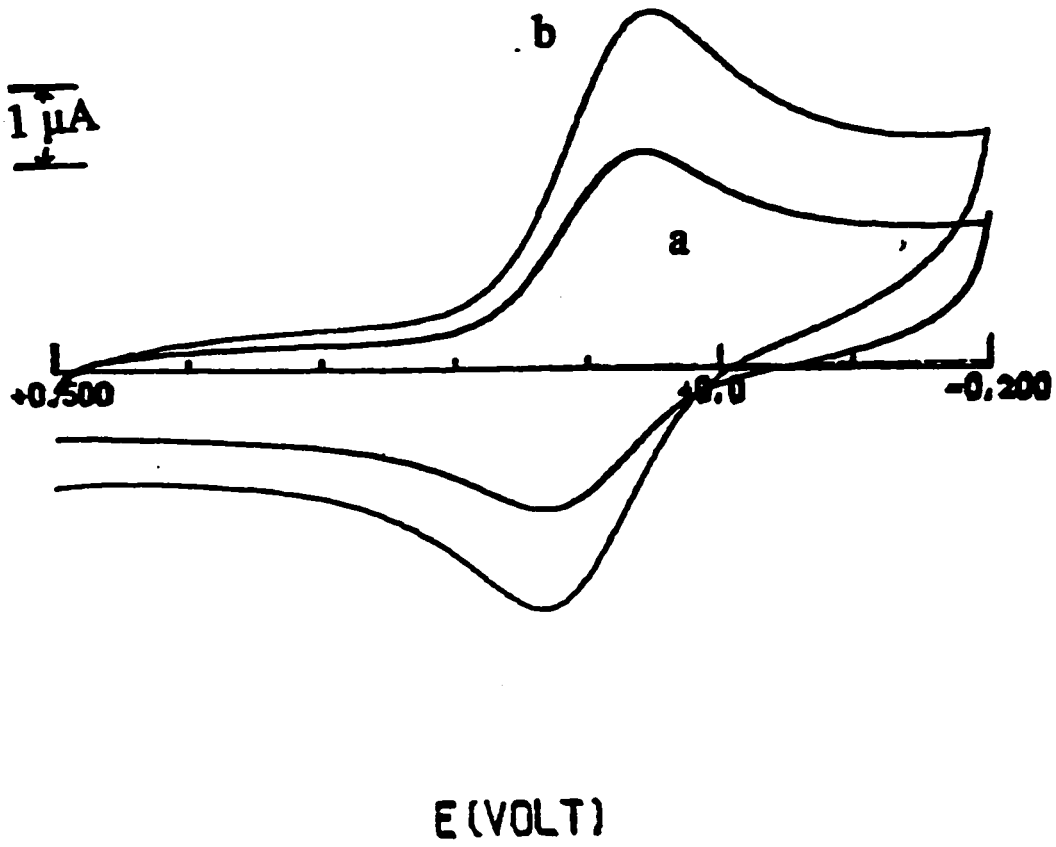

Figure 3.3 Cyclic voltammograms for (a) an unmodified GCE (b) a GCE modified with denatured calf thymus DNA. Conditions: 0.12 mM $Co(bpy)_3^{3+}$ 5 mM Tris pH 7.1, 20 mM NaCl, scan rate 50 mV/s.

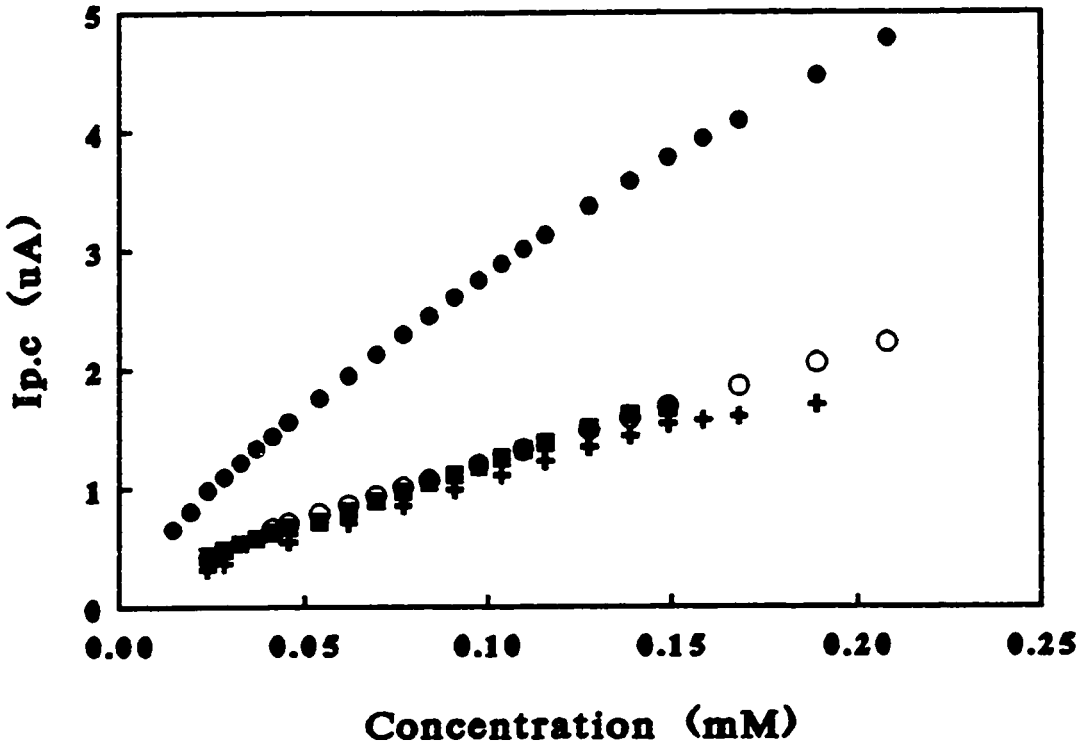

Figure 3.4 Peak Current vs concentration for a glassy carbon electrode unmodified (+), modified with native calf thymus DNA (■), and modified with denatured calf thymus DNA with EDC (●), and without EDC (○). Conditions as in Figure 3.3.

for poly(dA)-poly(dT) and poly(dG)poly(dC) modified GCEs were 1.5 μA and 3.7μA, respectively. As can be seen from the titration curve no significant change is observed between an unmodified electrode and an electrode modified with denatured poly(dA)-poly(dT). Significant increases in peak current are observed for immobilizations with denatured poly(dG)poly(dC). Attempts to immobilize denatured poly(dG)poly(dC) in the absence of the EDC coupling reagent showed no significant change in peak current from an unmodified GCE.

Titrations with $Co(bpy)_3^{3+}$ for three denatured poly(dG)poly(dC)-modified electrodes were conducted with two different analysis buffers, one containing 0.020 M and the other containing 0.050 M. Figure 3.6 demonstrates the difference in the magnitude of the peak current at poly(dG)-poly(dC) measured at two NaCl concentrations. As can be seen greater peak currents are obtained at lower NaCl concentrations. The peak current obtained at 0.020 M NaCl and 0.12 mM $Co(bpy)_3^{3+}$ is 5.0 μA, whereas at 0.050 M NaCl the peak current is 1.6 μA. The large difference in peak currents at different NaCl concentrations demonstrates the electrostatic component of the interaction between $Co(bpy)_3^{3+}$ and DNA. Similar results were acquired at calf thymus DNA-modified electrodes. Since a greater signal difference between unmodified and DNA-modified electrodes was acquired at lower NaCl concentrations all future analysis buffers contained 0.020 M NaCl.

Since only GCEs modified with denatured calf thymus DNA (42% GC content) and poly(dG)poly(dC) yielded significant increases in peak current for $Co(bpy)_3^{3+}$ reduction, then either deoxyguanosine or deoxycytosine residues are covalently bound to the activated GCE surface. Single-stranded oligonucleotides containing a twenty base repeating sequence of

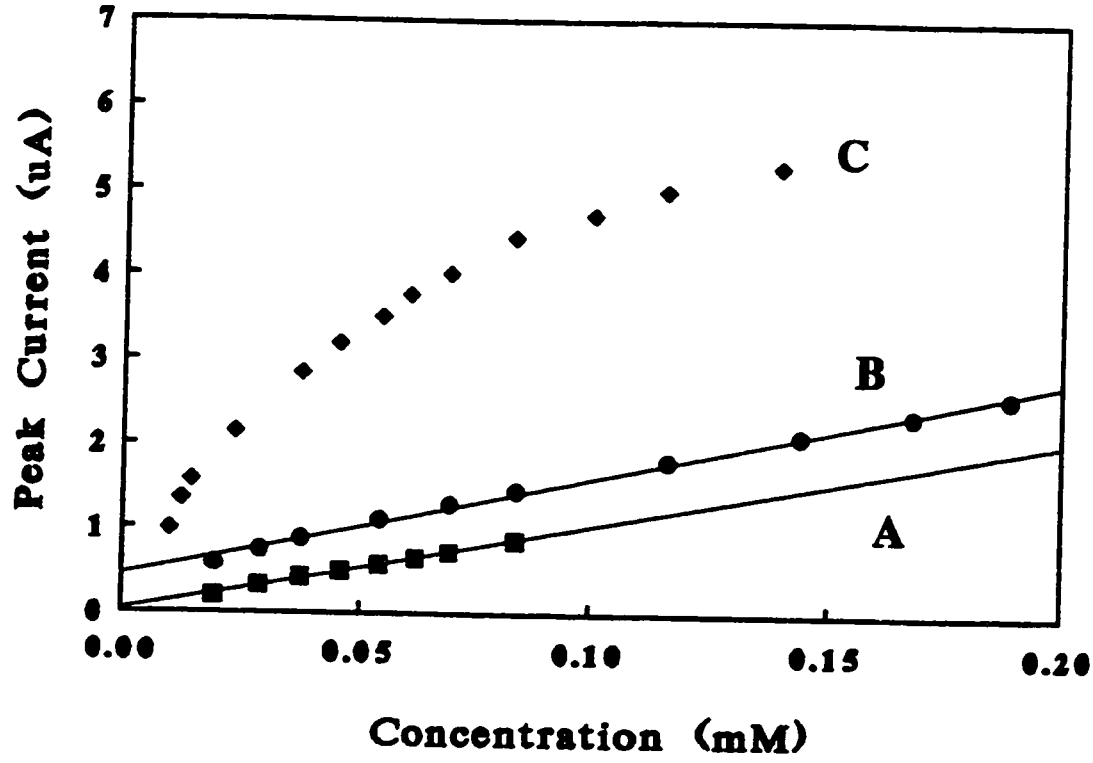

Figure 3.5 Voltammetric titrations with $Co(bpy)_3^{3+}$ (A) an unmodified GCEs, (B) a GCE reacted with denatured poly(dA)poly(dT), (C) and denatured poly(dG)poly(dC). Conditions as in Figure 3.3.

either guanosine or cytosine bases, oligo$(dG)_{20}$ and oligo$(dC)_{20}$ respectively, were then used to determine which nitrogenous base is reactive in the immobilization reaction. Table 3.2 summarizes the results obtained after immobilization with each of these oligodeoxynucleotides and hybridization to their complementary sequence.

Following hybridization with either denatured poly(dG)poly(dC) or oligo$(dC)_{20}$ immobilized oligo$(dG)_{20}$ shows the largest increase in peak currents. Oligo$(dC)_{20}$ was not reactive to the activated GCE surface, as determined by the slight decrease in response to $Co(bpy)_3^{3+}$ upon attempted hybridization with its complementary DNA. These results indicate that the functional group for the EDC coupling reaction is on the guanosine base.

3.2.1.2 EDC and NHS: A More Stable Intermediate

Oxidized GCEs were activated with EDC and NHS, as described in section 2.2.2.2 and then attempts were made to modify the GCEs with denatured calf thymus DNA, denatured poly(dA)-poly(dT), and denatured poly(dG)-poly(dC). The peak current responses obtained for 0.12 mM $Co(bpy)_3^{3+}$ at 50 mV/s were 1.24 μA, 1.26 μA, and 13.1 μA, respectively. No signal increase was observed in the absence of the coupling reagents. The activated GCEs were unreactive towards double-stranded poly(dG)poly(dC). Figure 3.7 shows three calibration curves for titrations with $Co(bpy)_3^{3+}$ at GCEs modified with denatured poly(dG)poly(dC) without a coupling reagent, with EDC as the coupling reagent, and EDC/NHS as coupling reagents. As shown in Figure 3.7 larger signals are obtained at (NHS/EDC) DNA-modified GCEs. Therefore the combination of NHS and EDC give better immobilizations than EDC alone. Successful coupling of poly(dG)poly(dC) to activated GCEs

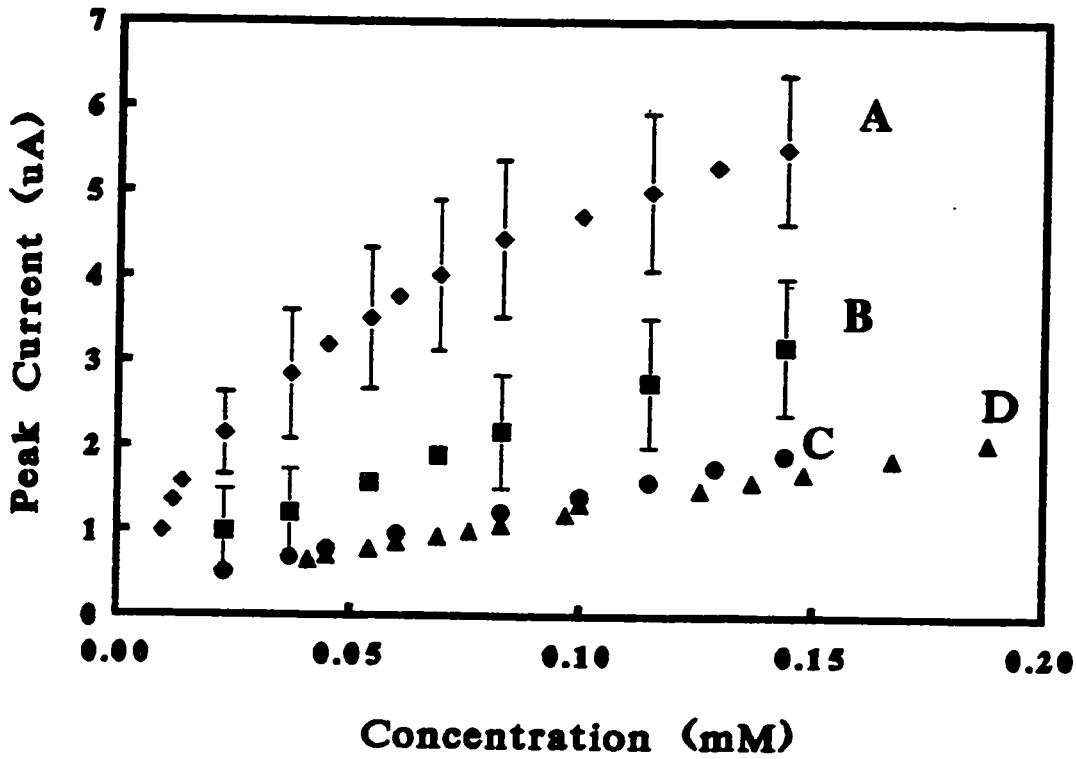

Figure 3.6 Voltammetric titrations of three denatured poly(dG)poly(dC)-modified GCEs in (A) 20 mM NaCl, (B) 50 mM NaCl, and (C) an unmodified GCE at 20 mM NaCl and (D) at 50 mM NaCl. Conditions: 5 mM Tris pH 7.1, scan rate 50 mV/s. (Each curve represents the averages for three DNA modifications, each sensor was analyzed in 50 mM NaCl and 20 mM NaCl.

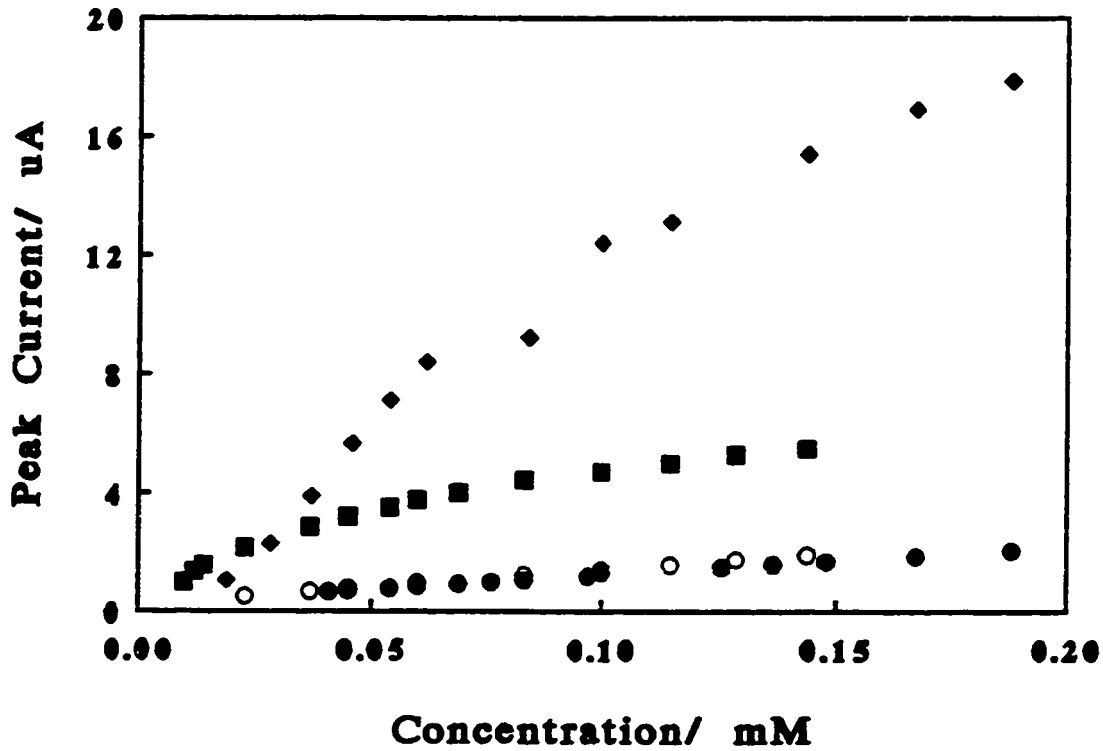

Figure 3.7 Voltammetric titrations with $Co(bpy)_3^{3+}$ at GCEs reacted with poly(dG)poly(dC) and EDC (■), or EDC/NHS (♦), or no coupling reagents (●), and unmodified (○). Conditions as in Figure 3.3.

was confirmed by UV-visible reflectance spectroscopy of an unmodified GCE and a poly(dG)poly(dC)-modified GCE.[12] Figure 3.8 shows the UV-visible reflectance spectra of unmodified and DNA-modified GCEs. The reflectance spectroscopy experiments show an increase in absorption at wavelengths between 240 and 280 nm at a DNA-modified GCE but not at an unmodified GCE.

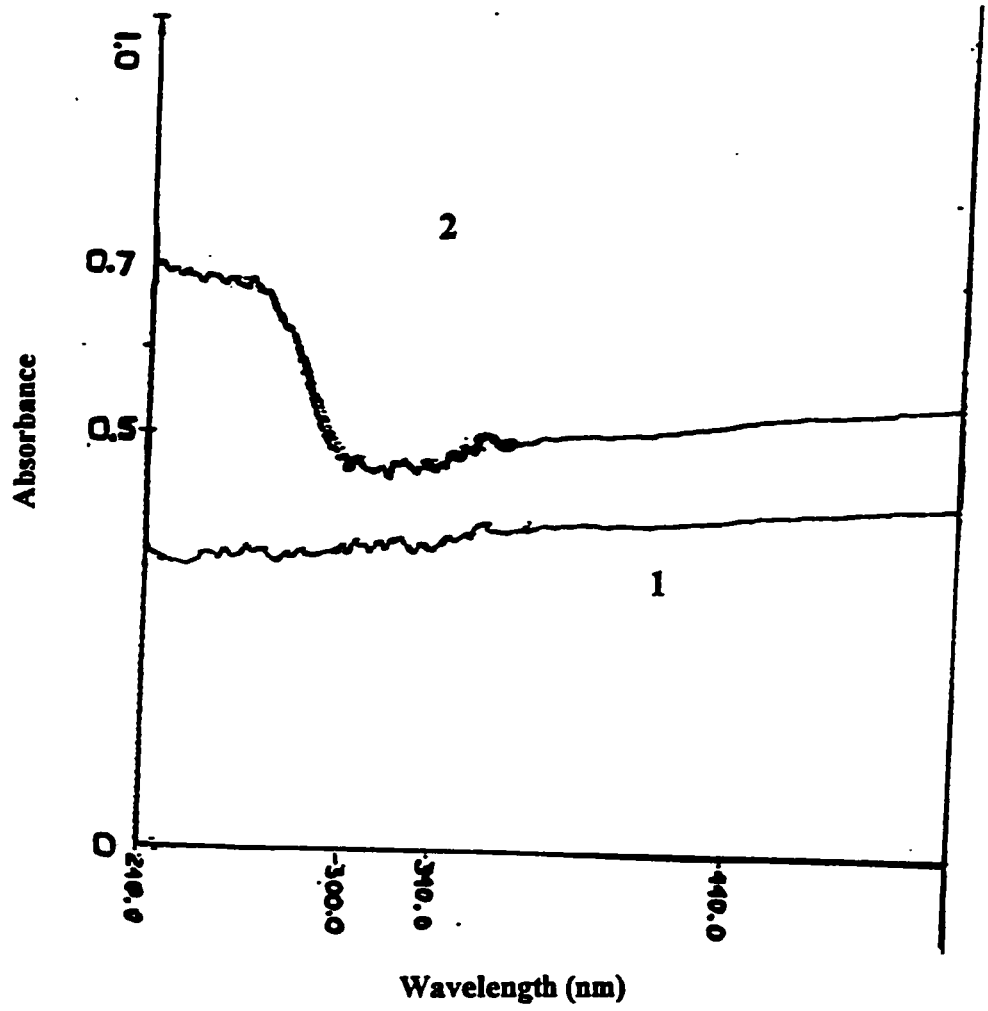

Figure 3.8 UV-Visible Reflectance Spectra of (1) an unmodified and (2) a poly(dG)poly(dC)-modified GCE.

Table 3.2 Cathodic Peak Currents for 0.12 mM $Co(bpy)_3^{3+}$ obtained at Modified Glassy Carbon Electrodes before and after Hybridization with Complementary DNA.

DNA Species Immobilized	DNA Species Hybridized	Cathodic Peak Current (μA)
$Oligo(dG)_{20}$	--------	1.3
$Oligo(dG)_{20}$	poly(dG)poly(dC)	1.9
$Oligo(dG)_{20}$	$oligo(dC)_{20}$	1.6
$Oligo(dC)_{20}$		1.3
$Oligo(dC)_{20}$	$oligo(dG)_{20}$	1.2

Cyclic Voltammetry was performed at 50 mV/s in 5 mM Tris pH 7.1, with 20 mM NaCl. The coupling reagent is EDC. The peak current values are single values obtained at one oligo(dG)-modified GCE (hybridized first with denatured poly(dG)poly(dC) followed by a hot rinse and then hybridized with oligo(dC), and at one oligo(dC)-modified GCE hybridized with oligo(dG).

The peak currents generated by 0.12 mM $Co(bpy)_3^{3+}$ at oligo(dG)-and oligo(dC)-modified electrodes before and after hybridization with complementary DNA were observed. Table 3.3 summarizes the results of these immobilizations and hybridizations. For an oligo(dG)-modified electrode the peak current increased substantially upon hybridization with both denatured poly(dG)poly(dC) and oligo(dC). Attempts made at immobilizing oligo(dC) onto a GCE provided only slight increases in peak currents upon hybridization with oligo(dG) or denatured poly(dG)poly(dC). The peak current generated at 0.12 mM $Co(bpy)_3^{3+}$ for a GCE with an attempted immobilization of oligo(dC) generated a signal response of 1.2 μA and upon hybridization with oligo(dG), 2.5 μA. It was highly possible that oligo(dG) reacted with some remaining active groups on the surface of the GCE. Thus it was necessary to add a blocking step. After immobilization with oligo(dC) any remaining active groups were reacted with 10 mM glycine at 25 C for 15 min. Glycine contains a primary amine which is

strongly nucleophilic and will deactivate any remaining NHS-esters. After the addition of glycine the modified GCEs are rinsed and hybridized with oligo(dG). When this blocking step is added the peak current after hybridization only increases slightly to 1.8 μA. These results show that covalent immobilization of DNA to activated GCEs occurs primarily through deoxyguanosine residues.

Table 3.3 Cathodic Peak Currents for 0.12 mM $Co(bpy)_3^{3+}$ obtained at Modified Glassy Carbon Electrodes before and after Hybridization with Complementary DNA.

Immobilized	Hybridized	Response, μA
none	poly(dG)+poly(dC)	1.0
oligo(dG)	none	1.3
oligo(dG)	oligo(dC)	5.7
$oligo(dG)_{20}$	poly(dG)+poly(dC)	4.5
$oligo(dC)_{20}$	none	1.2
$oligo(dC)_{20}$	$oligo(dG)_{20}$	2.5
$oligo(dC)_{20}$	poly(dG)+poly(dC)	1.5
$oligo(dC)_{20}$	glycine/ $oligo(dG)_{20}$	1.8

Poly(dG)+poly(dC) is denatured poly(dG)poly(dC).
Cyclic voltammetry was performed at 50 mV/s in 5 mM Tris, pH 7.1, with 20 mM NaCl. Uncertainty ≤ 0.2 μA. Coupling reagents are EDC and NHS.

3.2.2 Optimization of Sensor Response

3.2.2.1 Buffer Conditions for Coupling DNA onto GCEs

K_3PO_4 and Li_3PO_4 based buffers were compared to determine their influence on the immobilization reaction. Research indicates that the presence of potassium or sodium ions

promotes the formation of the G4 secondary structure whereas lithium does not.[13,14,15] Results show that 20 mM K_3PO_4 or 60 mM K^+ resulted in better immobilizations of DNA as indicated by larger increases in peak currents after immobilization relative to the unmodified electrode. Immobilizing denatured poly(dG)poly(dC) onto NHS-activated GCEs in the presence of K_3PO_4 gave increases in peak currents of 4 ± 1 μA (n=5), while modifications in the presence of 20 mM Li_3PO_4 (60 mM Li^+) gave relatively no increase in peak current 1.22 ± 0.01 μA as compared to 1.1 ± 0.01 μA for an unmodified GCE (n=3).

3.2.2.2 **Methods for Electrochemical Detection**

Three electrochemical techniques were evaluated for their ability to improve the sensitivity for the detection of dsDNA at the surface of an electrode. Cyclic voltammetry (CV), chronoamperometry (CA), and differential pulse voltammetry (DPV) were compared according to the percent increase in response for the same GCE before and after modification with poly(dG)poly(dC). Table 3.4 provides these results for CV, CA, and DPV (using different pulse amplitudes, 50, 100, 150, 200 mV). DPV provided the largest signal increase upon modification with poly(dG)poly(dC).

3.2.3 Electrochemical Characterization of DNA-modified GCEs.

DNA-modified GCEs were characterized by cyclic voltammetry, using the two electroactive complexes which associate selectively with dsDNA, $Co(bpy)_3^{3+}$ and $Co(phen)_3^{3+}$, and with two electroactive species which do not associate preferentially with dsDNA,

ferrocene carboxylic acid (FCA), and (dimethylaminomethyl) ferrocene (DAF). At pH 7, FCA is negatively charged and should not interact with polyanionic DNA, while DAF is positively charged and is expected to be nonselectively attracted to the DNA phosphate backbone. Table 3.5 summarizes the relevant chemical properties of all four complexes, which exhibit quasireversible one-electron redox activity.

Table 3.4 Percent Increase in Peak Current at a GCE after Modification with Poly(dG)poly(dC).

Electrochemical Method	Percent Increase in Signal (%)
CV	430
CA	492
DPV PA= 50 mV	615
DPV PA= 100 mV	680
DPV PA= 150 mV	683
DPV PA= 200 mV	857

Conditions for CV, CA, and DPV are described in Section 2.2.7, 2.2.9, and 2.2.8, respectively. PA = pulse amplitude.

Figure 3.9 shows calibration curves for the voltammetric titrations of these four complexes at an unmodified glassy carbon electrode. Linear behaviour is observed for all four complexes over the 0.05 - 0.3 mM concentration range. Regression of peak current; (μA) vs concentration (mM) for $Co(bpy)_3^{3+}$, $Co(phen)_3^{3+}$, DAF, and FCA gives y= 6.75x + 0.25 (R=0.9997), y= 7.45x + 0.09 (R= 0.9990), y= 9.41x + 0.00 (R= 0.9989), and y= 8.10x + 0.13

(R= 0.9998), respectively.

Table 3.5 Electrochemical and DNA-Binding Properties[16], of FCA, DAF, $Co(bpy)_3^{3+}$, and $Co(phen)_3^{3+}$

Species	$E^{o'}$ V vs SCE	D cm^2/s	K_{DNA}, M^{-1} (Site Size, BP)
FCA	0.275	3×10^{-6}	———
DAF	0.400	3×10^{-6}	———
$Co(bpy)_3^{3+}$	0.085	5.0×10^{-6}	1.4×10^4 (3)
$Co(phen)_3^{3+}$	0.137	3.7×10^{-6}	2.6×10^4 (5)

Voltammetric calibration curves for all four species at a poly(dG)poly(dC)-modified electrode are shown in Figure 3.10. Linear behaviour is observed for FCA and DAF with a regression of i_p vs concentration giving y= 16.11x - 0.16 (0.998) for DAF, and y= 7.97x - 0.19 (R= 0.991) for FCA. DAF exhibits a slight increase in slope for i_p vs concentration at a DNA-modified GCE as compared to an unmodified electrode. In contrast FCA exhibits a slight decrease in peak current at each concentration. This behaviour is expected since the DAF is positively charged and will be nonselectively preconcentrated near the surface of the electrode by electrostatic interactions with DNA. FCA is negatively charged and will be excluded from the DNA layer at the electrode surface. Large increases in peak current are observed at all concentrations of $Co(bpy)_3^{3+}$ and $Co(phen)_3^{3+}$ for a poly(dG)poly(dC)-modified electrode. In addition, the curves obtained are non-linear and suggest saturation binding to the immobilized DNA.

Peak currents were observed as a function of scan rate for a poly(dG)poly(dC)-modified GCE. For a diffusing species linear plots of i_p vs $v^{1/2}$ are observed (Randles-Sevcik equation: Equation 1), whereas for an adsorbed species linear plots for i_p vs v are observed. Figure 3.11 gives a plot of i_p vs $v^{1/2}$ at an unmodified and a poly(dG)poly(dC)-modified GCE for all four species tested. Linear plots of i_p vs $v^{1/2}$ were obtained for all four species at an unmodified electrode. At a DNA-modified electrode linear behaviour is observed for FCA, DAF, and $Co(bpy)_3^{3+}$. $Co(phen)_3^{3+}$ exhibits linear behaviour for i_p vs $v^{1/2}$ at a DNA-modified electrode up to 100 mV/sec. At higher scan rates the curve tends to level off.

The linear dependence of i_p vs $v^{1/2}$ at a DNA-modified GCE suggests diffusing behaviour for the redox-active complexes tested. This indicates that the microenvironment near the surface of a DNA-modified GCE extends into solution and that the electrode does not see the bulk solution. Therefore calibration data at DNA-modified and unmodified electrodes can be used to estimate the ratio of DNA-bound to free complex in this microenvironment.

Voltammetric titrations of $Co(phen)_3^{3+}$ with homogenous calf thymus DNA [17] and synthetic poly(dG)poly(dC) in 20 mM NaCl were fit to the standard form of the McGee-von Hippel model. The results gave $K = 1.3 \times 10^4 M^{-1}$, n = 3 bp for calf thymus DNA and $K = 1.8 \times 10^5 M^{-1}$, n = 4.4 bp for poly(dG)poly(dC). Figure 3.12 shows a Scatchard plot for the titration of homogeneous poly(dG)poly(dC) with $Co(phen)_3^{3+}$, fit to the standard form of the McGee-von Hippel model. A voltammetric titration was performed at a DNA-modified electrode in order to determine the K_a and n of $Co(bpy)_3^{3+}$ and $Co(phen)_3^{3+}$ with DNA immobilized onto a GCE. Since the DNA was immobilized onto a GCE its concentration

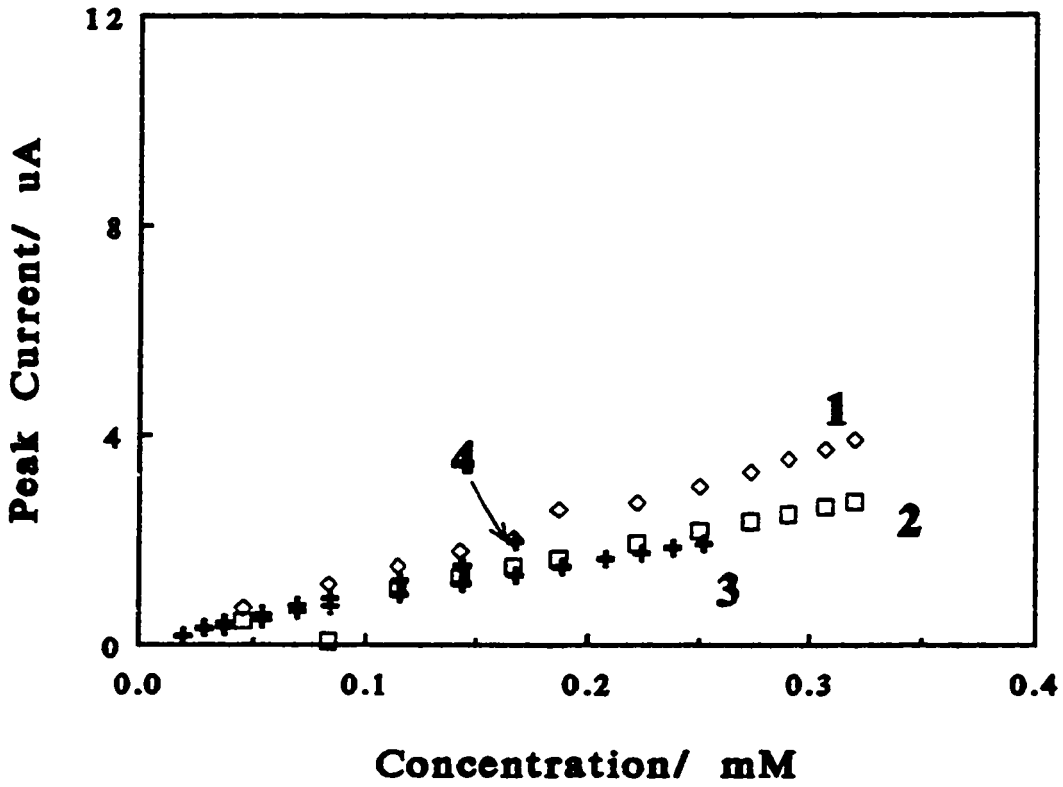

Figure 3.9 Voltammetric titrations at an unmodified GCE. Peak current vs concentration for (1) DAF, (2) FCA, (3) $Co(bpy)_3^{3+}$, and (4) $Co(phen)_3^{3+}$. Conditions: 5 mM Tris pH 7.1, 20 mM NaCl, scan rate 50 mV/s.

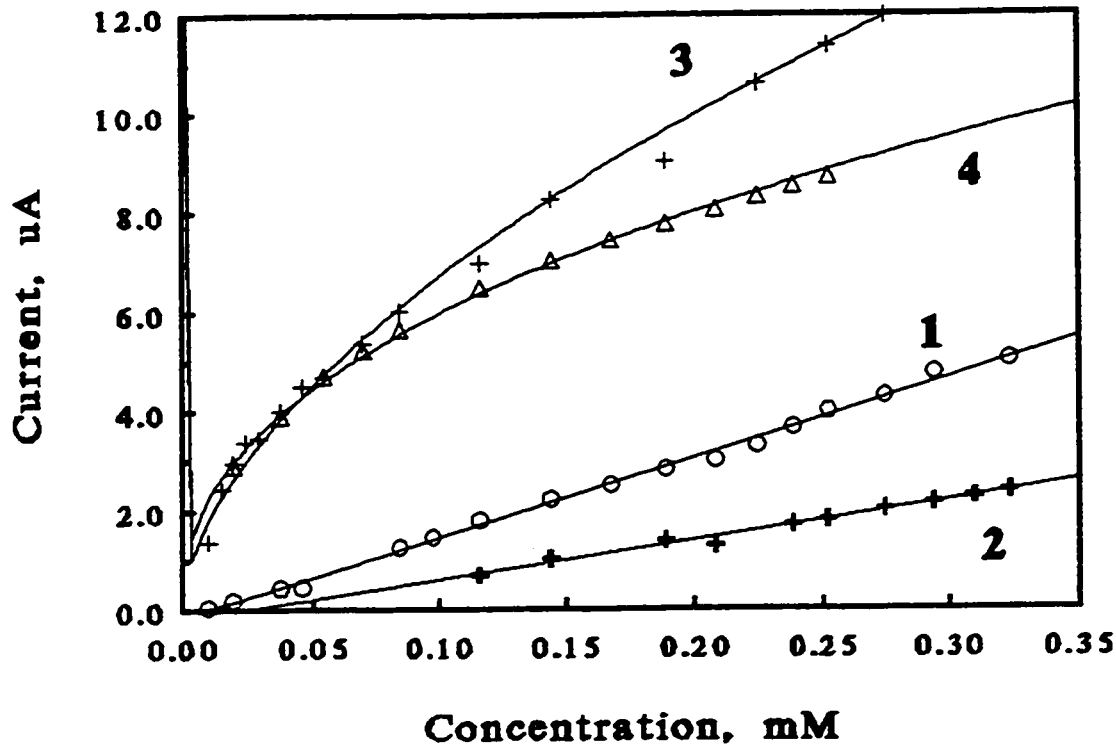

Figure 3.10 Voltammetric titrations at a poly(dG)poly(dC)-modified GCE. Peak current vs concentration for (1) DAF, (2) FCA, (3) $Co(bpy)_3^{3+}$, and (4) $Co(phen)_3^{3+}$. Conditions as in Figure 3.9.

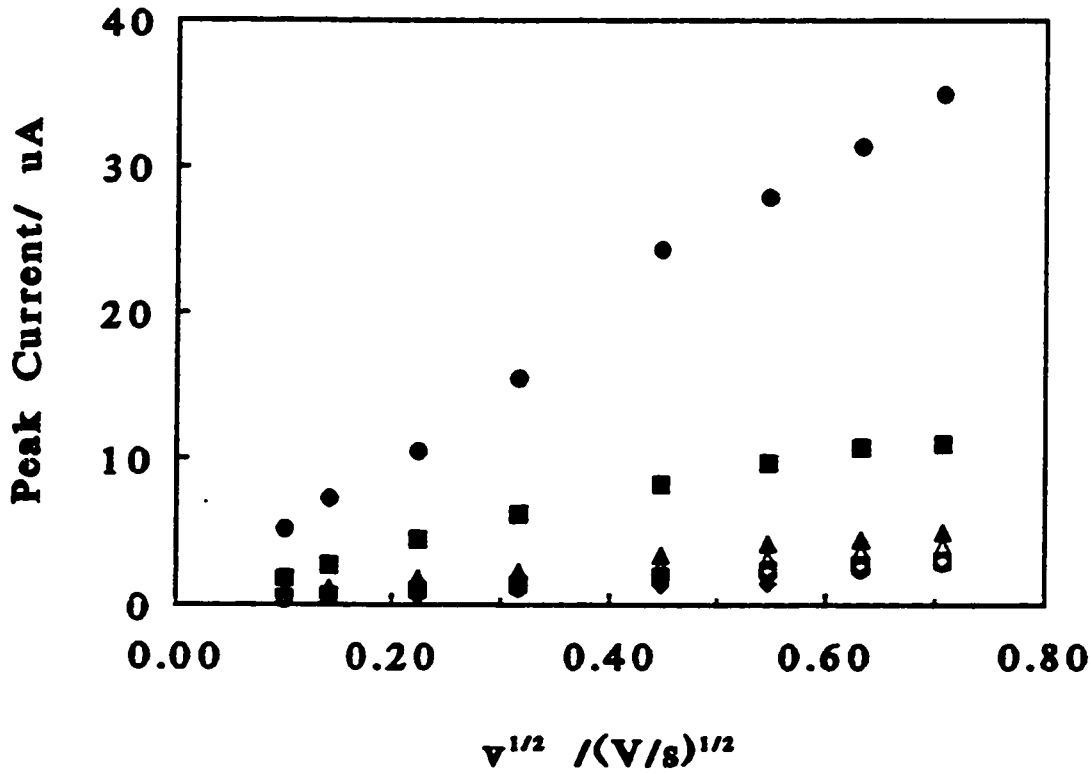

Figure 3.11 GC-modified GCE (solid symbols) and an unmodified GCE (open symbols), with 0.12 mM FCA (◇, ◆), DAF (△, ▲), $Co(bpy)_3^{3+}$ (○, ●), $Co(phen)_3^{3+}$ (□, ■). Conditions: 0.12 mM complex, 5 mM Tris pH 7.1, 20 mM NaCl.

remained constant and the concentration of transition metal complex was varied. For immobilized DNA the voltammetric titration data were fit to the McGee Von Hippel model and the concentrations of free and bound complex were determined by the following equations 13 and 14:

$$i_{p,u} = BC_f \tag{13}$$

$$i_{p,m} = B(C_b+C_f) \tag{14}$$

where $i_{p,u}$ and $i_{p,m}$ are the peak currents at an unmodified electrode and a modified electrode, respectively, B is the constant given in equation 4, and C_f and C_b have already been defined in equation 8. These equations allow the calculation of the ratio of free to bound forms by equation 15:

$$\frac{i_p - i_{p,c}}{i_p} = \frac{C_b}{C_f} \tag{15}$$

These data can be fit to the McGee Von Hippel equation. For $Co(phen)_3^{3+}$ equation 9 becomes equation 16, assuming nonspecific, noncooperative interaction of $Co(phen)_3^{3+}$ with dsDNA:

$$\frac{r}{[Co(phen)_3^{3+}]} = K(1-nr)\frac{(1-nr)}{(1-(n-1)r)}^{n-1} \tag{16}$$

where $r=[Co(phen)_3^{3+}]_b/[DNA]_t$, K is the intrinsic associatation constant of $Co(phen)_3^{3+}$, n is the binding site size in base pairs, and $[DNA]_t$ is the total concentration of DNA in base pairs per unit volume.

Since the DNA layer is considered to be a homogenous microvolume with the concentration of DNA constant within that layer, the McGee von Hippel equation can be applied to the association reaction between the transition metal complex; $(Co(phen)_3^{3+})$ and the DNA-modified electrode. Substituting $r = [Co(phen)_3^{3+}]_b/[DNA]_t$ and solving for $[DNA]_t$ gives equation 17:

$$[DNA]_t = \frac{[Complex]_b}{K[Complex]_f} \frac{[DNA]_t - (n-1)[Complex]_b^{n-1}}{([DNA]_t - n[Complex]_b} \qquad (17)$$

The voltammetric data from the calibration curve of i_p vs concentration for $Co(phen)_3^{3+}$ at a poly(dG)poly(dC)-modified and an unmodified electrode were used to estimate $[Co(phen)_3^{3+}]_b$ at each bulk $[Co(phen)_3^{3+}]_f$ value using equation 4. $[DNA]_t$ was then calculated using equation 17 by varying K (500-200000) and n (3-6) to minimize the standard deviation of $[DNA]_t$ over a range of 0.01 to 0.25 mM $[Co(phen)_3^{3+}]_f$. The best fit occurred for n= 5 and K= 1.74×10^3 M^{-1}, which gives $[DNA]_t = 8.6 \pm 0.2$ mM base pairs. Figure 3.13 shows the Scatchard plot of $r/[Co(phen)_3^{3+}]$ vs r, fit to the standard form of the McGee-Von Hippel equation. Similar analysis for the determination of K and n could not be done for $Co(bpy)_3^{3+}$ because of evidence which suggests adsorption of $Co(bpy)_3^{3+}$ at GCEs. The non-zero y-intercept of the calibration curve for $Co(bpy)_3^{3+}$ at the unmodified GCE (0.26 μA) in Figure 3.9 suggests adsorption. Adsorption of $Co(bpy)_3^{3+}$ onto glassy carbon electrodes has been documented elsewhere.[8]

In addition to changes in peak current observed at a DNA-modified GCE, shifts in formal potential occur as a result of the modification of the GCE with poly(dG)poly(dC).

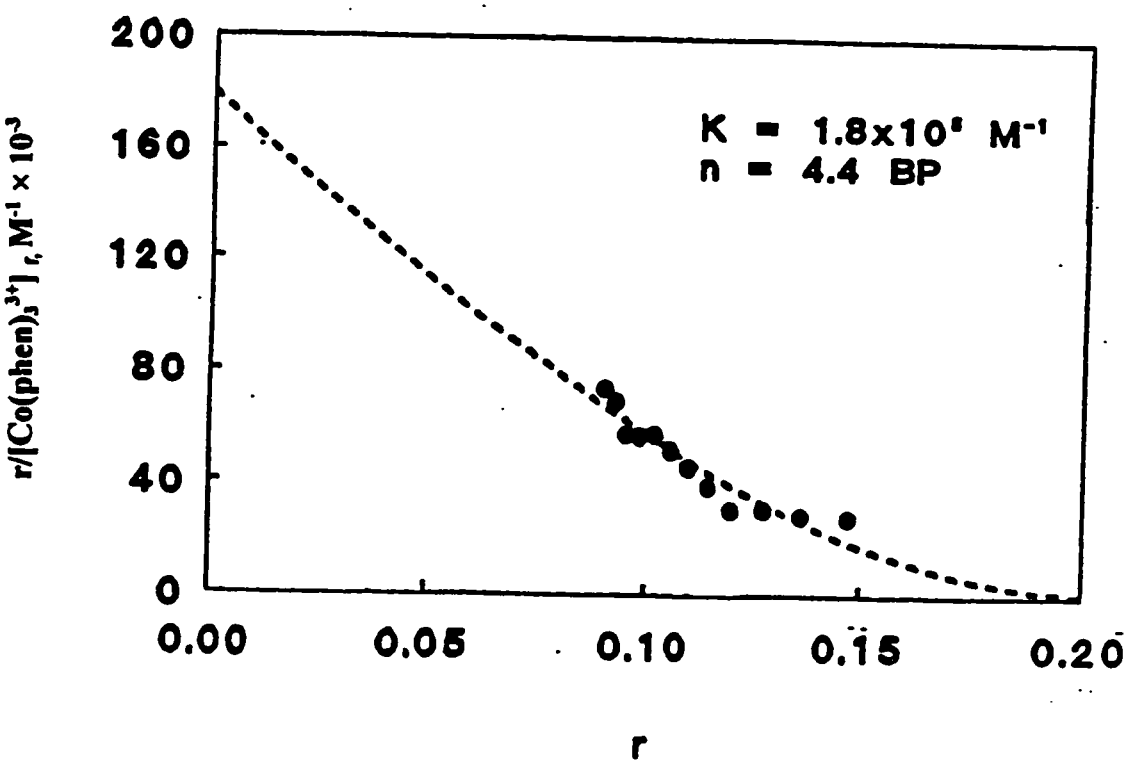

Figure 3.12 Scatchard Plot for a titration of $Co(phen)_3^{3+}$ with poly(dG)poly(dC). Conditions: 5 mM Tris pH 7.1, 20 mM NaCl, scan rate 50 mV/s. Dotted lines are calculated from equation 16.

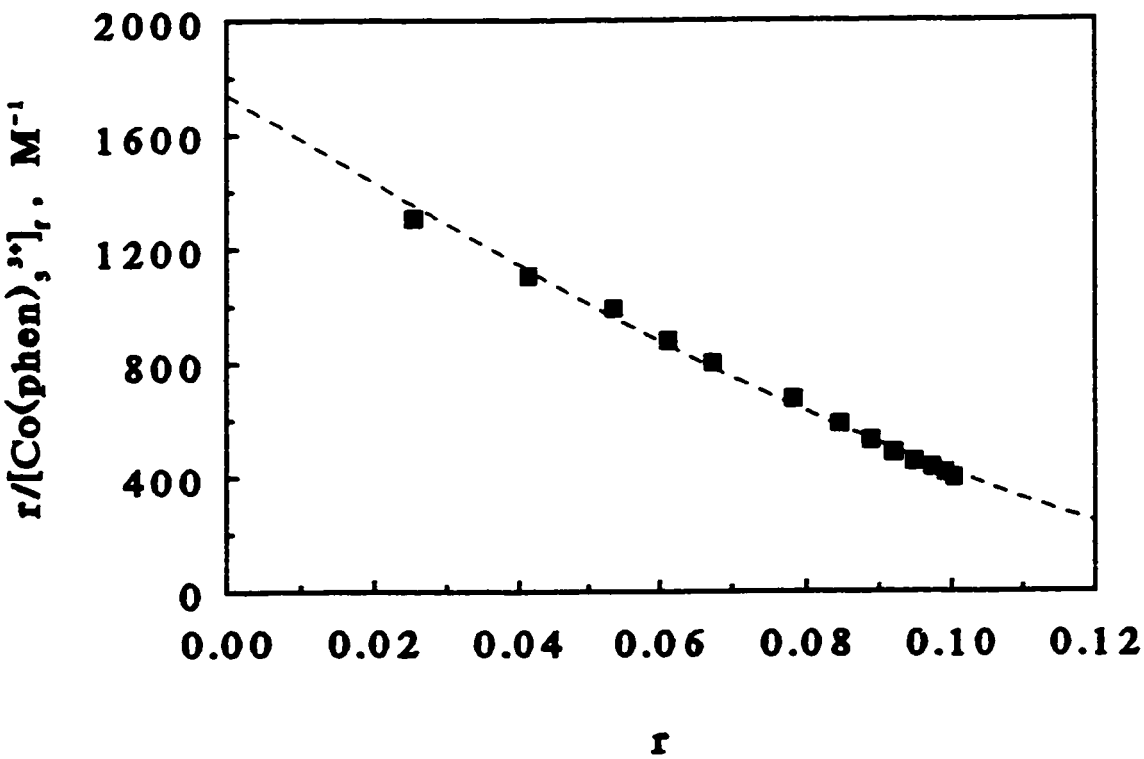

Figure 3.13 Scatchard plot for the binding of $Co(phen)_3^{3+}$ to poly(dG)poly(dC) immobilized onto the surface of a GCE in 5 mM Tris pH 7.1, 20 mM NaCl, scan rate 50 mV/s.

At 0.12 mM $Co(phen)_3^{3+}$ the formal potential $E^{\circ'}$ is 132.0 mV for a DNA-modified GCE and at an unmodified GCE it is 159.5 mV. This is a shift of -27.5 mV. This is in contrast to the +17 mV shift that Carter et. al observed after the addition of homogenous calf thymus DNA to a $Co(phen)_3^{3+}$ solution.[6] At 0.12 mM $Co(bpy)_3^{3+}$ there is a shift of -29.5 mV when the electrode is modified with DNA. Figure 3.14 illustrates this shift in $E^{\circ'}$ for both DNA-binding complexes. From equation 12 a negative shift suggests that the 3+ form is more strongly bound to DNA than the 2+ form.

The separation between the anodic and cathodic peak potentials (ΔE_p) of the complexes increase at a DNA-modified electrode. Electron transfer rates between a redox-couple and an electrode can be calculated from peak separations when the electrochemical reaction is not reversible, or when separation of peak potentials becomes greater than 60/n mV.[18] The standard heterogenous rate constant for electron transfer can be calculated from ΔEp provided that IR drop is compensated for. Nicholson developed a working curve of the variation of ΔE_p with the logarithm of ψ; the charge transfer parameter. Once ψ is obtained from this working curve the electron transfer rate between analyte and electrode can be obtained from equation 18.

$$\psi = \frac{\gamma^{\alpha} k_s}{\sqrt{\pi a D_o}} \qquad (18)$$

where $a = nfv/RT$, $\gamma = (D_o/D_R)^{1/2}$ and α is the charge transfer coefficient. Usually $D_o = D_R$ and γ^{α} is unity. Electron transfer rates for redox active complexes at unmodified and DNA-modified electrodes can be calculated and compared.

The separation of anodic and cathodic peak potentials were measured as a function

of scan rate for all four electroactive complexes used for the characterization studies. The peak separations were all corrected for IR drop. Resistance values measured at 0 V vs Ag/AgCl reference electrode were 598 ± 5 Ω at an unmodified GCE and 618 ± 3 Ω at a poly(dG)poly(dC)-modified electrode.

Figure 3.15 shows the peak separations for all four complexes at an unmodified and a DNA-modified GCE. For all four species an increase in peak separations and an increased scan rate dependence of peak separations are observed at the DNA-modified GCE. Table 3.6 gives the rate constants for heterogenous electron transfer calculated using the working curve and equation 18. Slower rate constants are observed for all four species at the DNA-modified GCE. The heterogenous electron transfer rates all decrease by as much as fivefold when an electrode is modified with DNA, the largest decreases observed for FCA and $Co(phen)_3^{3+}$. The smallest decrease was observed for DAF, in which there was no significant difference in electron transfer rates between a DNA-modified and an unmodified GCE. Heterogenous electron transfer between a DNA-modified electrode and FCA was the slowest which can be explained by the electrostatic exclusion of FCA from the DNA layer. Thus electron transfer between the electrode and FCA would occur over a greater distance.

3.2.4 A Prototype Sequence-Selective DNA-Sensor Based on an Oligo$(dT)_{20}$ Probe.

Oligo$(dT)_{20}$ was incubated with 1000 fold excess of dGTP in the presence of terminal transferase under the appropriate buffer conditions, as described in Section 2.2.5. The product was isolated and characterized by polyacrylamide gel electrophoresis, as described in Section 2.2.6. Figure 3.16 shows that the migration distance of denatured DNA molecular weight

markers are inversely proportional to the logarithm of molecular weight, y= -39.001x + 107.91 (R= 0.995).

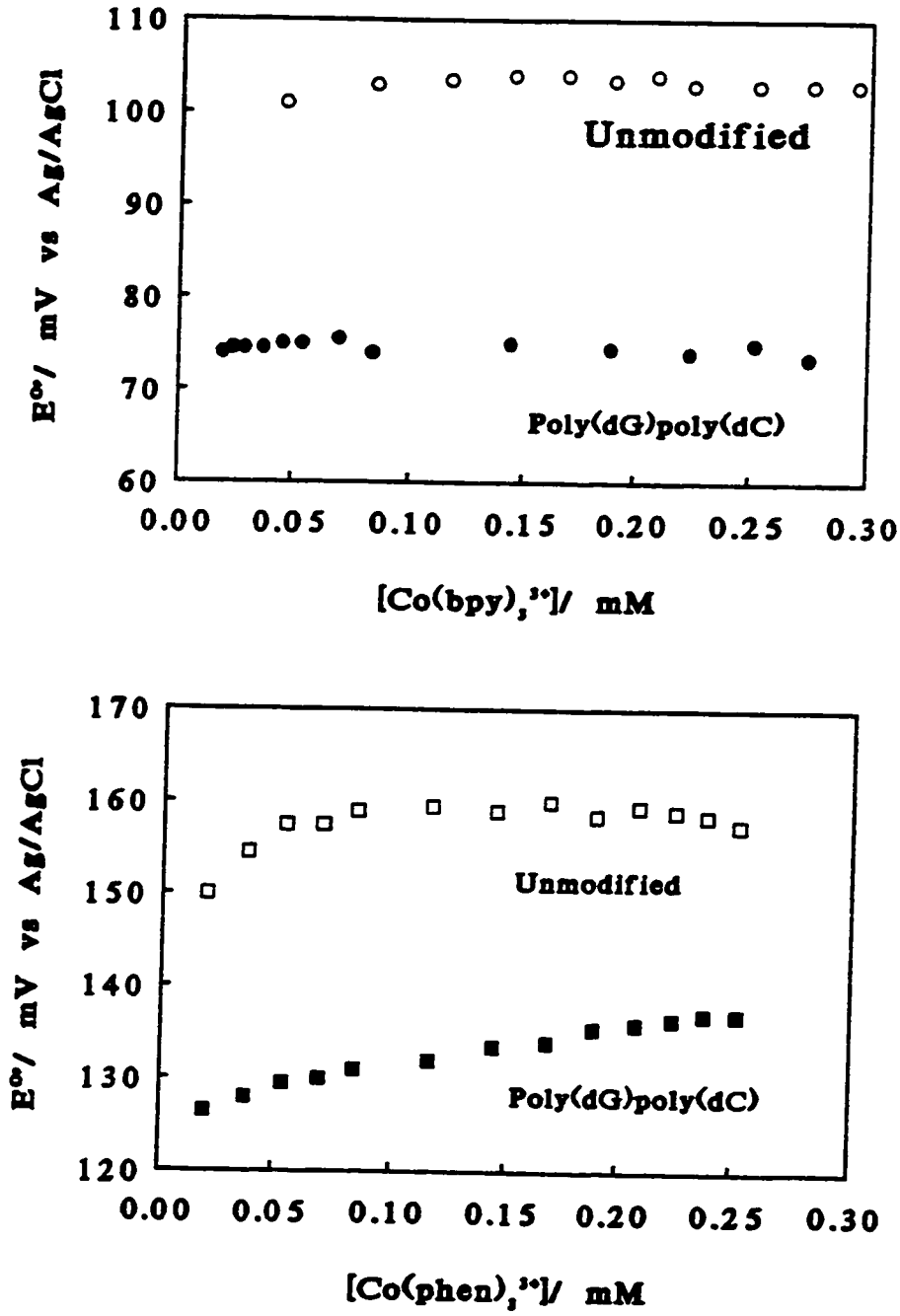

Figure 3.14 Formal potential vs concentration for (A) $Co(bpy)_3^{3+}$ and (B) $Co(phen)_3^{3+}$ at unmodified and poly(dG)poly(dC)-modified GCEs. Conditions: 5 mM Tris pH 7.1, 20 mM NaCl, at 50 mV/s.

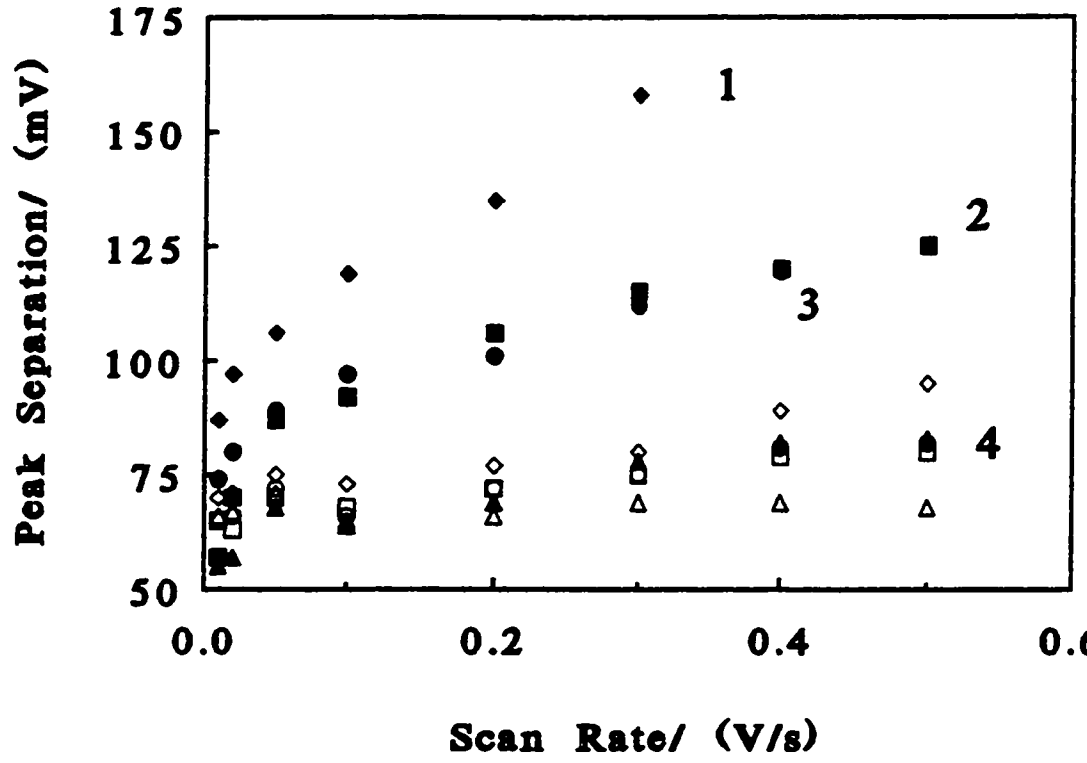

Figure 3.15 Peak separations for (1) FCA, (2) $Co(bpy)_3^{3+}$, (3) $Co(phen)_3^{3+}$ and (4) DAF at a poly(dG)poly(dC)-modified GCE (closed symbols) and the same complexes at an unmodified GCE (open symbols, symbol shape is same as for complexes above. Conditions as in Figure 3.14.

Table 3.6 Apparent Heterogenous Electron Transfer Rates
for all four species at an Unmodified and a poly(dG)poly(dC)-modified GCE.

Complex	Modification	k_o (cm/sec)*
$Co(bpy)_3^{3+}$	unmodified	0.02 ± 0.002
$Co(bpy)_3^{3+}$	DNA-modified	0.006 ± 0.001
$Co(phen)_3^{3+}$	unmodified	0.0160 ± 0.0003
$Co(phen)_3^{3+}$	DNA-modified	0.004 ± 0.002
FCA	unmodified	0.0101 ± 0.0009
FCA	DNA-modified	0.0020 ± 0.0001
DAF	unmodified	0.027 ± 0.001
DAF	DNA-modified	0.025 ± 0.002

* k_o was calculated from the average of 5 ΔE_p values at 8 different scan rates (10, 20, 50, 100,200, 300, 400, and 500 mV/s).
Conditions as in Figure 3.15.

The product of the terminal transferase reaction appeared as a single broad band with a migration distance of 27 ± 2 mm. This would correlate with an average DNA size of 119 bases with a range of 105 bases to 133 bases. Thus an average of 99 ± 14 dG residues were incorporated to the oligo$(dT)_{20}$ probe. The added dG residues are capable of being covalently bound to an activated GCE. The dG tail acts as an anchor to the electrode. The oligo$(dT)_{20}$ probe sequence should not be reactive and will not be covalently bound to the surface of the GCE. It will therefore be free in solution free to hybridize with its complement poly(dA) or oligo$(dA)_{20}$.

The product of the terminal transferase elongation reaction oligo$(dT)_{20}(dG)_{98}$ was covalently immobilized to an activated GCE through the dG residues. The ability of the

oligo$(dT)_{20}$ probe to hybridize to its complement was examined voltammetrically using $Co(bpy)_3^{3+}$ as the hybridization indicator. $Co(bpy)_3^{3+}$ was chosen since this species yielded the largest cathodic peak current at a poly(dG)poly(dC)-modified electrode, as shown in Figure 3.10. A slight increase in peak current at 0.12 mM $Co(bpy)_3^{3+}$ (1.5 ± 0.2 μA) was observed after modification of the GCE with oligo$(dT)_{20}(dG)_{99}$. This is expected since $Co(bpy)_3^{3+}$ will be nonselectively attracted to the negative phosphate groups on ssDNA. A much larger increase in peak current amplitude at the same concentration $Co(bpy)_3^{3+}$ is observed following hybridization of the probe with denatured poly(dA)poly(dT), (2.7 ± 0.2 μA).

Regeneration of the single-stranded probe after hybridizations was accomplished by rinsing the modified probe in hot (100°C) distilled H_2O for 10 minutes. Following this hot rinse step, peak currents at 0.12 Mm $Co(bpy)_3^{3+}$ were the same as those obtained at the probe modified surface prior to hybridization (1.5 ± 0.2 μA). Figure 3.17 illustrates the reusability of the oligo$(dT)_{20}$ prototype DNA sensor. It shows typical voltammograms obtained after hybridization, regeneration of the single-strand probe by rinsing in hot H_2O, and hybridization again. The results of repeat denaturation and regeneration cycles demonstrate that no significant deviations occur in the cathodic peak currents over ten such cycles, and the average responses after hybridization with denatured poly(dA)poly(dT) and regeneration of the ssDNA probe are 2.7 ± 0.2 μA and 1.5 ± 0.2 μA.

The ability of the oligo$(dT)_{20}(dG)_{99}$ probe to discriminate between complementary and non-complementary sequences was then examined. Figure 3.18 shows calibration curves for the peak current responses of this probe before and after hybridization to various synthetic sequences of DNA. Separate hybridization with oligo$(dA)_{20}$ and denatured poly(dA)poly(dT)

yielded significant increases in peak currents as shown in Figure 3.18 A. Attempts to hybridize this probe sequence to the denatured alternating copolymer poly(dAdT) and to denatured poly(dG)poly(dC) yielded no increase in peak currents as seen in Figure 3.18 B respectively. Thus the oligo$(dT)_{20}(dG)_{99}$ probe will not hybridize to these two possible interferents.

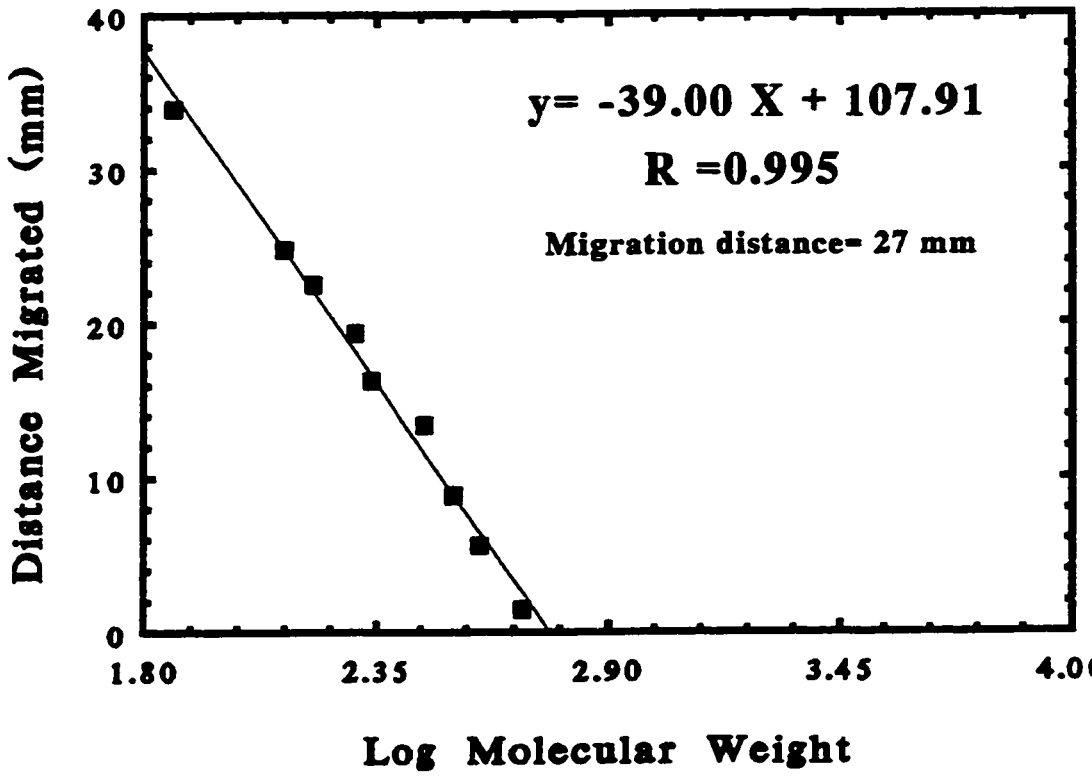

Figure 3.16 Migration distance vs log of the molecular weight of DNA molecular weight markers in 10% polyacrylamide with 7M urea. The dotted line represents the distance migrated by the terminal transferase product.

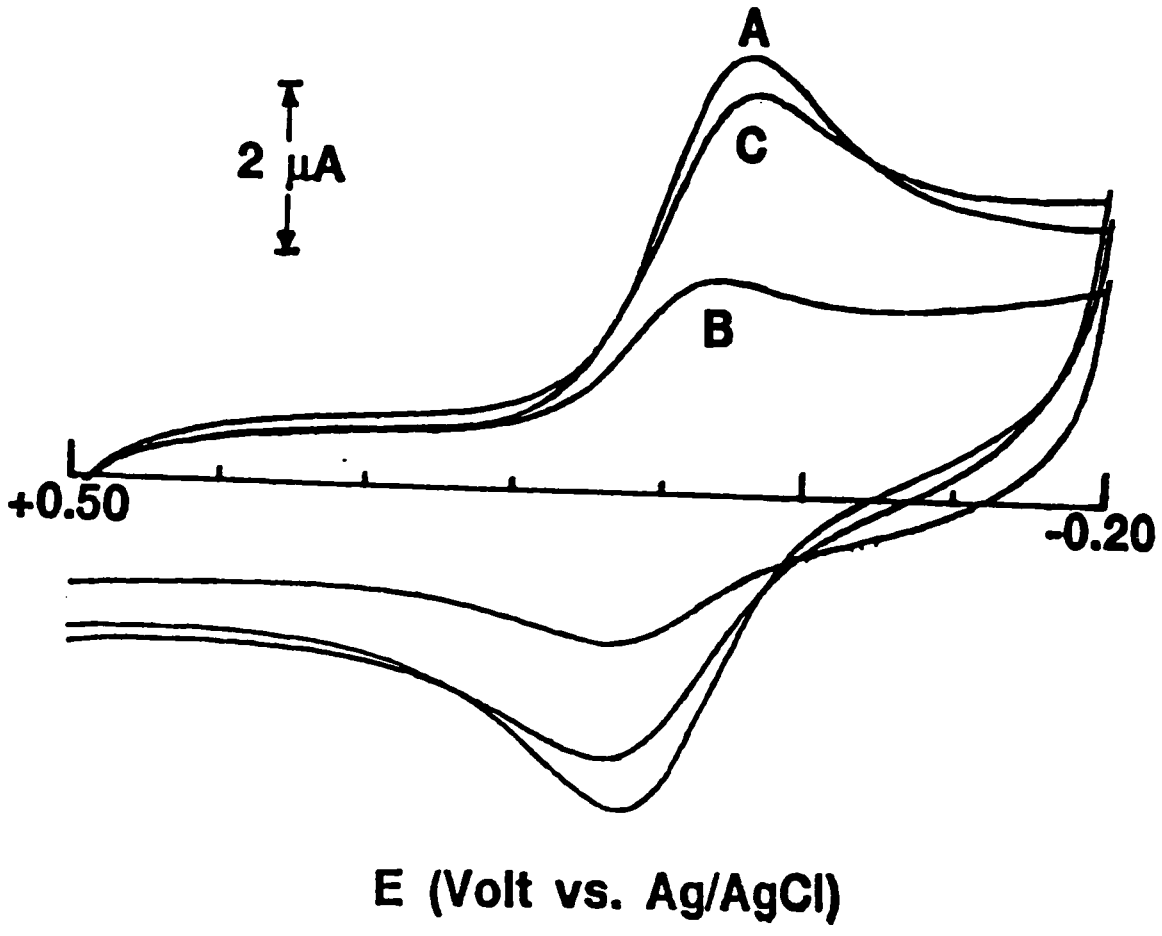

Figure 3.17 CVs at 0.12 mM $Co(bpy)_3^{3+}$ for an oligo$(dT)_{20}(dG)_{99}$-modified GCE (A) after hybridization with denatured poly(dA)poly(dT), (B) regeneration in 100 ° distilled water and (C) rehybridization.

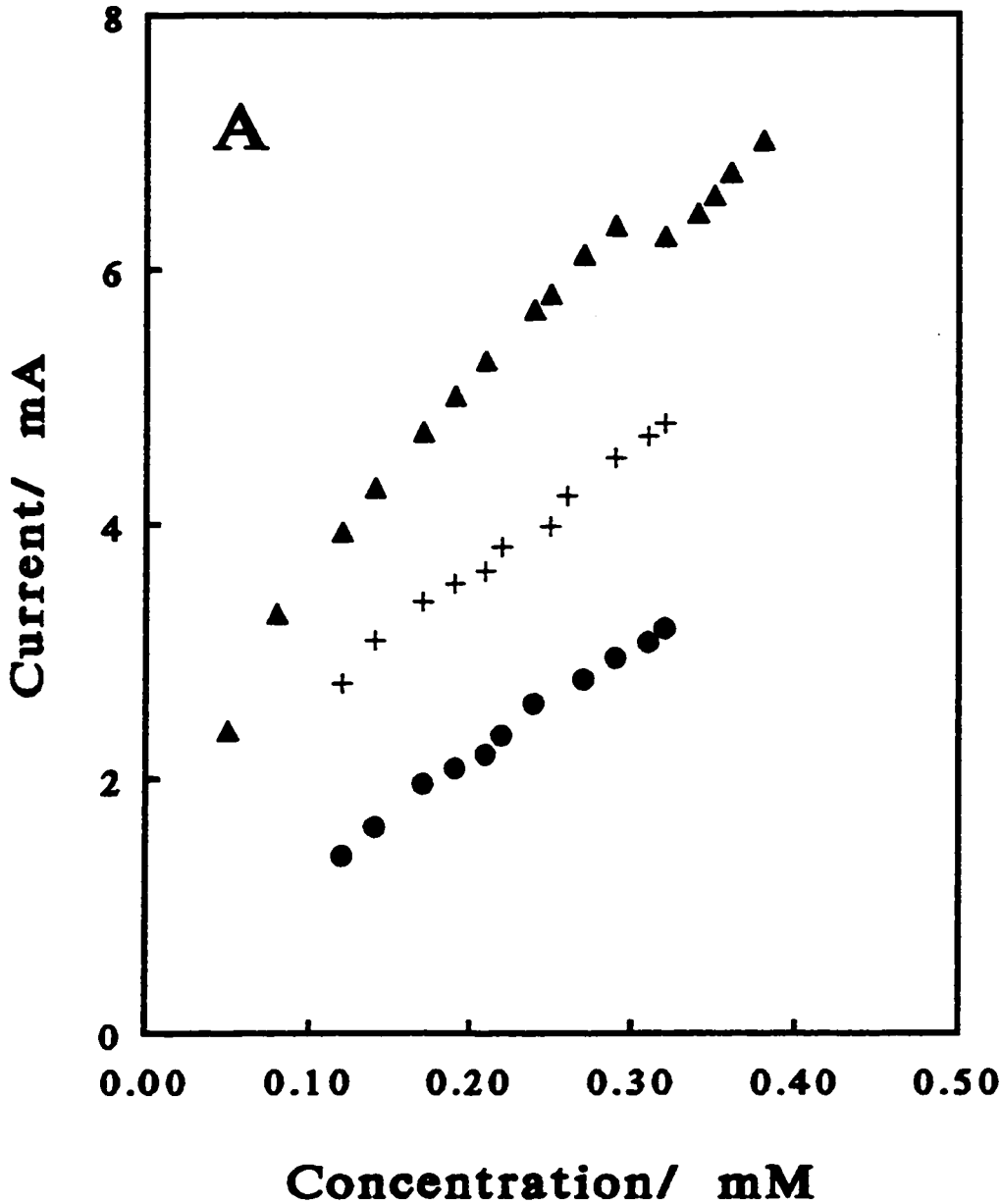

Figure 3.18 A Peak current vs $[Co(bpy)_3^{3+}]$ obtained at an oligo$(dT)_{20}(dG)_{99}$-modified GCE before, in its denatured single-stranded state (●) and after hybridization to different species of DNA. Attempted hybidization to complementary sequences (▲) denatured poly(dA)poly(dT) and (+) oligo(dA).

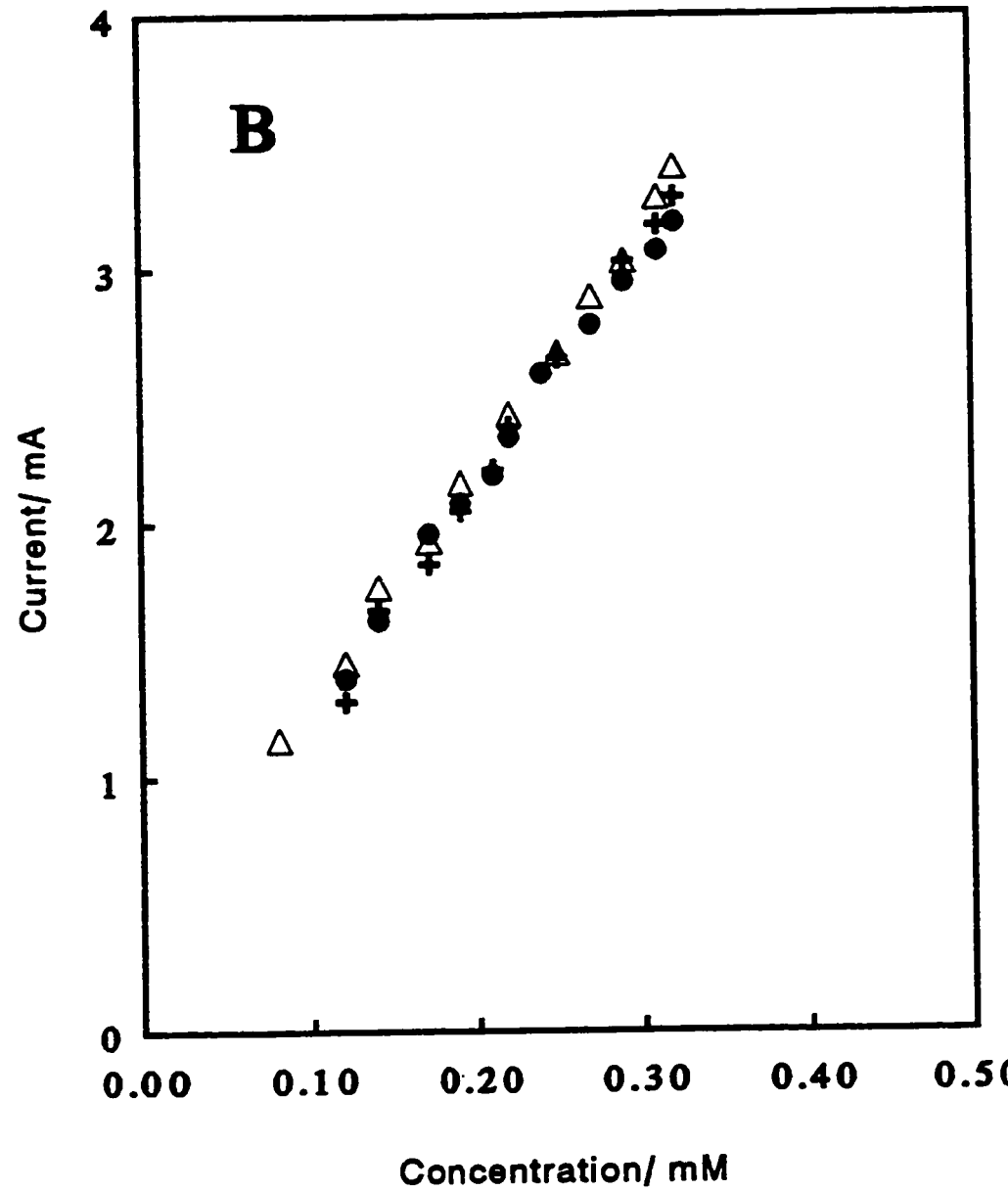

Figure 3.18 B Peak current vs $[Co(bpy)_3^{3+}]$ obtained at an oligo$(dT)_{20}(dG)_{99}$-modified GCE before (●) and after hybridization to different species of DNA. Attempted hybridization to noncomplementary sequences (+) Poly(dA)(dT) and (Δ) denatured poly(dG)poly(dC).

3.3 Discussion

Figures 3.3 to 3.7 and 3.9 and 3.10 show that the behaviours of $Co(bpy)_3^{3+}$ and $Co(phen)_3^{3+}$ at DNA-modified GCEs are different than at unmodified GCEs. The increase in peak currents, shifts in formal potential, increase in peak separation, at a DNA-modified GCE demonstrate the preconcentration of $Co(bpy)_3^{3+}$ in the DNA layer at the surface of the GCE. This provides indirect evidence that DNA is immobilized onto the GCE. UV-visible reflectance spectroscopy shows direct evidence of DNA immobilization since DNA absorbs between 240 -280 nm, see Figure 3.8.[12]

Denaturation of DNA to its single-stranded form is required for immobilization, as shown in Figure 3.4. This indicates that one of the bases is involved in the reaction, since the bases are exposed only in the single-stranded form, while the 5'-phosphate and 3'-hydroxyl are exposed both in the single and double-stranded forms. Also, the inability to immobilize denatured calf thymus DNA without the coupling reagents EDC or EDC/NHS provides evidence that DNA does not adsorb to the GCE surface under our experimental conditions (Figure 3.7). This has been documented elsewhere.[17] Experiments show no change in the electroactive surface area, measured by chronoamperometry, of a GCE throughout a titration with DNA up to 0.56 mM DNA. If DNA were to adsorb to the GCE a change in surface area would be expected.

To determine which base was reactive to the O-acylisourea at the electrode surface attempts were made to immobilize various synthetic sequences of DNA. With both the EDC and EDC/NHS reactions, significant increases in voltammetric responses were observed for immobilization with denatured poly(dG)poly(dC), but not for poly(dA)poly(dT), as illustrated

in Figure 3.5 and presented in Section 2.2.1.2. These results indicate that the reactive base is guanine or cytidine. This also provides evidence against the modification occurring at the 5'phosphate or the 3'-hydroxyl, since if these were reactive then the reaction would be independent of the base.

Attempts to immobilize oligo$(dG)_{20}$ and oligo$(dC)_{20}$ reveal that the coupling reaction occurs through the guanine base. Comparison of the results obtained at electrodes modified with calf thymus DNA (42% G-C content) and poly(dG)poly(dC) (100% G-C content) suggest that consecutive dG residues are required for immobilization. This is consistent with the reported nucleophilicity of the N-7 position of the guanine base and the influence of the molecular electrostatic potential at this position by the nearest-neighbour base pairs.[19,20] Most nitrogen mustards react with the nucleophilic N-7 position of guanine. However, the sites of greatest alkylation require runs of contiguous guanosine residues as compared to independent residues which have lower alkylation yields. The degree of reactivity was much greater than expected if only the number of guanosine residues were taken into consideration.

Studies with poly(dG)poly(dC)-modified electrodes reveal that the NaCl concentration affects the amplitude of the peak currents for $Co(bpy)_3^{3+}$ reduction, as shown in Figure 3.6. Smaller increases in peak current are observed for higher NaCl concentrations (0.050 M) than for lower NaCl concentrations (0.020 M). This demonstrates the electrostatic nature of the binding of $Co(bpy)_3^{3+}$ to DNA.

Two different buffer counterions were chosen to determine the effects of the counterion on the immobilization reaction. Results shows that K^+-containing buffers resulted in better immobilizations of poly(dG)poly(dC) as indicated by larger increases in peak

currents after immobilization relative to the unmodified electrode. Results from other studies indicate that G4 DNA forms more readily in the presence of potassium than lithium. In G4 DNA the deoxyguanosine residues form a crown ether-like association via hydrogen bonds with one another. These results suggest that the conformation of DNA is important in its reactivity towards the NHS-activated GCE surface.

Different electrochemical techniques were examined to optimize the sensitivity of the detection process. DPV gave the largest increases in peak current after immobilization of the GCE with poly(dG)poly(dC). The greater increase in signal observed at a DNA-modified GCE using DPV in comparison to CV or CA can be attributed to the enhancement of the faradaic current. In DPV, the potential is stepped by a finite amount, say 50 mV, and there is an initial surge of current that lowers the concentration of the redox complex within the surface layer around the electrode to the concentration required by the new potential. As the equilibrium concentration is approached, the current decays to a level which is described by diffusion, since charging currents decay rapidly.[21] At the surface of the DNA-modified GCE the redox complex is preconcentrated, and this diffusion-controlled current is much greater that at the unmodified GCE.

Electrochemical characterizations of poly(dG)poly(dC)-modified GCEs and unmodified GCEs reveal that electroactive species behave differently to DNA-modified electrodes than at unmodified electrodes. The two ferrocene species demonstrate the nonselective electrostatic component of interactions with DNA, as shown in Figures 3.9 and 3.10. These two complexes do not bind to specific sites on DNA and yield linear calibration curves at both DNA-modified and unmodified electrodes. However, because of electrostatic

interactions with the negative sugar phosphate backbone, slight increases in voltammetric peak currents are observed at a DNA-modified GCE with DAF, and slight decreases are observed for FCA relative to responses at the unmodified GCE. At DNA-modified GCEs much larger peak currents are observed with the cobalt complexes relative to an unmodified GCE, and at higher concentrations of complex the curves plateau, suggesting saturation binding of the complexes to the immobilized DNA.

At a DNA-modified electrode FCA, DAF, and $Co(bpy)_3^{3+}$ have linear plots for i_p vs $v^{1/2}$, Figure 3.11. This suggests that mass transport of these complexes occurs through diffusion, and provides evidence that the DNA layer extends into solution. The DNA-bound complex dissociates from DNA to diffuse to the surface of the electrode and then reassociates with DNA following electron transfer between the complex and the electrode surface. $Co(phen)_3^{3+}$, in contrast, shows curvature past 100 mV/s. This can be attributed to its intercalative binding mode which can cause relatively slow dissociation of the complex from the immobilized DNA. This is consistent with intercalative binding, since it has been demonstrated that DNA intercalators, such as the phenanthridines and acridines associate with DNA in a two step process; fast (electrostatic) and slow (intercalative).[22]

Since evidence suggests that the DNA microenvironment extends into solution and that the electrodes does not see the bulk solution, the data from the calibration curve of peak current vs $Co(phen)_3^{3+}$ concentration for a DNA-modified GCE in Figure 3.9 can be fit to equation 17 to provide an estimate of the DNA concentration in the microenvironment near the electrode surface. The binding site size (n) and the association constant (K) can also be estimated. Since the Scatchard equation gives overestimates for association constants for

complexes with overlapping binding sites, the McGee-von Hippel equation (eq. 9) was used. The validity of this approach for quantitative purposes has not been established, but the comparison of Figures 3.12 and 3.13 shows that qualitatively similar behaviour is observed for binding of the complex in the immobilized DNA layer and binding of the complex to free DNA in solution. The association constants for $Co(phen)_3^{3+}$ with calf thymus DNA, poly(dG)poly(dC), and poly(dG)poly(dC) immobilized at a GCE vary by orders of magnitude. The association constants for the binding of $Co(phen)_3^{3+}$ with homogeneous poly(dG)poly(dC) and immobilized poly(dG)poly(dC) differ considerably; $K = 1.8 \times 10^5$, n= 4 bp and $K = 1.74 \times 10^3\ M^{-1}$, n= 5 bp, respectively. The association constant decreases by two orders of magnitude for the interaction of $Co(phen)_3^{3+}$ with immobilized poly(dG)poly(dC) in comparison to homogeneous poly(dG)poly(dC). This suggests that poly(dG)poly(dC) may have a different conformation when immobilized onto a planar surface than it has when free in solution, and that this affects its interactions with DNA-binding compounds.

Further evidence to support the different binding behaviour of $Co(phen)_3^{3+}$ to soluble vs immobilized DNA is found in the changes in formal potential. For homogeneous calf thymus DNA a +17 mV shift in formal potential is observed for $Co(phen)_3^{3+}$ relative to its formal potential in the absence of DNA. This is in contrast to the -27.5 mV shift observed at a poly(dG)poly(dC)-modified GCE relative to an unmodified GCE, shown in Figure 3.14b. A positive shift in formal potential suggests intercalative binding because the 2+ form binds more strongly, as indicated by equation 11. At a DNA-modified electrode the negative shift in formal potential indicates that the +3 form of the complex interacts more strongly and this implies that the binding of $Co(phen)_3^{3+}$ to immobilized DNA is more electrostatic in nature.

For $Co(bpy)_3^{3+}$ the shift in formal potential between bound and free complex for both a homogenous solution of DNA and surface immobilized DNA is negative, indicating that for both cases the binding is highly electrostatic. These results are in agreement with the observed decreases in the $Co(phen)_3^{3+}$ association constants upon DNA immobilization, and also suggests that the conformation of DNA free in solution is different than DNA immobilized onto a planar surface.

DNA-modified GCEs display consistently larger charging currents relative to unmodified GCEs. This is apparent in Figure 3.7, where voltammograms for an unmodified GCE and a poly(dG)poly(dC)-modified electrode are shown. The larger apparent capacitance of a DNA-modified electrode suggests a larger apparent electroactive surface area, and that DNA can behave as an electronic conductor (ie. electron transfer can occur between an electroactive species and DNA and between DNA and the electrode). This supports the conclusion of other researchers that DNA can act as an electronic "wire".[23] In this study photoinduced electron transfer from $Ru(phen)_3^{2+}$ to $Co(bpy)_3^{3+}$ or $Co(phen)_3^{3+}$ in the presence and absence of homogenous calf thymus DNA show that DNA enhances electron transfer rates in 84-90% glycerol by one to two orders of magnitude. Since all three complexes associate with DNA, it has been proposed that DNA is the intervening medium for long-range electron-transfer between these complexes.

Table 3.6 shows that the rates of heterogenous electron transfer from FCA, DAF, $Co(bpy)_3^{3+}$ and $Co(phen)_3^{3+}$ to glassy carbon electrodes are slower at a DNA-modified electrode relative to an unmodified electrode. Although DNA may act as a mediator for electron transfer between the redox active complex and the GCE, electron transfer by this

mechanism must be slow relative to direct electron transfer between the complexes and the GCE surface. This kinetic evidence indicates that the cobalt complexes participate in the electrochemical reactions both with DNA and with the electrode surface, after dissociation from the DNA and diffusion to the electrode surface.

FCA is electrostatically excluded from the DNA microenvironment at the surface of the electrode. Thus electron transfer must occur from a greater distance and/or may use DNA as a mediator. Both processes would result in lower electron-transfer rates. DAF is electrostatically attracted to DNA and thus has free access to the electrode surface. Its rate of electron transfer is only slightly affected by immobilization of DNA at the electrode surface. $Co(bpy)_3^{3+}$ and $Co(phen)_3^{3+}$ interact selectively with DNA. Both their electron transfer rates are substantially decreased by immobilization of DNA at the surface of the GCE. These observations imply that electron transfer occurs both via DNA and directly at the GCE but that the preferred mechanism is the direct reaction at the GCE surface.

A prototype sequence-selective DNA sensor was prepared using single-stranded oligo$(dT)_{20}(dG)_{98}$, where the $(dT)_{20}$ acted as the recognition sequence and was anchored to the electrode surface through the $(dG)_{98}$ tail sequence. The recognition sequence $(dT)_{20}$ is capable of forming hybrids with its complementary sequences oligo$(dA)_{20}$ and poly(dA). The excess dG tail was not expected to alter the probes ability to hybridize selectively, since it has been demonstrated that the addition of a poly(dA)-tail to a β-globin probe does not significantly alter its hybridization properties.[24] In this study a 20mer complementary to the β-normal sequence was synthesized with a 3'tail of $(dA)_{15}$. Dot blots were prepared using the β-normal gene and the β-globin gene. Denaturation of the complementary gene sequence with

the probe was accomplished at 64 °C and at 57-58 °C for the noncomplementary sequence regardless of whether the oligo$(dA)_{15}$ tail was present on the probe.

The results in Figure 3.18 show that the oligo$(dG)_{99}$ tail does not affect the ability of the recognition sequence oligo$(dT)_{20}$ to discriminate between complementary and noncomplementary sequences. The oligo$(dT)_{20}$oligo$(dG)_{99}$ probe hybridizes with poly(dA), oligo(dA), but not with poly(dA)(dT) or poly(dG)poly(dC). Apparently, the dG anchor does not participate in the recognition process and does not hybridize with poly(dC).

In this prototype sequence-selective DNA sensor reversible binding processes are important for the reusability of the sensor. It is important that the hybridization indicators bind reversibly with DNA and that the single-stranded probe can be regenerated after recognition of the target sequence. The hybridization indicators bind reversibly to DNA as indicated by the decrease in peak current to base line levels after a rinse in a high salt buffer. Denaturation of double-stranded DNA to regenerate the single-strand probe at the surface of the electrode was accomplished by a rinse in hot (100 °C) distilled H_2O for 10 minutes. Cycles of hybridization and denaturation (Figure 3.17) demonstrate the regeneration of the single stranded probe at the surface of the electrode, and the reusability and reliability of the sensor over 10 cycles.

3.4 Conclusions

DNA has been covalently immobilized onto oxidized glassy carbon electrodes using water soluble carbodiimide and hydroxysuccinimide reagents. This promotes coupling between surface carboxylic acid groups and guanine bases. Immobilized DNA was detected

voltammetrically with $Co(bpy)_3^{3+}$ $Co(phen)_3^{3+}$, two complexes which exhibit quasireversible one electron redox activity and associate selectively with double-stranded DNA.

Voltammetric peak currents obtained with a poly(dG)poly(dC)-modified GCE depend on $Co(bpy)_3^{3+}$ and $Co(phen)_3^{3+}$ concentrations in a nonlinear fashion and indicate saturation binding with immobilized DNA. Ferrocene derivatives which do not bind selectively to dsDNA yield linear calibration curves (i_p vs concentration) at both DNA-modified and unmodified electrodes. The electrostatic interactions with the polyanionic deoxyribose phosphate backbone of the immobilized DNA cause the voltammetric peak currents to increase for DAF and decrease for FCA relative to the responses observed at unmodified electrodes. Voltammetric peak currents for $Co(phen)_3^{3+}$ reduction were used to estimate the constant local DNA concentration at the modified electrode surface; a binding site size of 5 base pairs and and association constant of $1.74 \times 10^3\ M^{-1}$ yield 8.6 ± 0.2 mM base pairs. Increases in voltammetric peak separations at a DNA-modified electrode relative to an unmodified electrode indicate that heterogenous electron transfer is slower at DNA-modified glassy carbon electrodes. The linearity of the i_p vs $v^{1/2}$ plots at a DNA-modified GCE (Figure 3.11) sugggests that mass transport occurs through diffusion for DAF, FCA and $Co(bpy)_3^{3+}$, which suggests fast dissociation of the complex from the immobilized DNA. $Co(phen)_3^{3+}$ displays curvature past 100 mV which can be attributed to its intercalative binding mode. This results in slower dissociation of the complex from the immobilized DNA. The results from the electrochemical characterization of the DNA-modified GCE demonstrate the use of electroactive hybridization indicators in a DNA sensor.

Buffers containing K^+ or Li^+ ions were compared to optimize conditions for

immobilization of poly(dG)poly(dC) onto GCEs. Results indicated that the buffer containing potassium provided better reaction conditions.

Different electrochemical techniques were examined to optimize the sensitivity of the detection process. DPV gave the largest increases in peak current after immobilization of the GCE with poly(dG)poly(dC).

A prototype sequence-selective DNA sensor was developed by immobilizing a 20-mer oligo$(dT)_{20}$, following its enzymatic elongation with dG residues, which yielded the species oligo$(dT)_{20}(dG)_{99}$. Cyclic voltammograms before and after hybridization with either poly(dA) or oligo$(dA)_{20}$ show increased voltammetric peak currents after hybridization. The single-stranded probe is regenerated after rinsing the sensor in hot distilled water. These results demonstrate that this sensor can be used as a reusable sequence-selective biosensor for DNA.

3.5 References

1. Millan, K. M.; Spurmanis, A. J.; Mikkelsen, S. R.; *Electroanalysis*, **1992**, 4, 929-932.

2. Millan, K. M.; Mikkelsen, S. R.; *Anal. Chem.*, **1993**, 65, 2317-2323.

3. A. J. Bard, L. R. Faulkner, *Electrochemical Methods*, John Wiley & Sons, N. Y., **1980**, p 26-34.

4. Maki, N.; Tanaka, N.; *Encyclopedia of Electrochemistry of Elements*; Bard, A. J., Ed.; Marcel Dekker; New York, 1975, Vol. 3, pp 188- 210.

5. (a) Barton, J. K.; Goldberg, J. M.; Kumar, C., V.; Turro, N., *J. Am. Chem. Soc.*, **1986**, 108, 2081- 2088.

6. Barton, J. K., *Science*, **1986**, 233, 727.

7. Pyle, A. M.; Rehmann, J. P.; Meshoyrer, R.; Kumar, C. V.; Turro, N. J.; Barton, J. K.; *J. Am. Chem. Soc.*, **1989**, 111, 3051-3058.

8. Carter, M. T.; Rodriguez, M.; Bard, A. J., *J. Am. Chem. Soc.*, **1989**, 111, 8901.

9. McGee, J. D.; Von Hippel; *J. Mol. Biol.*, **1974**, 86, 469-89

10. Rosen, I.; Rishpon, J. *J. Electroanal. Chem.* **1989**, 258, 27.

11.Staros, J. V.; Wright, R. W.; and Swingle, D. M.; *Anal. Biochem.*, **1986**, 156, 220.

12. Reflectance spectroscopy was performed by Darren Lawless, Department of Chemistry and Biochemistry, Concordia University.

13. Sen, D.; Gilbert, W.; *Nature*, **1988**, 334, 364.

14. Sen, D.; Gilbert, W.; *Nature*, **1990**, 344, 6265.

15. Sen, D.; Gilbert, W.; *Biochemistry*, **1992, 31, 65.**

16. Cass, A. E. G.; Davis, G.; Francis, G.D.; Hill, H.A.O., Aston, W.J.; Higgins, I.J.; Plotkin, E. V.; Scott, L.D.L, Turner, A.P.F.; *Anal. Chem.* **1984**, 56, 667-671.

17. Spurmanis, Alexandrs, Chemistry 450 Honors Project (1990), Department of Chemistry and Biochemistry, Concordia University.

18. Nicholson, R. S.; *Anal. Chem.*, **1965**, 36,11,1351-1355.

19.Pullman, A.; Pullman, B.; *Q. Rev. Biophys.*, 1981, 14, 289.

20. Harley, John A.; Forrow, Stephen M.; Souhami, Robert L.; *Biochemistry*, **1990**, 29, 2985-2991.

21. Skoog, D. A.; Leary, J. J.; *Principles of Instrumental Analysis*, Fourth Ed., Saunder College Publishing, USA, **1992**, pp. 554-556.

22. Wakelin, L.P. G.; Waring, M.J.; *J. Mol. Biol.*, 1980, 144, 183.

23. Purugganan, M. D.,; Kumar, C. V.; Turro, N. J.; Barton J. K.; *Science*, 1988, 241, 1645.

24. Woodhead, J. Lesley; Malcolm, Alan D. B.; *Biochem. Soc. Trans.*, **1986**, 14, 1168.

Chapter 4
DNA Biosensors Based on Carbon Paste Electrodes

4.1 Introduction

Carbon paste electrodes (CPEs) are prepared with a mixture of graphite powder and an organic liquid, such as mineral oil, which is immiscible with contacting aqueous solutions.[1] The mixture is packed tightly into an electrode holder, and polished to a smooth finish. CPEs have low background currents, a wide potential window, surfaces which are easily renewable, are capable of miniaturization, and have a low cost. The graphite/mineral oil mixture can include additives which provide functional groups for convenient modification.[2] The number of functional groups at the surface of the electrode can be more easily controlled with CPEs than with GCEs, by manipulating the quantity of modifier in the graphite mixture. With the DNA sensors described in Chapter 3, DNA immobilization involves three steps: electrode oxidation, activation with coupling reagents, and coupling with DNA. All three are heterogeneous processes, and all may contribute to irreproducibility in the quantity of DNA bound to the surface. Control of the quantity of functional groups on the surface of the transducer should, in theory, improve the reproducibility of the coupling reaction.

For DNA immobilizations onto CPEs, two modifiers were tested: octadecylamine and stearic acid. Both species are hydrophobic and soluble in mineral oil. Stearic acid contains a terminal carboxylate functional group. Modification of a stearic acid CPE (SACPE) with DNA proceeds via the NHS-ester intermediate, which reacts selectively with dG residues.[3] Denaturation of the DNA to be immobilized is required to expose the guanine base to the

NHS-ester. Octadecylamine contains a terminal primary amine group. In the presence of a carbodiimide reagent, the primary amin110e will form a phosphoramidate bond with the 5'-terminal phosphate group of DNA. EDC, 1-[3-(dimethylamino)propyl]-3-ethylcarbodiimide hydrochloride has been used previously to immobilize DNA via its 5'-terminal phosphate group onto a secondary amine present on the surface of derivatized polystyrene microtiter wells.[4] Since the 5'phosphate is the reactive site on DNA, denaturation of DNA prior to immobilization is not required and also DNA of any sequence can be immobilized.

The method of detection of the target DNA is the same as that used with the glassy carbon DNA-sensors. Three hybridization indicators were chosen for studies with the carbon paste electrodes; tris (1,10 phenanthroline) cobalt(III), $Co(phen)_3^{3+}$, tris(2,2'-bipyridyl)cobalt(III), $Co(bpy)_3^{3+}$, and tris(2,2'-bipyridyl)osmium(II)',$Os(bpy)_3^{2+}$. The first step in the development of a CPE-based DNA biosensor was to optimize the immobilization procedure. This consisted of determining the optimum quantity of modifier in the graphite paste mixture, the concentration of DNA which provided the greatest signals, and the effects of Li^+ and K^+ counterions in the immobilization buffers (cf. Section 3.1). The formation of G4-DNA may have an influence on the yield of immobilization of guanosine residues onto carboxylate groups on SACPE.[5,6,7]

Electrochemical characterizations of the DNA-modified CPEs were carried out by cyclic voltammetry (CV). A reversibly electroactive, diffusing species produces asymmetric voltammetric peaks. The peak current, i_p is proportional to the square root of the scan rate, $v^{1/2}$ as indicated by the Randles-Sevçik equation (Equation 1).

$$i_p = (2,69\times10^5)\, n^{3/2} A D^{1/2} \nu^{1/2} C \qquad (1)$$

In contrast Guassian-shaped voltammetric peaks indicate adsorption of the redox-active species at the electrode surface and a linear plot of i_p vs ν is observed.[8] Equations 2 and 3 show this relationship for an adsorbed species:

$$i_p = \frac{n^2 F 2}{4RT} \nu A \Gamma^* \qquad (2)$$

$$\Gamma^* = \Gamma_o(t) + \Gamma_R(t) \qquad (3)$$

where i_p is peak current, n is the number of electrons transferred in the redox process, F is the charge of one mole of electrons, R is a constant, T is temperature, ν is scan rate (mV/s), A is surface area of the electrode, $\Gamma_o(t)$ and $\Gamma_R(t)$ are the amounts of oxidized and reduced species adsorbed at time t (mol/cm^2). For an adsorbed species the peak potential is described by equation 4[8]:

$$E_p = E^{o\prime} - \frac{RT}{nF} \ln \frac{b_o}{b_r} \qquad (4)$$

where b_o and b_r are relative strengths of adsorption of the oxidized and reduced species, respectively. For an ideal Nernstian reaction under ideal Langmuir isotherm conditions, $E_{p,c}=E_{p,a}$. The relative strengths of adsorption of the oxidized and reduced species are found by the location of E_p with respect to $E^{o\prime}$. If the oxidized species is adsorbed more strongly than the reduced species ($b_o>b_r$) a postwave can result. If the reduced species is adsorbed more strongly ($b_r>b_o$) then a prewave may be observed. The effects of adsorption of the redox-

active species on the electrochemical response range from complete inactivation of the electrode response to catalytic enhancement of the heterogenous electron transfer reaction, to the appearance of a new electrochemical process.[1]

The adsorption of an electroinactive substance on an electrode surface can inhibit or completely block heterogenous electron transfer between the electrode and a redox-active compound. If the adsorbed species blocks electron transfer, the reaction must proceed at the uncovered surface of the electrode. If it inhibits the electrode process then the redox-active species must penetrate the adsorbed layer or transfer electrons through the film. Adsorption of electroinactive species can also facilitate the electrode reaction by double-layer effects.[9]

For SACPE immobilization occurs via deoxyguanosine residues. An oligo$(dT)_{18}$ probe was coupled to a SACPE via its $(dG)_{18}$ tail, in order to investigate the hybridization and denaturation properties of the CPE-immobilized probe. Denaturation is achieved by breaking the hydrogen bonds between complementary bases. This can be accomplished by raising the temperature higher than the melting temperature of the DNA heteroduplex or by adding a denaturant such as urea or guanidinium HCl.[10] The reusability of CPE-based DNA sensors was investigated using these denaturants. The regeneration of reproducible signal responses for the single-stranded probe and for the hybridized probe is crucial for a reusable DNA-sensor.

In addition to the transition metal DNA-binding complexes, a daunomycin-glucose oxidase conjugate was tested for use as a hybridization indicator. This conjugate combines the selectivity for dsDNA of a DNA intercalant with the catalytic properties of a redox enzyme. Daunomycin is an aromatic dye which selectively interacts with DNA through

intercalation.[11] Glucose oxidase (GOx) is an enzyme which catalyzes the oxidation of glucose to gluconolactone in the following reaction:

$$\text{Glucose} + O_2 \rightarrow \text{Gluconolactone} + H_2O_2.$$

The enzyme contains two molecules of flavin adenine dinucleotide which are responsible for its redox properties. Ferrocene is an excellent mediator for glucose oxidase. It exhibits a reversible redox behaviour with $E_{½}$ = 0.165 V vs SCE. In the presence of glucose and ferrocene the following reactions occur:

$$\text{Glucose} + GOx_{ox} \rightarrow GOx_{red} + \text{gluconolactone}$$

$$GOx_{red} + 2\ \text{Ferrocene}^+ \rightarrow GOx_{ox} + 2\ \text{Ferrocene} + 2H^+$$

$$2\ \text{Ferrocene} \rightleftharpoons 2\ \text{Ferrocene}^+ + 2e^- \text{ (at the electrode)}$$

Thus the reversible electron transfer step between ferrocene and the electrode, in which ferrocene is oxidized, is followed by a catalytic reaction which regenerates the reduced form of ferrocene. For this scheme the pseudo first order rate constant of the catalytic reaction, k_{cat} is large compared to a, where a = nFV/RT. Thus, the reduced ferrocene is continually replenished at the electrode producing a limiting or plateau current.[12]

The daunomycin-GOx conjugate was prepared by covalently binding the primary amine group of daunomycin to the free carboxylic acid groups on the surface of GOx. These conjugates were prepared and characterized previously in this laboratory.[13,14]

4.2 Results

4.2.1 Octadecylamine-Incorporated Carbon Paste Electrodes

Figure 4.1 shows three voltammograms for octadecylamine CPEs (ODA-CPE) at

0.12 mM $Os(bpy)_3^{2+}$ at an unmodified ODA-CPE (5% ODA w/w), an ODA-CPE modified with poly(dT), and the same poly(dT)-modified electrode after hybridization with poly(dA). The resulting peak currents were 1.15 μA, 2.12 μA, and 5.18 μA, respectively. Note the differences in the shapes of the voltammograms. The voltammogram for the unmodified ODA-CPE is asymmetric, with a ΔE_p of 92 mV. When ssDNA is immobilized ΔE_p is 72 mV and upon hybridization ΔE_p decreases to 42 mV and the peak shapes become more Gaussian. This suggests that the redox-active species are bound to the DNA very close to the surface of the electrode. This may be due to the adsorption of dsDNA at the CPE surface. Peak currents were measured as a function of scan rate to determine if adsorption occurs. Figure 4.2 shows that at an unmodified ODA-CPE, linear plots of i_p vs. $v^{1/2}$ are obtained for 0.12 mM $Os(bpy)_3^{2+}$ for scan rates between 0 and 100 mV/s ($y = 0.088 + 0.13$, $R = 0.9999$). At scan rates greater than 100 mV/s i_p levels off at greater scan rates. At a DNA-modified electrode upward curvature is observed for i_p vs $v^{1/2}$ and the plot of i_p vs v levels off at higher scan rates. Figure 4.3 shows the plot of i_p vs v for an unmodified and a DNA-modified ODA-CPE. These results suggests that the electrochemical behaviour of $Os(bpy)_3^{3+}$ is intermediate between diffusion-limited and the totally adsorbed cases at a DNA-modified CPE.

The ODA content of the CPEs was varied from 0.4% to 4% (w/w), while the concentration of denatured poly(dG)poly(dC) was held constant at 1 mg/mL. No voltammetric peaks were detected for $Co(bpy)_3^{3+}$ or $Co(phen)_3^{3+}$ reductions at any concentration within the range of 0.05 to 0.25 mM complex. After a 30 min incubation in 0.12 mM $Os(bpy)_3^{2+}$ anodic peak currents of 5.1 μA, 8.8 μA, and 7.0 μA were obtained for a poly(dG)poly(dC)-modified CPE with 0.4%, 0.8%, and 4% ODA, respectively. For calf

thymus DNA-modified CPEs 30 minute incubations in 0.12mM $Os(bpy)_3^{2+}$ gave anodic peak currents of 6.8 ± 0.8 μA (n=6), 6 ± 2 μA (n=2), 6.9 ± 0.9 μA (n=4) for 0.5%, 0.8%, and 2.0% (w/w) octadecylamine. At octadecylamine concentrations higher than 0.5% inconsistent results were obtained at unmodified and DNA-modified ODA-CPEs. Frequently no anodic peaks were generated at either the unmodified or the DNA modified ODA-CPEs for $Os(bpy)_3^{2+}$.

Two possible causes of these effects are (1) octadecylamine exchange for a bipyridine or phenanthroline ligand and (2) octadecylamine blockage of the surface electrode reaction. To determine whether electrode fouling was occuring, ferrocene carboxylic acid (FCA) was used as a probe. At CPEs without a modifier the anodic peak currents for 0.12 mM ferrocene carboxylic acid were observed throughout time following the addition of a saturated solution of ODA. A decrease in peak current was observed until no peak current was observed at all. Figure 4.4 shows two voltammograms at t=0 and at t= 22.45 hours. The voltammogram produced in the absence of ODA demonstrates a quasireversible diffusing species, $\Delta E_p = 74$. In the presence of ODA after 22.5 hours the separation of anodic and cathodic peaks becomes larger. The shape of the peaks become broad and less well-defined, characteristic of irreversible behaviour. These results suggest that octadecylamine fouls the CPE surface.

The ODA content of the CPEs was held constant at 0.4% and poly(dG)poly(dC) concentrations were varied to optimize DNA immobilizations. Figure 4.5 gives the anodic peak currents for 0.12 mM $Os(bpy)_3^{2+}$, where increased peak currents were observed at higher DNA concentrations. At concentrations of 1 and 2 mg/mL gelatinous strands were observed on the surface of the electrode after rinsing with buffer.

Polyacrylamide gel electrophoresis (Figure 4.6) showed that poly(dA) incubated with EDC, under the same buffer conditions used for immobilization, at 4 °C for 24 hours migrated more slowly through the polyacrylamide gel than poly(dT) not exposed to EDC

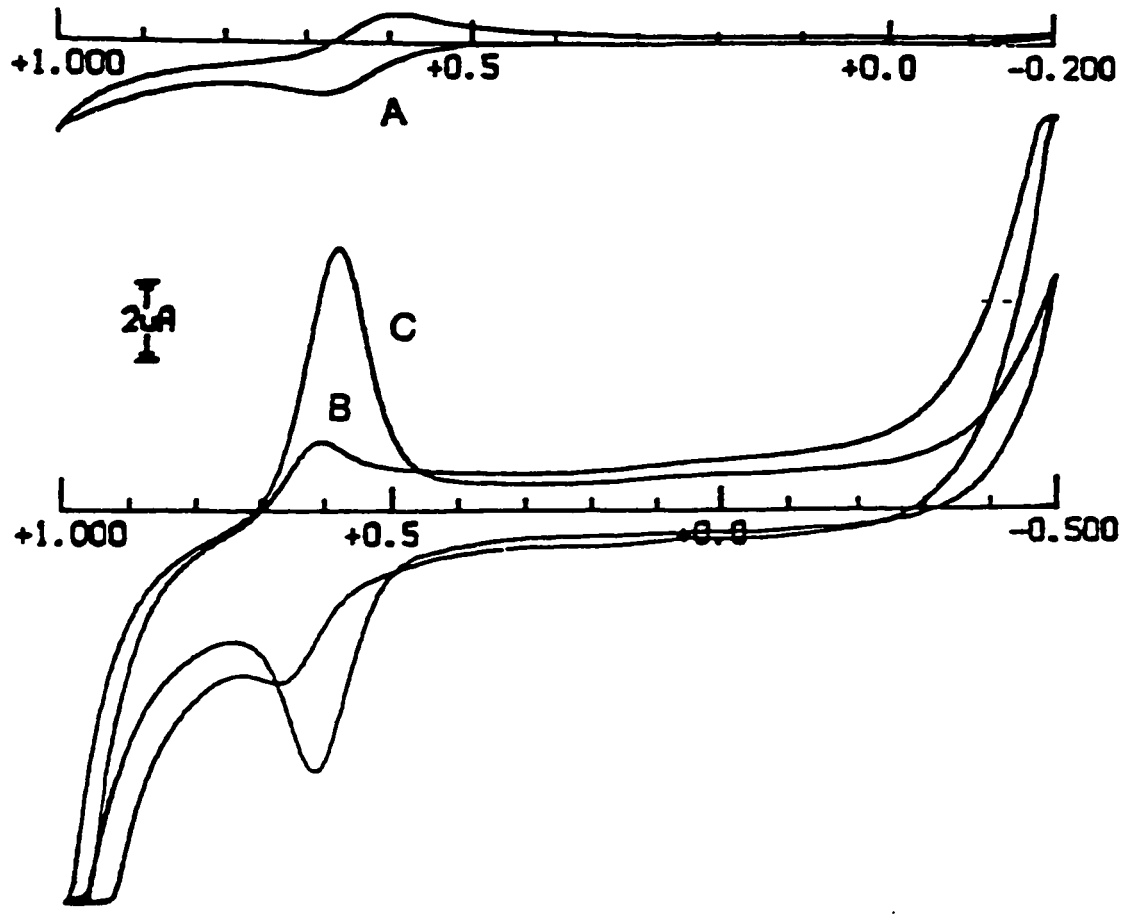

Figure 4.1 Cyclic voltammograms of DNA-modified ODA-CPEs (5% ODA) at 0.12 mM $Os(bpy)_3^{2+}$, 5 mM Tris pH 7.1, 20 mM NaCl, scan rate 50 mV/s (A) unmodified, (B) ODACPE modified with poly(dT), and (C) After hybridization with poly(dA).

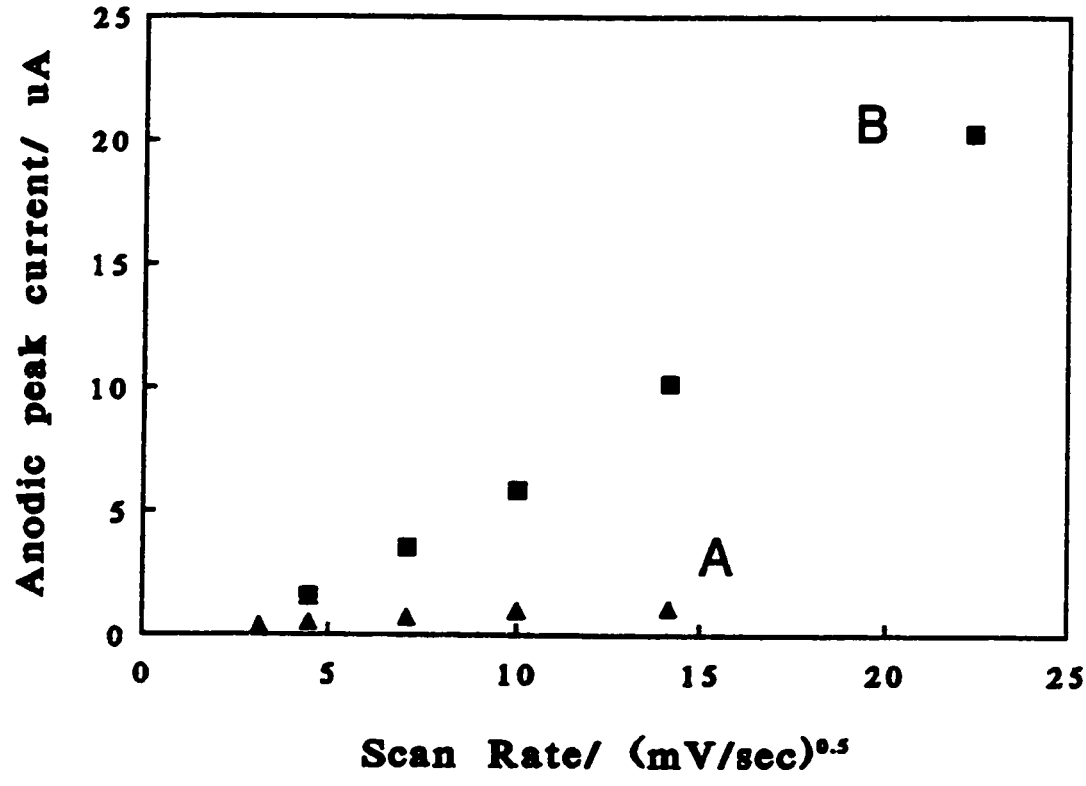

Figure 4.2 Anodic peak currents for 0.12 mM $Os(bpy)_3^{2+}$ as a function of the square root of scan rate for (A) an unmodified ODA-CPE (5% ODA) and (B) for a poly(dG)-poly(dC)-modified ODA-CPE (5% ODA). Conditions same as in Figure 4.1.

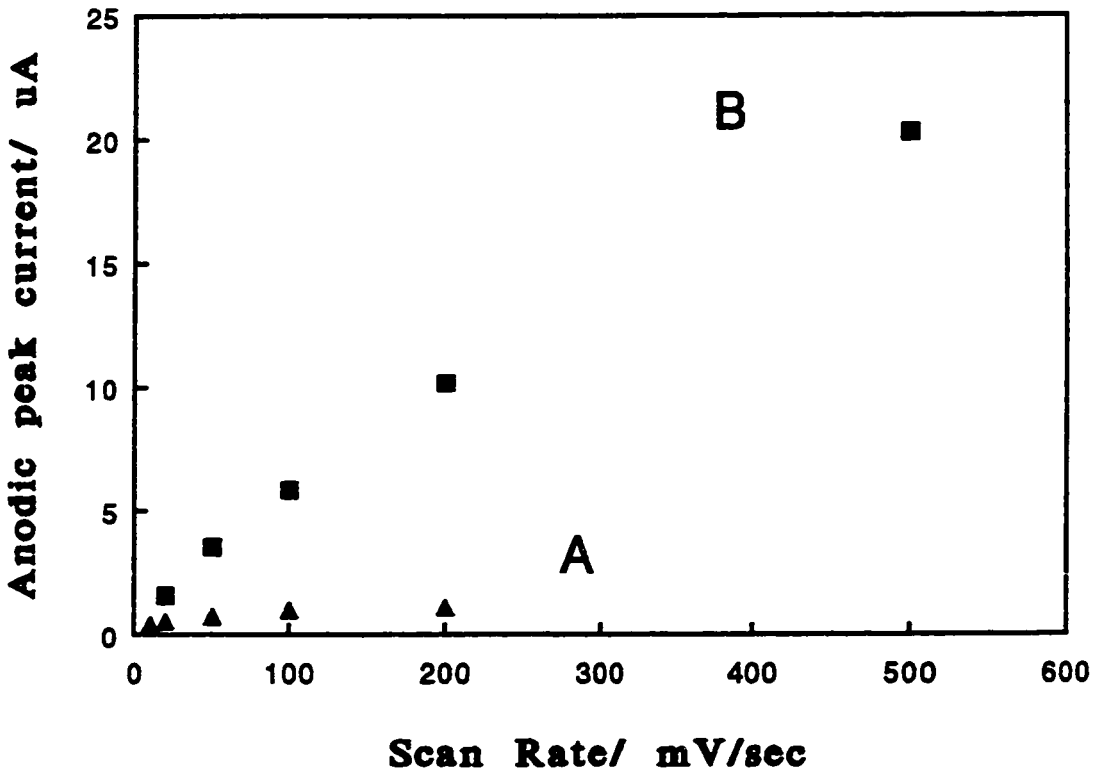

Figure 4.3 Anodic peak currents for 0.12 mM $Os(bpy)_3^{2+}$ as a function of scan rate for (A) an unmodified ODA-CPE (5% ODA) and (B) for a poly(dG)-poly(dC)-modified ODA-CPE (5% ODA). Conditions same as in Figure 4.2.

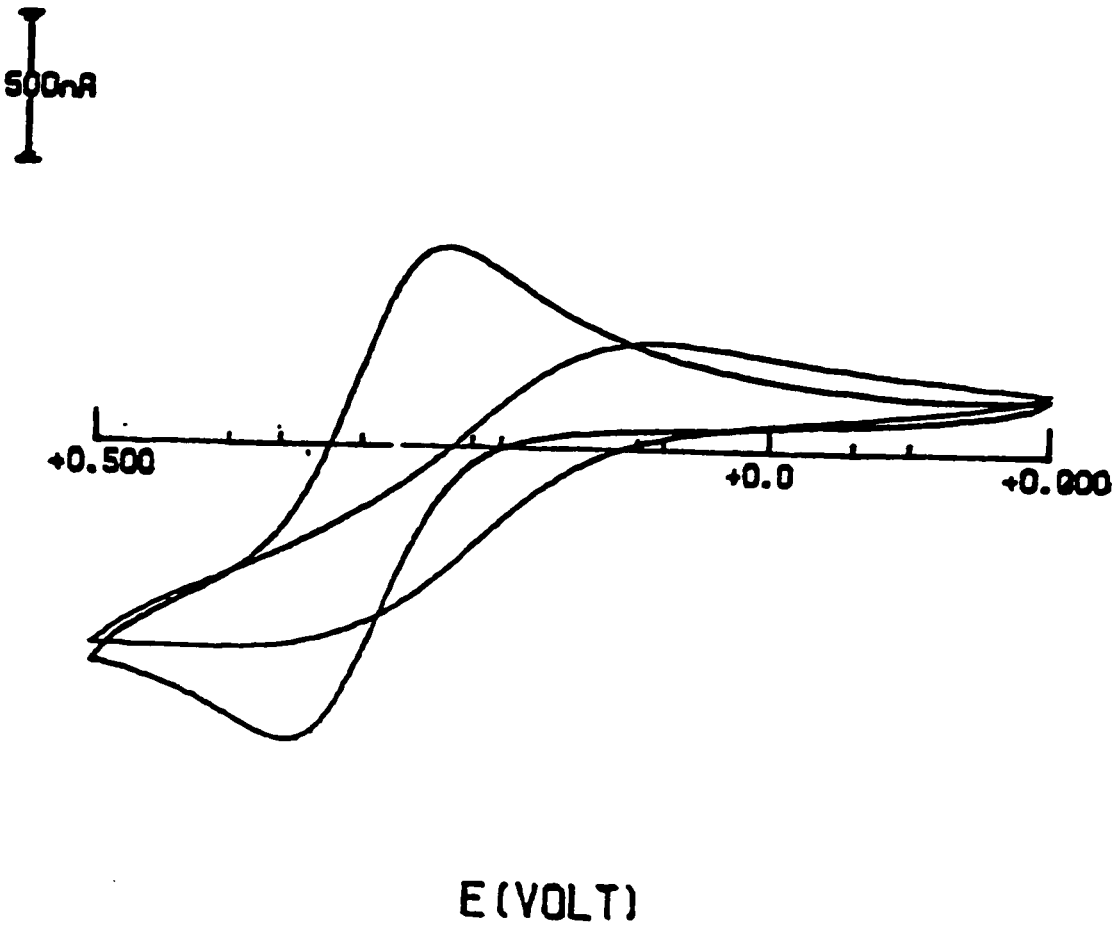

Figure 4.4 Cyclic voltammograms at 0.12 mM FCA, 5 mM Tris pH 7.1, 20 mM NaCl, scan rate 50 mV/s in the presence of ODA at (A) t= 0 and (B) t= 22.45 hours.

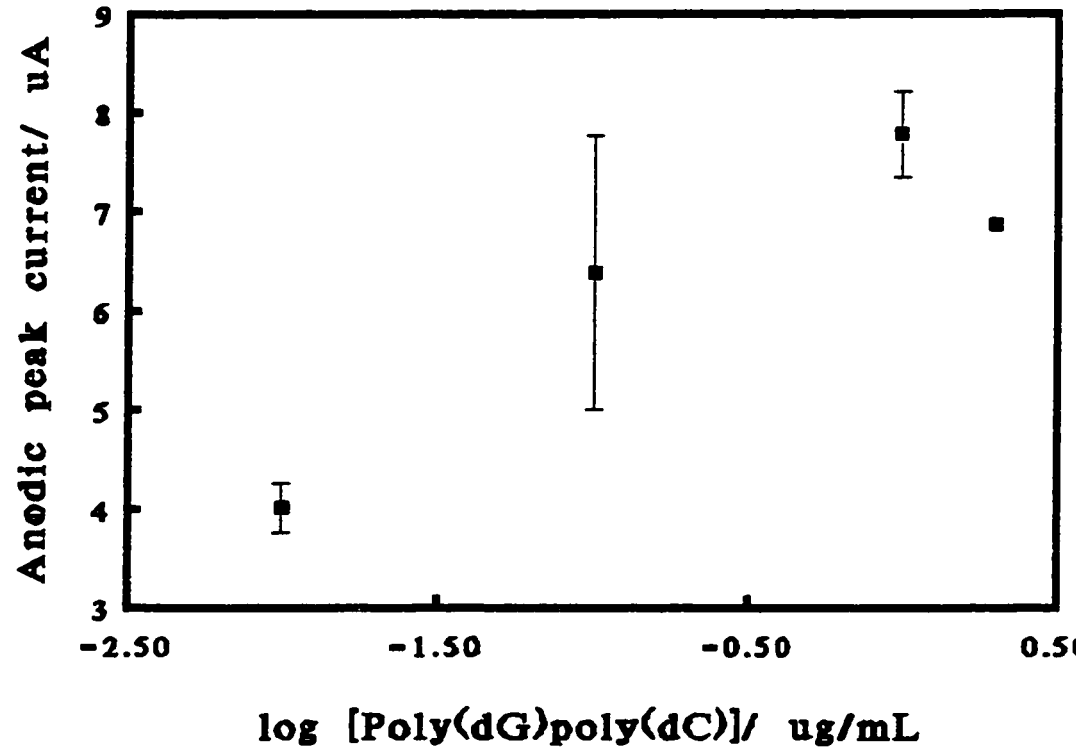

Figure 4.5 Anodic peak currents were measured at 0.12 mM $Os(bpy)_3^{2+}$ for ODA-CPEs (0.5% ODA) immobilized with varying concentrations of denatured poly(dG)poly(dC). Conditions the same as in Figure 4.1 (n=3, 3 different immobilizations).

This indicates that the DNA exposed to EDC is of higher molecular weight than before exposure to EDC which suggests that phosphodiester bonds are formed between the 5'-phosphate of one strand and the 3'hydroxyl of another. Polymerization of the DNA at the electrode surface eliminates this method for immobilizing DNA at the electrode surface for use in a DNA biosensor.

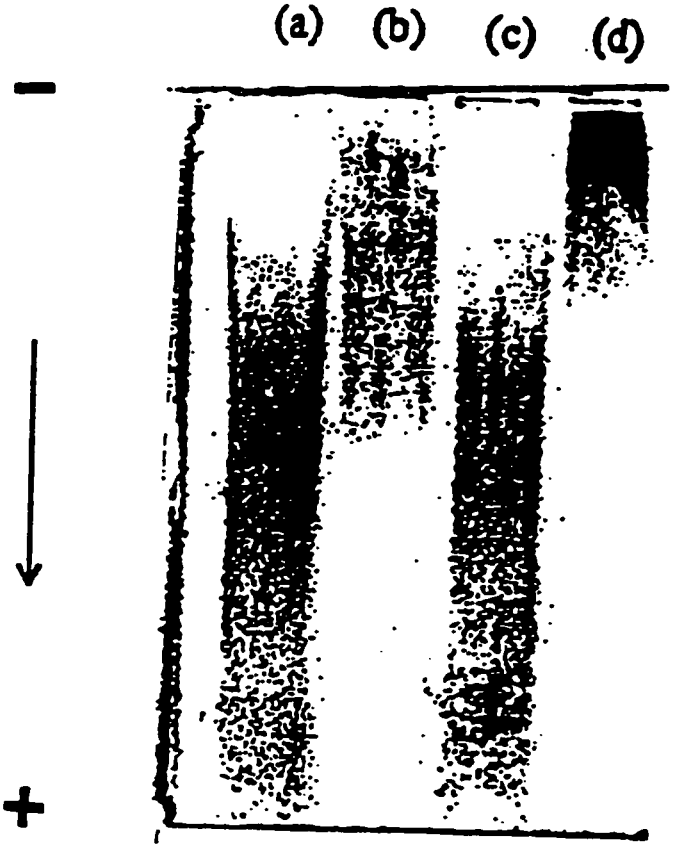

Figure 4.6 Poly(dT) in the presence and absence of EDC, separated by 5% polyacrylamide gel electrophoresis. Lane (a) 10 μL of 2 mg/mL poly(dT), (b) 10 μL of 2 mg/mL poly(dT) incubated with 0.2 M EDC, (c) 20 μL of 2 mg/mL poly(dT) (d) 10 μL of 2 mg/mL poly(dT) incubated with 0.2 M EDC. The average length of the initial poly(dT) mixture (curves a and c) was 4000 bases.

4.2.2 **Stearic Acid Modified Carbon Paste Electrodes (SACPEs).**

Stearic acid incorporated into the graphite/mineral oil mixture provides carboxylic acid groups on the surface ofthe CPE. These SACPEs can be activated by EDC and NHS to an NHS-ester which is reactive to deoxyguanosine residues. Optimum conditions for the coupling of denatured poly(dG)poly(dC) to SACPEs were determined by first varying the stearic acid concentration while maintaining the poly(dG)poly(dC) concentration constant. Figure 4.7 shows the cathodic peak currents for the reduction of 0.12 mM $Co(phen)_3^{3+}$ at SACPEs modified with 1 mg/mL denatured poly(dG)poly(dC) with varying percent stearic acid. An optimum was achieved with 4.5% stearic acid (w/w) in the graphite paste.

Using 4.5% stearic acid in the carbon paste mixture, the concentration of poly(dG)poly(dC) was varied from 1 μg/mL to 1mg/mL. The peak currents are normalized for day-to-day variation in the immobilization yields; the absolute magnitudes of the peak currents vary considerably. Table 1 shows these day-to-day variations for different concentrations of DNA tested. Peak currents are normalized to the maximum value obtained on a given day, which was assigned a value of 100%. These results are shown in Figure 4.8, as a plot of normalized peak current versus the logarithm of the concentration of poly(dG)poly(dC). The optimum concentration for poly(dG)poly(dC) immobilization was 10 μg/mL. A comparison of voltammograms from an unmodified SACPE and a DNA-modified SACPE under optimum conditions (4.5% stearic acid, 10 μg/mL) are shown in Figure 4.9.

Immobilizations at a 4.5% stearic acid CPE with 10 μg/mL poly(dG)poly(dC) were attempted with two phosphate buffers at pH 6.8, containing either Li^+ or K^+ counterions at 60 mM concentration. G4-DNA or any higher ordered deoxyguanosine structures should not

Table 4.1 DNA Concentration Studies
Day to Day Variation of Signal[1]

[G-C]mg/mL	1	0.1	0.03	0.01	0.003	0.001
$i_{p,c}$ Day 1	8.91	11.86		17.10		
$i_{p,c}$ Day 2	7.08	10.91	5.20	6.82		
$i_{p,c}$ Day 3	4.90		6.40	6.70		4.2
$i_{p,c}$ Day 4		3.78		17.86	9.47	

[1] Variations in response to 0.12 mM $Co((phen)_3^{3+}$ for different concentrations of poly(dG)poly(dC), [G-C]. Immobilization conditions: 1 mg/mL EDC, 2 mg/mL s-NHS in phosphate buffer pH 6.8.

form in the presence of Li^+ but should form in the presence of K^+ [5-7]. With SACPEs immobilizations of poly(dG)poly(dC) with the Li^+ containing buffer, cathodic peak currents of 7.3 ± 1.6 μA (n= 3) at 0.12 mM $Co(phen)_3^{3+}$ were observed. With K^+ present in the immobilization buffer the peak current was 4.5 ± 0.6 μA (n= 2).

The shapes of the voltammograms obtained at the unmodified SACPEs suggests diffusion of the redox-active species. For the DNA-modified electrodes the Guassian peak shapes suggests adsorption, as was observed for the ODA-CPE. A decrease in ΔE_p is observed for all three complexes at DNA-modified SACPEs. At the unmodified SACPE ΔE_p is 78 mV, 67 mV, and 78 mV for 0.12 mM $Co(bpy)_3^{3+}$, $Co(phen)_3^{3+}$, and $Os(bpy)_3^{2+}$, respectively. At a poly(dG)poly(dC)-modified CPE ΔE_p is 44 mV, 50 mV, and 60 mV, for these complexes, respectively.

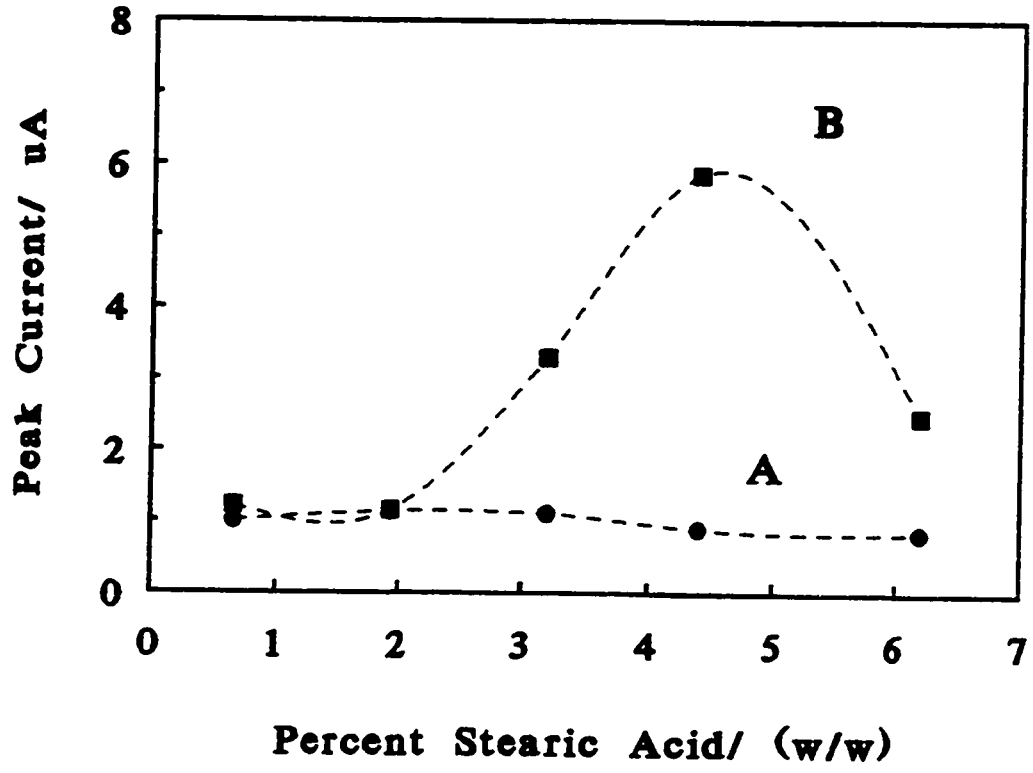

Figure 4.7 Cathodic peak current for 0.12 mM $Co(phen)_3^{3+}$ as a function of percent stearic acid in CPE (A) before and (b) after modification with denatured poly(dG)-poly(dC). Conditions: 5 mM Tris pH 7.1, 20 mM NaCl, 50 mV/s.

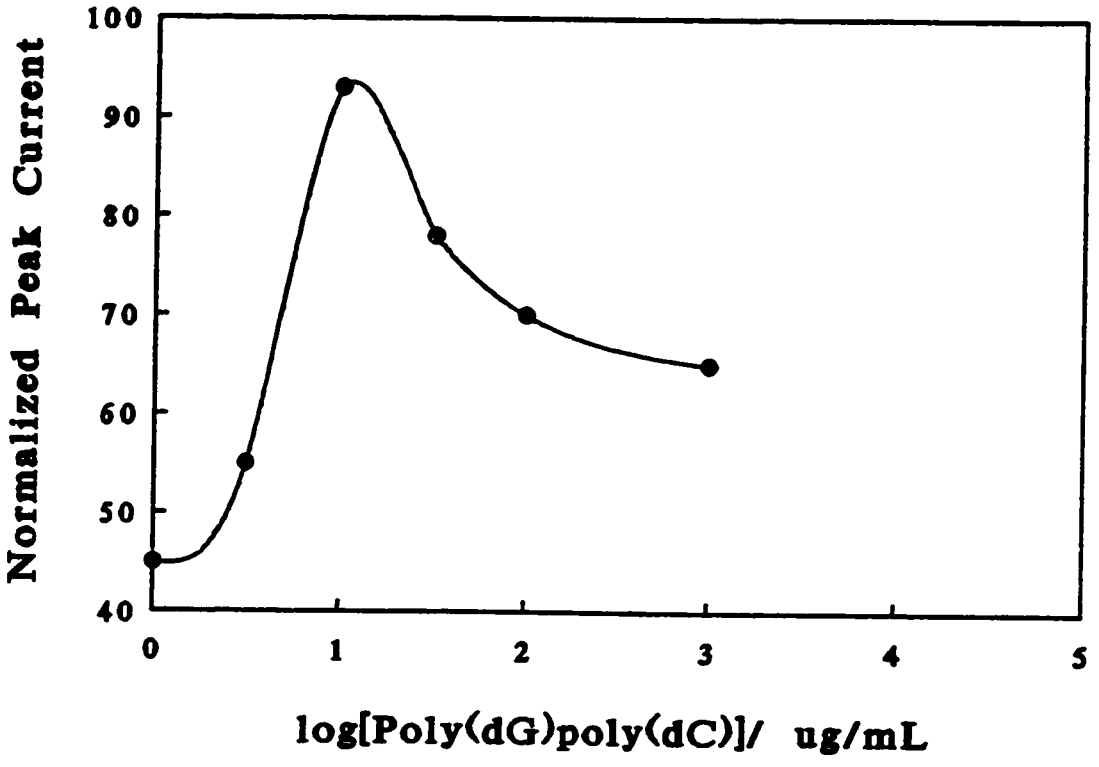

Figure 4.8 Normalized peak current as a function of concentration of denatured poly(dG)poly(dC) used for immobilizations onto SACPEs. Conditions: 0.12 mM $Co(phen)_3^{3+}$, 5 mM Tris pH 7.1, 20 mM NaCl, 50 mV/s.

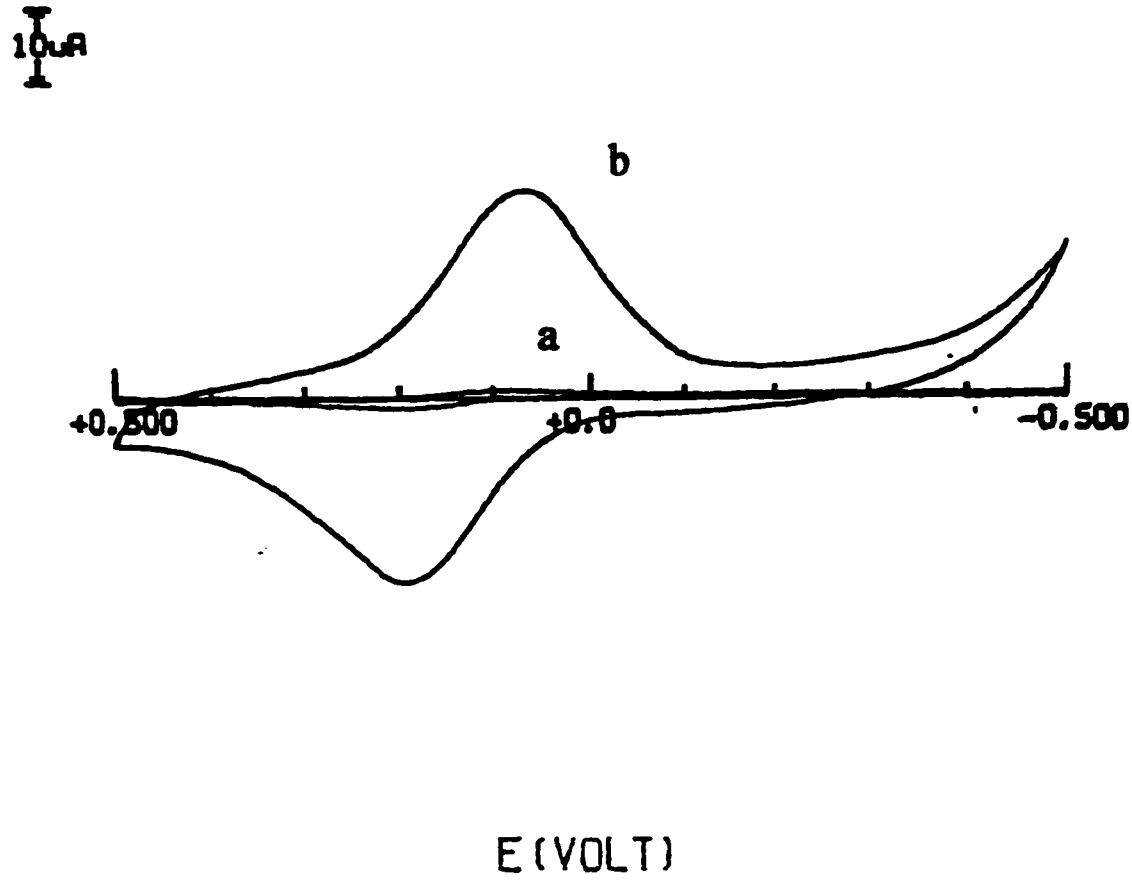

Figure 4.9 Cyclic voltammograms of (A) an unmodified and (B) a poly(dG)poly(dC)-modified SACPE at 0.12 mM $Co(phen)_3^{3+}$, 5 mM Tris pH 7.1, 0.020 M NaCl, scan rate 50 mV/s.

Peak currents were measured as a function of scan rate over the 10 to 200 mV/s range for $Co(bpy)_3^{3+}$, $Os(bpy)_3^{2+}$, and $Co(phen)_3^{3+}$, at an unmodified and a DNA-modified CPE as shown in Figure 4.10. Plots of peak current vs the square root of scan rate show upward curvature, at scan rates below 200mV/s, as shown in Figure 4.10. At scan rates above 200 mV/s the curves level off. The plots of i_p vs $v^{1/2}$ for unmodified SACPEs are linear for all three complexes which indicate diffusional behaviour. For $Os(bpy)_3^{2+}$ y= 0.23x -0.25, R= 0.995 , y= 0.14x - 0.14, R= 0.991 for $Co(bpy)_3^{3+}$ and for $Co(phen)_3^{3+}$ (y= 0.12 + 0.11, R= 0.997 for the unmodified SACPEs. In plots of i_p vs v the curves for all three complexes level off at higher scan rates, as shown in Figure 4.11. These results indicate that the behaviour of these three DNA-binding complexes is intermediate between diffusion and adsorption at a DNA-modified SACPE.

The shift in formal potential for a Nernstian redox reaction between a DNA-modified electrode and an unmodified electrode has been employed to determine the electrostatic and intercalative components of the binding of the electroactive hybridization indicators to immobilized DNA.[15] Table 4.2 summarizes the changes in formal potential for the three transition metal complexes upon DNA modification of a SACPE.

An oligo$(dT)_{18}$ probe was enzymatically elongated with deoxyguanosine residues with terminal deoxynucleotidyl transferase. Polyacrylamide gel electrophoresis showed that there were two main oligonucleotide products of this reaction, a 84 ± 2 base oligo$(dT)_{18}$oligo$(dG)_{66}$ and a 51 ± 2 base oligo$(dT)_{18}$- oligo$(dG)_{33}$, and some high molecular weight substances which can be attributed to the enzyme itself. Table 4.3 provides the migration distance of these products. The calibration of the molecular weight standards gave a linear response for

migration distance versus the logarithm of number of bases ($y = -34.76x + 100.55$, $R = 0.99$). The oligo$(dG)_x$ provided an anchor for the oligo$(dT)_{18}$ probe. Figure 4.12 shows calibration curves of peak currents for a 4.5% SACPE unmodified, modified with oligo$(dT)_{18}$-oligo$(dG)_x$, and the oligo$(dT)_{18}$ modified CPE hybridized to oligo$(dA)_{20}$, for $Co(phen)_3^{3+}$ concentrations between 0.01mM and 0.3 mM. A slight increase in peak current is detected at all concentrations of $Co(phen)_3^{3+}$ for the oligo$(dT)_{18}$-modified electrode. But a much larger increase is observed when the probe is hybridized to its complementary sequence. This shows that $Co(phen)_3^{3+}$ can discriminate between ssDNA and dsDNA immobilized at a carbon paste electrode.

The reusability of the SACPE based DNA sensor was investigated. Three methods routinely used for the denaturation of DNA to its single-stranded form were tested. A hot rinse in distilled water which was successful in denaturing the hybridized target with the glassy carbon based DNA-sensor[3], was not effective with the carbon paste electrode. A rinse in 100 °C distilled water caused the carbon paste matrix to break apart. A hot rinse in 70 °C for 30 minutes was sufficient to have the peak currents return to the same magnitude as that for the original probe-modified CPE. For repeated hybridization /denaturations cycles, ΔE_p increased from 62mV to 194mV after the second complete cycle. The signal upon the third cycle of rehybridization with a complementary sequence increased to 6.3 μA from the first hybridization of 2.83 μA. Figure 4.13 shows the voltammograms obtained with this electrode after the second hybridization, second regeneration, and third hybridization steps.

Other routinely used methods for denaturation are rinsing in 8M urea or 8M guanidinium HCl[10]. These methods were not compatible with maintaining an intact carbon

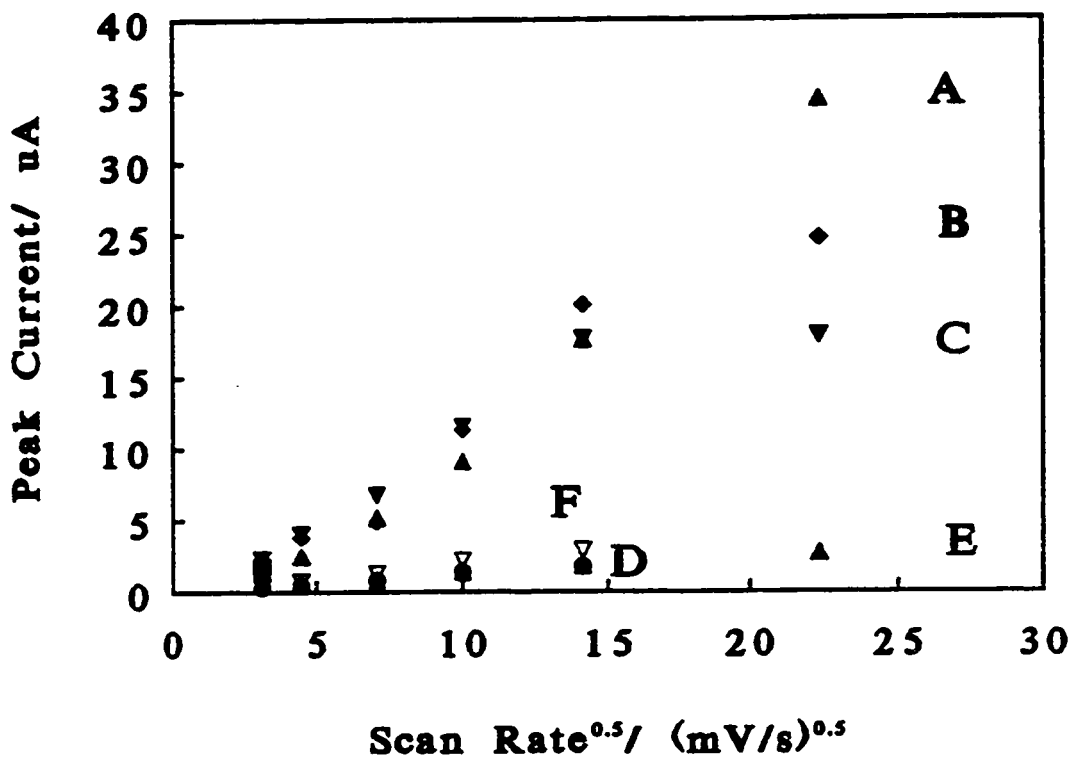

Figure 4.10 Peak current vs the square root of scan rate at DNA-modified SACPEs for (A) ● $Co(bpy)_3^{3+}$, (B) ■ $Co(phen)_3^{3+}$ (C) ▲ $Os(bpy)_3^{2+}$ and at unmodified SACPEs (D) ● $Co(bpy)_3^{3+}$, (E) ▲ $Os(bpy)_3^{2+}$, (F) ▽ $Co(phen)_3^{3+}$. Conditions 0.12 mM complex, 5 mM Tris pH 7.1 and 20 mM NaCl.

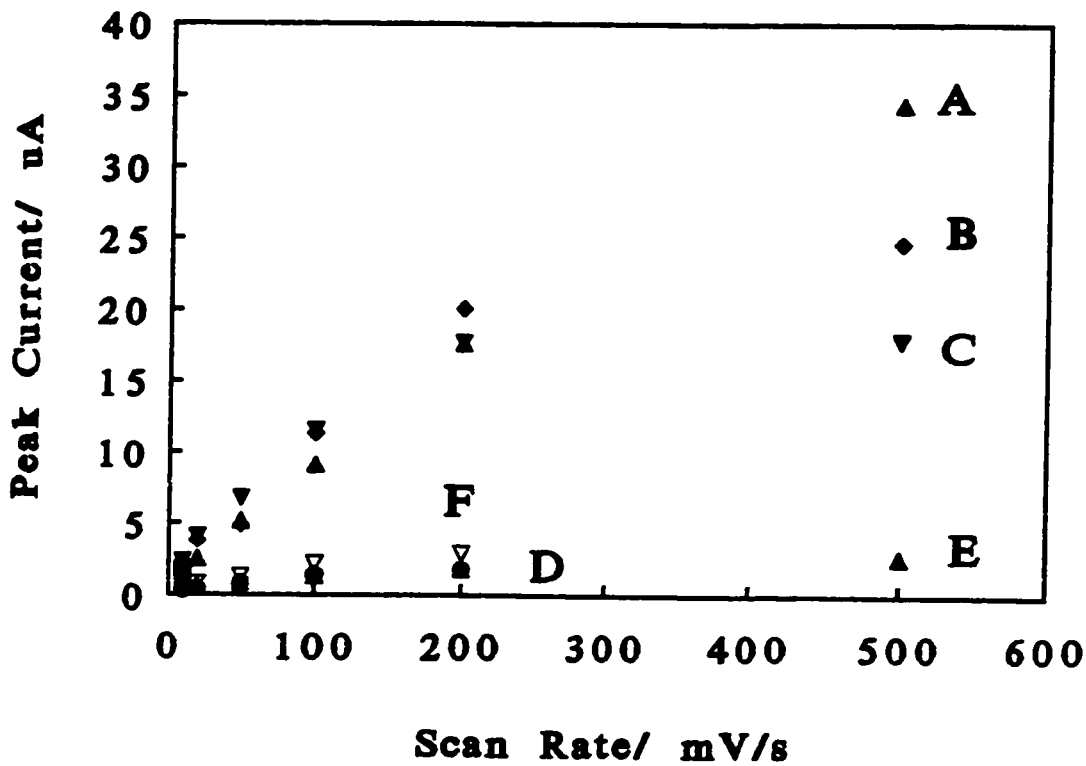

Figure 4.11 Peak current vs the scan rate at DNA-modified SACPEs for (A) $Co(bpy)_3^{3+}$, (B) $Co(phen)_3^{3+}$ (C) $Os(bpy)_3^{2+}$ and at unmodified SACPEs (D) $Co(bpy)_3^{3+}$, (E) $Os(bpy)_3^{2+}$, (F) $Co(phen)_3^{3+}$. Conditions 0.12 mM complex, 5 mM Tris pH 7.1 and 20 mM NaCl

Table 4.2 The shift in $E^{\circ\prime}$ between an unmodified and a DNA-modified SACPE

Complex	unmodified (mV)	DNA-modified (mV)	Shift in $E^{\circ\prime}$ (mV)
$Co(bpy)_3^{3+}$	132	121.4	-10.6
$Os(bpy)_3^{2+}$	639.4	674.2	+34.8
$Co(phen)_3^{3+}$	169.75	218.5	+49.2

Table 4.3 The major bands from a terminal transferase reaction with oligo$(dT)_{18}$

Corrected Position of Each Band	Percent Area	Molecular Weight
13.73	16.55	314.56
33.74	12.38	83.57
41.17	19.61	51.08

paste surface. This suggests that the mechanical stability of the carbon paste does not permit its use in a reusable DNA-sensor unless other, less extreme, methods can be developed for regeneration of the single-stranded probe at the surface of the electrode.

There were many problems associated with carbon paste electrodes for use in this type of DNA sensor. For both ODA-CPEs and SACPEs the peak currents and peak potentials for $Co(bpy)_3^{3+}$, $Co(phen)_3^{3+}$, and $Os(bpy)_3^{2+}$ were not stable through time. At unmodified and DNA-modified SACPEs peak currents decreased, resistances increased, and peak separations increased through time. Table 4.4 provides the peak current, ΔE_p, and resistance at various times for different CPEs incubated in $Co(bpy)_3^{3+}$ and ferrocenemethanol. A 4.5% SACPE incubated in ferrocenemethanol at 25 °C was observed through time to determine if the

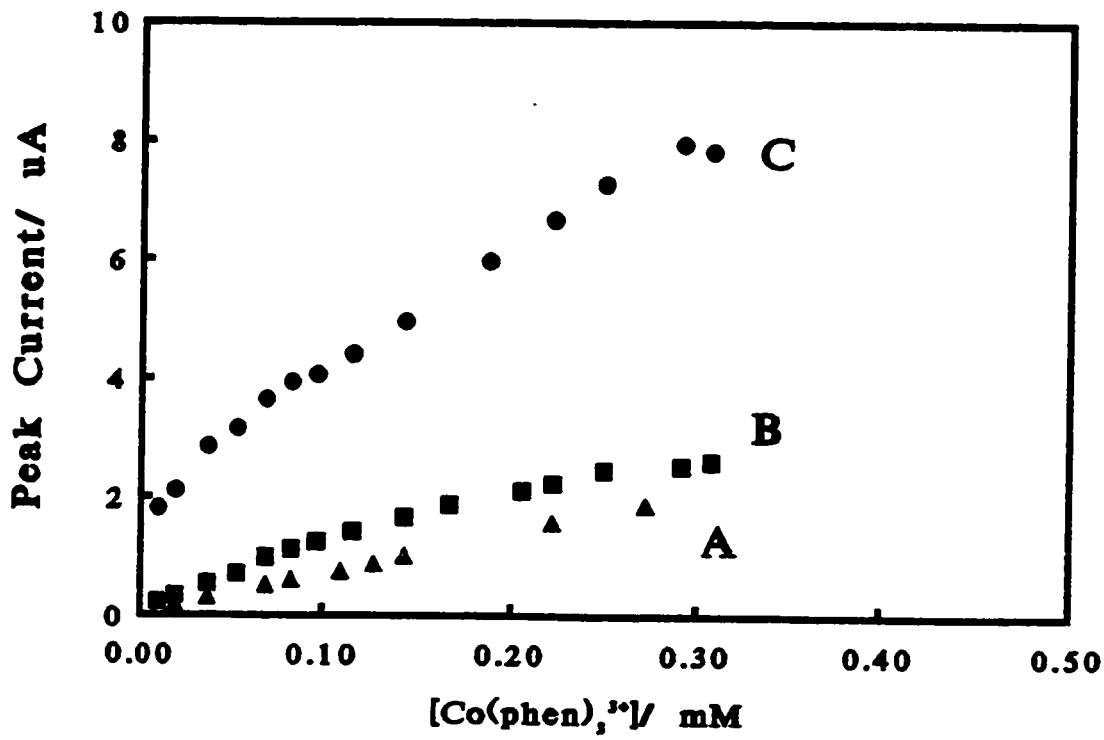

Figure 4.12 Peak current as a function of $Co(phen)_3^{3+}$ concentration at (a) an unmodified (b) an $oligo(dT)_{18}oligo(dG)_x$-modified SACPE and (c) same as (b) but after hybridization with $oligo(dA)_{20}$. Conditions: 20 mM NaCl, 5 mM Tris pH 7.1, scan rate 50 mV/s.

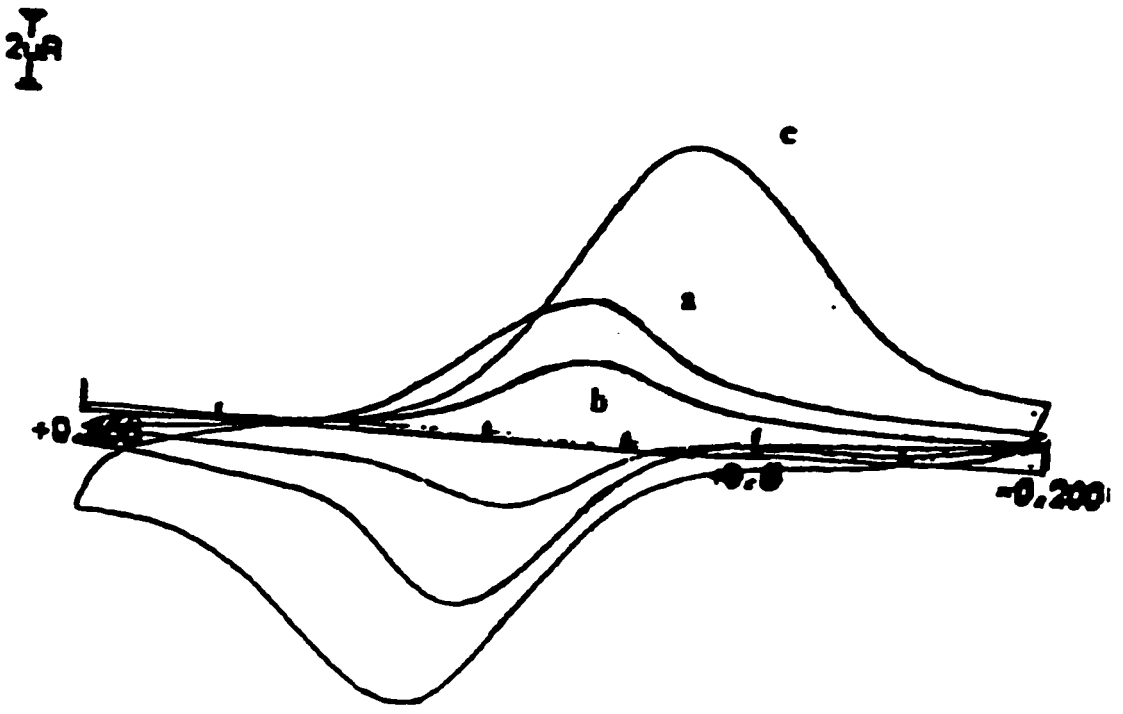

Figure 4.13 Third cycle of regeneration of the single-stranded probe by a rinse in hot, deionized H_2O (70°C). Conditions for CV: 50 mV/s scan rate, 5 mM Tris pH 7.1, 20 mM NaCl, 0.12 mM $Co(phen)_3^{3+}$. Voltammograms corresponding to an electrode with the (a) single-stranded probe after the second hybridization to its complementary sequence, (b) after regeneration to the single-stranded probe and (c) after the third cycle of hybridization.

effects seen are due to an interaction of the modifier and the charged complexes. Incubated in a solution of ferrocenemethanol the peak currents increased only slightly with time, the ΔE_p increased from 53 mV to 111 mV and the resistance increased from 400 Ω to 900 Ω after 7 hours. To study whether the differences observed between ferrocenemethanol and $Co(bpy)_3^{3+}$ are due to interactions between the stearic acid and the redox complex, a CPE without modifier was incubated in $Co(bpy)_3^{3+}$ and the peak currents, resistances, and peak potentials were measured through time. Table 4.4 shows that after 48 hours of incubation in the redox complex no significant changes were observed for peak currents, and only slight changes were observed for resistances, and ΔE_p decreased from 76 mV at t=0 to ΔE_p= 69 mV after 48 hours.

Changes in mineral oil content, analysis temperature, and activation of the carbon by heat or oxidation in basic medium did not affect resistance, peak currents or peak separation changes with time. The mineral oil content of the carbon paste mixture was varied from 20% to 40%. The unmodified SACPE with 20% mineral oil gave the most reversible electrochemistry for $Co(bpy)_3^{3+}$ with ΔE_p= 75 mV while the 40% mineral oil SACPE gave ΔE_p= 84 mV. Table 4.5 gives the peak currents and resistance values for SACPEs with varying mineral oil concentration. Independent of mineral oil concentration modification of SACPEs with poly(dG)poly(dC) caused the peak currents to increase, the peak seperations to decrease and the resistances to decrease. With DNA-modified and unmodified SACPEs the resistance values increased with time from R= 897 Ω (t= 5 minutes) to R= 336981 Ω (t= 846 minutes) and the peak currents decreased until no peaks were observed.

Table 4.4 Electrochemical behaviour of $(C_5H_5)Fe(C_5H_4CH_2OH)$ and $Co(bpy)_3^{3+}$ as a function of time.

Compound	Electrode	Time (min)	i_p (μA)	ΔE_p (mV)	R (ohms)
$Co(bpy)_{33+}$	CPE	5	0.93	76	497
		3025	1.06	69.75	502
$Co(bpy)_3^{3+}$	SACPE	5	1.22	78	487
		851	0.28	104	9674
Fe(MeOH)	SACPE	5	0.49	53	357
		1909	0.70	111	900

Conditions: Cyclic voltammetry was performed at 0.12 mM $Co(bpy)_3^{3+}$ and 0.88 mM Fe(MeOH) in 5 mM Tris, 20 mM NaCl at 50 mV/s scan rate.

Changes in the temperature of the redox reaction from 15 °C to 38 °C had no effect on the increases in resistance or decreases in peak potential. Activation of the graphite by heating at 100 °C overnight prior to preparation of the graphite mixture did not significantly improve the stability of the SACPE. Activation of the SACPE by electrochemical oxidation in basic solution also did not improve the stability of the SACPE.

4.2.3 A DNA Intercalant-Redox Enzyme Conjugate Hybridization Indicator

Preliminary studies tested a daunomycin-GOx conjugate as a possible redox hybridization indicator. The catalytic current generated by the daunomycin-GOx conjugate in the presence of 0.05 mM ferrocene carboxylic acid (FCA) and 20.0 mM glucose was tested

Table 4.5 Stability of the SACPE with varying mineral oil content.

Mineral oil Content	Time (minutes)	Peak Currents (μA)	Resistances (Ω)
20%	5	1.22	993
	1146	0.28	9674
30%	5	1.11	897
	846	0.34	33691
40%	5	0.72	576
	1440	0.58	10259

If observed for longer periods of time the peak currents continue to decrease until no peaks are observed.

and compared at an unmodified SACPE and a poly(dG)poly(dC)-modified SACPE (4.5% SA). Adsorption and hybridization of the conjugate was tested by adding Daunomycin-GOx to the surface of the SACPE and poly(dG)poly(dC)-modified SACPE for 10 minutes, rinsing, and then measuring its cataytic current in the presence of glucose and FCA. No catalytic current was observed at the unmodified electrode which suggests that this conjugate does not adsorb to the SACPE. Figure 4.14 compares the catalytic current generated at the unmodified and the poly(dG)-poly(dC)-modified SACPE. This demonstrates the ability of the daunomycin-GOx conjugate to act as a redox hybridization indicator. The limiting current produced at the unmodified electrode is 0.6 μA, and at the DNA-modified electrode it increases to 4.08 μA. The percent increase in response at the DNA-modified electrode is 580%. Table 4.6 provides the conditions under which the daunomycin-GOx conjugate was tested and the associated signal. The conjugate was tested for its catalytic properties by examining the currents produced in the presence and absence of FCA.

Table 4.6 The Daunomycin-GOx Conjugate as an Electrochemical Hybridization Indicator.

Electrode	Conditions*	Catalytic Current (μA)
Unmodified	**Daunomycin-GOx Glucose**	**0.17**
Unmodified	**Daunomycin-GOx FCA, Glucose**	**0.60**
Poly(dG)poly(dC) modified	**Daunomycin-GOx Glucose**	**2.10**
Poly(dG)poly(dC) modified	**Daunomycin-GOx FCA, Glucose**	**4.08**

* The electrodes used had 4.5% SACPE. Buffer conditions 0.1 M potassium phosphate buffer pH 7.0. Cyclic voltammetry was performed with a scan rate 5 mV/s from an initial potential of 0 mV to a final potential of 650 mV.

4.3 Discussion

Two different modification procedures were used to immobilize DNA onto CPEs. In the first procedure, the 5'-phosphate of the probe DNA is covalently bound to the primary amine group of octadecylamine incorporated into the graphite mixture, creating a phosphoramidate bond. Reversible behaviour was not observed with $Co(phen)_3^{3+}$ or $Co(bpy)_3^{3+}$ at the octadecylamine CPE. $Os(bpy)_3^{2+}$ was chosen as the hybridization indicator since it displays quasireversible electrochemistry with the ODA-CPE and appears to associate selectively with dsDNA in a manner analogous to $Co(bpy)_3^{3+}$. This selective association with dsDNA over ssDNA is demonstrated in Figure 4.2. The peak current for the reduction of 0.12 mM $Os(bpy)_3^{2+}$ at an unmodified ODA-CPE is 1.15 μA. The anodic peak current shows a mild increase to 2.12 μA when poly(dT) is bound to the electrode surface and a much greater increase to 5.18 μA upon hybridization with poly(dA). There is an 84% increase in signal

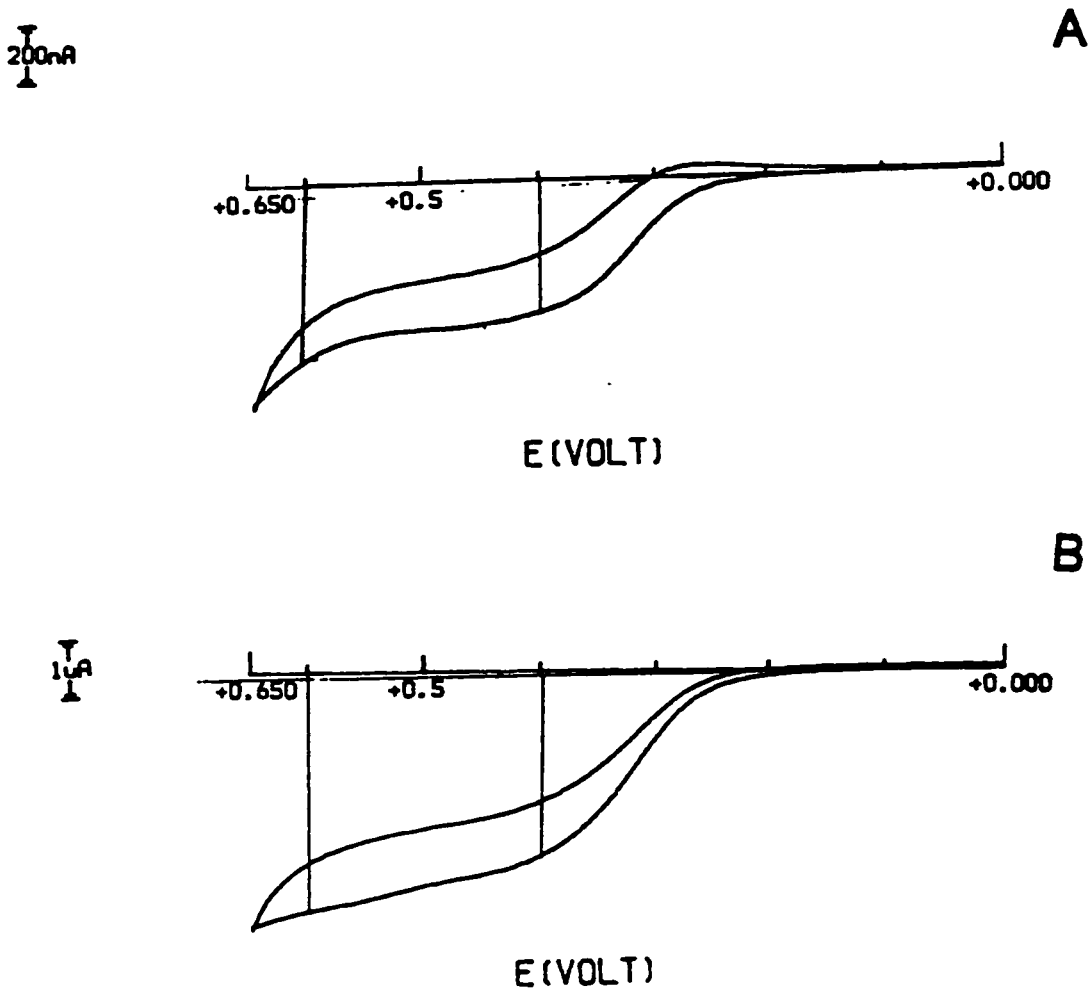

Figure 4.14 Cyclic voltammetry at an (A) unmodified (4.5%) SACPE and (B) a poly(dG)poly(dC)-modified SACPE in the presence of 20 mM glucose, 0.05 mM FCA, and 0.1 M potassium phosphate, pH 7.0. Scan rate 5 mV/s. Previous to CV the daunomycin-GOx conjugate (50 μL) was placed on the surface of each electrode and incubated at room temperature for 10 minutes to allow for adsorption or hybridization to occur.

between the unmodified electrode and single-stranded DNA immobilized onto the electrode surface. However there is a 144% increase in peak current between ssDNA and dsDNA at the surface of the electrode. This demonstrates the selective interaction of $Os(bpy)_3^{2+}$ with dsDNA.

At DNA-modified CPEs, with both octadecylamine and stearic acid as modifiers, a large background current is observed relative to the unmodified electrode. The separation of anodic and cathodic peak currents also becomes smaller at DNA-modified ODA-CPEs and SACPEs. At 50 mV/s and 0.12 mM $Os(bpy)_3^{2+}$ ΔE_p is 92 mV for an unmodified ODA-CPE and 42 mV for a dsDNA-modified octadecylamine-incorporated CPE. Peak currents were measured as a function of scan rate to determine the behaviour of the electroactive species at both the unmodified and the DNA-modified CPEs. The plots of i_p vs ν and i_p vs $\nu^{1/2}$ for the redox complexes at the unmodified CPEs, both stearic acid and octadecylamine, reveal diffusion limited redox processes. At the DNA-modified CPE, stearic acid and octadecylamine, the plots indicate behaviour intermediate between a purely diffusing and purely adsorbed species for all three complexes. This suggests that the DNA strand is closely bound at the surface of the electrode. The redox species are bound to DNA and therefore behave as adsorbed electroactive species. Another part of the DNA strand may be at some distance from the electrode surface and the electroactive species bound in this region may diffuse to the electrode surface in order to participate in the electrode reaction. The shift in formal potential for a Nernstian redox reaction between a DNA-modified electrode and an unmodified electrode has been employed to determine the electrostatic and intercalative components of the binding of the electroactive hybridization indicators to immobilized DNA.[3].

At the DNA-modified SACPE shifts in individual peak potentials result both from differences in DNA-binding and adsorption. Thus changes in E°' can reflect the strength of the binding of the charged redox species to DNA. For a Nernstian electron transfer, in a system in which both the oxidized and reduced forms associate with third species in solution (DNA), equation 5 can be used to determine the relative strength of binding of the oxidized and reduced forms of an electroactive DNA-binding complex

$$E_b^{o'} - E_f^{o'} = 0.059 \log \frac{K_{2+}}{K_{3+}} \qquad (5)$$

where $E_b^{o'}$ and $E_f^{o'}$ are the formal potentials of the 3+/2+ couple for the reduction of the 3+ complex to the 2+ complex. For $Co(phen)_3^{3+}$ a positive shift of 49.2 mV indicates that the 2^+ ion is about 6.82 times more tightly bound to DNA than the 3^+ ion. For $Co(bpy)_3^{3+}$ the -10.6 mV shift shows that the 3^+ ion is bound 1.5 times more strongly than the 2^+ ion. With $Os(bpy)_3^{3+}$, since it undergoes an electrochemical oxidation at the electrode, a + 34.8 mV shift demonstrates that the 3^+ ion is more tightly bound to DNA by a factor of 3.88.

Optimum conditions for covalently coupling denatured poly(dG)poly(dC) to an octadecylamine CPE were obtained by keeping the octadecylamine content constant at 0.5% and varying the concentration of DNA. ODA was held constant at 0.5% since at higher concentrations of ODA irreversible behaviour was observed for $Os(bpy)_3^{2+}$. The concentration of denatured poly(dG)poly(dC) was varied between 0.01 mg/mL to 2 mg/mL and the optimum was achieved at concentrations equivalent and higher than 1 mg/mL. However, at the higher concentrations gelatinous strands of DNA were visible on the surface of the electrode. Polyacrylamide gel electrophoresis demonstrated that DNA incubated in EDC and

imidazole yielded higher molecular weight DNA. It is probable that the 5'-terminal phosphate reacts with the 3'-terminal hydroxyl to yield higher molecular weight DNA immobilized onto the ODA-CPE.

With SACPEs the optimum quantity of stearic acid for immobilizing denatured poly(dG)poly(dC) was 4.5% stearic acid (w/w). The optimum DNA concentration was determined to be 10 μg/mL. The smaller peak currents obtained with higher DNA concentrations can be the result of competition between renaturation of poly(dG) with poly(dC) and immobilization with free deoxyguanosine bases. At higher DNA concentrations the kinetics of renaturation are increased, leaving fewer deoxyguanosine residues available for the immobilization reaction. DNA immobilization at higher DNA concentrations may also be influenced by steric or conformational factors.

The most suitable buffer for immobilizing DNA onto SACPEs via dG residues is one which does not contain a strong nucleophile and one which permits the reactive site on the guanosine base to participate in the coupling reaction. Since G4 DNA is the product of deoxyguanosine bases hydrogen bonding to other dG residues via Hoogsteen pairing it would seem that this self-association may interfere with the coupling reaction. G4 DNA is formed in the presence of potassium and sodium cations but not if lithium is the only alkali cation present.[7] G4 DNA requires a neutral pH and at low ionic strength intramolecular foldback structures and antiparallel structures form. Complex structures will form at ion concentrations between 5 mM and 1 M. The rate of complex structure formation increases with DNA concentration. The rate of complex structure formation, for concentrations between 0.1 and 10 μg/mL at 60 °C, is very slow (greater than 5 days), and increases linearly with time.[6] This

demonstrates that the system is far from equilibrium. Thus, the yield of the coupling reaction should be dependent on the cation of the buffer and its concentration. Lithium phosphate was compared to potassium phosphate and the results indicate that better immobilizations were achieved with lithium phosphate. In the presence of lithium G4 DNA should not form and thus the Hoogsteen bonding between dG residues should not interfere with coupling of dG residues to the electrode surface. These results contrast with those in section 3.2.1.2, where larger peak currents were obtained when K^+ was present as opposed to Li^+.

For the investigation of the effects of Li^+ and K^+ on immobilization of DNA onto GCEs and CPEs poly(dG)poly(dC) was used and all conditions (temperature (room temperature), time between denaturation and exposure to electrode, and evaporation conditions remained constant. One possible explanation for the differences observed for the effect of the ion in the immobilization of DNA onto GCEs and CPEs is that the surfaces of the two electrodes are different. Therefore conformational differences in the DNA induced by different ions may affect the interaction of the guanine base with the electrode surface.

Many problems were encountered with carbon paste electrodes as transducers for a DNA biosensor. At octadecylamine CPEs no peaks were observed for $Co(bpy)_3^{3+}$ and $Co(phen)_3^{3+}$. At concentrations greater than 0.5% ODA irreversible behaviour was frequently observed for $Os(bpy)_3^{2+}$. A CPE without modifier at 0.12 mM FCA showed no substantial change in peak current or peak potential with time. Upon the addition of a saturated solution of octadecylamine a continuous decrease in peak current was observed until no peaks were observed at all. This suggests that octadecylamine adsorbs onto the CPE and inhibits the heterogenous electron transfer between the redox complex and electrode. Carbon paste

electrodes can extract some substances from an aqueous solution into the organic phase of the electrode itself.[16] In this specific case it seems that octadecylamine was extracted from the analysis buffer and that it can interfere with the electrode reaction. Octadecylamine has been incorporated into CPEs to eliminate interference by analytes such as dopamine during the highly selective detection of hexacyanoferrate (III).[17] In this study optical microscopy of ODACPEs and CPEs revealed that there is a higher surface coverage of binding agent (liquid paraffin) in the former.

Problems associated with SACPEs were similar to those found for ODACPEs. At unmodified SACPEs, and ODA-CPEs, the peak currents for the electroactive complexes decreased, and increases in resistance across the electrode were observed with time. Scanning tunnelling microscopy has characterized the distribution of conductive and insulating regions at the CPE surface. The fraction of insulating regions is dependent on mineral oil content; a lower mineral oil content gives a decrease in the fraction of insulating regions and an increase in proportion of conducting regions. A 10-20% mineral oil content is the dry graphite limit with which the surface appears to be fully conductive.[18] Heterogenous electron transfer rates are more rapid with CPEs having an increased graphite fraction.[19] The addition of pasting liquids decreases the electron transfer rate. It has been suggested that chemical and electrochemical oxidative pretreatments of carbon paste electrodes increase the electron transfer rate by removing the organic layer at the surface of the electrode, since oxygen-containing surface states are formed. Therefore to improve the stability of SACPEs the mineral oil content was varied between 20 to 40%. With time, regardless of mineral oil content, the resistances increased and the peak currents decreased until no signals were

observed. Changes in the analysis temperature, activation of the graphite by heat, and electrochemical activation did not improve the stability of the CPEs.

The large changes observed in the behavior of $Co(bpy)_3^{3+}$ at SACPEs with time, and the stability of the peak currents and resistances with time at SACPEs (Table 4.4) indicates that the modifier (SA) causes instability. One possible explanation for these results is that the modifiers (SA and ODA) are amphiphilic, thus having a hydrophobic component and a polar head group; a primary amine in the case of octadecylamine and a carboxylate group in the case of stearic acid. The polar head groups face the sample solution and may be solubilized by the aqueous media. This may lead to preferential wetting of the graphite by the solution leading to dissolution of the modifier, or the modifier may be concentrated at the surface, after time in contact with an aqueous solution. This in fact may be the case since it was observed that after incubation in aqueous solution the surface of the SACPE became white and uneven instead of its initial shiny black flat surface.

The daunomycin-GOx conjugate provided a 580% increase in signal at the poly(dG)poly(dC) SACPE in comparison to the unmodified SACPE. This is a significant increase in response, comparable to that seen with $Co(bpy)_3^{3+}$ at a poly(dG)poly(dC)-modified GCE where the current increased from 1.0 μA to 13.1 μA (see section 3.2.1.2). Furthermore, adsorption of the conjugate at the surface of the SACPE was not observed.

4.4 **Conclusions**

ODACPEs have been modified with DNA via a phosphoramidate bond between the 5'-phosphate and the primary amine of octadecylamine. This reaction caused DNA

polymerization at the CPE surface. Also, fouling of the electrode surface by octadecylamine eliminated this type of electrode for use as a DNA sensor in aqueous medium.

SACPEs have been modified with DNA via the activation of the carboxylic acid group of stearic acid to an NHS-ester which is reactive to the guanine base. Optimum conditions for immobilization have been established including buffer conditions, DNA concentration and concentration of modifier. One significant problem associated with SACPEs is that they are unstable in aqueous solutions.

Due to problems associated with carbon paste electrodes other electrode materials, such as glassy carbon, gold, and platinum, are suggested transducers for an electrochemical DNA sensor.

Further studies with the daunomycin-GOx conjugate are suggested in order to optimize its effectiveness as a hybridization indicator in an electrochemical DNA sensor. This conjugate can be examined in conjunction with other electrodes for a new DNA sensor.

4.5 References

1. P. T. Kissinger and W. R. Heineman, "Laboratory Techniques in Electroanalytical Chemistry", Marcel Dekker Inc, New York, **1984**, pp 294 -302.

2. Kulys, J.; Gorton, L.; Doninguez, E.; Jarskog, H.; *J. Electroanal. Chem.*, **1994**,372, 49-55.

3. Millan, K. M.; Mikkelsen S. R.; *Anal. Chem.*, **1993**, 65, 2317-2323.

4. Rasmussen, S. R.; Larsen, M. R.; Rasmussen, S. E.; *Anal. Biochem*, **1991**, 198, 138.

5. Sen, D.; Gilbert, W.; *Nature*, **1988**, Vol. 334, 364.

6. Sen, D.; Gilbert, W; *Nature*, **1990**, Vol. 344, 6265, 410.

7. Sen, D.; Gilbert, W.; *Biochemistry*, **1992**, 31, 65

8. A. J. Bard and L. R. Faulkner, "Electrochemical Methods", John Wiley & Sons, N.Y., **1980**, pp 26-34.

9. A. J. Bard and L. R. Faulkner, "Electrochemical Methods", John Wiley & Sons, N.Y., **1980**, pp 538.

10. G. H. Keller and M. M. Manak, "DNA Probes", MacMillan (Stockton Press), New York, **1989**, pp 1-80.

11. Combatsiaris, C; Chemistry 419 Thesis, Concordia University, **1991**.

12. Cass, A. E. G.; "Biosensors A Practical Approach", Oxford University Press, London, **1990**, p 23-24.

13. Battaglini, F.; Koutroumanis, M.; English, A. M.; Mikkelsen, S. R.; *Bioconj. Chem.*, **1994**, 5, 430.

14. Kolakowski, B. M.; M.Sc. Thesis, Concordia University, **1995**.

15. Carter, M. T.; Rodriguez, M.; and Bard, A. J.; *J. Am. Chem. Soc.*, **1989**, 111, 8901-8910.

16. Chambers, C. A.; Lee, J. K.; *J. Electroanal. Chem*, **1967**, 14, 309.

17. Amine, A.; Deni, J., Kauffmann, J.; *Anal. Chem.*, **1994**, 66, 1595- 1599.

18. Wang, J.; Martinez, T.; Yaniv, D.R.; McCromich, L.; *J. Electroanal. Chem.*, **1990**, 286, 265-272.

19. Rice, M. E.; Galus, Z.; Adams, R. P.; *J. Electroanal. Chem.*, **1983**, 143, 89-102.

Chapter 5

Hybridization Kinetics of CPE-immobilized DNA.

5.1 Introduction

For individual base-pairing reactions the rate of formation of base pairs is so fast that the reaction is diffusion controlled. As the number of bases in a strand increases beyond 4 bases the complexity of the reaction increases. Initially oligonucleotide duplex

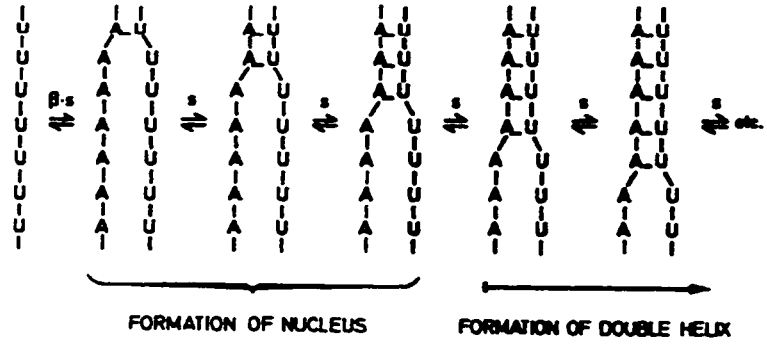

Figure 1 Model for the formation of oligonucleotide duplex formation.[1]

formation was assumed to be diffusion controlled, that only aligned duplexes form and that a unique nucleation site exists. Figure 5.1 is a cartoon depiction of this model for the kinetics of oligonucleotide duplex formation.

Temperature-jump relaxation kinetic experiments demonstrated that the rate constants of duplex formation were much slower than predicted by simple collision of the two strands. A simple elementary kinetic step cannot have a negative activation energy, E_a. Duplex formation between two complementary strands the reaction is described by equation 1:

$$A+B \underset{k_2}{\overset{k_1}{\rightleftharpoons}} A-B \qquad (1)$$

Experimental results indicate that the forward rate constant does not fit the Arrhenius equation.

$$\frac{d(\ln k_1)}{d(\ln(1/T))} = -\frac{E_a}{R} \qquad (2)$$

The forward rate constant k_1 decreases with increasing temperature for oligonucleotides without G-C pairs. Figure 5.2 shows the Arrhenius plot of k_{obs} for duplex formation as a function of temperature. The results of this plot reveal a negative activation energy for duplex formation. A large positive E_a was determined for the reverse rate constant k_{-1}. Duplex formation for oligomers with G-C pairs only have a slightly positive E_a for k_1 and a much larger E_a for k_{-1}.Also the rate constants of duplex formation for a variety of oligomers are of the order of 10^5 to 10^7 M^{-1} sec^{-1}. This rate is much slower than the rate of base pairing for monomers and is too slow for a diffusion controlled process. These results suggests that duplex formation is not a simple elementary kinetic reaction, and that k_1 and k_{-1} are composite rates consisting of a combination of individual steps. It also suggests that the formation of the first base pairs is not rate-limiting. It has been suggested that the first few base-pairs exist in a rapid pre-equilibrium in which a critical intermediate exists which can more rapidly dissociate than it can associate to form dsDNA.[1] The activation energies of duplex formation helps evaluate how many base pairs exist in a pre-equilibrium state before base pairing predominates over dissociation. The longer the pre-equilibrium region the more negative the

total activation energy will be.[2] From the relaxation experiments on duplex formation by Craig et. al.[2] the following model of hybridization has been proposed. DNA hybridization in solution results from the collision of complementary strands and follows second-order kinetics. The first step is collision followed by the formation of the first base pair. The first base pair forms more slowly than a base pair at the end of a helix. The formation of the first

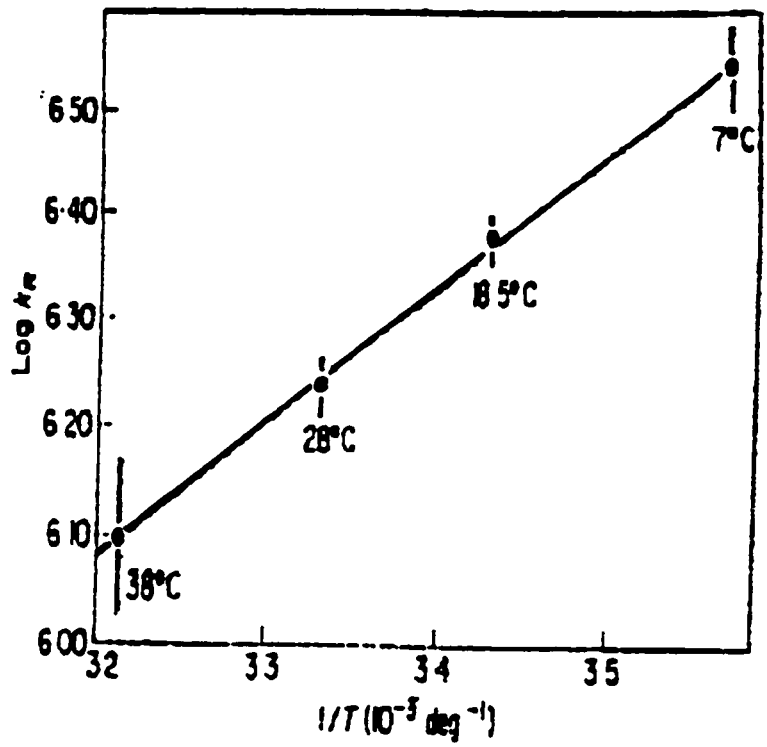

Figure 2 Arrhenius plot for duplex formation[1]

pair is concentration-dependent and base follows a second-order process. It is not stabilized by stacking free energy, as is the case for following base pair formations. A pre-equilibrium

state of formation and dissociation exists prior to helix growth. Two to three base pairs form the critical intermediate for which dissociation to single bases predominates over renaturation to the double helix. When there is sufficient base pairing to form a stable nucleus, such that base pairs form more rapidly than they dissociate, then the formation of more base pairs is stabilized by stacking free energy and a limiting rate of base pair addition will be achieved.

Hybridization of complementary strands of DNA free in solution is dependent on frictional resistance to the rotation of helix and coil forms in solution[1], DNA sequence complexity (each strand must find its complementary sequence for nucleation), length of DNA strand, temperature and ionic strength.[3] Experimentally, renaturation rates are optimum at 25 °C below the melting temperature (T_m) of the duplex.[3] At this temperature the effects of intramolecular secondary structures are minimized. The T_m of oligonucleotide-target heteroduplexes is relatively low. Under these conditions intramolecular secondary structures are present and inhibit oligonucleotide-target hybridization.[4] The equilibrium of duplex formation has a strong salt dependence. ^{1}H NMR experiments of base-pairing reactions of oligonucleotides determined that 1.4 ± 0.2 sodium ions associate for an octamer with the sequence d(GGAATTCC) during the rate-limiting helix association step.[5] Ideal conditions for solution DNA hybridization include a temperature 25 °C below T_m, a pH between 5.0 and 9.15 and high ionic strength ([NaCl] ≥ 0.4M).[3] Under these conditions the rate constant is described by the Wetmur and Davidson relationship:

$$k=3.5\times10^{5}L^{0.5}N^{-1}(M^{-1}s^{-1}) \qquad (3)$$

where L is the length of the DNA strand involved in hybridization and N is molecular

complexity (total number of base pairs in a nonrepeating sequence). The time at which half of the target DNA has annealed ($t_{½}$) is given by equation 4[3]:

$$t_{½} = \frac{\ln 2}{kC} \qquad (4)$$

where k is the first-order rate constant and C is the probe concentration in mol nucleotide/L. Equations 3 and 4 can be combined to yield equation 5 which provides an expression for the time required to anneal half the probe DNA to its target under optimum conditions.

$$t_{½} = \frac{N \ln 2}{3.5 \times 10^{5} L^{0.5} C} \qquad (5)$$

These equations predict that hybridization time is minimized by using probes of low complexity and longer length, at high concentrations. However, longer probes does not always decrease hybridization times for mixed phase hybridizations since some immobilized target sequences may not be accessible to long probe molecules.

Hybridization of complementary strands of DNA free in solution is different than hybridization with one strand immobilized onto a solid surface. Hybridization at solid surfaces is about 10 to 100 times slower than hybridization free in solution.[6] The kinetics of DNA hybridization at a solid surface are difficult to study since the exact concentration of immobilized DNA available for hybridization is unknown. This leads to difficulty in determining the mechanism for DNA hybridization at a solid support. If the amount of target DNA free in solution is in excess of support-bound DNA then pseudo-first order kinetics are observed.[3]

The kinetics of hybridization of RNA to membrane filter-immobilized DNA have been

investigated.[6] It was discovered that such hybridization could not be described in the same terms as solution hybridization. Instead a stable hybrid intermediate exists throughout the hybridization reaction. The rate of formation of the complete double helix is comparable to the rate of dissociation of the intermediate stable hybrid. The kinetic complexity of hybridization increases when one DNA strand is immobilized onto a surface, and consists of more than one kinetically significant step. This is in contrast to solution hybridization in which the crucial step is formation of a well-defined hybrid nucleus. One possible expalantion for this difference is that when ssDNA is immobilized, its movement is restricted and this inhibits the hybridization process.

For membrane filter-immobilized DNA, the rate equation for hybridization is:[7]

$$-\frac{d[C]}{dt} = k_s[C_s]\,[C] + k_a[C]^2 + J \qquad (6)$$

where C_s is the concentration of filter-bound ssDNA, C is the concentration of ssDNA free in solution, k_s and k_a are rate constants for hybridization at the surface of the filter and between two strands in solution, respectively, and J is a diffusion term which is a function of the concentration gradient and the diffusion coefficient. The term $k_a[C]^2$ represents the kinetics of reassociation of homogeneous DNA. Reassociation can complicate the kinetics of filter hybridization. As much as 30% of solution DNA can reassociate and thus be unavailable for hybridization with immobilized DNA.

When solution DNA is present in vast excess over immobilized DNA ($C >> C_s$) diffusion can be ignored. Ignoring reassociation and diffusion, and assuming pseudo-first

order conditions the kinetics can be described by equation 7:

$$\frac{dX}{dt} = k_{obs}(C_s - X) \tag{7}$$

where X is the concentration of dsDNA at the surface, C_s is the concentration of ssDNA on the surface, and $k_{obs} = k_s C$ and is the apparant first order rate constant. Integration from time zero to time t gives:

$$C_s - X = C_s e^{-k_{obs} t} \tag{8}$$

A plot of log(concentration ssDNA remaining C_s-X) vs time gives a straight line with a slope equal to $-k_{obs}$.

Recently acoustic network anlaysis has been used to study the kinetics of DNA hybridization.[7] This method was designed for use in a DNA sensor, as described in Chapter 1.[8] DNA probe molecules in solution are transported to the TSM sensor, where the complementary sequence is immobilized. Hybridization of immobilized DNA is detected by changes in series resonant frequency measurements. DNA hybridization kinetics can be measured by series resonant frequency changes resulting from viscosity changes over time. These experiments were performed with a vast excess of probe DNA (cDNA). Thus diffusion can be ignored and a steady-state condition can be assumed. The reaction mechanism has been described by equations 9, 10, and 11.

$$cDNA_{sol} \frac{k_1}{k_2} cDNA_{surf} \tag{9}$$

$$ssDNA_{immob} + cDNA_{surf} \frac{k_3}{k_4} DNA_{intermediate} \quad (10)$$

$$DNA_{intermediate} \frac{k_5}{k_6} dsDNA_{surf} \quad (11)$$

where $cDNA_{sol}$, $cDNA_{surf}$, $ssDNA_{immob}$, $DNA_{intermediate}$, $dsDNA_{surf}$ symbolize different species of DNA. $cDNA_{sol}$ and $cDNA_{surf}$ are probe DNA in solution and at the surface of the support. $ssDNA_{immob}$ is the immobilized target sequence, $DNA_{intermediate}$ represents DNA molecules which are specifically bound but only partially hybridized, and $dsDNA_{surf}$ represents the more stable immobilized dsDNA. DNA probe molecules in solution are transported to the surface of the TSM sensor interface-liquid region, the $cDNA_{surf}$ collides with $cDNA_{immob}$ to produce an intermediate DNA structure which is followed by "zippering up" of all the bases to produce the final product, $dsDNA_{surf}$.

The results of the experiments for hybridization on a TSM sensor indicate that an intermediate hybrid accumulates during hybridization. A possible explanation for the accumulation of partially hybridized DNA is that immobilized ssDNA may be restricted and this slows the annealing process.

Previous studies of DNA adsorbed on a TSM sensor show that only 10% of immobilized ssDNA reacts with its complementary DNA.[8] These results indicate that this procedure of immobilizing DNA somehow interferes with its ability to hybridize to cDNA. This has also been observed for DNA adsorbed on membrane filters,[6] and may be related to how the ssDNA is bound to the surface in these two immobilization reactions. Immobilization may involve interactions of the solid surface to form hydrogen bonds with the DNA bases at

locations necessary for base pair associations.

In this chapter, hybridization kinetics are examined for ssDNA immobilized onto stearic acid carbon paste electrodes (SACPEs). A poly$(dT)_{4000}$ sequence was bound to the SACPE via deoxyguanosine residues which were enzymatically added onto the 3'terminus of the probe. Hybridization of this immobilized probe was studied to determine the rate constants and to determine the detection limits for the target sequence. Hybridization of a probe immobilized through a terminal group or groups which do not participate in hybridization may yield different results than a probe immobilized through adsorption of the bases onto a TSM sensor or a membrane filter. The interactions of DNA at different surfaces may result in the ssDNA taking on different conformations.

Hybridization kinetic studies were simplified by creating pseudo-first order conditions, with the concentration of target DNA being in vast excess of immobilized probe. This also eliminates the diffusion term in equation 3 and knowledge of the concentration of immobilized ssDNA is not required. Also reassociation of complementary DNA in solution is eliminated by hybridizing by using soluble sspoly(dA) as the target sequence. Thus, solution hybridization can be neglected. Finally, the complexity of the DNA strand is minimized by having a homogenous DNA strand with N=1.

Hybridization kinetics were examined using the voltammetric DNA-biosensor based on SACPEs. Hybridization is measured indirectly by the preconcentrating effect dsDNA has on the electroactive hybridization indicators $Co(bpy)_3^{3+}$, $Os(bpy)_3^{2+}$, and $Co(phen)_3^{3+}$. Thus the extent of hybridization is directly proportional to the increase in peak currents. The binding of the indicators to dsDNA is assumed rapid relative to the hybridization process.

Hybridizations were performed in the presence of a hybridization indicator in low ionic strength and in high NaCl concentrations in the absence of a hybridization indicator.

5.2 Results

5.2.1 *In Situ* Hybridization Kinetics

A 4.5% stearic acid carbon paste electrode was modified with dG-elongated poly(dT)$_{4000}$, as described in Section 2.2.5. The extent of hybridization was measured by an increase in cathodic peak current resulting from the preconcentration of hybridization indicator by increasing quantities of dsDNA at the surface of the electrode. At t=0 the exact complement of poly(dT)$_{4000}$, poly(dA)$_{4000}$ was added to a solution of 0.06 mM hybridization indicator and the cathodic peaks were measured through time for several hours. Figure 5.3 shows that upon addition of poly(dA) the peak currents increase with time.

The hybridization reactions appear to be complete after one hour, when a maximum peak current is obtained. Since 10 μg/mL of complement should be in vast excess of the concentration of immobilized poly(dT), poly(dA) concentrations should change significantly as a result of hybridization. Therefore pseudo-first order rates can be assumed. A plot of $-\ln(i_{inf}-i_t)$ versus time; where i_{inf} is the maximum peak current and i_t is the peak current at time t, gives straight lines for $Co(bpy)_3^{3+}$, $Co(phen)_3^{3+}$, and $Os(bpy)_3^{2+}$. Figure 5.4 shows these first order plots for all three complexes. The results give an observed rate constant of $0.82 \pm 0.4 \times 10^{-3}$, $0.50 \pm 0.3 \times 10^{-3}$, and $0.45 \pm 0.8 \times 10^{-3}$ s^{-1} for hybridization of immobilized poly(dT) with 10 μg/mL poly(dA) in the presence of $Co(bpy)_3^{3+}$, $Co(phen)_3^{3+}$, and $Os(bpy)_3^{3+}$, respectively.

Similar in situ hybridization experiments were performed by varying poly(dA) concentration over the 1 μg/mL to 10 μg/mL range, and using immobilized poly(dT). Figure 5.5 compares plots of peak current versus time for these hybridizations.

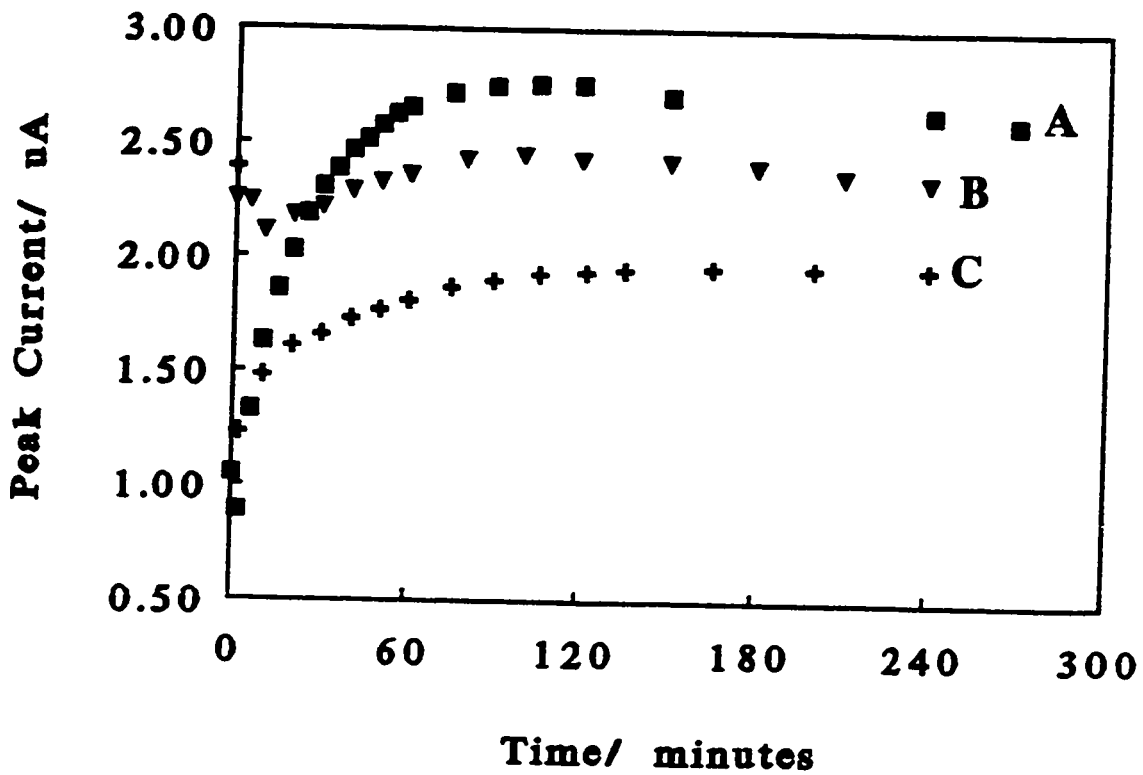

Figure 5.3 Peak current vs time at a poly(dT)$_{4000}$-modified CPE/ At t= 0 poly(dA)$_{4000}$ is added. Hybridization was performed in 5 mM Tris pH 7.1, 20 mM NaCl, and 60 μM (A) $Co(bpy)_3^{3+}$, (B) $Os(bpy)_3^{3+}$, or (C) $Co(phen)_3^{3+}$ under constant stirring being interrupted only during a voltammetric run. Cyclic voltammetry was performed at a scan rate of 50 mV/s.

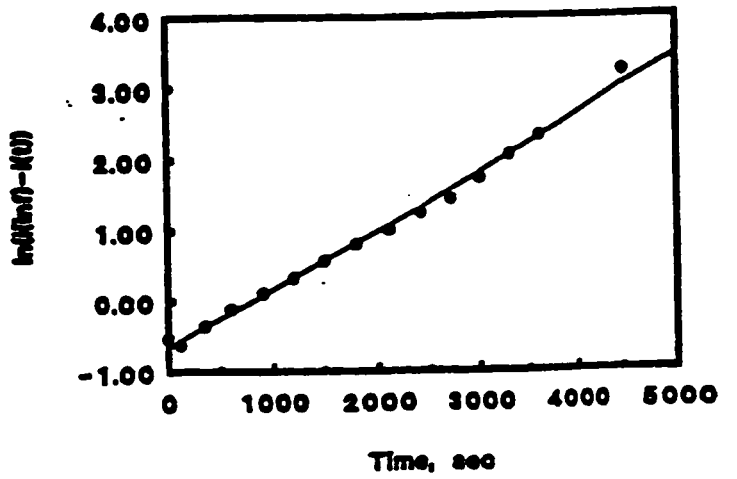

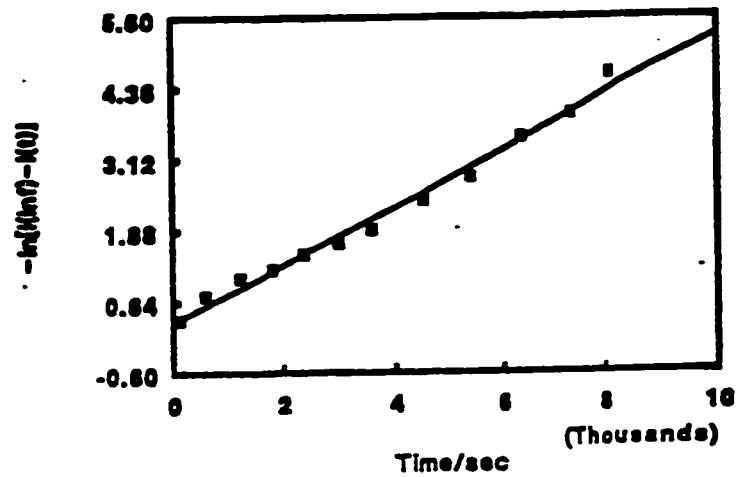

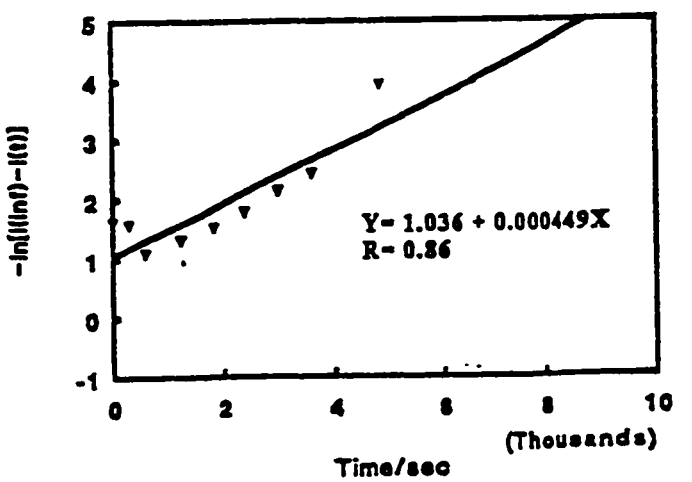

Figure 5.4 First order plots of $-\ln(i_{inf} - i_t)$ against time for (A) $Co(bpy)_3^{3+}$, (B) $Co(phen)_3^{3+}$, or (C) $Os(bpy)_3^{3+}$. Conditions as in Figure 5.3.

From this figure it can be seen that there are differences in the magnitude of the initial peak currents after immobilization at t=0 and after completion of hybridization at time t. Variability of peak currents for different immobilizations reflects the irreproducibility of the immobilization reaction. The *in situ* hybridization rate constants for $Co(phen)_3^{3+}$ and $Co(bpy)_3^{3+}$ for varying concentrations of poly(dA) are given in Table 5.1.

Table 5.1 *In Situ* Hybridization Rate Constants.
Conditions: 5 mM Tris pH 7.1, 20 mM NaCl, 0.06 mM complex.

[Poly(dA)] µg/mL	k_{obs}, $s^{-1} \times 10^3$ $Co(bpy)_3^{3+}$	k_{obs}, $s^{-1} \times 10^3$ $Co(phen)_3^{3+}$
1	2.6 ± 0.3 R= 0.94	0.96 ± 0.4 R= 0.84
5	1.5 ± 0.5 R= 0.965	0.5 ± 0.3 R= 0.991
10	0.8 ± 0.4 R= 0.997	0.50 ± 0.3 R= 0.994

Over the concentration range of 1 - 10 µg/mL, the observed rate constants (k_{obs}) did not increase with increasing poly(dA) concentration. The magnitude of the increase in peak current displays a similar inconsistency, for 1 µg/mL

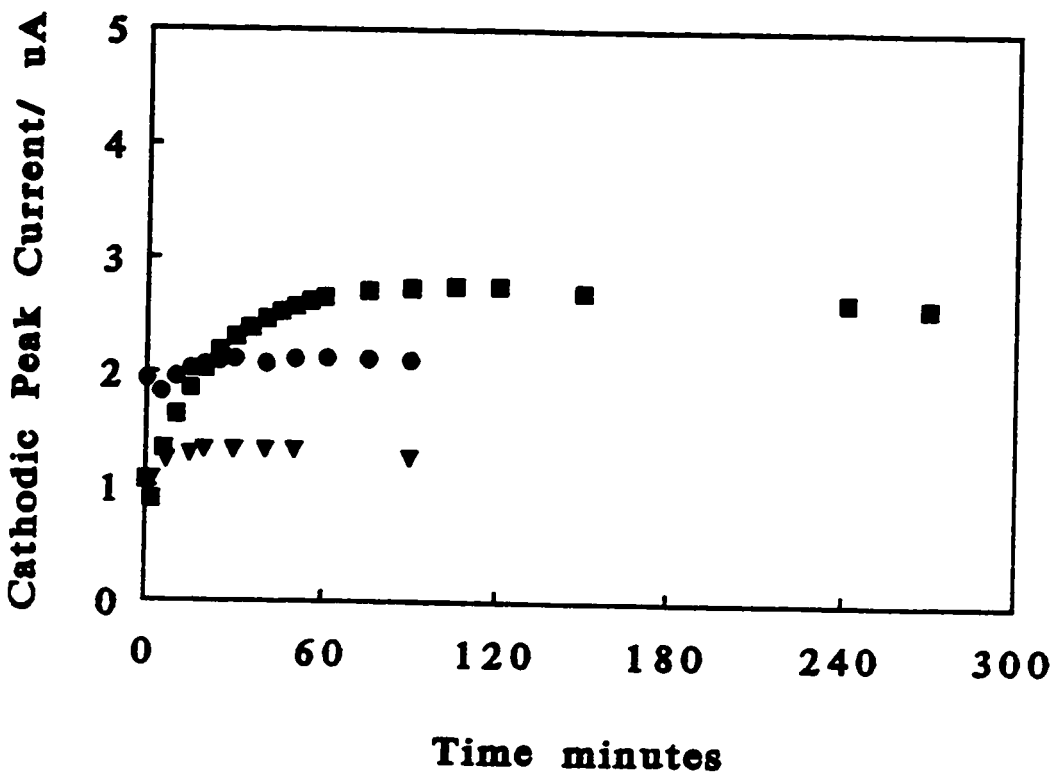

Figure 5.5 Peak current vs time for hybridizations of immobilized poly(dT) with [poly(dA)] = (▾) 1, (●) 5, and (■)10 μg/mL. Conditions: 60 μM $Co(bpy)_3^{3+}$ mM Tris pH 7.1, 20 mM NaCl, ν = 50 mV/s.

5.2.2 **Batch Hybridizations**

Batch hybridizations at varying poly(dA) concentrations were carried out at high ionic strength separately from detection. Hybridizations were performed at 28 °C, in 0.5 M NaCl, 5 mM Tris pH 7.1 in the absence of hybridization indicators. Hybridizations were periodically interupted by removal of the sensor for voltammetric analysis in a solution of hybridization indicator (analysis buffer). The sensor was equilibrated in the analysis buffer for 5 minutes before voltammetric analysis. In these experiments hybridizations were completed after less than 10 minutes of exposure to poly(dA) for all poly(dA) concentrations within the range of 1 ng/mL to 1 μg/mL. Figure 5.6 shows the cathodic peak current vs time of hybridization for typical batch hybridizations with poly(dA) concentrations equal to 1 μg/mL, 0.1 μg/mL, 10 ng/mL and 1 ng/mL.

In both batch and *in situ* hybridization experiments the magnitude of the peak current both before and after hybridization with target DNA varies considerably between sensors. Figure 5.7 shows the peak current vs hybridization time with a poly(dA) concentration equal to 1 μg/mL for three separate sensors. It demonstrates the variability in magnitude of the peak current throughout the hybridization process. A comparison of curve A, in which hybridization is complete within 10 minutes versus curves B and C in which hybridization is complete after 30 and 50 minutes, respectively, also demonstrates the variability of hybridization times at separate poly(dT)poly(dG)-modified CPEs. For the hybridization experiment shown in Figure 5.7 (Curve B) the rate constant k was calculated to be 9×10^{-4} s^{-1}.

Due to the variability in the magnitude of the peak current response, the percent

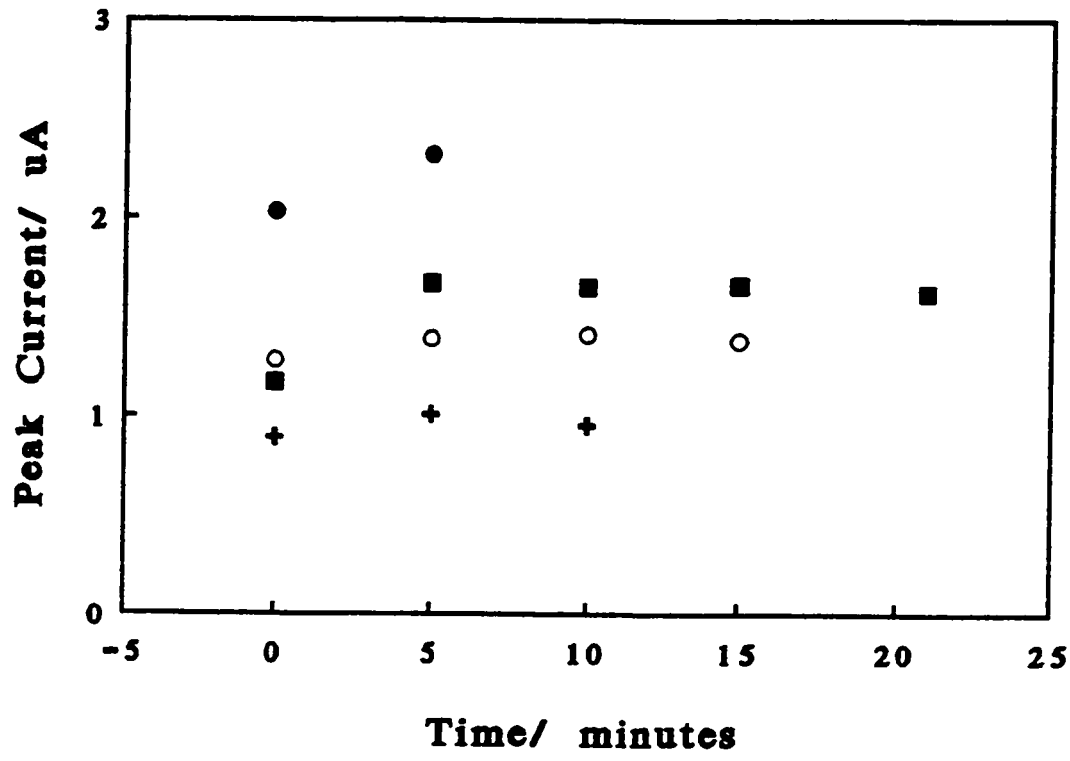

Figure 5.6 Cathodic peak current vs hybridization time for poly(dT)$_{4000}$-poly(dG)$_x$-modified SACPEs. Hybridizations were performed in 0.5 M NaCl, 5 mM Tris pH 7.1. Analysis were performed in 60 μM $Co(bpy)_3^{3+}$, 20 mM NaCl, 5 mM Tris pH 7.1, ν = 50 mV/s. [Poly(dA)] = (●) 1 ng/mL, (■) 1.0 μg/mL, (+) 0.1 μg/mL, (O) 10ng/mL.

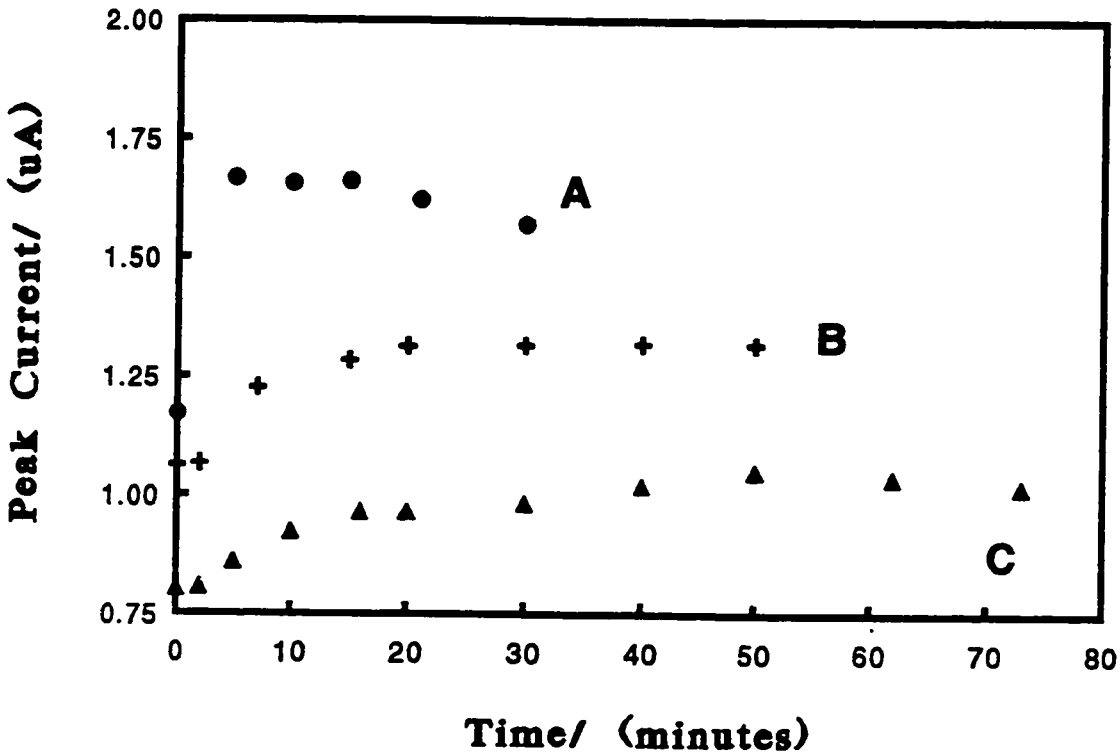

Figure 5.7 Cathodic peak current vs hybridization time for three poly(dT)$_{4000}$-poly(dG)$_x$-modified SACPEs. Hybridizations were performed in 0.5 M NaCl, 5 mM Tris pH 7.1. Analysis were performed in 60 μM $Co(bpy)_3^{3+}$, 20 mM NaCl, 5 mM Tris pH 7.1, ν = 50 mV/s. [Poly(dA)] = 1 μg/mL

increase in current upon hybridization was determined for each sensor in order to determine the detection limits for both the in situ and batch hybridizations, as shown if figure 5.8. The results of these studies show that hybridization reactions performed in high NaCl cocentrations in the absence of hybridization indicators yield detection limits which are two orders of magnitude lower than that for *in situ* hybridizations, for a 25 to 30% increase in peak current. The detection limits are 10 μg/mL poly(dA) for *in situ* hybridizations and 0.1 μg/mL for batch hybridizations.

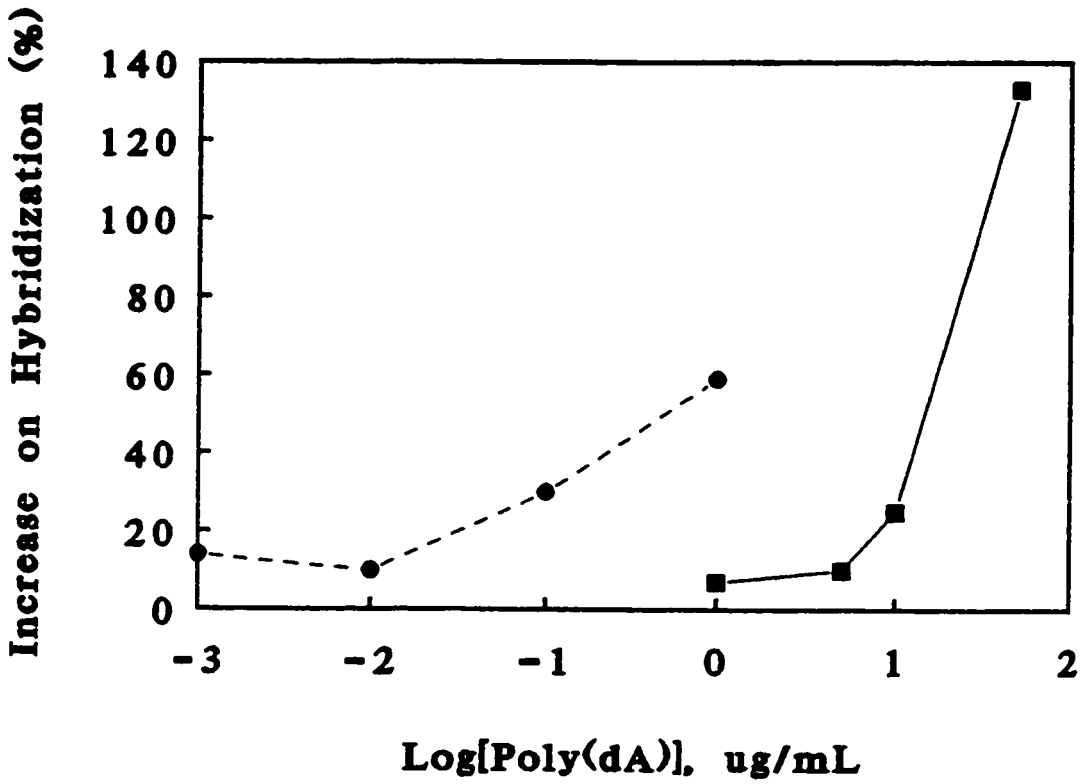

Figure 5.8 Detection Limits of analyte DNA. Percent increase in cathodic peak current of 60 μM $Co(bpy)_3^{3+}$ at a poly(dT)$_{4000}$-poly(dG)$_x$-modified SACPE as a function of [poly(dA)]. Analysis buffer conditions: 60 μM $Co(bpy)_3^{3+}$, 20 mM NaCl, 5 mM Tris pH 7.1. *In situ* hybridizations are represented by (■) and batch hybridizations by (●). Analysis of the extent of hybridization was performed separately with low NaCl concentrations, in the presence of a hybridization indicator, and at 25°C.

5.3 Discussion

Two procedures for hybridization were examined. In situ hybridizations had only one buffer system, hybridizations and analysis were performed in the presence of a hybridization indicator with low NaCl concentrations, and at 25°C. In the batch hybridization procedure hybridizations were performed under optimal conditions with [NaCl] = 0.5 M, and at a temperature 25°C below the T_m of the duplex (53 - 25°C = 28°C), in the absence of a hybridization indicator. Analysis of the extent of hybridization was performed separately with low NaCl concentration, in the presence of a hybridization indicator, and at 25 °C.

The rate of hybridization is limited by diffusion when there are high amounts of DNA immobilized onto a membrane filter.[7] This is characterized by hybridization rates which are extremely fast, by an increase in rate by stirring or shaking the hybridization solution, a decreased rate of hybridization with an increase in size of the target DNA in solution, and an independence of rate on DNA sequence complexity. This is not true under the conditions in which hybridization is carried out in our experiments. It can be assumed that the total quantity of poly(dA) in solutions with a greater than 1 μg/mL concentration are in vast excess of the of the total quantity of poly(dT) immobilized onto the surface and that hybridization on the membrane itself is rate limiting. Thus the solution reassociation and diffusion terms from equation [6] can be ignored[7] and pseudo-first order kinetics can be applied to the hybridization reactions with excess poly(dA) concentrations.

In the *in situ* experiments hybridizations were carried out in the presence of either $Co(bpy)_3^{3+}$, $Co(phen)_3^{3+}$, or $Os(bpy)_3^{2+}$. These transition metal complexes bind to DNA electrostatically, and in the case of $Co(phen)_3^{3+}$ also through intercalation. A high ionic

strength medium will result in lower association constants and therefore a lower voltammetric response.[9,10] Therefore, low ionic strength conditions are required for detection. The hybridization conditions are therefore not optimum. Under these conditions the rates of hybridization were much lower than that predicted by theory for solution hybridizations (equation 3). For a poly(dA) concentration of 10 μg/mL (8×10^{-9} M) at 28°C at [NaCl]≥ 0.4M the theoretical k_{obs} is 0.17 s^{-1} and 0.017 s^{-1} for [poly(dA)]= 1μg/mL. Hybridization in the presence of $Co(bpy)_3^{3+}$, $Co(phen)_3^{3+}$, or $Os(bpy)_3^{2+}$ had rates of $8 \times 10^{-4} s^{-1}$, $5 \times 10^{-4} s^{-1}$, and $5 \times 10^{-4} s^{-1}$. This difference between theoretical and experimental hybridization rates indicates that under the *in situ* hybridization conditions hybridization is not straightforward and that collision of poly(dA) with immobilized poly(dT) is not rate limiting. This is further substantiated by results which show no correlation between increasing poly(dA) concentrations and an increase in rate. By using an excess of poly(dA) its concentration is maintained nearly constant and the corresponding term in the rate law does not change, and pseudo-first order conditions are assumed. Under these conditions k_{obs} should vary linearly with [poly(dA)] with a slope equal to k_s ($k_{obs} = k_s$ [C]). This was not observed, negative slopes for k_{obs} vs [C] were found for DNA hybridizations in the presence of $Co(bpy)_3^{3+}$ and $Co(phen)_3^{3+}$. It is possible that surface immobilization of one of the DNA strands and/or the DNA-binding complexes decreases the rate of DNA hybridization.

Batch hybridizations were carried out in a solution separate from DNA-binding complexes. It was believed that hybridization would occur at a faster rate since hybridization and detection are performed in two steps and the conditions for both hybridization and detection can be optimized. The results could also be compared to theoretical values since the

conditions of hybridization are the same.

Under these conditions the maximum peak currents were obtained in less than 10 minutes after the addition of poly(dA) with concentrations of 1 ng/mL to 0.1 μg/mL. The time to obtain the maximum peak current due to hybridization decreased substantially in the absence of a DNA-binding complex. At all concentrations of poly(dA) the maximum peak current was obtained in less than 10 minutes of exposure to poly(dA). However, a longer hybridization time was observed for two hybridization experiments with a poly(dA) concentration of 1 μg/mL (t= 30 and 50 minutes). The k_{obs} for one hybridization (30 minutes) was calculated to be 9×10^{-4} s^{-1} which is much less than the value of 0.017 s^{-1} predicted by equation 3. Although the time for completion of hybridization is decreased in the absence of DNA-binding complex, the inconsistency in the results makes for difficult interpretation about the kinetics of hybridization.

The results for the *in situ* and the batch hybridization experiments suggest that both the presence of the hybridization indicators and the fact that one of the DNA strands is surface-bound may affect hybridization kinetics. Also, the initial interaction of the two DNA strands at low [NaCl] is not rate-limiting. It is possible that the DNA-binding complexes interfere with hybridization by inducing a conformational change in ssDNA by electrostatic binding. A lower rate of hybridization is expected when one strand is immobilized even if immobilization does not bind the bases involved in hybridization. In solution, both strands can diffuse freely; however, immobilization of one strand of DNA to a surface eliminates its diffusion, which will reduce the rate of hybridization. Also, the binding of ssDNA to a solid surface can affect its conformation and interfere with the normal hybridization process. The

conformation of ssDNA bound to the surface of a CPE is unknown.

For both the batch and the in situ hybridization experiments the magnitude of the peak current change during hybridization depends on individual immobilizations. The immoblilization of poly(dT)poly(dG)$_x$ is highly inconsistent and may contribute significantly to the variability in the initial signal magnitude after immobilization and the final signal magnitude after the completion of hybridization. This was also observed for poly(dG)poly(dC) immobilizations at both GCEs and SACPEs, as observed in Chapters 3 and 4. One factor which seems to influence immobilization yield is evaporation rate, but the determination of other variables requires further study. Because of this variability in absolute peak currents, the percent increase in current response between hybridized and ssDNA is a better measure for the detection of analyte DNA. Hybridizations at high ionic stength without DNA-binding complexes give better detection limits for poly(dA) by about 2 orders of magnitude for a 25-30% increase in peak current in comparison to in situ hybridizations. A 4000 base sequence is easily detectable at 100 ng/mL, which is equivalent to a 10 ng/mL quantity produced by a typical PCR reaction product of 400 bases in length. The volume used for hybridization can be as low as 25 μL which indicates that a total of 250 pg of analyte DNA can be detected for each hybridization reaction. This corresponds to a limit of detection of 1.8 fmol. The possibility of lowering the detection limits of a CPE based DNA-sensor is hopeful since the detection limits of another voltammetric DNA-sensor based on the same concept has a detection limit of 0.1 amol.[11] In this work gold electrodes and Hoechst 33258 were used, as described in Chapter 1.

5.4 **Conclusions**

The kinetics of hybridization of an immobilized poly(dT) probe at high ionic strength in the absence of a hybridization indicator and at low ionic strength in the presence of a hybridization indicator were compared. It was determined that hybridization was much faster under high ionic strength conditions in the absence of a hybidization indicator. Under these conditions the detection limit for a 4000-base target sequence was found to be 100 ng/mL. This technique should be readily adaptable to analysis of a PCR amplified sequence of 400 bases.

5.5 **References**

1. Porsche, D.; Eigen, M.; *J. Mol. Biol.*, **1971**, 62, 361.

2. Craig, M. E.; Crothers, D. M.; Doty, P.; *J. Mol. Biol.*, **1971**, 62, 383.

3. Meinkoth, J.; Wahl, G.; *Anal. Biochem.*, **1984**, 138, 267.

4. Gamper, H. B.; Cimino, G. D.; Hearst, J. E.; *J. Mol. Biol.*, **1993**, 197 (2). 349.

5. Braunlin, W. H.; Bloomfield, V. A.; *Biochemistry*, **1991**, 30, 754.

6. Brunemann, H.; *Nucleic Acids Res.*, **1982**, 10, 7181.

7. Su, H.; Thompson, M.; *Biosens. and Bioelectron.*, **1995**, 329.

8. Su, H.; Yang, M.; Kallury, K. M. R.; Thompson, M., *Analyst*, **1993**, 118, 309. Su, H., Kallury, K. M. R.; Thompson, M.; Raoch, A.; *Anal. Chem.*, **1994**, 66, 769. Thompson, M.; Kipling, A. L.; *Analyst*, **1991**, 116, 881.

9. Barton, J. K.; Goldberg, J. M.; Kumar, C. V.; Turro, N. J.;*J. Am. Chem. Soc.*, **1986**, 108, 2081.

10. Figure 3.4 demonstrates the effect of ionic strength on peak current of $Co(bpy)_3^{3+}$ to a poly(dG)poly(dC)-modified GCE.

11. Hashimoto, K.; Ito, K.; Ishimori, Y.; *Anal. Chem.*, **1994**, 66, 3830.

Chapter 6

Detection of the Cystic Fibrosis ΔF508 Mutation

6.1 Introduction

The cystic fibrosis gene is located in the q arm of chromosome number 7. It is approximately 230 kb of genomic DNA and has 27 exons. Molecular cloning has permitted the isolation of a region of DNA which contains the CF gene.[1] This gene has been analysed by chromosome walking and jumping from flanking, linked polymorphic markers on genomic DNA[2,3], by the analysis of yeast artificial chromosomes and by pulsed-field genetic mapping.[4a] The CF gene product is named the Cystic Fibrosis Transmembrane Conductance Regulator (CFTR). This 1480 amino acid protein is composed of two membrane-spanning domains, each containing six hydrophobic subunits, followed by a hydrophilic region containing the nucleotide binding fold (NBF). These two domains are separated by the regulatory domain which contains multiple substrate binding sites for protein kinase A and C.[4a] Cystic fibrosis is an autosomal recessive hereditary disorder caused by mutations which result in a defective CFTR protein.[5]

The first DNA mutation was detected by comparing the sequences derived from CF patients and individuals without signs of the disease.[1] It is a deletion of three base pairs which results in the absence of a phenylalanine amino acid at position 508 of the protein product, and is called the ΔF508 mutation. Approximately 70% of patients with cystic fibrosis from northern Europe and North America have the ΔF508 mutation.[2] Over 500 mutations have been identified, although most have only been found in one or a few patients. Most mutations are missense mutations, single-base substitutions, nonsense mutations, frame-shift mutations,

splice mutations, or small insertions or deletions. Many mutations may not be associated with a diseased state, and the protein product may not be affected, depending on where the mutation is located.[4a,b]

Genetic screening for cystic fibrosis has been complicated by the over 500 mutations already identified. However cystic fibrosis is a model for genetic screening because the carrier frequency in North American and European caucasian populations is so high (1/25), with approximately 8 million Americans being a carrier.[6] One caucasian child in 2500 has the disease.[6] Cystic fibrosis has become the test case for the economic, ethical, and analytical issues of genetic screening since many of the problems associated with CF testing are general for most hereditary disorders.[6] The development of effective methods for gene therapy in affected individuals is ongoing. A clinical trial of gene therapy for the respiratory symptoms of CF began in 1993 and indicates that it is possible to transfer and express the normal CFTR cDNA to the airway epithelium *in vivo* in patients with cystic fibrosis.[5] With the development of an effective treatment for the manifestations of cystic fibrosis, the need for cost-effective neonatal screening is essential. Until a universal treatment is available genetic screening for carriers is helpful in genetic counselling.

The first diagnostic test for cystic fibrosis was the sweat test developed in 1953.[7] The sodium and chloride levels in the sweat of CF patient is very high relative to individuals without the disease. This method was improved by pilocarpine iontophoresis to stimulate sweat. Sweat is collected and the quantity of sodium and chloride ions are determined by routine analytical methods.[8] This test has been routinely used for over 30 years. However, false negatives have been a problem, since normal sweat Cl^- quantities have been found in

patients with mild symptoms of cystic fibrosis.[9]

Another diagnostic test is the Meconium Test. Meconium is a dark green mucilaginous material in the intestine.[10] It has been determined that the albumin content of meconium from CF infants is elevated due to pancreatic insufficiency, but the use of quantitative[11] analysis of meconium albumin has serious problems with its reliability.[12] The Meconium Test has both a relatively high false positive incidence (>0.5 %) and a high false negative occurence (> 25%).

Cystic fibrosis has also been diagnosed by screening for blood immunoreactive trypsin. In CF infants of a few weeks of age the immunoreactive trypsin (IRT) levels in the blood are elevated. However, due to significant variability between the IRT levels in children, this test must be used in conjunction with other tests for a positive diagnosis.[13]

Since the discovery of the CF gene and the mutations which cause CF, genetic testing has become available as a diagnostic test. Different methods of DNA analysis have been applied to the detection of mutations of the CF gene. Most of these methods require primer-directed PCR amplification of the region of interest (see chapter 1, section 1).[14]

The most routinely used method for detection of mutations is PCR-RFLP analysis. A sequence of DNA surrounding the area of interest is amplified by PCR. The DNA to be amplified must contain the region where a mutation will result in the creation or elimination of a site recognized by a restriction endonuclease. The restriction endonuclease will cleave only a specific sequence. The amplified region is also chosen such that only one restriction site for a particular endonuclease is present. After PCR the product of amplification is incubated with the restriction enzyme and then analyzed by electrophoresis. The mutated

sequence has a different mobility than the normal sequence since one will have been cleaved by the restiction enzyme and the other will not.

Figure 6.1a shows a photograph of a 2% agarose gel, stained with ethidium bromide, of the fragments created by the restriction endonuclease HhaI.[15] The presence of the CF mutation CS.7/HhaI polymorphism results in the creation of a HhaI restriction site. This mutation can then be determined by the visualization of a fluorescent band, after ethidium bromide staining, which corresponds to a fragment 165 bp long. In the absence of this mutation a fragment 330 bp in length can be seen. A heterozygote is determined by the presence of both fragments. The problem with this being a universal method for genetic screening is that the mutation must result in the creation or elimination of a restriction site, and this is not always the case.

Another method for detecting mutations is Single-Stranded Conformational Polymorphism analysis (SSCP). The fragment of interest is amplified by PCR and the product is denatured and analysed by high resolution, nondenaturing PAGE. Under these conditions a single strand of DNA can fold back onto itself conferring a unique secondary structure dependent upon the sequence of the strand. Mutations will alter the sequence and create a conformation different from the non-mutated sequence. Therefore strands of DNA with exactly the same size that differ in base composition will have different electrophoretic migration rates.[16] This assay has been applied to identify novel mutations of the cystic fibrosis gene.[17]

Small-size polymorphisms, such as insertion or deletions, as in the ΔF508 three base pair deletion, can be detected by non-denaturing or denaturing polyacrylamide gel

electrophoresis. A size difference of three base pairs between fragments can be resolved on a 10-12% non-denaturing or an 8% denaturing polyacrylamide gel. The fragment surrounding the area of the potential deletion is amplified by PCR, resolved by electrophoresis, and followed by Southern blotting and detection using ^{32}P probes. Figure 6.2 shows the different migrations of a DNA fragment with the ΔF508 deletion and the non-deleted fragment of the normal sequence.[15]

Denaturing gradient gel electrophoresis (DGGE) has also been applied to detect single base changes in PCR products. This method relies on the different melting properties of DNA with different base composition.[18] This method has been applied to the diagnosis of cystic fibrosis which results from non ΔF508 mutations.[19]

A recently developed method is called Chemical Cleavage of Mismatch (CMM). A specified region of DNA is amplified and then denatured and allowed to hybridize with a control sequence which does not contain the mutation. Any mismatch will result in a base which is not hybridized. Mismatched cytosines are chemically modified by hydroxylamine, and thymidines are modified by osmium tetroxide. These modified bases are susceptible to cleavage by piperidine.[20] The resulting fragments are then separated by PAGE. This technique has been applied to diagnosis of non-ΔF508 deletions of the CF gene.[21]

For cystic fibrosis, as well as many heritable disorders, more than one mutation is responsible. Thus many researchers have focused on the diagnosis of multiple mutations simultaneously. The amplification refractory mutation system (ARMS), has been modified such that more than one mutation can be diagnosed concurrently. The ARMS test is a PCR-based diagnostic assay. It is based on the fact that oligonucleotides which have a

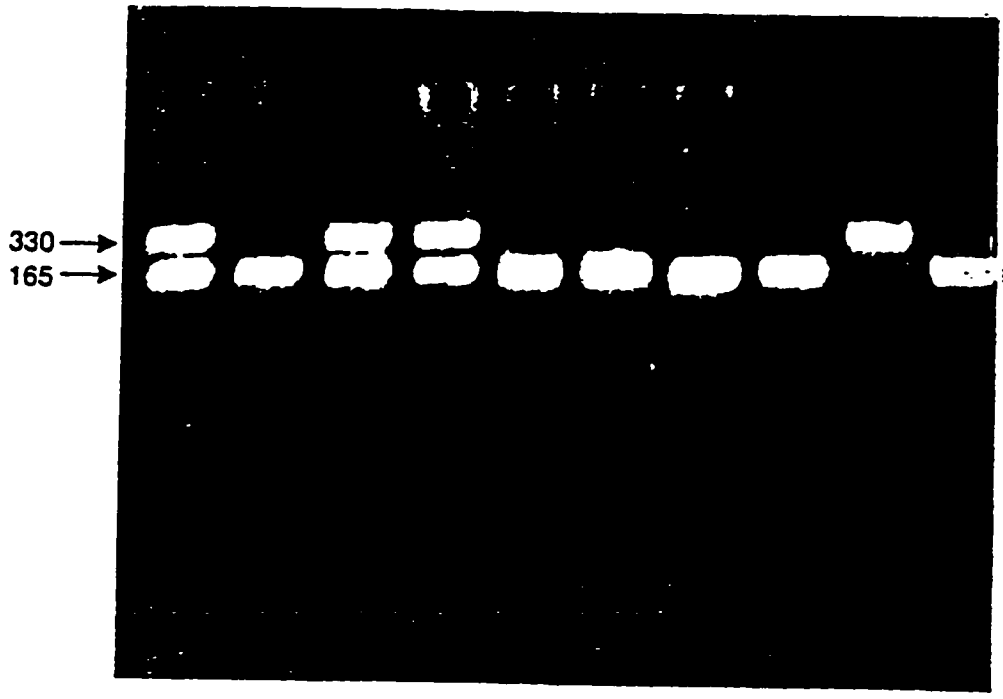

Figure 6.1 PCR-RFLP analysis of CS.7/Hha polymorphism. The DNA samples were amplified for 30 cycles, digested with HhaI, and electrophoresed in a 2% agarose gel.

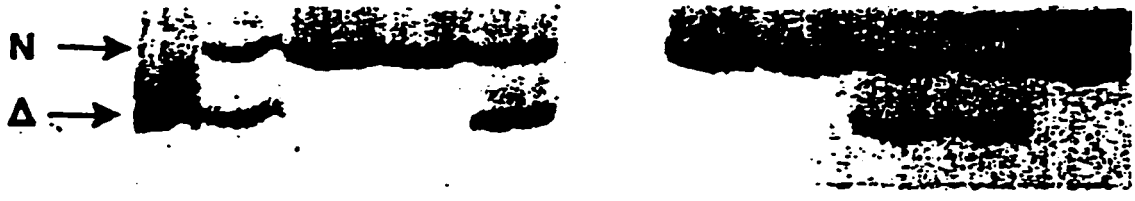

Figure 6.2 Separation of small sized polymorphism by PAGE. The ΔF508 deletion migrates a further distance from the normal gene. N represents the normal gene and Δrepresents ΔF508.[15]

complementary sequence to the target DNA, except for the 3'terminal hydroxyl base will not act as a primer in the PCR reaction, and it will not amplify the target DNA. The primer is chosen such that the 3' terminal base is located at the site of a mutation. The ARMS test consists of two reactions, one with a primer which will only amplify the normal sequence and one which will only amplify the mutant sequence. A heterozygote is identified by the presence of a PCR product in both reactions, a homozygote normal only has an amplification product in the reaction with the non-mutant primer, and a homozygote only has product from the reaction with the mutant primer.[22] This ARMS assay has been modified to analyze multiple mutations concurrently. In this assay primers complementary to sites of different CF mutations are used in a PCR reaction. In addition to their sequence the primers are chosen such that each site being amplified will have a different molecular weight. Two complementary reactions are performed; one for the mutated primers, and one for the non-mutant primers. After the PCR reaction is completed the PCR products are separated by gel electrophoresis in order to identify which sites contain the mutation and which are normal. Each site is identified by its molecular weight, and its genotype is identified by the absence or presence of a PCR product in the normal or mutant reaction.[23]

Another simultaneous multiple mutation detection assay is based on allele-specific oligonucleotides (ASOs). An ASO can be designed to detect any mutation.[24] However each ASO differs in its T_m and thus hybridizations with different regions of DNA must be performed separately. However, recently the ASO method has been adapted to allow for the simultaneous analysis of 12 cystic fibrosis mutations. This assay involves the multiplex PCR amplification of many regions of DNA in which CF mutations have been identified, followed

by dot-blot hybridization with pooled ASOs. The differences in T_ms of the many ASOs used were eliminated by the use of tetramethylammonium chloride. Tetramethylammonium chloride eliminates the dependency of the T_m on G-C content. In the presence of tetramethylammonium chloride the T_m is dependent only on length, and the stringency of hybridization is improved such that single-base changes can be detected. Therefore one hybridization reaction can be performed for a pool of ASOs which can identify many mutations.[25]

A DNA enzyme immunoassay has been designed as a non-isotopic assay for the detection of the ΔF508 deletion which results in the most common form of cystic fibrosis. This enzymatic immunoassay is based on the selective hybridization of target DNA with an microtiter-immobilized probe. The hybrid is detected with an anti-DNA monoclonal antibody, which specifically reacts with dsDNA but not ssDNA, in a colorimetric assay.[26]

Screening for CF has also been accomplished by a technique termed solid-phase minisequencing. In this technique 5'-biotinylated amplified DNA is bound to a solid phase, denatured and hybridized to a detection probe. This probe is complementary to the site which ends immediately before the site where the mutation is known to occur. Taq DNA polymerase will ligate a base 3' to the detection probe which is complementary to the target sequence. In the presence of a mutation, one radioisotopic base will be incorporated, and if the sequence is normal another radioisotopic base will be incorporated. This method was applied to the detection of the ΔF508 deletion. If the deletion is present, [^{3}H]dTTP can be detected, while with the nonmutated sequence [^{3}H]dCTP is detected.

In this chapter the DNA biosensor based on an electroactive hybridization indicators

is applied to the detection of the ΔF508 deletion of the CF gene. The ΔF508 DNA sensor is applied to the detection of its complementary sequence, and reproducibilities are evaluated. The voltammetric sensor is then applied to the analysis of human DNA samples which have been amplified by PCR. Probe sequences were designed so that each will selectively hybridize only with their exact complementary sequence, under stingent conditions of temperature and ionic strength. The probes were 18 bases long for recognition of a unique sequence. In addition the mutation/ 3 base deletion was positioned near the center of the sequence to maximize thermal instability of mismatch hybridization which would improve selective hybridization with only their exact complement.[27]

6.2 **Results**

6.2.1 A Prototype DNA Sensor for the ΔF508 Deletion of the Cystic Fibrosis Gene Sequence.

6.2.1.1 *Carbon Paste Electrodes*

Two probe sequences were designed so each will selectively hybridize only with their exact complementary sequence, under stringent conditions of temperature and ionic strength. The probes CFPD and CFPN were enzymatically elongated with deoxyguanosine residues using the enzyme terminal deoxynucleotidyl transferase as described in section 2.2.5. The sizes of the elongated probes were determined by polyacrylamide gel electrophoresis as described in section 2.2.6. For both reactions (elongation of Probe CFPD and CFPN) there were two main products which were 38 and 53 bases in length. Stearic acid-modified carbon paste electrodes (5% w/w) were modified with these terminal transferase products according

to section 2.2.2.2. The elongated probes are referred to by their probe number, with Probe CFPD having the ΔF508 deletion and Probe CFPN which identifies the normal sequence. The oligonucleotides with complementary sequences to these probes are identified by the CFTD and CFTN, respectively. Table 6.1 gives the peak currents, for 9 different SA-CPEs: 6 modfified with Probe CFPD, 3 modified with Probe CFPN, at the probe-modified electrodes, before and after hybridization with the target DNA. A slight increase in peak current was observed after immoblization of the probe to the CPE. Upon hybridization to the complementary sequence the cathodic peak current increases substantially. Cyclic voltammograms for an unmodified, Probe CFPD modified CPE, and the sensor hybridized to its complementary sequence are illustrated in Figure 6.3.

Table 6.1 Reproducibility of a cystic fibrosis gene DNA sensor. Cathodic peak currents were measured at 1.2×10^{4} M $Co(bpy)_3^{3+}$ for SA-CPEs modified with the probe sequence(either CFPD or CFPN), before and after hybridization with their target DNA. The average peak current at 1.2×10^{4} M $Co(bpy)_3^{3+}$ for unmodified SA-CPEs was 1.07 ± 0.08 μA (n = 9).

Species Immobilized	Peak Current (μA)	Species Hybridized	Peak Current (μA)
CFPD	1.09 ± 0.11 (n = 3)	CFTD	2.48 ± 0.19 (n = 3)
CFPN	1.22 ± 0.09 (n = 6)	CFPN	2.57 ± 0.11 (n = 6)

To determine whether the probe sequences can selectively hybridize with their complementary target sequences the probe-modified SA-CPEs were hybridized to both their

noncomplementary and complementary sequences. At room temperature, both the normal and the CF sensors (CPEs modified with probe CFPD and CFPN respectively) did not discriminate between complementary and noncomplementary sequences. For the CFPD probe, an increase in cathodic peak current from 1.60 μA for the single strand probe to 3.40 μA at 1.2×10^{-4}M was observed after hybridization with the normal (noncomplementary) target (CFTN). For the CF_{normal} probe (Probe CFPN), the peak current obtained after probe immobilization was 1.16 μA, and increased to 2.40 μA after hybridization with the cystic fibrosis target sequence (CFTD). The stringency of the hybridization reaction can be adjusted by altering temperature, ionic strength, or formamide concentration. Since the concentration of target sequences in clinical samples will be small and the rate of hybridization is dependent on ionic strength, hybridization times will be more rapid if performed with high NaCl concentrations. Thus temperature is the most easily manipulated of the variables which affect stringency. The melting temperature for probes larger than 30 bases can be calculated by equation 1:[28]

$$T_m = 81.5°C + 16.6 \log M + 0.41(\%G+C) - \frac{500}{n - 0.61(\%F)} \qquad (1)$$

where M is the Na^+ concentration in M, n is the length in bases of the smallest oligonucleotide participating in hybridization, % G+C is the percent guanosine and cytosine content, and %F is the percent formamide concentration. A different calculation is required for probes 14 to 20 bases in length, equation 2:[27]

$$T_m = 4\ °C \text{ per GC pair} + 2\ °C \text{ per AT pair} \quad (2)$$

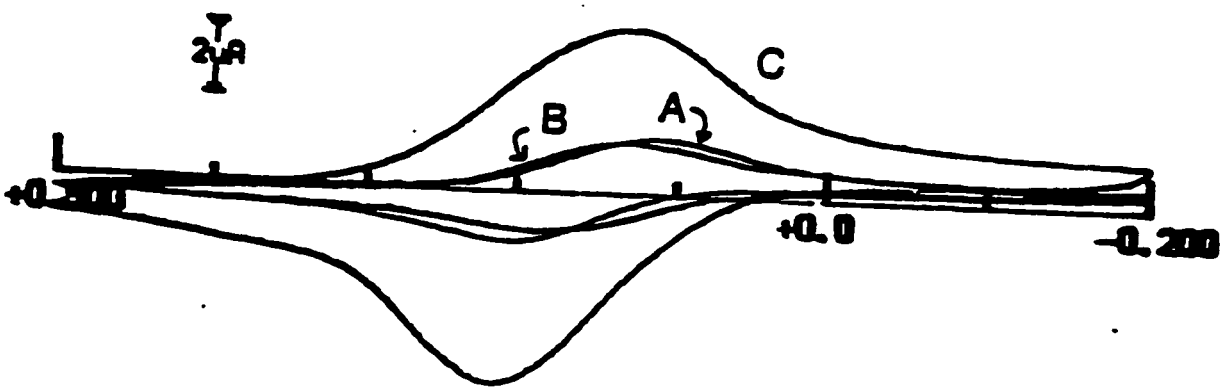

Figure 6.3 Cyclic Voltammograms of an unmodified (A), a CF probe-modified stearic acid CPE (B), and (C) hybridized to its complementary sequence. Conditions: 1.2×10^{-4} M $Co(bpy)_3^{3+}$, 0.020 M NaCl, 5 mM Tris pH 7.1, scan rate 0.050 V/s.

Hybridization occurs most readily at 5 °C below the T_m. The theoretical hybridization temperature, T_H for the cystic fibrosis probes CFPD and CFPN at high ionic strength (above 0.5 M) are 41 and 43 °C,respectively. The CF sensors (CPEs modified with CFPD and CFPN) were hybridized at room temperature (22 °C), 42 °C, and 43 °C. At room temperature the probes did not discriminate between their complementary and noncomplementary sequences. Table 6.2 shows the signal amplitude generated at the two sensors after hybridization at 42 and 43 °C with their complementary and noncomplementary sequences. Hybridizations were performed as described in section 2.2.3.2 in an incubator with the temperature controlled. These temperatures were chosen due to the measured fluctuation in temperature of the incubator by ± 1 °C. A solution of 5 mM Tris pH 7.1, 20 mM NaCl at the same temperature as the hybridization temperature was used to rinse the sensor after hybridization. In Table 6.2 five electrodes were modified with either the normal CF gene sequence probe (CFPN) or the CF deletion sequence probe (CFPD). The numbers 1 through 5 represent a single modification. Since it was determined that DNA sensors based on carbon paste electrodes are not reusable (see Chapter 4), hybridization with the noncomplementary sequence was attempted prior to hybridization with the complementary sequence. As can be seen from Table 6.2, both immobilized probes are capable of selectively detecting their complementary sequence at 42-43 °C. However greater selectivity was achieved at a T_m of 43 °C.

6.2.1.2 *Glassy Carbon Electrodes.*

Carbon paste electrodes are unstable under DNA denaturing conditions (Chapter 5); however, it has been determined that glassy carbon electrodes are stable at temperatures

required to denature DNA. Therefore, GCEs were used to determine the variability in signals at a probe-modified electrode, in its denatured and renatured states. For a ΔF508 probe bound to a GCE and its denatured state the signal at 1.2×10^{-4} M $Co(bpy)_3^{3+}$ is 1.00 ± 0.01 μA (n= 4), which represents a 1% error. This sensor, after hybridization with its synthetic complement gives a signal of 1.42 ± 0.07 μA (n=4), which represents a 5% error, under the same conditions. This demonstrates that for a given DNA sensor, the signals obtained with the denatured and hybridized probes are reproducible. However, between-electrode variability is large. For example, the signal variability between glassy carbon electrode-based DNA sensors can be attributed to the irreproducibility of generating carboxylic acid groups on the electrode surface, to the activation of the carboxylic acid groups with coupling reagents, and to the coupling of DNA to the electrode surface. Both the activation and DNA-coupling reactions are heterogenous, and this may contribute to variability.

6.2.2 The ΔF508 Probe: Detection of Human PCR-amplified Target Sequences.

Two probes were prepared for the sequences of DNA which are complementary to the region surrounding the ΔF508 deletion. One probe is complementary to the gene sequence which results from the 3-base deletion and is referred to as ΔF508M. Two other probes were designed which are complementary to nonmutated sequences and are referred to as ΔF508NA and ΔF508NB. Probe complementarity for the region surrounding the ΔF508 deletion can be verified in Table 6.3 in which the sequence of the cystic fibrosis gene between bases 1621 and 1680 is given along with the sequences of the two probes used for the sensor. All three probes have a 3' deoxyguanosine tail which is 15 bases in length, and acts as the anchor to the

electrode surface. The ΔF508 probes were immobilized onto GCEs following the procedure outlined in sections 2.2.1 and 2.2.2. It was demonstrated in Chapter 3 that $Co(bpy)_3^{3+}$ binds preferentially to double-stranded DNA and is preconcentrated at the surface of an electrode with double-stranded DNA coupled to it. Successful coupling of DNA to the electrode surface was therefore verified by determining the percent increase in signal at a constant

Table 6.2 CF Gene DNA sensors. Cathodic peak currents were measured at SA-CPEs modified with the probe sequence (either # CFPD or CFPN), after hybridization to the noncomplementary synthetic target (# CFTD or CFTN), and after hybridization with the complementary sequence at either 42 or 43 °C. Hybridization conditions: 5 mM Tris pH 7.1 and 0.020 M NaCl. Conditions for cyclic voltammetry were 1.2×10^{-4} M $Co(bpy)_3^{3+}$, 5 mM Tris pH 7.1, 0.020 M NaCl. The complementary sequences to the probe are indicated by *. Numbers 1 through 5 indicate an individual sensor.

Species Immobilized	Peak Current (μA)	Species Hybridized	Peak Current (μA)	Hyb. Temp(°C)
(1) CFPN	1.00	CFTD	1.49	42
(1) CFPN	1.00	CFTN*	2.78	42
(2) CFPN	1.21	CFTD	1.49	43
(2) CFPN	1.21	CFTN*	3.36	43
(3) CFPD	1.87	CFTN	2.40	42
(3) CFPD	1.87	CFTD*	3.43	42
(4) CFPD	2.30	CFTN	2.39	43
(4) CFPD	2.30	CFTD*	3.80	43
(5) CFPD	2.31	CFTN	2.40	43
(5) CFPD	2.31	CFTD*	3.43	43

Table 6.3 The cystic fibrosis transmembrane conductance regulator gene sequence between bases 1621 and 1680. The ΔF508 deletion occurs within this region. The probes ΔF508M (CF probe) and probe ΔF508NB (normal probe) are also given.$(GGG)_5$ is an abbreviation for 15 G residues which bind to the electrode.

Probe Name	Sequence 5'-3'
CFTR Gene Sequence (Bases 1621-1680)	ATT ATG CCT GGC ACC ATT AAA GAA AAT ATC AT*C TT*T GGT GTT TCC TAT GAT GA ATA TAC
Probe ΔF508M	GAA ACA CCA ATG ATA TTT $(GGG)_5$
Probe ΔF508NA	GAA ACA CCA AAG ATG ATA $(GGG)_5$
Probe Δf508NB	CAC CAA AGA TGA TAT TTT $(GGG)_5$

concentration of hybridization indicator before and after hybridization to its synthetic complement. An increase in peak current of 25% or more at 1×10^{-4} M $Co(bpy)_3^{3+}$ was used to indicate that the probe was successfully immobilized onto the surface of the GCE. From studies with a ΔF508M probe-modified GCE, section 6.2.1.2, the sensor gave an initial signal of 1.00 ± 0.01 which increased to 1.42 ± 0.07 μA (n= 4) after hybridization with its complement.

6.2.2.1 Detection of the Cystic Fibrosis ΔF508 Deletion Sequence.

Probe ΔF508M was coupled to the surface of a glassy carbon electrode, as described in Sections 2.2.1.1 and 2.2.2.2. Its peak current before hybridization was 1.36 μA which increased to 1.81 μA upon hybridization with its complementary strand. This is a 33%

increase in signal which indicates successful coupling of the probe to the GCE surface. The sensor was then submerged in hot (100 °C) deionized H_2O to denature the hybridized probe. By rinsing in hot H_2O regeneration of the single-stranded probe was achieved as indicated by a decrease in peak current to a value obtained by the probe before hybridization.

Attempts were then made to hybridize the probe with human DNA samples. PCR-amplified sequences of the region where the ΔF508 deletion occurs were diluted 21-fold with 0.5 M NaCl in 5 mM Tris (pH 7.1). The samples were then heated to 100 °C to denature the double-stranded PCR product. The sensor surface was exposed to the heated PCR samples and the test samples were allowed to cool to 43 °C using a Perkin Elmer® DNA Thermal Cylcler, as described in section 2.2.3.3. The block temperature for this thermal cylcler is accurate within 1 °C for programmed temperatures between 33 °C and 99 °C. The sensor and samples were then incubated at 43 °C for 30 minutes. The sensor was removed from the test sample and rinsed with 5 mM Tris pH 7.1, 0.020 M NaCl. Detection of the target sequence was accomplished by cyclic voltammetry following a 5 minute incubation in 1×10^{-4} M $Co(bpy)_3^{3+}$ in the low ionic strength buffer.

Incubation with a test sample from an individual homozygous for the nonmutated CF gene gave a 1% increase, wheras an increase in peak current response was observed when the target DNA was present as in the case of the PCR sample from individuals heterozygous (N/F) and homozygous (F/F) for the ΔF508 deletion, as indicated by an increase in peak current response of 37% and 34%, respectively. Table 6.4 provides the results of the analysis of human PCR-amplified test samples with this ΔF508M sensor.

6.2.2.2 Detection of the Normal Cystic Fibrosis Gene Sequence.

Probe ΔF508NB was coupled to a GCE and at 1.2×10^{-4} M $Co(bpy)_3^{3+}$ the peak current was 0.87 μA. Upon hybridization with its synthetic complement a 65 % increase in peak current was observed. The PCR-amplified DNA was diluted and denatured as described above. The sensor was then immersed in the hot DNA solution, the temperature was allowed to cool to 43 °C, and the sensor was incubated at 43 ± 1 °C for 2.0 hours.

Hybridization times were varied for the same electrode. No increase in peak current was observed for hybridization times less than one hour for the PCR samples analyzed. Table 6.3 gives the results obtained after attempted hybridizations of a ΔF508NB sensor with samples

Table 6.4 GCEs were modified with ΔF508M probe sequence. Hybridizations were performed at 43 °C for 0.5 hour, 0.5 M NaCl, 5 mM Tris pH 7.1. Detection conditions were 1.2×10^{-4} M $Co(bpy)_3^{3+}$, 5 mM Tris pH 7.1, 0.020 M NaCl.

Test Sample	Peak Current Before Test (μA)	Peak Current After Test (μA)	Percent Increase
Synthetic Target Sequence	1.36	1.81	33
N/N	1.38	1.39	1
CF/CF	1.35	1.80	34
N/CF	1.37	1.88	37

Table 6.5 GCEs were modified with ΔF508NB probe sequence. Hybridizations were performed at 43 °C for two hours, 0.5 M NaCl, 5 mM Tris pH 7.1. Detection conditions were 1.2×10^{-4} M $Co(bpy)_3^{3+}$, 5 mM Tris pH 7.1, 0.020 M NaCl.

Test Sample	Peak Current Before Test (μA)	Peak Current After Test (μA)	Percent Increase
Synthetic Target Sequence	0.87	1.44	66
N/N	0.88	1.28	47
CF/CF	0.86	0.90	5
N/CF	0.86	1.35	57

from individuals that are homozygous normal (N/N), heterozygous for the deletion (F/N), and homozygous for the deletion (F/F).

To verify that the probe was hybridized within 1.5 hours the same ΔF508NB-sensor was incubated with 100 μg/mL of its synthetic complement in 0.5 M NaCl, 5 mM Tris pH 7.1 and the hybridization time recorded. The sensor was periodically removed from the solution containing the target sequence for analysis. The extent of hybridization was measured via cathodic peak current after incubation for 5 minutes in a solution of 1.2×10^{-4} M $Co(bpy)_3^{3+}$. Figure 6.4 illustrates the increase in peak current versus hybridization time. It demonstrates that the hybridization is complete within 10 minutes for a 100 μg/mL solution of target DNA.

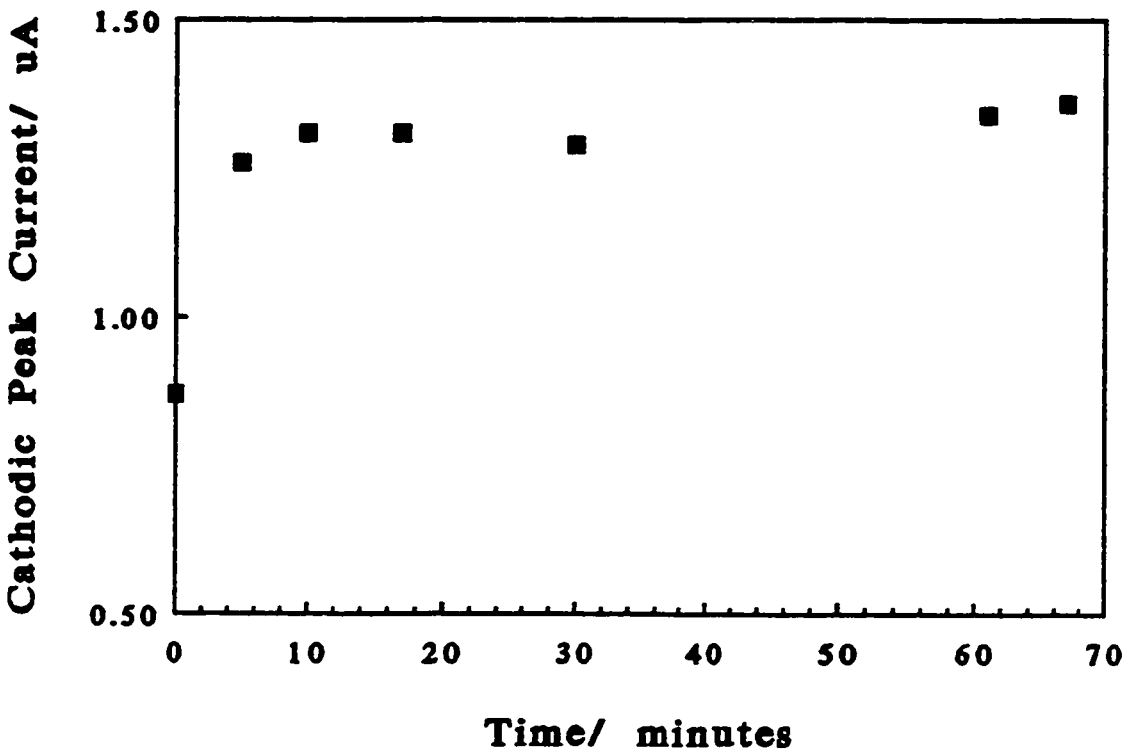

Figure 6.4 A ΔF508NB-probe modified sensor is incubated with 100 μg/mL of single-stranded target DNA, 0.5 M NaCl 5 mM Tris pH 7.1 and the time recorded. The sensor is periodically removed from the analyte solution for cathodic peak current measurements at 1.2 × 10^{-4} M $Co(bpy)_3^{3+}$, 5 mM Tris pH 7.1, with a scan rate of 0.050 V/s.

6.3 Discussion

The results from the CPE based DNA sensor show that immobilization of an oligonucleotide probe through a dG tail does not abolish the ability of the probe to recognize and hybridize to its complementary sequence. The immobilized cystic fibrosis sequence probe and its normal equivalent were capable of hybridization with their complementary strands. These probe sequences were also capable of selectively discriminating between their exact complement and the same sequence with a three base deletion, under appropriate conditions of temperature and ionic strength. At 42-43 °C both probe sequences hybridize with only their exact complement.

The variability associated with different electrode modifications was determined by measuring the signal before and after hybridization at a probe-modified CPE. The reproducibility between CPE-based DNA sensors is poor. An 11% and 8% coefficient of variation is associated with different immobilizations and hybridizations (with a target sequence) of an 18-mer DNA probe at CPEs, respectively.

The variability of response for a single sensor was determined by measuring the signal at a GCE-modified with a probe, before and after multiple hybridizations with the synthetic complement to the probe. For a single sensor the percent error in peak current after immobilization of the single-strand probe is 1%, and 5% after hybridization with its target sequence. Thus within-sensor variation is very low and the reliability of the signal is excellent.

Improvements are required to increase the reproducibility of the signals for different sensors. This can be accomplish by focussing on improving the reproducibility of the coupling reaction.

CPEs are unstable under conditions necessary to denature double-stranded DNA. Thus tests on human genomic samples were performed with a GCE-based DNA sensor. Three probes were designed all of which were complementary to the region surrounding the three base deletion. The main difference between the probe which recognizes the mutant sequence and the probe which recognizes the normal sequence is the three base deletion, referred to as the ΔF508 deletion. Two oligonucleotides, with different sequences complementary region surrounding the ΔF508 mutation of the normal gene, were used as probes for the normal gene sequence (see Table 6.3). One was successful(ΔF508NB), and the other unsuccessful (ΔF508NA) as a probe for this sensor.

The ΔF508 deletion is a recessive mutation, thus two copies of the gene are required to show manifestations of the disease. Thus detection of both copies of the ΔF508 gene sequence is necessary to determine the genotype of the patient for diagnosis of the disease. Individuals heterozygous for the gene do not have any symptoms of the disease. However, heterozygous individuals can pass the gene on to their offspring. Therefore genetic screening is also necessary for genetic counselling and family planning.

Two sensors, one for the normal gene and one for the mutation, will be able to determine which sequence or sequences are present. A positive result at both sensors will indicate that the patient is heterozygous for the gene. A positive results at only one of the sensors will indicate that the individual is either homozygous normal or homozygous for the mutated gene.

The results of the studies with the PCR-amplified human genome samples indicate that the coupling methods do not interfere with the probe's ability to selectively hybridize with its

target sequence. This method for electrochemical detection of hybridization at an electrode surface has now been shown to provide reliable results with real PCR samples for patients being screened for the ΔF508 deletion.

The results shown in Section 6.2.2 demonstrate that DNA sensors for the ΔF508 mutation can properly identify the three base ΔF508 deletion and that with the two sensors, for the normal and mutated sequence, the presence of one or two copies can be determined.

This novel electrochemical DNA sensor incorporates the high selectivity of DNA as the recognition agent with a highly sensitive, inexpensive and portable electrochemical transducer. In comparison to the standard DNA diagnostic methods for heritable disorders and infectious disease (PCR in conjunction with electrophoresis, the use of ^{32}P probes, Southern Blotting, etc), electrochemical DNA sensors are relatively inexpensive, less hazardous, portable due to their size, and require little expertise. This would be of great benefit in developing countries.

The electrochemical transducer provides more advantages than do the other transducers for use in hybridization sensors. In Chapter 1 the various types of transducers used for DNA sensors was reviewed. Piezoelectric devices rely on a method that requires great expertise, lengthy processing times, and to date has not provided better detection limits than electrochemical transduction. Optical and electrochemiluminescent transducers lack the portability and detection limits that electrochemical transduction offers.

To date the DNA sensor with the best detection limits is based on electrochemical detection, with a gold electrode, of the hybridization event via Hoechst 33258, an organic dye which binds selectiveley to dsDNA.[29] This work was based on our DNA sensor and gives an

indication that the detection limits for our DNA sensor can be improved.

6.4 **Conclusions**

DNA sensors selective for the cystic fibrosis ΔF508 deletion region of human DNA were prepared and characterized with synthetic and PCR-amplified human DNA targets. These sensors were capable of selectively detecting their target sequences when hybridization occurred at 43 °C in 5 mM Tris with 0.5 M NaCl.

6.5 **References**

1. Riordan, J. R.; Rommens, J. M.; Kerem, G.; Alon, N.; Rozmahel, R.; Grzelczak, Z.; Zielenxki, J.; Lok, S.; Plavsic, N.; Chou, J.; Drumm, M. L.; Iannuzzi, M. C.; Collins, F. S.; Tsui, L.; *Science*, **1989**, 245, 1066.

2. Kerem, B.; Rommens, J. M.; Buchanan, J. A.; Markicwicz, D.; Cox, T. K.; Chakravarti, A., Buchwald, M.; Tsui, L.; *Science*, **1989**, 245, 1073.

3. Rommens, J. M; Iannuzzi, M. C.; Kerem, B. S.; et al.; *Science*, **1989**, 245, 1059.

4. a)Harris, A.; *British Medical Bulletin*, **1992**, 48 (4), 738. (b) Clavel, C.; Pennaforte, F.; Pigeon, F; Mozelle, M.; Boutterin, M.C.; Duval-Binninger, I.; F-erec, C.; Birembaut, P.; *Ann. Biol. Clin. (Paris)*, **1996**, 54, 67.

5. Horst, R. J.; McElvaney, N. G.; Chu, S. -S.; Rosenfeld, M. A.; Mastrangeli, A.; Hay, J.; Brody, S. L.; Eissa, T.; Danel, C.; Jaffe, H.A.; Crystal, R. G.; *Am J. Respir. Crit. Care Med.*, **1995**, 151, s75.

6. Silverman, L. M.; Highsmith Jr., W. E.; *Clin. Chem.* (editorial), **1992**, 38, 1, 7.

7. Darling, R. C.; diSant'Agnese, P. A.; Perera, G. A.; Anderson, D. H.; *Am. J. Med. Sc.*, **1953**, 225, 67.

8. Gibson, L. E.; Cooke, R. E.; *Pediatrics*, **1959**, 23, 545.

9. Stewart, B.; Zabner, J.; Shuber, A. P.; Welsh, M. J.; McCray Junior, P. B.; *Am J. Respir. Crit. Care. Med*, **1995**, 151, 899.

10. "Dorland's Pocket Medical Dictionary", W. B. Saunders Company, Philadelphia, 1959.

11. Stephan, U.; Busch, E. W.; Kollberg, H.; Hellsing, K.; *Pediatrics*, **1975**, 55, 35.

12. Ryley, H. C.; Goodchild, M. C., Dodge, J. A.; *Brit. Med. Bull.*, **1992**, 48 (4), 804.

13. Crossley, J. R.; Elliott, R. B.; Smith, P. A.; *Lancet*, **1979**, i, 472.

14. Saiki, R. K.; Glefand, D. H.; Stoffel, S.; Scharf, S. J.; Higuchi, R.; Horn, G. T.; Mullis, K. B.,; and Erlich, H. A.; *Science* , **1988**, 239, 487.

15. McPherson, M. J.; Quirke, P.; Taylor, G. R.; " PCR: A Practical Approach" , IRL Press, New York.

16. (a) Orita, M.; Suzuki, Y.; Sekiya, T.; Hayashi, K.; *Genomics*, **1989**, 5, 874. (b) Orita, M.; Iwahana, H.; Kanazawa, H.; Hayashi, K.; Sekiya, T.; *Proc. Natl. Acad. Sci. USA*, **1989**, 86, 2766.

17. Dean, M.; White, M. B.; Amos, J.; Gerrard, B.; Stewart, C.; Khaw, K. -T.; Leppert, M.; *Cell*, **1990**, 61, 863.

18. Myers, R. M.; Maniatis, T.; Lerman, L.; *Meth. Enzym.*, **1987**, 155, 501.

19. (a) Vivaud, M.; Fanen, P.; Martin, J.; Ghanem, N.; Nicolas, S.; Gossens, M.; *Hum. Genet.*, **1990**, 85, 446. (b) Devoto, M.; Ronchetto, P.; Fanen, P.; et al.; *Am. J. Hum. Genet.*, **1991**, 48, 1127. (c) Romey, M. -C.; Aguilar-Martinez, P.; Demaille, J.; Claustres, M.; *Hum. Genet.*, **1993**, 92, 627.

20. Cotton, R. G. H.; Rodrigues, N. R.; Campbell, R. D.; *Proc. Natl. Acad. Sci. USA*, **1988**, 85, 4397.

21.(a) Chalkley, G.; Harris, A.; *J. Med. Genet.*, **1991**, 28, 875. (b) Strong. T. V.; Smit, L. S.; Turpin, et al. *New Engl. J. Med.*, **1991**, 325, 1630.

22. Newton, C. R.; Graham, A.; Hepstinstall, L. E.; Powell, S. J.; Summers, C.; Kalsheker, N.; Smith, J. C.; *Nucleic Acids Res.*, **1989**, 17, 2503.

23. Ferrie, R. M.; Schwarz, M. J.; Robertson, N. H.; Vaudin, S.; Super, M.; Malone, G., Little, S.; *Am. J. Hum. Genet.*, **1992**, 51, 251.

24. Saiki, R. K.; Bugawan, T. L.; Horn, G. T.; Mullis, K. B.; Erlich, H. A.; *Nature*, **1986**, 324, 163.

25. Shuber, A. P.; Skoletsky, J.; Stern R.; Handelin, B. L.; *Hum. Mol. Gen.*, **1993**, Vol 2, 2, 153.

26. Mazza, C.; Mantero, G.; Primi, D.; *Mol. and Cell. Probes*, **1991**, 5, 459.

27. Cotton, B. J.; Reyes, A. A.; Morin, C.; Itakura, K.; Teplitz, R. L.; Wallace, R. B.; *Proc. Natl. Acad. Sci. USA*, **1983**, 80, 278.

28. Keller, G. H.; Manak, M. M.; "DNA Probes" Stockston press, **1989.**, pp 15.

29. Hashitoma, K.; Ito, K.; Ishimori, Y.; *Anal. Chem.*, **1994**, 66, 21, 219.

Chapter 7

Reactivity of Deoxyguanosine with N-Hydroxysuccinimide Esters

7.1 Introduction

Results presented in the preceeding chapters show that poly(dG) can be covalently immobilized onto oxidized glassy carbon and stearic acid modified carbon paste electrodes using a water-soluble carbodiimide 1-(3-dimethylaminopropyl-3-ethyl-carbodiimide (EDC), alone or in conjunction with N-hydroxysuccinimide (NHS), as coupling reagents.[1,2] These reagents have been previously used for protein immobilizations,[3] in which EDC couples available carboxylic acid groups to primary amine groups. The mechanism for amide bond formation is shown in Figure 7.1:

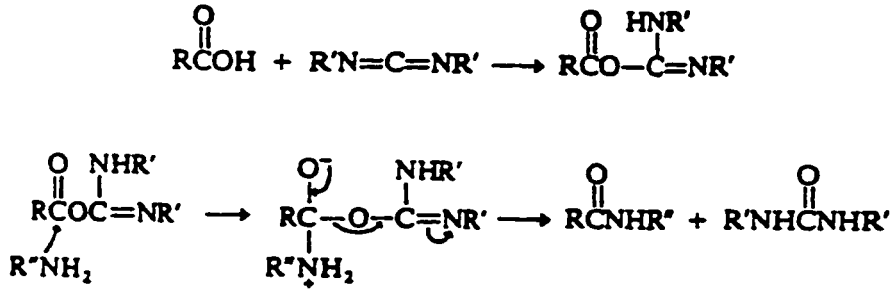

Figure 7.1 Mechanism for the conversion of carboxylic acid groups to a reactive acylating reagent by carbodiimides.[4]

The carboxylic acid adds to the imide carbon of the carbodiimide to generate an O-acylisourea. There is a strong driving force for elimination of the urea group from the O-acylisourea which makes it a very stong acylating agent. In the presence of an amine group the O-acylisourea reacts to form a very stable amide group.[5] In the absence of an amine the O-acylurea can be converted to an anhydride with another carboxylic acid group acting as the nucleophile. This anhydride can also react with an amine producing an amide and regenerating one of the carboxylic acids. The O-acylisourea intermediate is subject to hydrolysis in aqueous media to regenerate the acid, and this can significantly decrease the overall yield of the amide. In addition, the acyl group can transfer to an adjacent nitrogen, forming a stable N-acylisourea.[6]

The activated O-acylisourea can be transformed into a more hydrolysis-resistant reactive intermediate, to increase reaction yields. N-hydroxysuccinimide esters are hydrophilic active esters that hydrolyse slowly compared with their rate of reaction with primary amines.[7] The carboxylate functional group will form an acyl amino ester with NHS, and this product is highly selective for reactions with strong nucleophiles, like primary amines. The sulfo-NHS derivative has greater solubility in aqueous media than NHS. The addition of sulfo-NHS to the carbodiimide coupling reaction significantly increases coupling yields and selectivity in aqueous solutions at neutral pH. Figure 7.2 depicts the coupling of a peptide with a carboxylic acid functional group and a protein with a primary amine under aqueous conditions at neutral pH. N-hydroxysuccinimide has been used to couple active carboxylic acid derivatives of agarose to primary amines proteins through an amide linkage.[8]

Water-soluble carbodiimides have been used to modify DNA. In one study

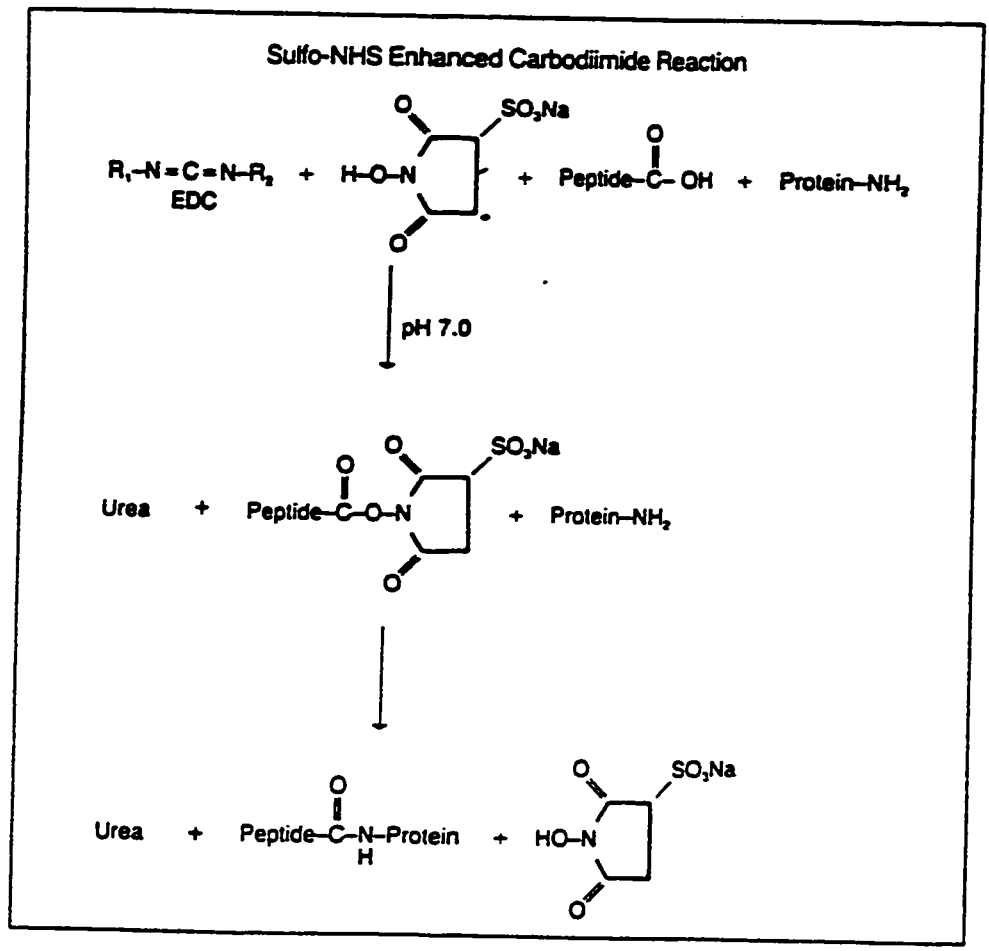

Figure 7.2 Sulfo-NHS Enhanced Carbodiimide Reaction.[9]

N-acylureas of albumin and transferrin prepared with EDC have been shown to bind reversibly to DNA.[10] Two types of binding between N-acylisourea and DNA could be distinguished, a weak binding which developed at the beginning of the interaction and a tight binding which developed on further incubation with the complex. This study showed that binding of DNA by N-acylurea proteins is dependent on ionic strength and therefore seems to be electrostatic. Another study with N-acylurea proteins showed that initially ion pairing occurs between the DNA phosphates and the N-acylisourea. A second step occurs in which the base guanine reacts with elements of the N-acylurea by hydrogen bonding and a glyoxal-type addition.[11] Water soluble N-cyclohexyl-N-(4-methylmorpholinium)ethyl carbodiimide (CMC) has been shown to react with imino sites of unpaired guanine and thymidine in DNA, with guanine being the most reactive. Figure 7.3 shows the two possible products of the reaction between a protein coupled to guanosine via carbodiimide coupling. N-alkyl-N-nitrosureas react preferentially with runs of guanines, specifically at the N7-position of guanine. This correlates with the molecular electrostatic potential by the nearest-neighbor base pairs.[12] It has been suggested that the neighboring guanines might increase the reactivity of the guanine N7-positon via electrostatic interactions with a local increase in the electronegativity near the guanine N7 position.[13]

In order to determine which site is reactive with an NHS-ester, NHS-fluorescein was reacted with 2',3',5' triacetylguanosine (TAG), as described in section 2.2.11. TAG is a derivative of deoxyguanosine in which the hydroxyl groups are replaced with acetyl groups, thereby eliminating their reactivity. NHS-fluorescein is commercially available, and is a commonly used reagent for fluorescent labelling of proteins. In addition, guanosine

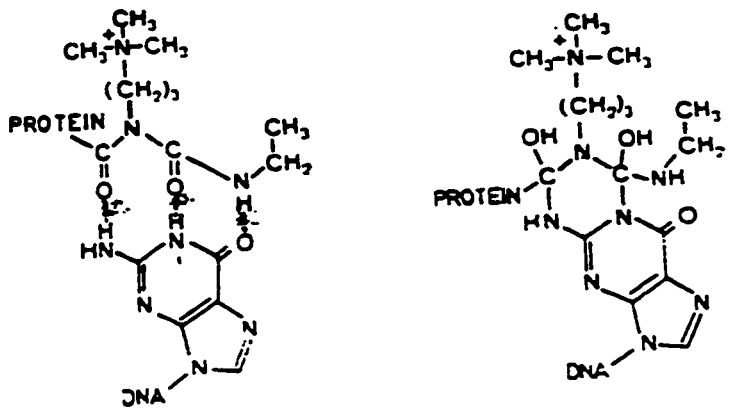

Figure 7.3 The structure of the carbodiimide and its binding to guanosine.[12]

triphosphate and fluorescein were reacted via the coupling reagents EDC and NHS. The products and reactants were examined by ^{1}H NMR spectroscopy for structure elucidation. Possible reactive groups of the guanine base are the N7 position, the imino nitrogen (N1), and the aromatic amine (N2) under neutral pH, which can tautomerize to an imine under basic condition. Figure 7.4 shows the structures of triacetylguanosine, guanosine 5' triphosphate, fluorescein, and fluorescein-NHS.

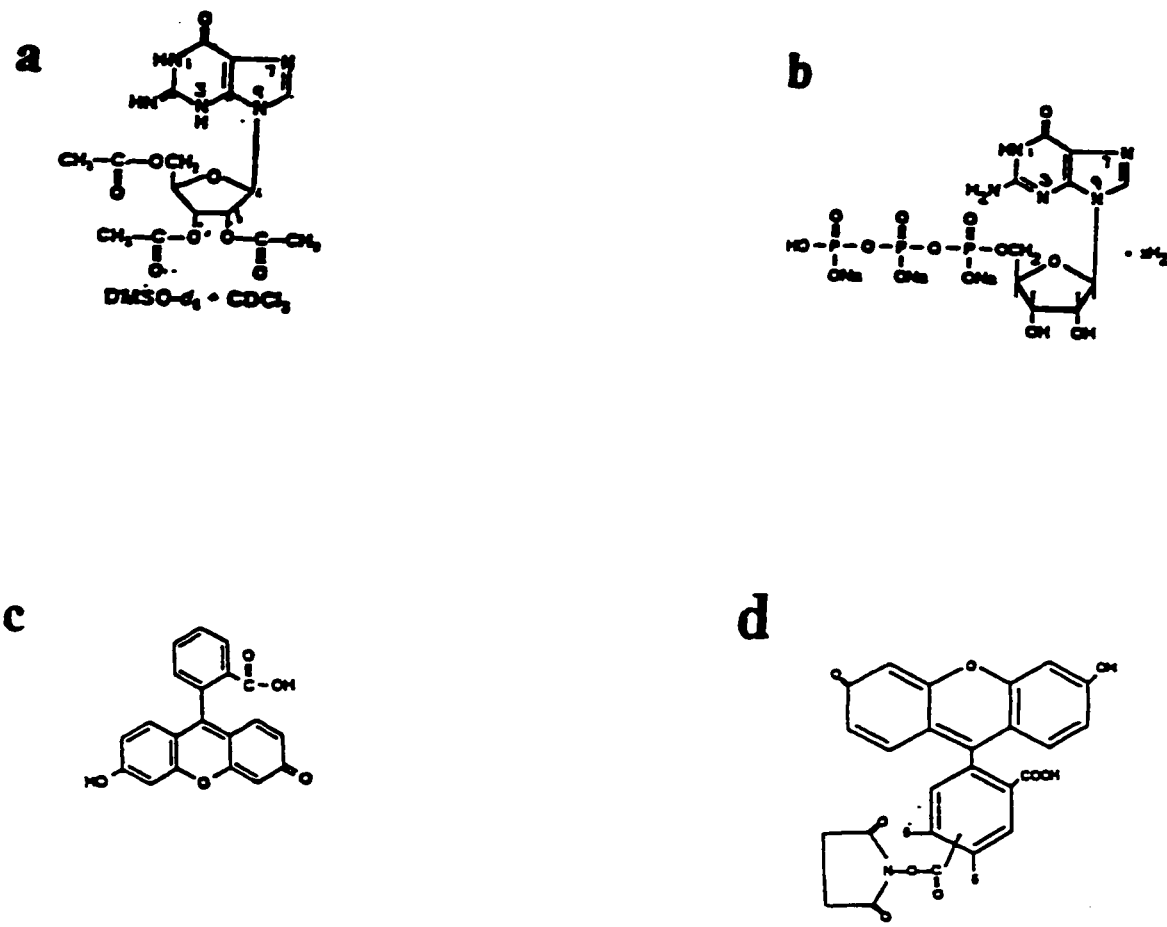

Figure 7.4 Chemical structures of (a) triacetylguanosine, (b) guanosine 5' triphosphate, (c) fluorescein, and (d) fluorescein-NHS.

7.2 Results

7.2.1 Purification of the Fluorescein-Triacetylguanosine Conjugate by HPLC.

TAG was reacted with an excess of NHS-fluorescein in dimethylformamide (DMF), as described in section 2.2.11. The DMF was removed by vacuum distillation and reconstituted in 40% aqueous acetonitrile (ACN). The products of this reaction were purified by isocratic reverse phase HPLC with a UV/Visible detector set at an absorbance wavelength of either 254 nm or 496 nm. Initially, the reaction products were chromatographed on a phenyl column with a flow rate of 1.2 mL/min and a mobile phase of 40% aqueous ACN. Figures 7.5 (a and b) show chromatograms of the reactants, triacetylguanosine and NHS-fluorescein, respectively, under the above conditions. As can be seen from the chromatography of NHS-fluorescein, there are many species present. This is NHS-fluorescein is present as a mixture of isomers, as shown in Figure 7.4 (d).

Figure 7.6 is a chromatogram of the products of the reaction between NHS-fluorescein and triacetylguanosine, under the same conditions. Comparing the chromatograms of the reactants and products it can be seen that there were several species present in the reaction mixture. Comparison of retention times suggests that peaks 3 and 4, from Figure 7.6 (a and b) result from unreacted NHS-fluorescein. Peak 1 is the void volume which may contain unreacted TAG and an isomer from the NHS-fluorescein mixture. The broad chromatographic peak labelled number 5 (a and b) in Figure 7.6 had a retention time which did not appear in the chromatograms of the reactants. Peak number 5 a, which absorbed at 490 nm and 256 nm was collected and further purified by HPLC with a mobile phase with 20% ACN in water on a phenyl column, as illustrated in Figure 7.7. Two peaks were resolved

under these conditions. These fractions, 12 and 13, were collected and injected onto a C18 column with a flow of 0.5 mL/min to determine their purity. Figure 7.8 (a and b) are chromatograms of these fractions, where one main peak is observed for each. These fractions were collected and stored at 4 °C until a significant amount was collected (31 days). However, under these conditions decomposition occurred, and four peaks were observed in the chromatogram (Figure 7.9).

Decomposition also occurred with the products of the guanosine 5' triphosphate-fluorescein coupling reaction. Eight fractions were collected and examined by UV-Visible and fluorescence spectroscopy. All of these fractions absorbed at 260 nm and were fluorescent. Several of these products were then examined by NMR spectroscopy, and the complexity of the spectra indicated that the products had decomposed. This made determination of their chemical structure impossible.

7.2.2 NMR Spectroscopy of the Fluorescein-Triacetylguanosine Conjugate

Simple ^{1}H NMR spectroscopy was used to investigate which group(s) of triacetylguanosine were reactive with the NHS-ester of fluorescein. ^{1}H NMR spectroscopy was performed on NHS-fluorescein, triacetylguanosine, and products (Fractions 12 and 13) in CD_3OD. Figure 7.10, 7.11, 7.12 and 7.13, respectively, show the NMR spectra for triacetylguanosine, NHS-fluorescein, and Fractions 12 and 13 after storage for 50 days. The only compound for which the chemical shifts could be assigned is TAG, and these are given in Figure 7.10. The NHS-fluorescein spectrum is difficult to assign, because it is a misture of positional isomers. This can also be seen by chromatography (Figure 7.5 (b)) which shows

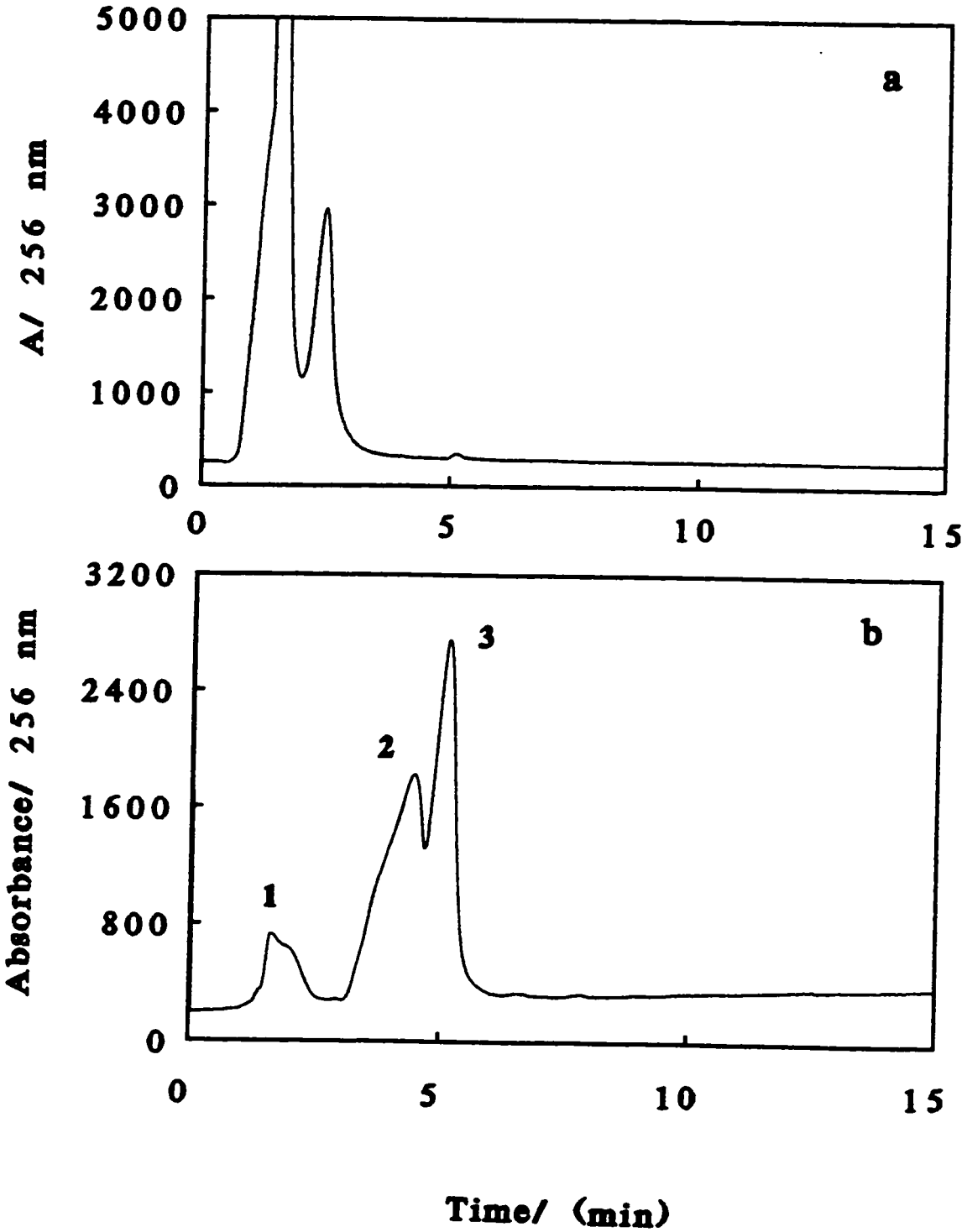

Figure 7.5 Elution of (a) 2',3',5', triacetylguanosine and (b) NHS-fluorescein by reverse phase HPLC with 40:60 ACN:H_2O on a phenyl column (15 cm). The wavelength of the detector was set at 256 nm.

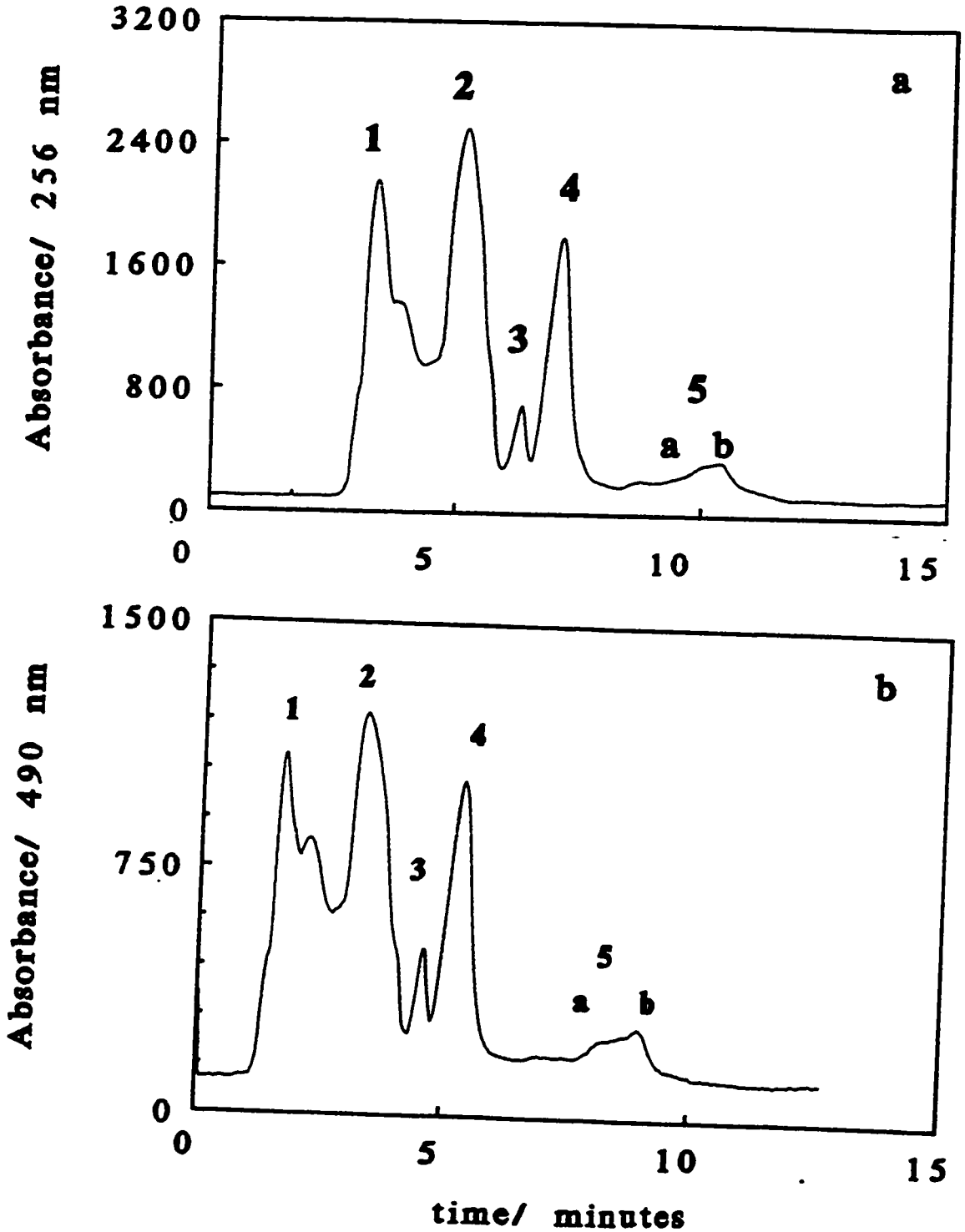

Figure 7.6 Elution of the TAG NHS-fluorescein reaction products by reverse phase HPLC with 40% ACN in water on a phenyl column, (a) with the absorbance detector was set at 256 nm and (b) with the absorbance detector set at 490 nm.

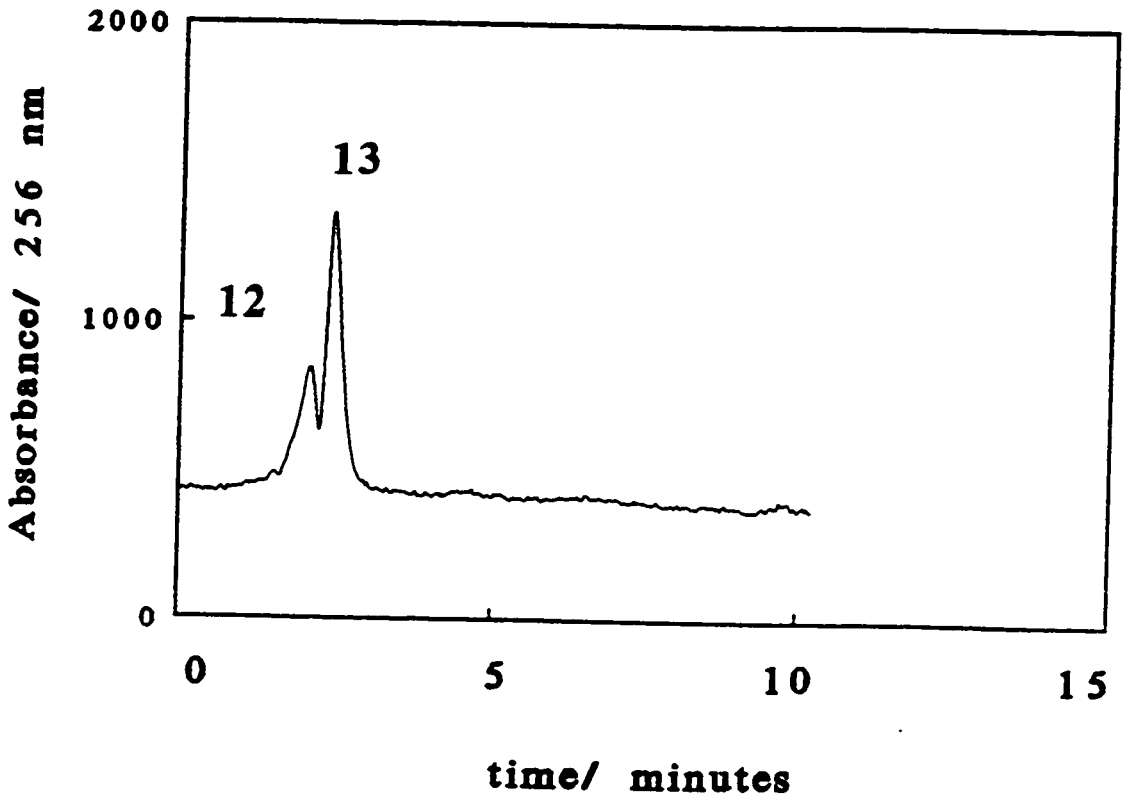

Figure 7.7 Elution of the reaction product associated with Peak 5 from Figure 7.6, by isochratic reverse phase HPLC with 20% ACN in deioinized water on a phenyl column (15 cm). Two peaks are observable, called Fraction 12 and 13.

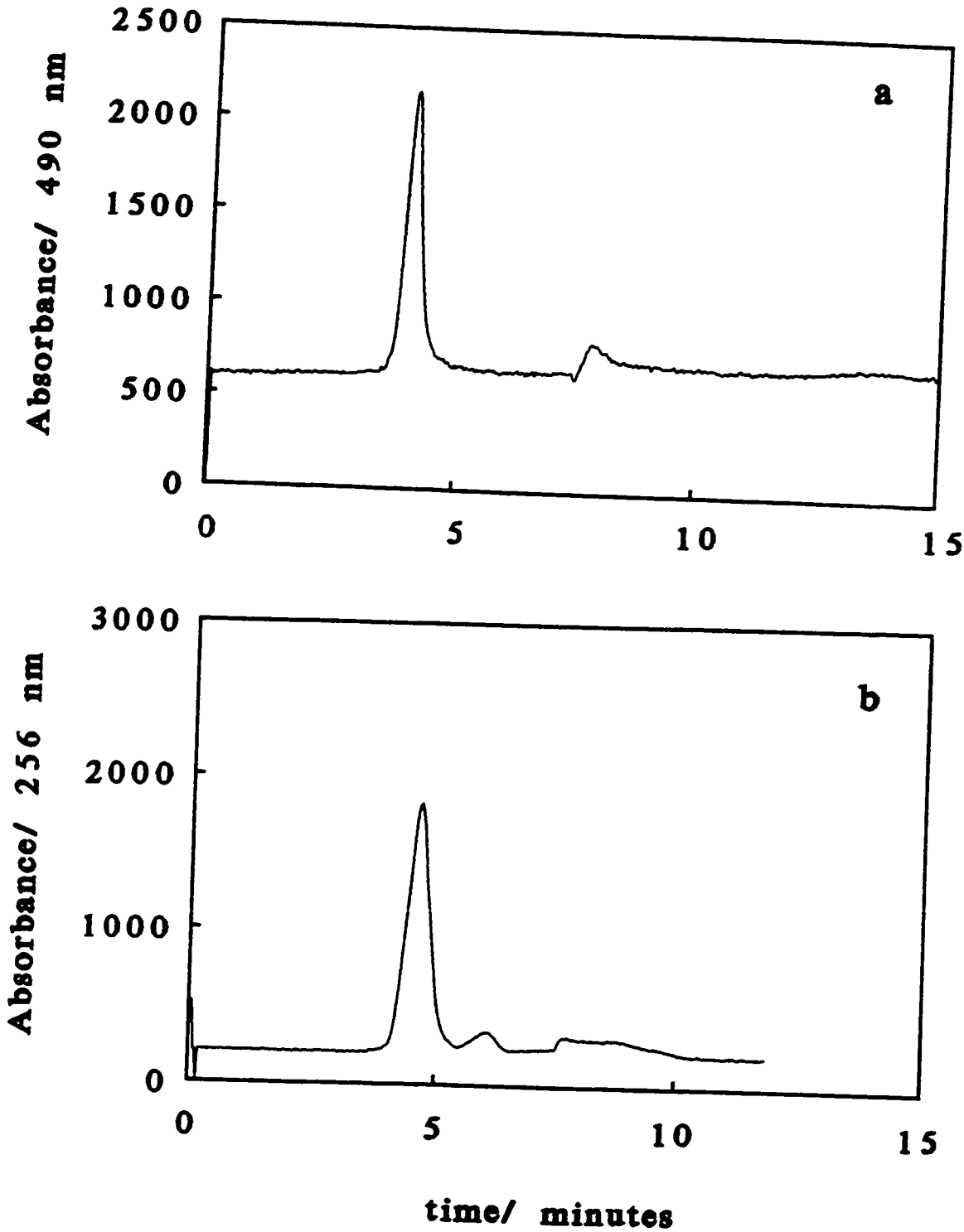

Figure 7.8 Elution of (a) Fraction 12 and (b) Fraction 13 by isochratic reverse phase HPLC with 10% ACN on a C18 column.

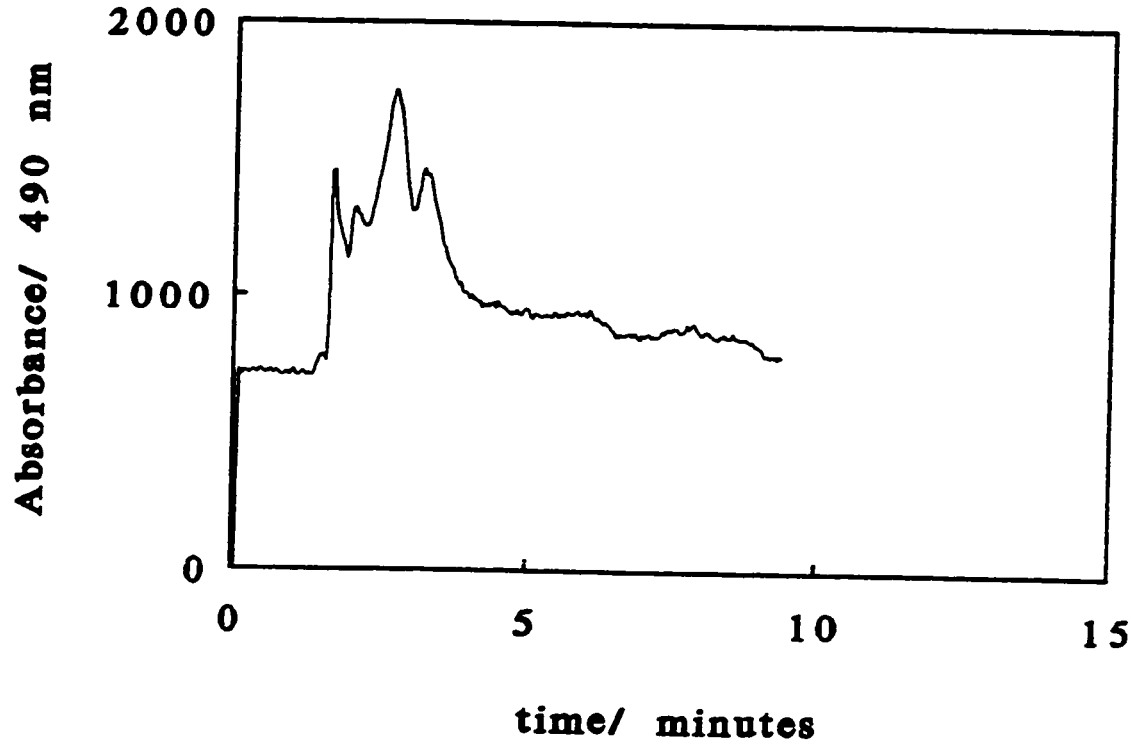

Figure 7.9 Analysis of the stability of fraction 13 by isochratic reverse phase HPLC on a C18 column with a mobile phase of 10 % ACN in deionized water. (Storage period = 31 days at 4 °C.

many peaks eluting from the phenyl column. The NMR spectra of fractions 12 and 13, as shown in Figure 7.12 and 7.13, suggest that the products in these fractions are not pure, possibly as a result of decomposition. Three chemical shifts assigned to the protons of the ribose sugar (δ = 5.65 (triplet), 5.94 (triplet), 6.05 ppm (doublet)) in TAG are not seen in the spectra of the reaction products.

Solubility of both the starting materials (especially TAG) and products limited the choice of NMR solvents to CD_3OD and D_6-DMSO. With CD_3OD, the deuterium is extremely labile and can exchange with the primary amine protons at position 2 on the base and the imino proton at position 1, both possible sites for reaction with the NHS-ester.

The reaction between NHS-fluorescein and TAG was repeated. However, because of product instability, purification proceeded by precipitation of the reaction mixture with water. TAG, NHS-fluorescein and products in the precipitate and supernatant were examined by ^1H NMR spectroscopy as shown in Figure 7.14, 7.15, 7.16 and 7.17 respectively. The chemical shifts of interest are for the C8 proton (s, 1H, δ = 7.8 ppm), N1 imino proton (s, 1H, δ = 10.8 ppm) and the aromatic NH_2 (s, 2H, δ = 6.5 ppm). A comparison of the spectra of triacetylguanosine and the the aqueous and nonaqueous products show that the chemical shift associated with the guanosine base, N1 (s, 1H, δ = 10.8 ppm), C8 (s, 1H, δ = 7.9), and NH_2 (s, 2H, δ = 6.5 ppm) all shifted downfield after the reaction with NHS-fluorescein.

In a separate experiment, fluorescein was reacted with EDC and sulfo-NHS under aqueous conditions. A precipitate formed immediately and the product mixture was centrifuged to separate the supernatant from the precipitate. The precipitate was reacted with guanosine 2',3',5' triphosphate in DMF. The product precipitated out of solution by the

Chemical Shift δ (ppm)	Multiplet	Assignment	# Protons
7.8	S	C-8	1
6.05	D	C-1'	1
5.94	T	C-2'	1
5.65	T	C-3'	1
4.4	Multiplet	C-4' and C-5'	1 for C-4' 2 for C-5'
2.15	S	acetyl	9
2.12	S	?	2
2.06	D	?	4

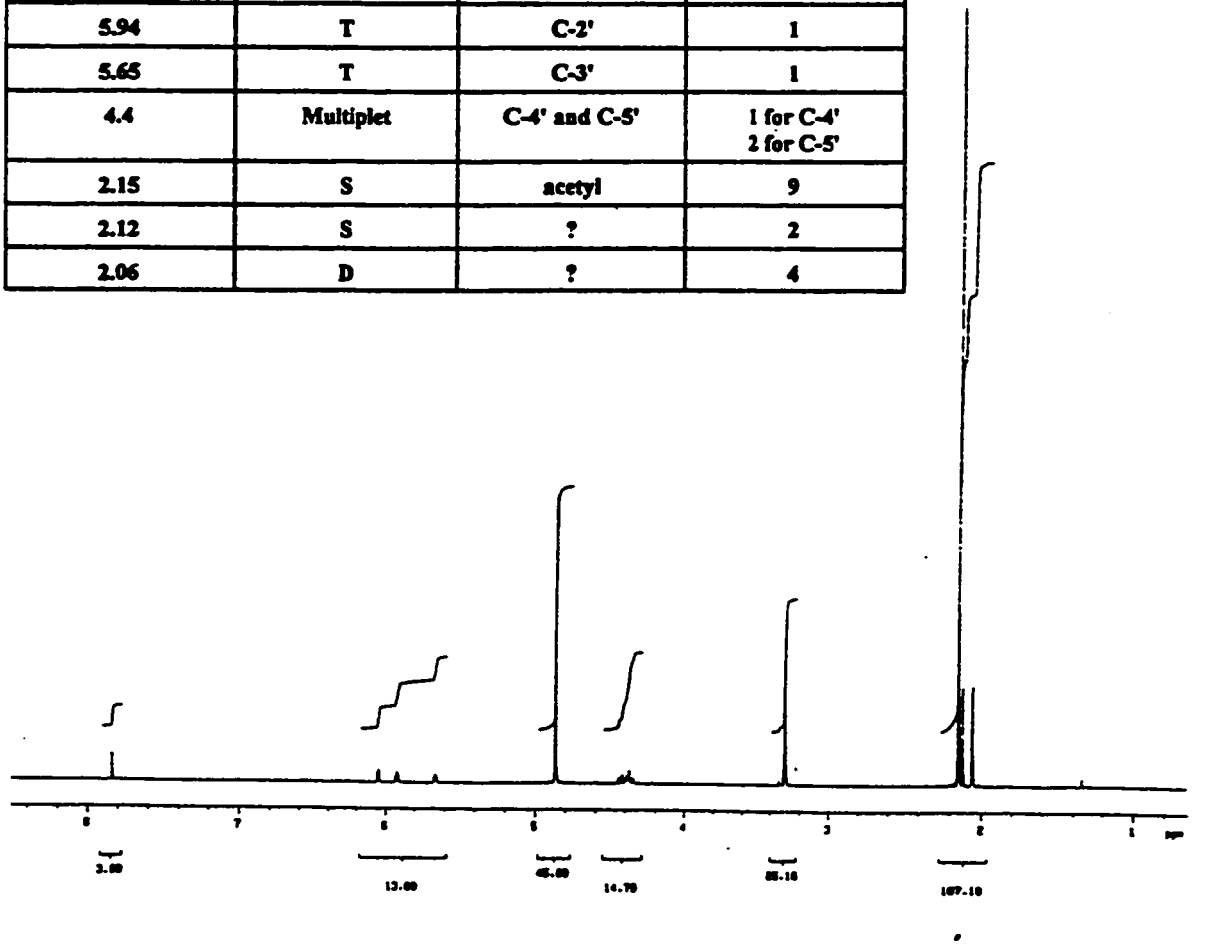

Figure 7.10 ^{1}H NMR spectrum of 2', 3', 5', triacetylguanosine, with the proton chemical shift assignments.

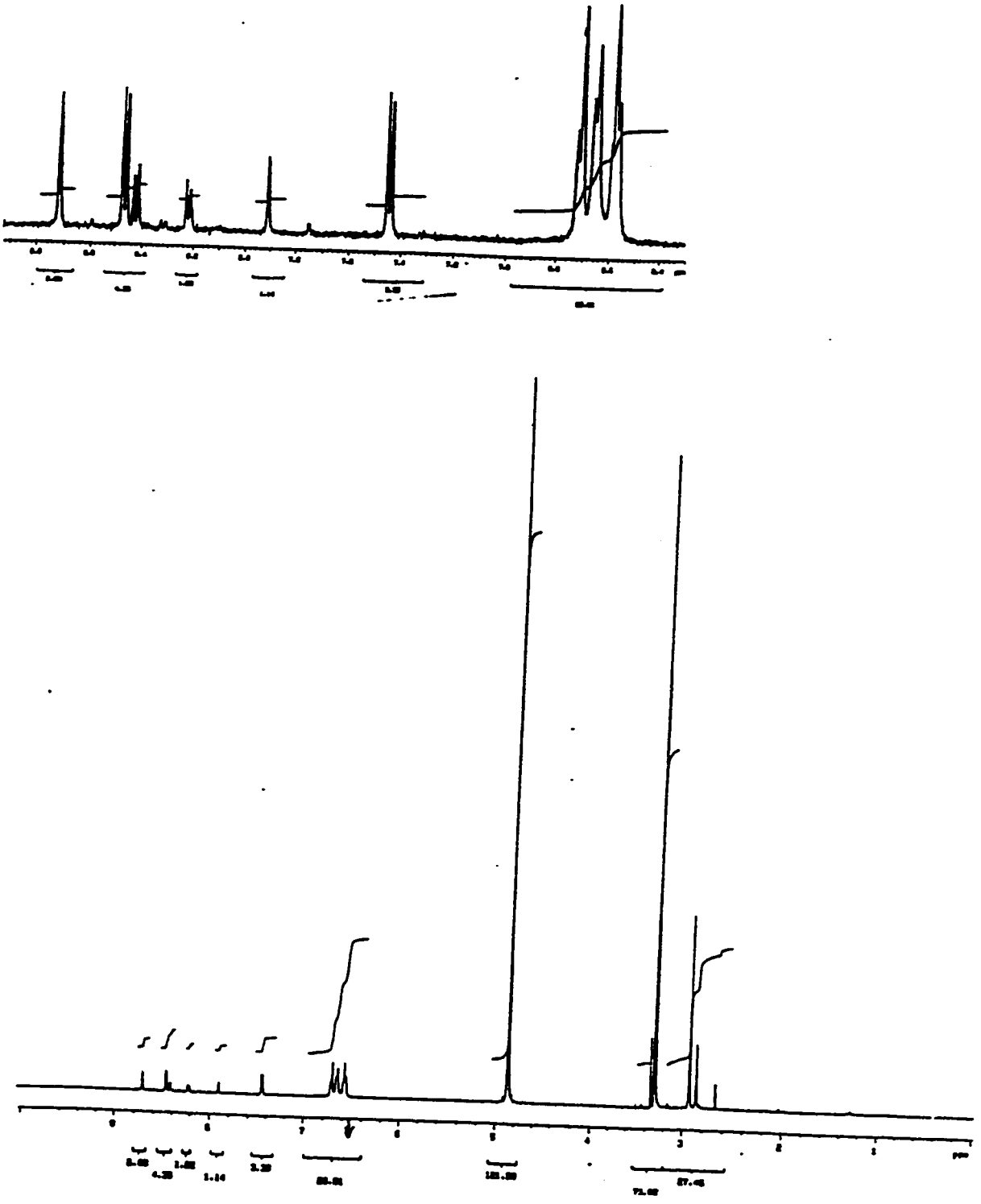

Figure 7.11 ^{1}H NMR spectrum of NHS-fluorescein. Conditions: Solvent CD_3OD.

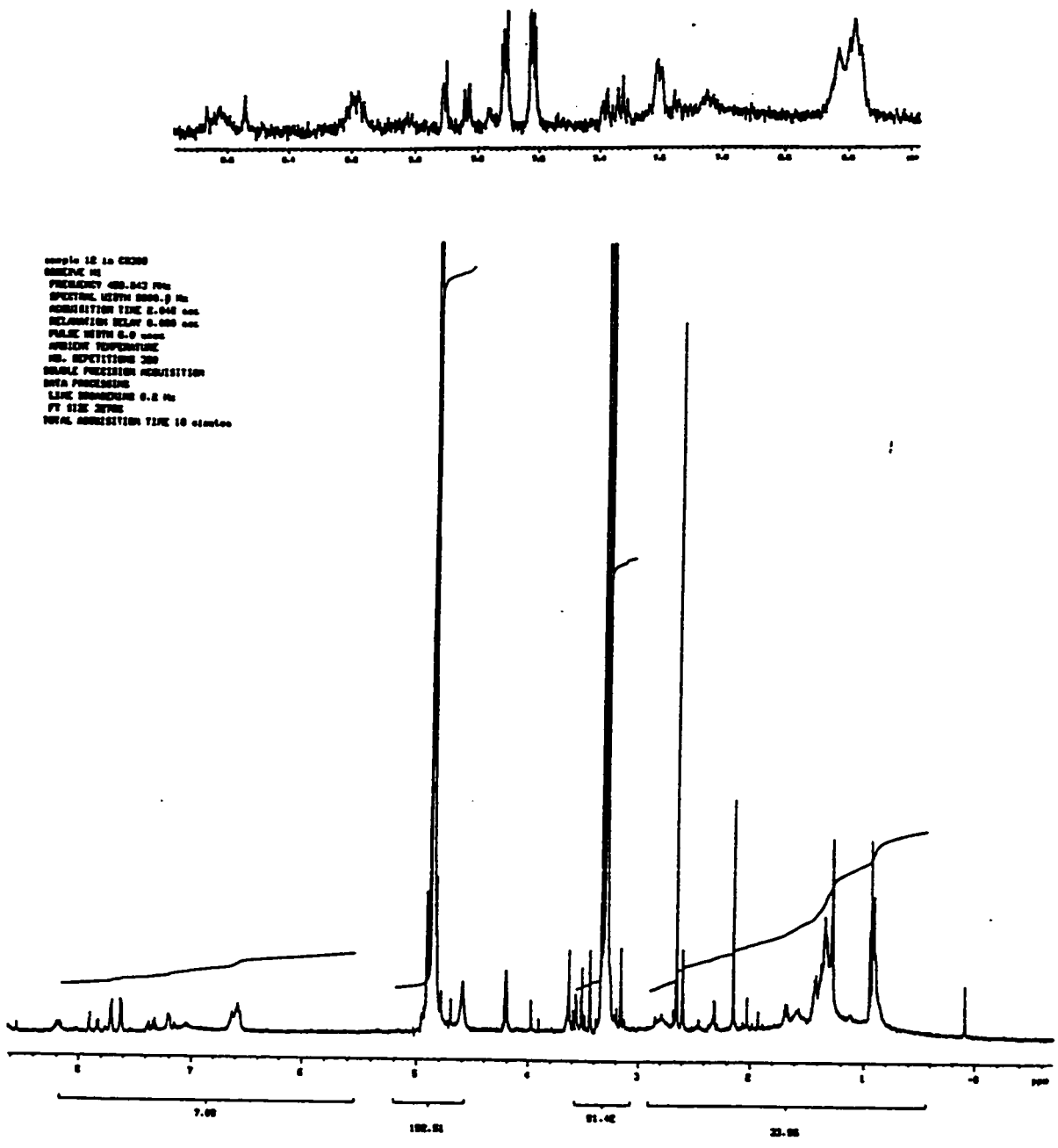

Figure 7.12 ^{1}H NMR spectrum of Fraction 12. Conditions: Solvent CD_3OD.

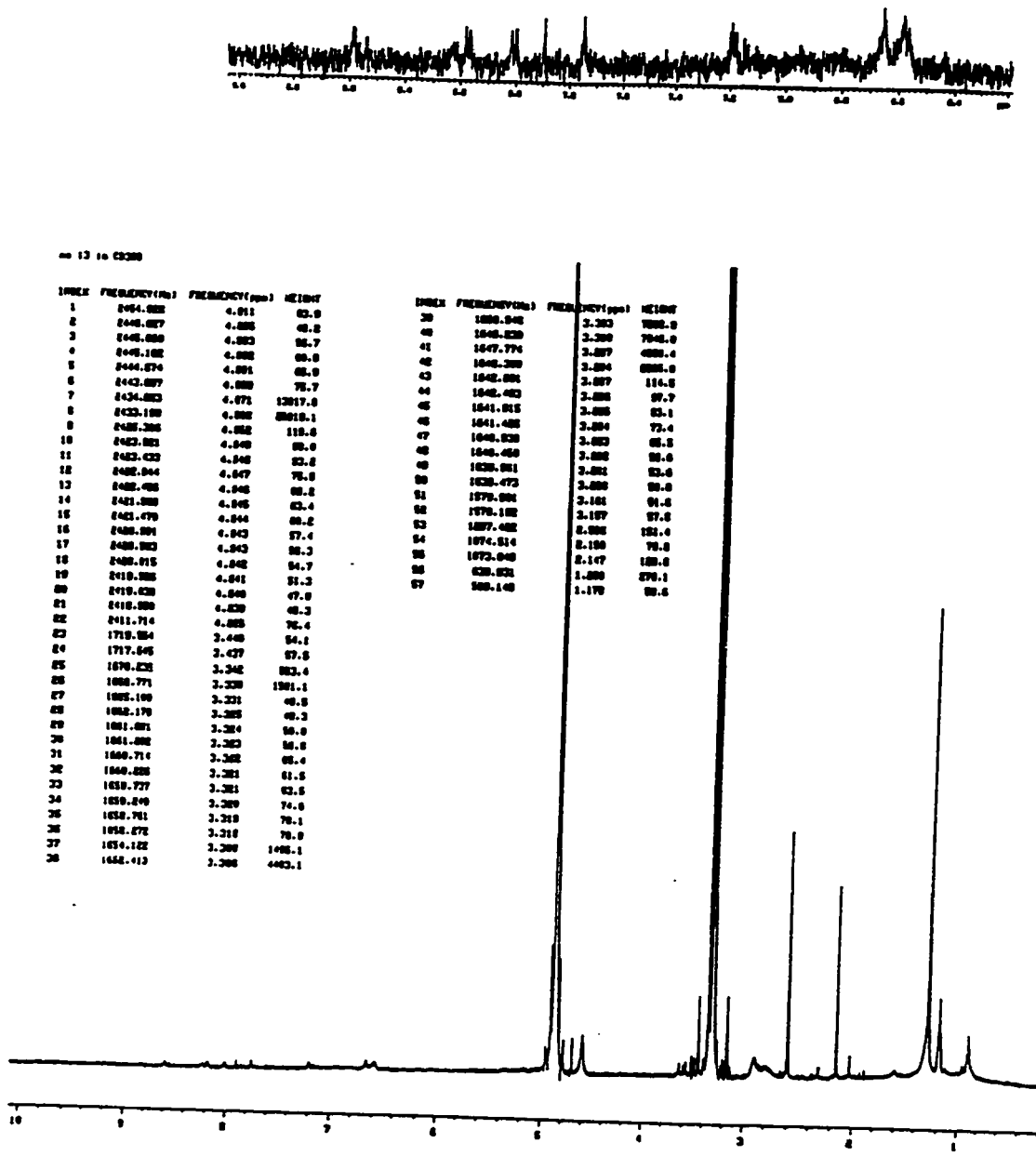

Figure 7.13 ^{1}H NMR spectrum of Fraction 13. Conditions: Sovlent CD_3OD

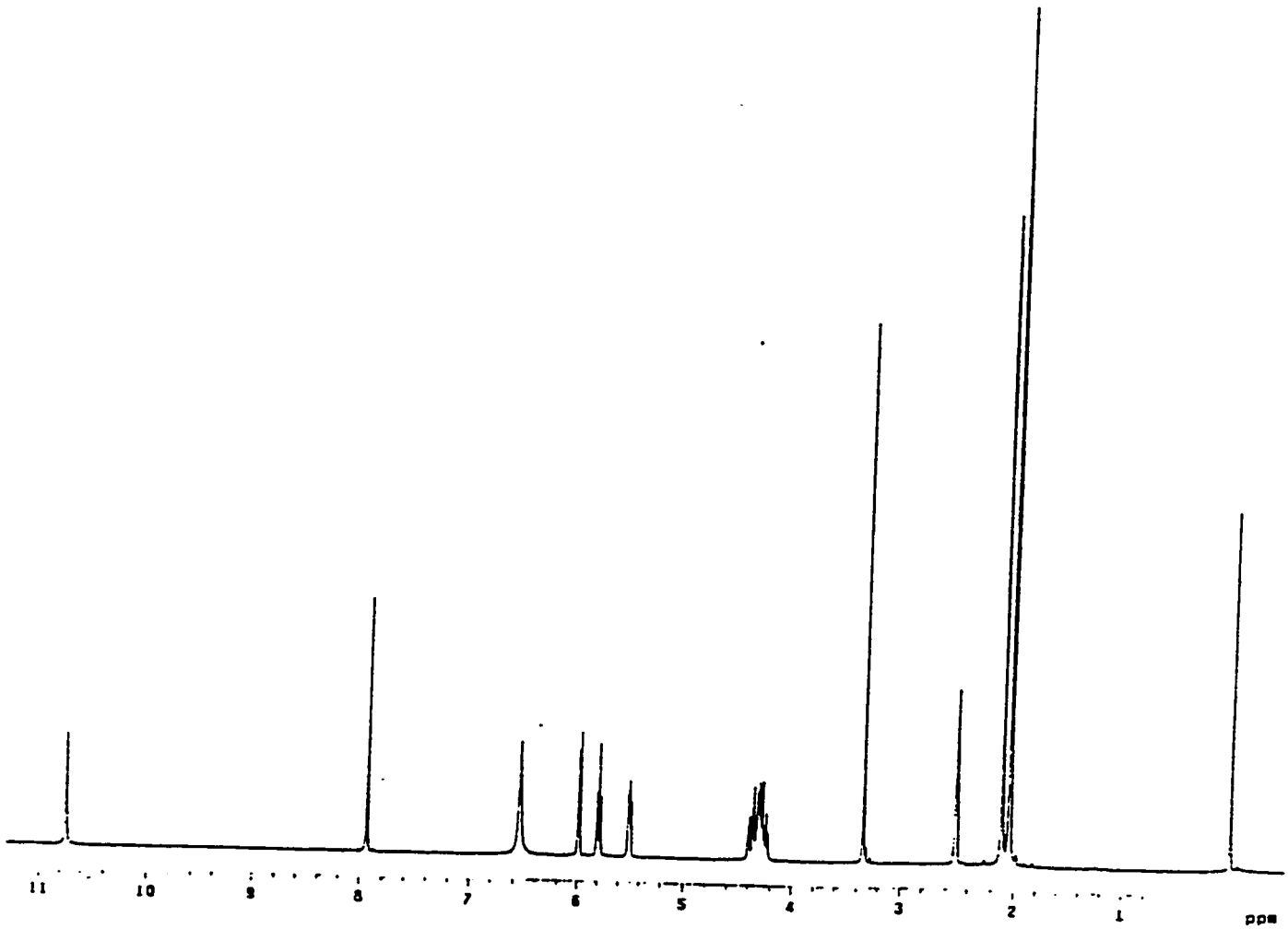

Figure 7.14 ^{1}H NMR spectrum of TAG in D_6-DMSO

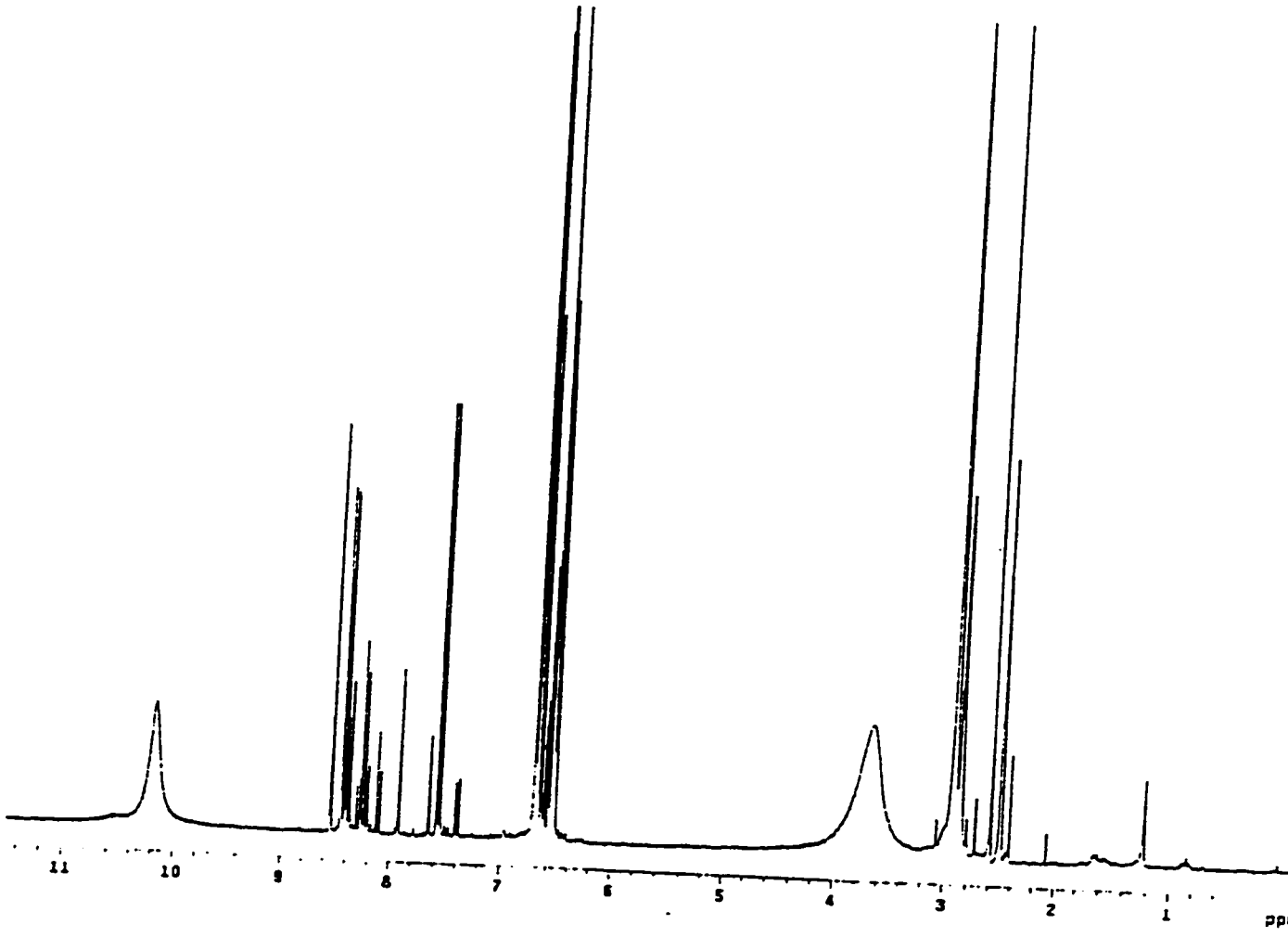

Figure 7.15 ^{1}H NMR spectrum of NHS-Fluorescein in D_6-DMSO.

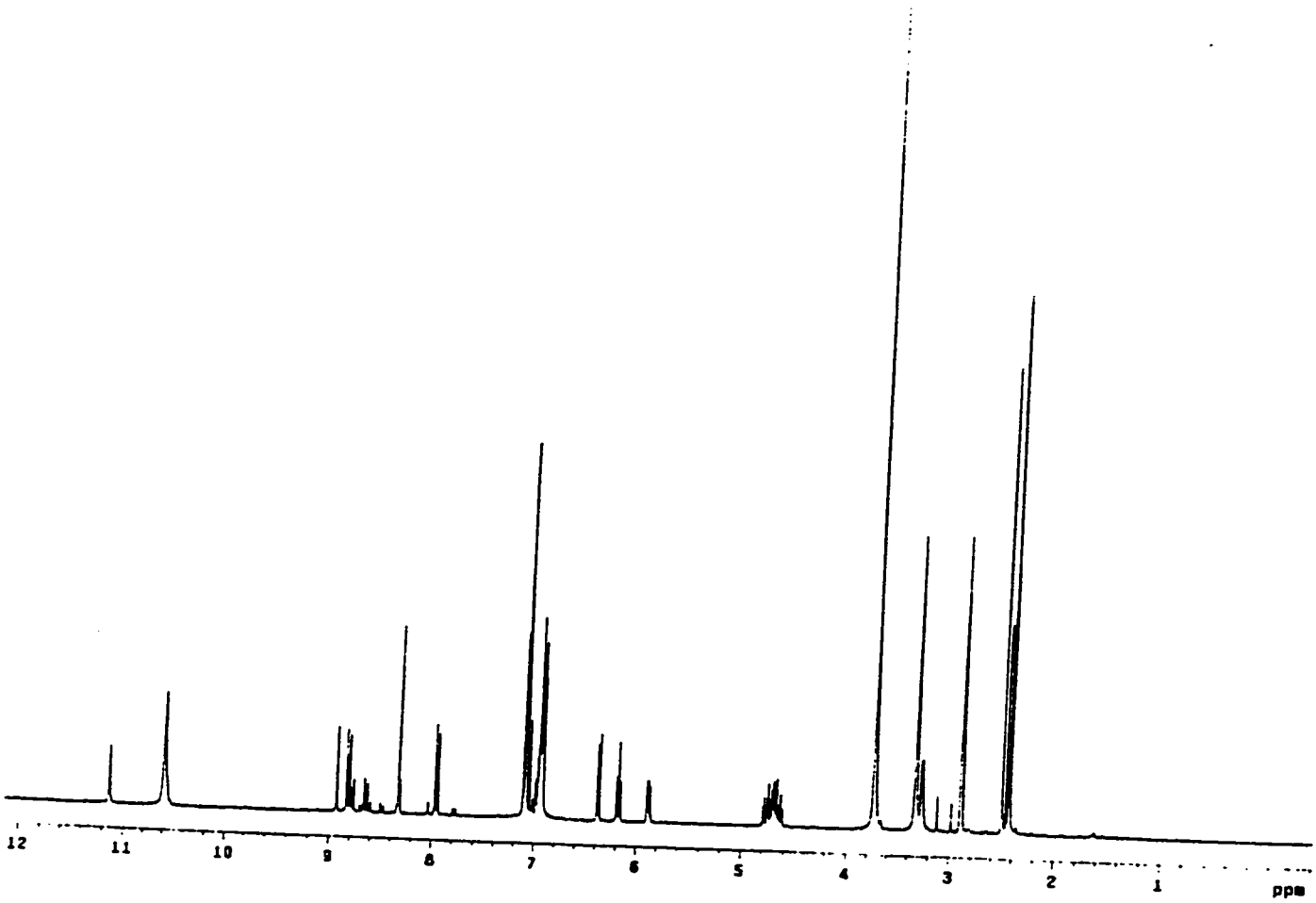

Figure 7.16 ^{1}H NMR spectrum of the product of the NHS-fluorescein TAG reaction (precipitate) dissolved in D_6-DMSO.

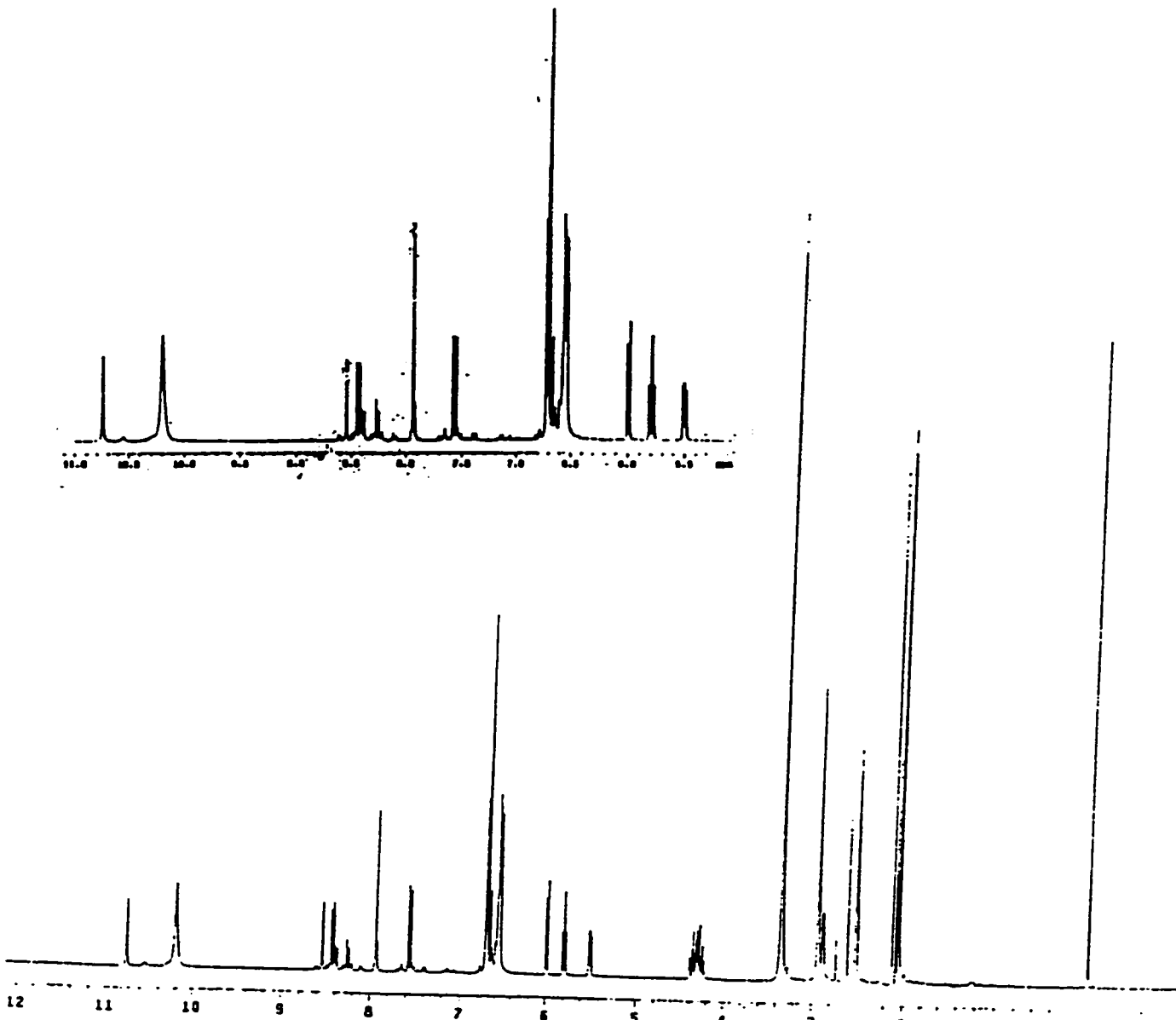

Figure 7.17 ^{1}H NMR spectrum of the product of the NHS-fluorescein TAG reaction (supernatant) dissolved in D_6-DMSO.

addition of water. The reaction mixture was centrifuged and the supernatant and precipitate were isolated and examined by ^{1}H NMR spectroscopy. Figure 7.18 and 7.19 shows the ^{1}H NMR spectrum of the products form the precipitate and the supernatant, respectively. As can be seen the chemical shift of N1 in both the products from the precipitate and supernatant (δ = 10.8) is lost. The chemical shifts associated with protons of the ribose sugar also disappear. In addition the sharp chemical shift associated with the carboxylate of fluorescein disappeared and a broad shift is observed between δ = 10.2 - 10.4 ppm. Interpretation of the NMR spectrum of this product is difficult since both fluorescein and guanosine have protons which have accidentally equivalent chemical shifts in the region of δ = 7.8-8.0 ppm and δ = 6.5 - 6.8 ppm.

7.3 Discussion

From the chromatograms it was determined that the reaction between NHS-fluorescein and TAG produce many species, two of which were isolated. These products absorbed at both 256 nm and 490 nm, the absorption maximum for guanosine and NHS-fluorescein, respectively[14,15], and have different retention times than the reactants. This suggests that these compounds are products of guanosine coupled to fluorescein. However, it could not be determined which grops on the guanosine base react with the NHS-ester of fluorescein.

If the NHS-fluorescein reacted at the N7 position on the guanosine base the signal for the C8 proton would shift due to the ring currents of the aromatic fluorescein bound at the N7 position. Another possiblity would be to lose the C8 proton in a manner similar to that

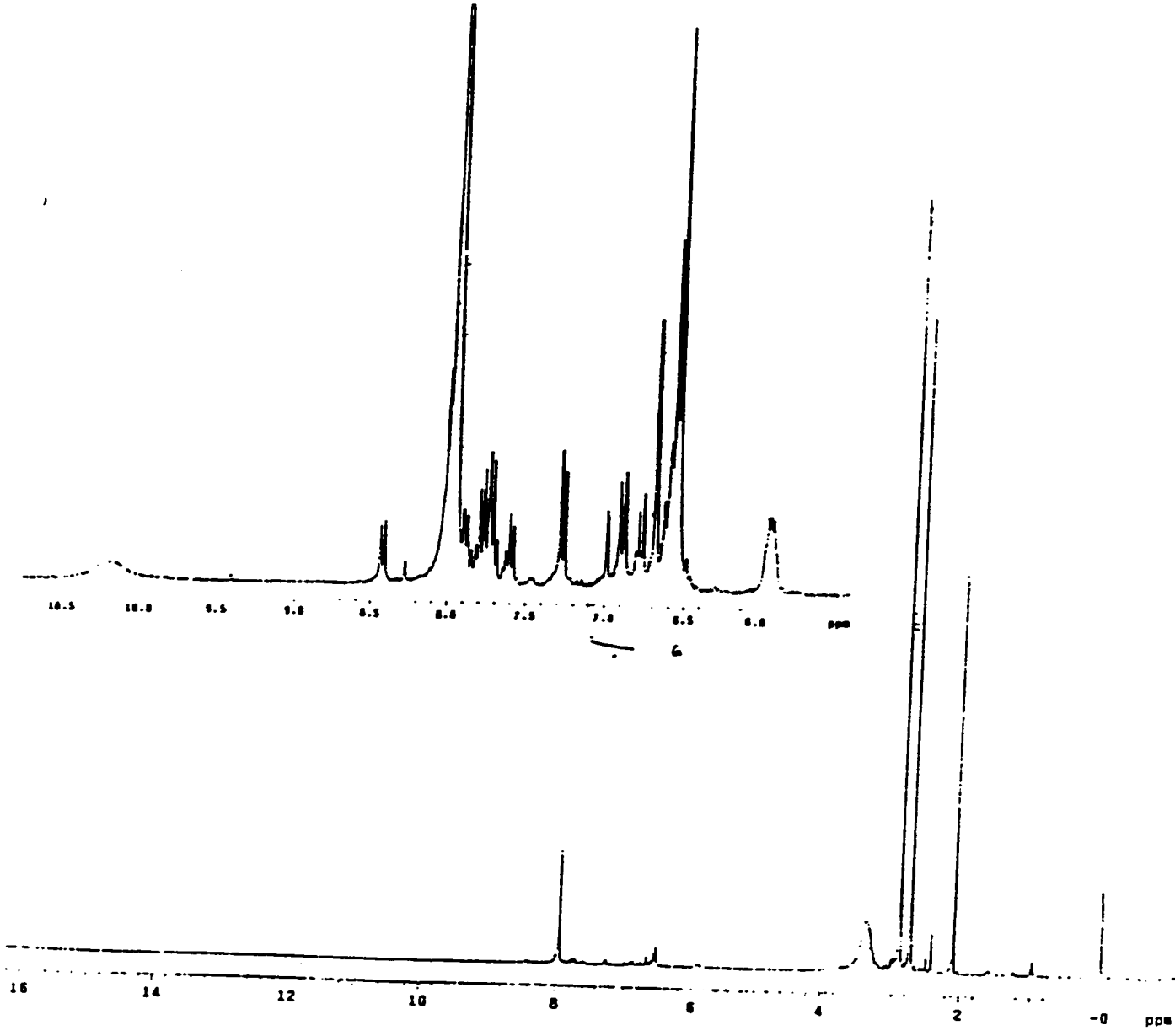

Figure 7.18 ^{1}H NMR spectrum of the product of the fluorescein dGTP reaction (precipitate) dissolved in D_6-DMSO.

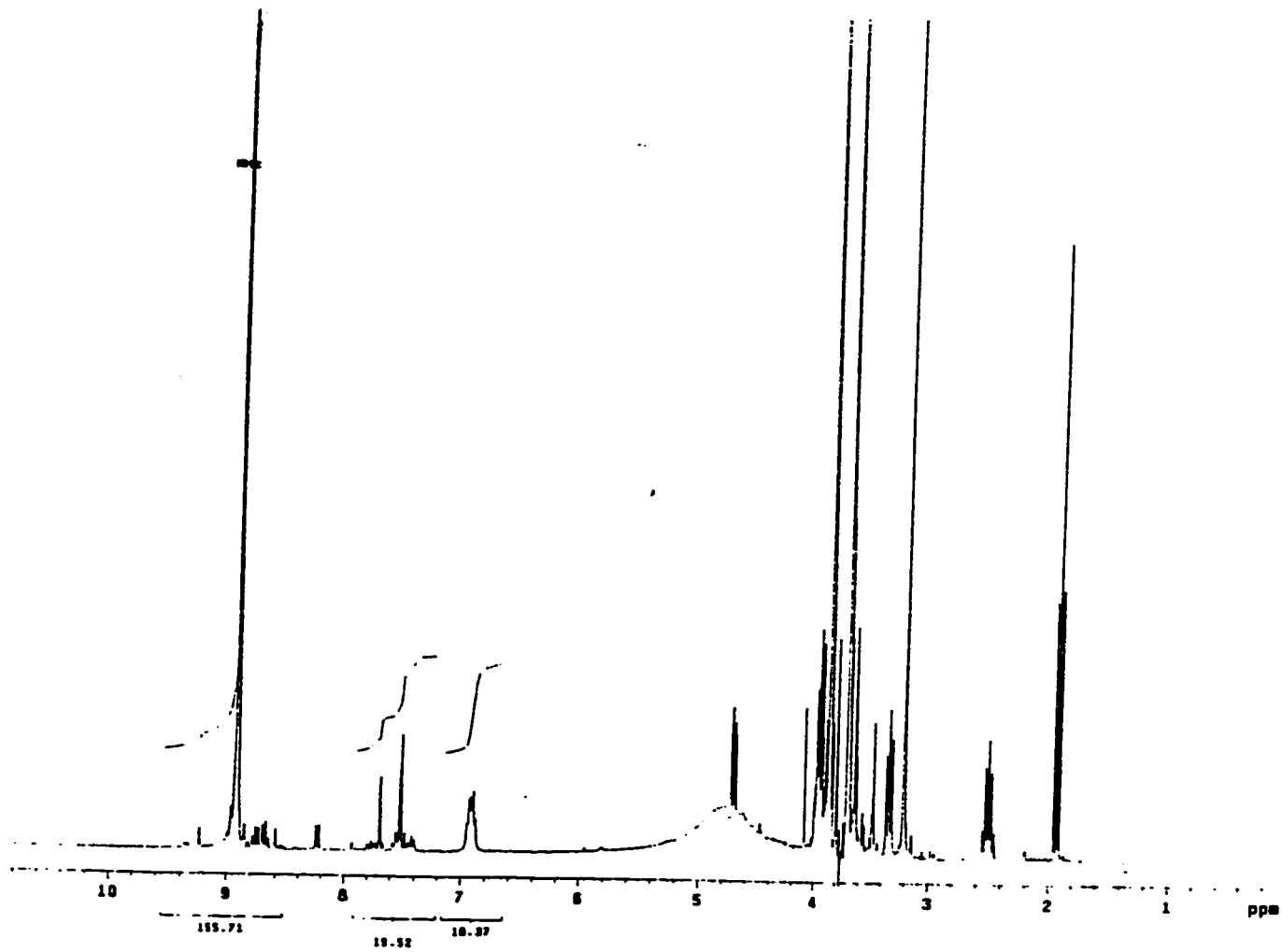

Figure 7.19 ^{1}H NMR spectrum of the product of the fluorescein dGTP reaction (supernatant) dissolved in D_6-DMSO.

which occurs when guanosine is reacted with DMSO under basic conditions. DMSO is a strong nucleophile which reacts at the N7 position of guanine. This creates a positive charge at the C8 position, which can then be attacked by a base (^-OH), as shown in Figure 7.20.[16] If NHS-fluorescein reacted with the aromatic NH_2 of guanosine the chemical shift associated with this group would move downfield and the integration would indicate only one proton, rather than two. Loss of the signal for the imino nitrogen (N1) $\delta = 10.8 - 12.5$ would indicate that NHS-fluorescein reacted at this site on the base.

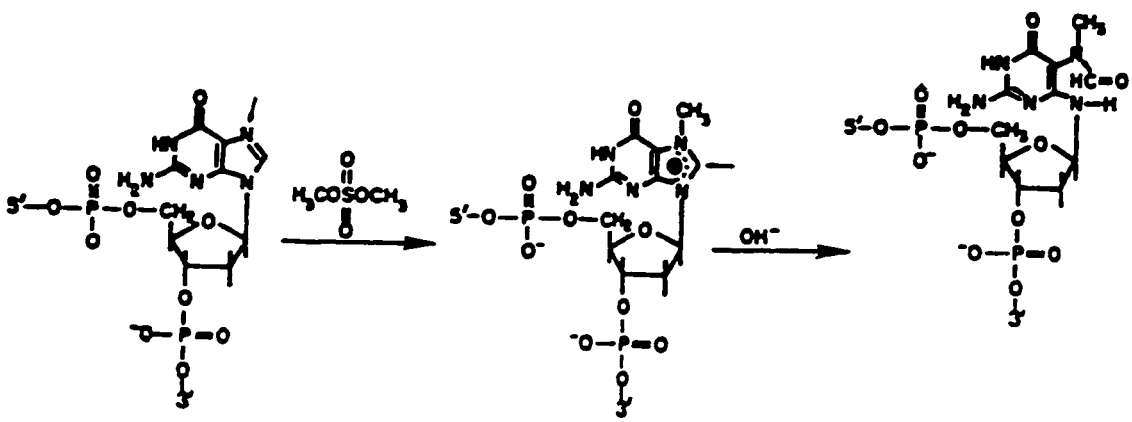

Figure 7.20 Reaction mechanism for the nucleophilic attack of DMSO with the C-8 position of the guanine base.

The NMR spectra of Fractions 12 and 13 show that the doublet at $\delta = 6.05$ ppm, the triplet at $\delta = 5.94$ ppm , and the triplet at 5.65 ppm for the single protons corresponding to the C-1', the C-2', and the C-3' positions, respectively, of the guanosine ribose sugar all disappear. This provides evidence that the ribose sugar may have reacted in the solvent methanol via transesterification or H^+ or OH^- catalyzed hydrolysis. Another possibility is that fluorescein was coupled to the N7 nitrogen and that this led, in the presence of a hydroxyl group to the elimination of the ribose sugar. The lack of sufficient product, impurities in the sample due to decomposition, and accidently equivalent protons in NHS-fluorescein and triacetylguanosine make it impossible to elucidate the structure of this species by simple ^1H NMR.

When dGTP was reacted with a 10-fold excess of fluorescein using EDC and sulfo-NHS as coupling reagents the chemical shift at $\delta \approx 10.8$ ppm, which has been assigned to the imino proton, disappears. In addition, the sharp chemical shift at $\delta = 10.2$ ppm which is found in NHS-fluorescein disappears. At $\delta = 10.2 - 10.4$ ppm a broad chemical shift is observed. This can be due to the protons of the primary amine, a carboxylate, or a hydroxyl group exchanging. The positions of resonances of protons in COOH, OH, and NH groups are subject to significant variation. These groups can exchange and form hydrogen bonds.[17] Another broad peak at $\delta = 3.4$ ppm can be assigned to a hydroxyl group. Two possibilities for the loss of the proton resonances of COOH and the N1 imino groups, (1) fluorescein is coupled to guanosine at the N1 imino position on the base or (2) the N-acylurea biproduct reacted with the N1 position of guanine. Elucidation of the products of the reaction between fluorescein and guanosine is difficult since the two reactants have chemical shifts in the same

region. In guanine the C8 proton has a singlet at $\delta \approx 7.8 - 8.0$ ppm and fluorescein (or NHS-fluorescein) has a proton with a singlet at $\delta \approx 7.9$. In addition, fluorescein has a multiplet at 6.5 - 6.8 ppm, exactly in the region of the aromatic amine of guanosine (s, 2H, $\delta = 6.5$ ppm).

In order to determine which group(s) on the guanine base are reactive, this following changes in purification and structure determination can be made. Isolating the pure product of the modified mononucleotide was difficult due to its decomposition. Flash chromatography on a reverse phase column can purify the products at a much faster rate, thereby decreasing the likelihood of the isolated products decomposing by the time an NMR spectrum is obtained. The ^{1}H NMR spectra of the products that have been obtained are too complex to assign chemical shifts. Complex spectra can be simplified by ^{15}N and ^{1}H heteronuclear 2D NMR exerpiments. However, due to the insensitivity of this nuclide, caused by a small gyromagnetic ratio and a small magnetic moment, and the low natural abundance of 0.37%, a large quantity of the purified product must be obtained. However, ^{15}N enriched guanosine is commercially available (Cambridge Isotopes). In addition, the ratio of fluorescein to guanosine residues in the product could be determined by fast atomic bombardment (FAB) mass spectrometry.

It is possible that the mononucleotide is less reactive with NHS-esters than a polynucleotide with runs of guanines. This would agree with the increase in electronegativity of the N7 position imposed by neighbouring guanines. It has been suggested that the neighbouring guanines might increase the nucleophilicity of the N7-positon of guanine via electrostatic interactions with a local increase in the electronegativity near the guanine N7 position.[13] To determine if NHS-fluorescein is more reactive with runs of guanines than the

mononucleotide, a purified NHS-fluorescein isomer or NHS-rhodamine could be reacted with guanosine and oligo$(dG)_x$ with x = 4 -20 bases.

7.4 Conclusions

To determine the site on the guanine base which reacts with the electrode surface using EDC and NHS as coupling reagents, products of the reaction between NHS-fluorescein and TAG were purified by HPLC and examined by NMR spectroscopy. Many problems were encountered which made elucidation of the structures of the products impossible, including decomposition of the products and accidentally equivalent protons in TAG and NHS-fluorescein. Further experiments are required to determine the reactive site on the guanine base.

7.5 References

1. Millan, K. M.; Spurmanis, A. J.; Mikkelsen, S. R.; *Electroanalysis*, **1992**, 4, 929.

2. (a) Millan, K. M.; Mikkelsen, S. R.; *Anal. Chem.*, **1993**, 65, 2317. (b) Millan, K. M.; Saraullo, A.; Mikkelsen, S. R.; *Anal. Chem.*; **1994**, 66, 2943.

3. Rosen, I.; Rishpon, J.; *J. Electroanal. Chem.*, **1989**, 258, 27.

4. Carey, F. C.; and Sundberg, R. J.; "Advanced Organic Chemistry" Part A, **1977**, Plenum Press, New York.

5. DeTar, D. F.; Silverstein, R.; *J. Am. Chem. Soc.*, **1966**, 88, 1013-1020.

6. Kurzer, F.; Douraghi-Zadeh, K.; *Chemical Reviews*, **1967**, 67, 2, 107-140.

7. Staros, J. V.; Wright, r. W.; and Swingle, D. M.; *Anal. Biochem.*, **1986**, 156, 220-222.

8. Cuatrecasas, P.; Parikh, I.; *Biochemistry*, **1972**, 11,12, 2291.

9. Pierce Catalogue, **1995**, p. T-165.

10. Huckett, B.; Gordhan, H.; Hawtrey, r.; Moodley, N.; Ariatti, M.; Hawtrey, A.; *Biochem. Pharma.*, **1986**, 35,8, 1249-1257.

11. Ariatti, M.; Hawtrey, A. O.; *Medical Hypothesis*, **1987**, 24,29.

12. Pullman A., Pullman, B.; *Biochem.*, **1990**, 29, 2985.

13. Pullman, A.; Pullman, B.; *Q. Rev. Biophys.*, **1981**, 14, 289.

14. Keller, G. H.; Manak, M. M.; "DNA Probes", **1989**, Stockton Press, pp. 243-244.

15. Harlow, E.; Lane, D.; "Antibodies: A laboratory manual", Cold Spring Harbor Laboratory, **1988**, New York, p 562.

16. Lawley, P.D.; Brookes, P.; *Biochem. J.*, **1963**, 89, 127.

17. Horst, Friebolin; "Basic One-and Two-Dimensional NMR Spectroscopy", Second Ed., VCH Publishers, New York, 1993. pp. 57-58.

Chapter 8

Summary and Suggestion for Future Research

8.1 Summary

From the results presented in Chapters 3-6 the following conclusions can be made:

1) DNA was immobilized onto the glassy carbon electrodes (GCEs) by coupling of the guanosine base with carboxylic acid groups electrochemically generated at the surface of the electrode via an N-hydroxysulfosuccinimide-carbodiimide coupling intermediate.

2) Electrochemical characterization of a DNA-modified GCE indicates that the transition metal complexes, $Co(bpy)_3^{3+}$ and $Co(phen)_3^{3+}$ can be used as redox-active hybridization indicators. Although the heterogeneous electron transfer rate at a DNA-modified GCE is slower than at the unmodified GCE, there is significant enhancement of the signal magnitude at the DNA-modified GCE. $Os(bpy)_3^{2+}$ binds selectively to dsDNA but does not provide a large enough signal difference between ssDNA and dsDNA. A daunomycin-glucose oxidase conjugate can also be used as an electrochemically-detectable hybridization indicator. Upon optimization of conditions it may provide larger signals than the transition metal complexes due to catalytic amplification.

3) The reproducibility of the DNA modification of the GCE is poor. Thus, between-sensor reproducibility is poor. However once the probe sequence is immobilized onto the GCE the reproducibility of detection of hybridization and regeneration of the probe is very good. In contrast,

the reproducibility of DNA immobilization at carbon paste electrodes is better, but these electrodes are highly unstable. Therefore, carbon paste electrodes should not be used as transducers in DNA sensors.

4) Two phosphate buffers were evaluated for the immobilization of poly(dG)poly(dC) at GCEs and SACPEs. One contains Li^+ counterions and the other K^+. These ions affect the formation of G4 DNA, with potassium increasing the formation of G4 DNA and lithium decreasing the ability to form G4 structures[1,2,3], as discussed in Chapters 3 and 4. In theory, since guanosine is involved in hydrogen bonding with other guanosine bases, the formation of G4 DNA structures should inhibit the coupling of DNA to GCEs and SACPEs. Experimental results do not support this fact. In fact, reverse results are obtained at GCEs and SA-CPEs where Li^+ improves coupling of guanosine at SA-CPEs and decreases coupling at GCEs (with virtually no coupling observed), while K^+ improves coupling at GCEs. This indicates that the surfaces of these two electrodes are very different and that the conformation of ssDNA influences the reaction yield of coupled ssDNA.

5) Three electrochemical methods were evaluated to determine which would provide the best detection limits for a DNA sensor: differential pulse voltammetry, chronoamperometry, and cyclic voltammetry. DPV provided the largest percent differences in signal between an unmodified and a DNA-modified GCE. This suggests that for the DNA sensor DPV should be the method of choice since these results indicate that it will provide the best detection limits.

6) The hybridization times, detection limits, and kinetics of hybridization of the immobilized probe

were examined. In the presence of an excess concentration of target DNA and the hybridization indicators, pseudo-first-order kinetics were observed. However, hybridization times were substantially reduced when hybridizations occurred in the absence of these transition metal complexes, at 28 °C, and in a high ionic strength buffer.

7) A DNA probe was synthesized which contained the sequence complementary for the ΔF508 mutation which codes for the three base deletion which causes cystic fibrosis, another for the complementary sequence for same region without the deletion which codes for the normal sequence. A sensor with these probes could positively identify the ΔF508 sequence and the normal sequence respectively, in human genomic PCR samples.

8) Preliminary results with model compounds indicate that the N1 imino group on the guanosine base is reactive to NHS esters. Other experiments must be performed to verify this result. There are other products of this reaction; however, their identities have not been determined.

8.2 Suggestions

On the basis of these experimental results and research in other laboratories and our own, a number of recommendations can be made.

The first is in the design of the probe sequence and the length of the dG tail. The probe sequence should not contain repeats of guanosine residues greater than three since guanosine residues can hydrogen bond with other guanosine residues. To improve the detection limits studies should be

performed to examine the effect of the length on the dG tail. Perhaps the formation of G4 structures will bring the probe sequence closer to the surface of the electrode. The optimal length which provides the best detection limits should be determined. In addition the detection limits of the DNA sensor may be improved by optimizing conditions for employing the daunomycin-GOx conjugate as the hybridization indicator in conjunction with gold, glassy carbon or platinum electrodes. The addition of hybridization accelerators, such as polyethylene glycol, should be included during hybridization of the probe with its target sequence to increase the rate of hybridization.

The specificity of the recognition process may be improved by using DNA analogues. It has recently been demonstrated that peptide nucleic acids (PNAs) have been used as probes for a sequence-selective DNA biosensor. These PNAs have higher thermal stability, can be formed at low ionic strength and show a higher specificity in the recognition of the target DNA. These PNA probes have been used in a DNA biosensor.[4]

The reproducibility between different sensors may be improved by increasing the reproducibility of the immobilization reaction. There are a few ways in which this may be accomplished, from using a less extreme anodization of the GCE to create carboxylic acid groups, to using different coupling reactions. Less extreme oxidizing conditions would include holding the potential at varying voltages for varying times under different buffer conditions. For example, anodization of the electrode has been achieved by holding at 1.8 V for 60 seconds in an acetate buffer with a pH = 5.0.[4,5] Another method for DNA immobilization which can be evaluated would involve the irreversible adsorption of oligonucleotides modified with a sulfhydryl group onto gold electrodes. Cystamine has been coupled to the 5'-terminal phosphate of the oligonucleotide by a phosphoramidate bond.[6] This would bind the 5'-cysteine of the modified oligonucleotide to the electrode surface,

thereby leaving the probe free to hybridize with its complementary sequence.

In addition to improving the reproducibility, a DNA sensor should be designed which has the ability to discriminate between a point mutation and the complementary sequence without the need for strict temperature control of hybridization. The hybridization reaction can be performed in the presence of varying concentrations of formamide. Also enzymatic or chemical cleavage at the site of a point mutation can be used. The design of this sensor would be an increase in signal upon hybridization. However, the probe will not discriminate between its complementary and noncomplementary sequence. The addition of a chemical or enzyme which cleaves DNA at the site of a base mismatch will decrease the length of dsDNA and produce a decrease in peak current. Therefore, the sequence can be properly identified by the decrease or lack of change in peak current associated with the extent of the preconcentration of the hybridization indicator, after incubation of the sensor with the enzyme or chemical cleavage complexes. S1 nuclease is an enzyme which reacts with mismatched bases in a DNA-DNA heteroduplex.[7] RNase A reacts with mismatched bases in RNA-RNA and DNA-RNA duplexes.[8,9] Osmium tetroxide and hydyroxylamine react with T and C mismatches and C mismatches, respectively.[10,11] The reaction of these reagents with mismatched C and T bases leads to cleavage of the DNA chain following the subsequent reaction with piperidine.

Another system which can be designed would be to use two probe oligonucleotides, a capture probe and a detection probe. One oligonucleotide, which is selective for one region of the target DNA, would capture the target sequence at the electrode surface. A second oligonucleotide, conjugated to an enzyme such as glucose oxidase, would be selective for another region of the target sequence, would be brought close to the electrode surface via hybridization with the target sequence. In the presence of a modifier such as ferrocene and excess co-substrate, a catalytic current will be

produced only when both the capture probe and the detection probe are complementary to the target sequence. This type of setup would be excellent for detection of unique sequences such as bacterial or viral sequences for the diagnosis of infectious diseases.

8.3 References

1. Sen, D.; Gilbert, W.; *Nature*, **1988**, 334, 364.

2. Sen, D.; Gilbert, W.; *Nature*, **1990**, 34, 6265, 410.

3. Sen, D.; Gilbert, W.; *Biochemistry*, **1992**, 31, 65.

4. Wang, J.; Palecek, E.; Nielsen, P. E.; Gustavo, R.; Cai, X.; Shiraishi, H.; Dontha, N.; Luo, G.; Farias, P. A. M.; *J. Am. Chem. Soc.*, **1996**, 118, 7667-7670.

5. Wang, J.; Cai, X.; Rivas, G.; Shiraishi, H.; Farias, P. A. M.; Dontha, N.; *Anal. Chem.*, **1996**, 68, 2629-2634.

6.Chu, b. C. F.; Orgel, L. e.; *Nucl. Acids Res.*, **1988**, 16, 3671.

7. Shenk, T. E.; Rhodes, C.; Rigby, P. W. J.; Berg, P.; *Proc. Natl. Acad. Sci. USA*, **1975**, 72, 989-983.

8. Myers, R. M.; Larin, Z., Maniatis, T.; *Science*, **1985**, 230, 1242-1246.

9. Winter, E.; Yamamoto, F.; Almoguera, C.; Perucho, M.; *Proc. Natl. Acad. Sci. USA*, **1985**, 82, 7575-7579.

10. Cotton, R. G. H.; Campbell, R. D.; *Nucleic Acid Res.*, **1989**, 20, 4223-4233.

11.Cotton, R. G. H.; Rodrigues, N. R.; Campbell, R. D.; *Proc. Natl. Acad. Sci. USA*, **1988**, 85, 4397-4401.

TEST TARGET (QA-3)

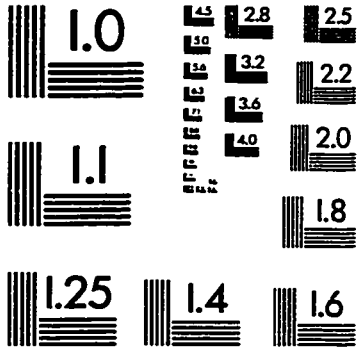

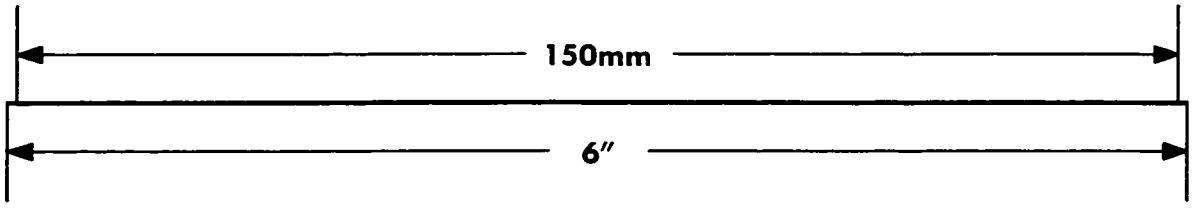

APPLIED IMAGE, Inc
1653 East Main Street
Rochester, NY 14609 USA
Phone: 716/482-0300
Fax: 716/288-5989